

The Development of Novel Electrochemical Sensors

From Redox Polymer Modified Electrodes

by

Andrew Patrick Doherty

A thesis submitted for the Degree of

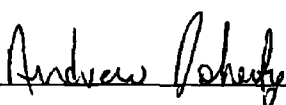
Doctor of Philosophy

Dublin City University

August 1992

Declaration

I hereby declare that the contents of this thesis, except where otherwise stated, is based entirely on my own work, which was carried out at the School of Chemical Sciences, Dublin City University, Dublin



Andrew Patrick Doherty

Johannes G Vos

(Supervisor)

To my loved ones

Acknowledgements

I would like to express my deepest gratitude to my supervisor, Dr Johannes G Vos for his faith, constant support, and encouragement throughout the course of this work. I would also like to thank Prof M R Smyth for his advice and encouragement.

Thanks also to the current and former members of the Vos research group, Alan, Dave, Margaret, Helen, Tia, Boris, Robert, Donal, Ellie and Ren Yi for their encouragement and help.

Thanks to the technical staff, Veronica, Fintan, Peig, Hugh, Morris Dawn and Damien for their invaluable help.

And finally, sincere thanks to John for the computer facilities used for the production of this thesis, and Mary, for diligent proof reading, and to my parents and Paul for never-ending faith and support.

Contents	Page No
Title Page	(i)
Declaration	(ii)
Dedication	(iii)
Acknowledgements	(iv)
Table of Contents	(v)
Abstract	(xii)

Chapter 1	Theory and Analytical Applications of Modified Electrodes	1
1 1	Introduction	2
1 2	Preparation of Modified Electrode Surfaces	4
1 2 1	Covalent Attachment	5
1 2 1 1	Silanisation	5
1 2 1 2	Direct Bonding	6
1 2 2	Adsorption	6
1 2 3	Polymeric Coatings	7
1 2 3 1	Preformed Polymers	8
1 2 3 1 1	Prefunctionalised Preformed Polymers	8
1 2 3 1 2	Post Coating Functionalisation of Preformed Polymers	9
1 2 3 2	Simultaneous Polymer Formation and Coating	11
1 3	Electrocatalysis	12
1 3 1	General Considerations	12
1 3 2	Theory of Mediated Electrocatalysis at Redox Polymers	15
1 4	Analytical Voltammetry and Amperometry	28
1 4 1	Introduction	28
1 4 2	Electrochemical Processes	30
1 4 3	Voltammetric and Amperometric Techniques	34
1 4 3 1	Cyclic Voltammetry	34
1 4 3 2	Chronoamperometry	40
1 4 3 3	Hydrodynamic Amperometry	40
1 4 3 3 1	Mass Transfer Under Hydrodynamic Conditions	42
1 5	Analytical Application of Modified Electrodes	45

1 5 1	Introduction	45
1 5 2	Preconcentration	46
1 5 3	Perm-selectivity	51
1 5 4	Electrocatalysis	54
1 6	Conclusions	58
1 7	Scope of Thesis	58
1 8	References	59
Chapter 2	The Development of a Sensor for Nitrite Based on [Os(bipy)₂(PVP)₁₀Cl]Cl Modified Electrodes	68
2 1	Introduction	69
2 2	Experimental	73
2 2 1	Materials and Reagents	73
2 2 1 1	Synthesis of High Molecular Weight Poly(4-vinylpyridine)	73
2 2 1 2	Determination of Poly(4-vinylpyridine) Molecular Weight	73
2 2 1 3	Synthesis of [Os(bipy) ₂ Cl ₂]	74
2 2 1 4	Preparation of [Os(bipy) ₂ (PVP) ₁₀ Cl]Cl	74
2 2 1 5	Electrolytes and Solutions	75
2 2 2	Procedures	75
2 2 2 1	UV/Visible Spectroscopy	75
2 2 2 2	Luminescence Spectroscopy	75
2 2 2 3	Cyclic Voltammetry and Rotating Disc Electrode Voltammetry	77
2 2 2 4	Flow Injection Analysis	77
2 2 2 5	Determination of Nitrite in Saliva	79
2 3	Results and Discussion	79
2 3 1	General Electrochemistry	79
2 3 2	Mechanism of Mediated Reduction of Nitrite	88
2 3 3	Modified Electrode Kinetics	96
2 3 4	Amperometry and Sensor Characterisation	108
2 3 4 1	Effect of Applied Potential	109
2 3 4 2.	Sensor Response Characteristics	111
2 3 4 3	Effect of Carrier Electrolyte Flow Rate	118

2 3 4 4	Effect of Carrier Electrolyte pH	120
2 3 4 5	Effect of Polymer Surface Coverage	120
2 3 5	Analysis of Nitrite in Saliva	122
2 4	Conclusions	122
2 5	References	125

Chapter 3 (Part A)	Development of a Dual Sensor for the Speciation Analysis of Fe(II)/Fe(III)	129
3 1	Introduction	130
3 2	Experimental	134
3 2 1	Materials and Reagents	134
3 2 1 1	Synthesis of $[\text{Ru}(\text{bipy})_2\text{Cl}_2] \cdot 2\text{H}_2\text{O}$	134
3 2 1 2	Synthesis of $[\text{Ru}(\text{bipy})_2(\text{PVP})_{10}\text{Cl}]\text{Cl}$	134
3 2 1 3	Electrolyte and Solutions	135
3 2 2	Procedures	135
3 2 2 1 1	UV/Visible Spectroscopy	135
3 2 2 2	Luminescence Spectroscopy	135
3 2 2 3	Cyclic Voltammetry and Rotating Disc Electrode Voltammetry	136
3 2 2 4	Flow Injection Apparatus	136
3 3	Results and Discussion	138
3 3 1	Characterisation of $[\text{Ru}(\text{bipy})_2(\text{PVP})_{10}\text{Cl}]\text{Cl}$	138
3 3 1 1	Absorption and Emission Spectroscopy	138
3 3 2	Mediated Oxidation/Reduction of Fe(II) and Fe(III) by Osmium and Ruthenium Containing Metallo-Polymers	139
3 3 3	Principle of Operation of Dual Sensor	143
3 3 4	Operational Performance of Dual Sensor	145
3 3 4 1	Sensor Response Attributes	145
3 3 4 2	Effect of Carrier Electrolyte Flow Rate	149
3 3 4 3	Effect of Applied Potential	149
3 3 4 4	Effect of Electrolyte pH	152
3 3 4 5	Effect of Polymer Surface Coverage	152
3 3 4 6	Electrode "Cross Talk"	154
3 3 4 7	Recoveries from Analytical Samples	155
3 3 4 8	General Considerations	157

3 4	Conclusions	159
3 5	References	161
Chapter 3 (Part B)	Electroanalysis of Nitrate using a Cu/Cd Reductor Column and a [Ru(bipy)₂(PVP)₁₀Cl]Cl Modified Electrode	164
3 6	Introduction	165
3 7	Experimental	168
3 7 1	Materials and Reagents	168
3 7 2	Procedures	168
3 7 2 1	Construction of Copperised Cadmium Reductor Column	168
3 7 2 2	<i>In Situ</i> Copperisation of Cadmium Chips	169
3 7 2 3	Flow Injection Apparatus	169
3 7 2 4	Analysis of Nitrate in Commercial Fertiliser using the Modified Electrode	170
3 7 2 5	Potentiometric Determination of Nitrate in Commercial Fertiliser	171
3 8	Results and Discussion	172
3 8 1	Mediated Oxidation of Nitrite by a [Ru(bipy) ₂ (PVP) ₁₀ Cl]Cl Modified Electrode	173
3 8 2	Optimisation of Carrier Electrolyte	173
3 8 3	FIA System Responses	175
3 8 4	Effect of Applied Potential	179
4 8 5	Effect of Carrier Electrolyte Flow Rate	179
3 8 6	Efficiency of Nitrate to Nitrite Conversion	182
3 8 7	Analysis of Nitrate in Commercial Fertiliser	184
3 9	Conclusions	185
3 10	References	186
Chapter 4	Physical Stabilisation of Electrode Surfaces Modified with [Os(bipy)₂(PVP)₁₀Cl]Cl Using Cross-linking Agents	188

4 1	Introduction	189
4 2	Experimental	194
4 2 1	Materials and Reagents	194
4 2 1 1	<i>In Situ</i> Cross-linking of $[\text{Os}(\text{bipy})_2(\text{PVP})_{10}\text{Cl}]\text{Cl}$	194
4 2 1 2	Electrolytes and Solutions	195
4 2 1 3	Cyclic Voltammetry and Rotating Disc Electrode Voltammetry	197
4 2 1 4	Flow Injection Apparatus	197
4 2 1 5	Infra Red Spectroscopy	198
4 3	Results and Discussion	198
4 3 1	General Observations and Considerations Concerning Stability	198
4 3 2	Infra Red Analysis of Solid State Cross-linking Reaction	201
4 3 3	Stability of Uncross-linked $[\text{Os}(\text{bipy})_2(\text{PVP})_{10}\text{Cl}]\text{Cl}$	202
4 3 4	Stability of Cross-linked $[\text{Os}(\text{bipy})_2(\text{PVP})_{10}\text{Cl}]\text{Cl}$	206
4 3 5	Charge Transport Characteristics	208
4 3 6	Nernstain Behaviour	214
4 3 7	Surface Behaviour of Cross-linked $[\text{Os}(\text{bipy})_2(\text{PVP})_{10}\text{Cl}]\text{Cl}$	217
4 3 8	Kinetics of Fe(III) Reduction at Cross-linked Redox Polymers	219
4 3 8 1	1,10-Dibromodecane	220
4 3 8 2	1,5-Dibromopentane	224
4 3 8 3	p-Dibromobenzene	227
4 3 8 4	Polymer Cross-linking and Mediated Electrocatalysis	230
4 4	Conclusions	231
4 5	References	234
 Chapter 5	 Synthesis, Characterisation and Analytical Application of $[\text{Os}(\text{bipy})_2(\text{PS})_{7.5}(\text{DMAP})_{2.5}\text{Cl}]\text{Cl}$	 237
5 1	Introduction	238
5 1 1	Charge Transport Properties of Redox Polymers	239

5 1 2	Activation Parameters	244
5 2	Experimental	245
5 2 1	Materials and Reagents	245
5 2 1 1	Synthesis of $[\text{Os}(\text{bipy})_2(\text{PS})_7 5(\text{DMAP})_2 5\text{Cl}]\text{Cl}$	245
5 2 2	Procedures	246
5 2 2 1	UV/Visible Spectroscopy	246
5 2 2 2	Luminescence Spectroscopy	247
5 2 2 3	Cyclic Voltammetry and Rotating Disc Electrode Voltammetry	247
5 2 2 4	Coulometry	248
5 2 3	Flow Injection Analysis	248
5 2 4	Spectrophotometric Determination of Iron in Therapeutic Formulation	249
5 3	Results and Discussion	249
5 3 1	Characterisation of $[\text{Os}(\text{bipy})_2(\text{PS})_7 5(\text{DMAP})_2 5\text{Cl}]\text{Cl}$	249
5 3 1 1	Absorption and Emission Spectroscopy	253
5 3 1 2	Electrochemistry	254
5 3 2	Electrochemistry and Charge Transport Properties of $[\text{Os}(\text{bipy})_2(\text{PS})_7 5(\text{DMAP})_2 5\text{Cl}]\text{Cl}$	254
5 3 3	Mediated Electrocatalytic Reduction of Fe(III) by $[\text{Os}(\text{bipy})_2(\text{PS})_7 5(\text{DMAP})_2 5\text{Cl}]\text{Cl}$	265
5 3 4	Analytical Application of $[\text{Os}(\text{bipy})_2(\text{PS})_7 5(\text{DMAP})_2 5\text{Cl}]\text{Cl}$	274
5 4	Conclusions	279
5 5	References	281
 Chapter 6	 Sensor Characterisation and Performance	 286
6 1	Introduction	287
6 2	Experimental	288
6 2 1	Procedures	288
6 2 1 1	Cyclic Voltammetry and Rotating Disc Electrode Voltammetry	288
6 2 1 2	Flow Injection Apparatus	289
6 2 2	Materials and Reagents	289

6 3	Results and Discussion	289
6 3 1	Sensor Sensitivity Control	289
6 3 2	Interference/Selectivity Control	297
6 3 3	Background/LOD/Linear Ranges	309
6 3 4	Inter-Electrode Variability	313
6 4	Conclusions	314
6 5	References	316
 Chapter 7	 Concluding Comments	 319

Abstract

The use of osmium- and ruthenium-containing redox polymer modified electrodes for the development of novel electrochemical sensors has been investigated. The kinetics and transport parameters for the electrocatalytic reactions of a number of important substrates at the modified electrodes have been analysed using conventional theory for mediated electrocatalysis. Using this information, a series of novel sensors have been constructed, and the operational performance of these devices assessed. A sensor for the reductive detection of nitrite was constructed from an $[\text{Os}(\text{bipy})_2(\text{PVP})_{10}\text{Cl}]\text{Cl}$ modified electrode. The mechanism of nitrite reduction at the modified electrode appears to proceed through the nitrosonium ion. The cross-exchange reaction occurs throughout the polymer film and is controlled by the rate constant for the cross-exchange reaction. Slow reaction kinetics allows measurement of limiting currents independent of solution mass transport. Under these conditions, an equation relating sensor response directly to known parameters can be obtained, this equation can be used for the internal calibration of the sensor. The sensor was applied to the determination of nitrite in saliva. A novel dual sensor for the speciation analysis of redox couple $\text{Fe}(\text{II})/\text{Fe}(\text{III})$ was constructed from osmium- and ruthenium-containing redox polymer modified electrodes. The principle of operation is described, and is based on the free energy differences for both the oxidation and reduction of the analytes at their respective sensors. The detection system exhibits considerable advantages compared to existing speciation techniques. The operational performance of the dual sensor is discussed in relation to existing methods for this speciation analysis. The recoveries of $\text{Fe}(\text{II})$ and $\text{Fe}(\text{III})$ from water samples was assessed. The physical stabilisation of the redox polymers by chemical cross-linking and by manipulation of the polymer back-bone was attempted. The effects of the stabilisation procedures on the charge / mass transport and electrocatalytic properties of the modified electrodes was investigated, and are discussed in relation to the requirements of operational sensors. Finally, the performance of sensors constructed from redox polymer modified electrodes is discussed with respect to control of sensor sensitivity, selectivity and potential interferences. General strategies for the control and optimisation of sensor performance are also discussed.

Chapter 1

Theory and Analytical Applications of Modified Electrodes

1.1. Introduction

The field of electrochemistry has a long association with analytical chemistry. With the development of potentiometry and polarography in the early decades of this century, electrochemistry produced the first forms of instrumental analysis. These developments were achieved due to the sensitivity, selectivity and simple equipment required for electroanalysis. However, from the outset, electrochemistry was plagued with problems of electrode instability caused by passivation of electrode surfaces and slow rates of heterogeneous electron transfer. In addition, these problems were compounded by the lack of suitable electrode materials. With the development of the dropping mercury electrode, (DME), which provided a reproducible renewable surface, a revolution occurred in electrochemistry. Through the pioneering work of Heyrovsky¹, considerable advances in both fundamental and applied electrochemistry were made during the middle part of this century. Unfortunately, the inherent difficulties associated with mercury, and the advent of highly sensitive and selective spectroscopic techniques, caused a decline in interest in electrochemistry as an analytical tool. This decline continued until the appearance of the first enzyme electrode² in the late 1960's and chemically modified electrodes in 1973^{3,4}. The concept of "tailoring" the electrode surface, and therefore, the properties of the electrode, caused a renaissance in electrochemistry. Suddenly, the prospect of "designer electrodes" became a reality, and along with this the possibility of large commercial returns created the impetus for modified electrode research.

It has long been recognised that the structure of the electrode/electrolyte interface is of manifest importance for electrode reactions. The use of surfactants for the elimination of maxima in polarography is a prime example of the importance of controlling the interfacial properties of electrodes. The concept of direct electrode modification was first introduced by Lane and Hubbard^{3,4} with the chemisorption of olefinic groups on platinum electrodes. The significance of this development was soon recognised, and resulted in intense research activity. The number of reviews which have appeared over the last decade concerning chemically modified electrodes lay testimony to their importance in electrochemistry⁴⁻⁸. It has been suggested that this area of

research “offers some of the greatest promises for advance in all chemistry” ⁷ Numerous approaches have been adopted for electrode modification, and the range of modifying materials is vast, but the universal theme is an attempt to seize control of the properties and reactivity of the electrode surface and the development of novel applications for the modified electrode surface. The types of materials used for electrode modification range from metal deposits, metal oxide layers, organic materials, enzymes and polymers. The range of applications envisaged for modified electrodes is huge, already their unique features are exploited in diverse areas such as electrochemical sensors ⁸, heterogeneous electrocatalysis ^{9,10}, solar energy conversion ^{11,12}, electrochromics ^{13,14}, energy storage ^{15,16} and information storage ^{17,18}. In all of these applications, the observed response of the device is directly related to the properties of the coating. In this literature survey, only the application of modified electrodes as electrochemical sensors will be discussed.

No area of modified electrode research has been more prolific than that of electroanalysis. The sheer scope and number of applications is impressive, and it appears that the only limitation of modified electrode design is the function which it must perform and the imagination of the chemist ¹⁹. The underlying purposes of electrode modification for electroanalysis are few and simple. In general, electrode modification is carried out to drive thermodynamically favourable reactions not observed at unmodified electrodes, improve electrode sensitivity and decrease limits of detection, to increase electrode selectivity and to prevent surface fouling. These themes are inexorably linked, as any modification used to effect one property tends to affect another. This can be used to advantage by exploiting several properties from a single modification scheme. In general, electrode modification is used to either promote or inhibit certain electrode reactions ¹⁹. Processes such as preconcentration, perm-selectivity and electrocatalysis have been utilised to produce electrochemical sensors with improved operational performance compared to conventional electrode surfaces.

Early examples of electrode modifiers were monolayers of electro-active materials either adsorbed ^{3,4} or covalently attached to the electrode surfaces *via* organosilane linkages ^{20,21}. Although elegant, these electrodes suffered severe stability problems, difficulty in preparation, and generally only monolayer derivatised surfaces could be prepared. With the advent of

electronically conducting polymers ²² and redox polymers ²³, modified electrodes tended to be constructed from polymeric materials due to their inherent physical stability, ease of preparation and synthetic variability. The ability to control the chemistry of the modifier is of great importance as this allows control of properties such as analyte transport, charge transport, redox site loading and the electrocatalytic properties of the modifier. Such control favours the construction of stable, sensitive and selective sensors.

In this chapter, the theories of analytical voltammetry and mediated electrocatalysis will be presented. In addition, a general discussion of the preparation of modified electrodes and a detailed account of the analytical application of such devices will be presented. This survey is not intended to be exhaustive rather it is an overview of the most interesting and relevant work in the field of modified electrode research. In the introduction to subsequent chapters, more specific accounts concerning the study being addressed will be given.

1.2. Preparation of Modified Electrode Surfaces

The origin, development and current interest in the area of modified electrodes stems from the desire to control the properties and reactivity of the electrode surface. ⁸ The reactivity of any electrode is determined firstly by its electrochemical potential, which can be controlled instrumentally, and secondly, by the nature and structure of the electrode/electrolyte interface. Other methods of achieving this objective remain difficult, therefore, the modification of electrodes is frequently exploited because of the ability to pre-select the response of an electrode by judicious choice of the modifier. The most important methods for the modification of electrode surfaces can be summarised as follows:

(1) Covalent Attachment

(a) Silanisation

(b) Direct bonding

(2) Adsorption

- (a) Electro-deposition
 - (b) Direct non-specific adsorption
- (3) Polymeric Coatings
- (a) Polymer solution casting
 - (b) Electro- and photo-deposition

1 2 1 Covalent Attachment

1 2 1 1 Silanisation

Silanisation was the first direct chemical technique to be utilised for electrode modification, (this work was stimulated by the successes in bonded phase high performance liquid chromatography (HPLC) technology ²¹ This involves the formation of surface hydroxy or oxide groups on the electrode surface which are subsequently reacted with trialkoxy- or trichloro-silanes to form, one to three covalent bonds to the underlying electrode surface ²⁴⁻²⁶ The silane groups can bear amine or pyridyl groups which can undergo further reaction for the surface synthesis of immobilised electro-active centres ²⁰ As these modifications involve covalent bonding, these electrodes are referred to as Chemically Modified Electrodes (CME's) These modification techniques generally give rise to monolayer modifications, although the preparation of multilayers is possible ²⁷ The range of base electrode materials to which the silanisation reactions can be applied include traditional electrode materials such as glassy and pyrolytic carbon ^{28,29}, platinum ³⁰ and gold ³¹ Metal oxides ³² and semiconductor materials ³³ can also be modified in this way In an alternative approach, reactive carboxylic acid groups can be generated by thermal or radio frequency plasma pre-treatments of electrode surfaces ³⁴⁻³⁶ Such reactive groups can be used directly as anchors for the subsequent chemical derivatisation of the surface Alternatively these groups can be converted to acid chloride groups prior to reaction Acid chloride is particularly useful as it can undergo a facile condensation reaction with amine groups ³⁷ Examples of this include the immobilisation of tetrakis(p-aminophenyl) porphyrins to electrode surfaces The covalent modification of carbon can be accomplished easily using these techniques, as surface carboxyl groups can be easily formed on carbon surfaces Metals such as platinum and gold can be modified *via*

surface oxide groups formed by such oxidation techniques ³⁸ Metal oxide electrodes generally possess sufficient surface oxide groups to facilitate covalent modification directly *via* ester or ether bonding with surface hydroxyl groups ³⁹ Other materials which have been modified in this way include Si and Ge semiconductors ⁴⁰

1 2 1 2 Direct bonding

Direct bonding is achieved by exposing the underlying bulk material such as carbon or platinum to various materials under the influence of argon radio-frequency plasma discharge ⁴¹, mechanical abrasion ⁴² or vacuum pyrolysis ⁴³ Materials which have been deposited in this manner include allylamine for condensation with ferrocenecarbaldehyde ⁴⁴ This approach is not widely practiced due to uncertainty of the resulting modifier structure Such modified electrodes are also difficult to prepare reproducibly, are frequently unstable and are therefore of little interest in the development of sensors

1 2 2 Adsorption

The adsorption of electro-active and electro-inactive materials at electrode surfaces has long been realised Several examples of this phenomena have been used to modify electrodes Lane and Hubbard studied the electro-sorption of olefins at platinum ^{3,4} The exact nature of the adsorption process is little understood but it appears that some form of Pt-C bonding takes place Another example is the adsorption of disulphide-containing enzymes to mercury electrodes ⁴⁵ The modifying species can not be thought of as covalently bound as slow desorption occurs Bilayer arrangements have been used to prevent loss of electro-active material from the surface ⁴⁶ Adsorption has been studied as a function of aromaticity of the adsorbate and it appears that some degree of aromaticity is required for strong adsorption ^{47,48} Thus for monomeric compounds, no adsorption may be observed, while irreversible adsorption may be found with the corresponding polymeric material ¹⁹ This approach to electrode modification is of little use in electroanalysis as the adsorption process is frequently of an equilibrium type, which results in

the desorption of the electro-active component when placed in electrolyte devoid of the modifying species

The modification of electrode surfaces by sublimation⁴⁹ and deposition from solution has also been investigated. In these cases physisorption is believed to be responsible for the adsorption process. Normally van der Waals forces and coulombic interactions are responsible for physisorption, but again at modified electrodes, the nature of the processes is not well understood.

1.2.3 Polymeric coatings

With the advent of electronically conducting and redox polymers in the late 1970's^{22,23}, the widespread use of polymer modified electrodes began. Polymeric materials offered considerable advantages compared to the chemically modified electrodes used previously. Polymeric materials are inherently more stable than monomeric modifiers, therefore, devices constructed from such materials are potentially more robust, which is desirable from the applied perspective. The field of polymer chemistry is mature and provides a readily available source of materials and synthetic strategies to produce electro-active polymers with desirable, and more importantly, controllable physical properties. This offers the prospect of synthetic variability which is vital for the development of operational devices such as electrochemical sensors. Polymers also offer the possibility of up to 10^5 molecular layers of electro-active species⁸ at high surface concentration (up to 10 M) at the electrode surface compared to conventional monolayer derivatised surfaces.¹⁹ This feature allows polymer modified electrodes to react with substrates in a three dimensional zone rather than a two dimensional region at monolayer modified electrodes. This provides the possibility of heterogeneous catalysis at the polymer modified electrode competing with solution phase homogeneous catalysis and the resulting advantages associated with this development.⁷

The preparation procedure for polymer modified electrodes can be classified by the synthetic strategy used for the preparation of the modified electrode. This approach gives an overview of how immobilisation can be carried out and highlights the relative merits and limitations of the different strategies. The principle division is whether preformed polymers are used

for coating or whether polymerisation/coating processes are performed simultaneously. In either case, further derivatisation of the polymer film is possible.

1.2.3.1 Preformed Polymers

1.2.3.1.1 *Prefunctionalised Preformed Polymers*

Redox polymers classified under this heading are generally formed from vinyl monomers. Poly(N-vinylimidazole)⁵⁰ (PVI) and poly 4-(vinylpyridine) (PVP)^{23,51} are the most common examples of this mode of preparation. Two strategies are used to produce polymers with the desired redox site loading.²³ Firstly, the polymer may be preformed and subsequently functionalised with a stoichiometric amount of functionalised reagent. Secondly, functionalised monomer may be co-polymerised with unfunctionalised monomer. Both of these approaches are elegant with respect to synthetic variability and the ability to characterise the redox material with respect to molecular weight, redox chemistry, glass transition temperature, tacticity and solubility prior to deposition. However in the second approach, the polymerisation process is less well understood, and control of the properties of the resulting redox polymer may be difficult. One of the most important advantages of this approach is that the electro-active centre is bonded by coordination, or covalently, to the polymer, consequently the electro-active centre is immobilised in the polymer and can not be leached by the action of solvents or ion-exchange processes. In addition, the modification procedures are simple. Both these types of polymer have been applied to electrode surfaces by procedures such as spin-coating, droplet evaporation, adsorption from solution, electro-precipitation, and photo-deposition.¹⁹ The mechanism of adsorption of the polymers on electrode surfaces is poorly understood. It appears that adhesion is a function of non-specific adsorption and insolubility in the contacting electrolyte. Control of the polymer layer thickness is of great importance as this frequently affects the catalytic efficiency of the electrode, charge transport rates, stability and preconcentration effects. This is accomplished by controlling the amount of material deposited on the electrode surface. Spin-coating and droplet evaporation are useful techniques as these allow control of the amount of material deposited. The

other methods mentioned above are less controllable and are therefore less useful

The ability to further derivatise the polymer coating to effect changes in the physical or chemical properties of the modifier is desirable. An example of this has been demonstrated by the photo-chemically induced ligand substitution of $[\text{Ru}(\text{bipy})_2(\text{PVP})_5\text{Cl}]\text{Cl}$.⁵² An example of this can be seen in Fig. 1.1. This results in a positive shift in half-wave potential of the electrocatalyst couple by 0.1 V. Such behaviour may prove valuable in the “fine tuning” of the electrocatalytic properties of the modifier such that reactions of interest can be observed while excluding potential interfering reactions. This may also be used to enhance the sensitivity of the electrochemical sensor.

1.2.3.1.2 *Post-Coating Functionalisation of Preformed Polymers*

This approach involves the coating of an electrode with a preformed polymer, followed by *in situ* functionalisation of the polymer with an electro-active moiety. Functionalisation can involve ligand displacement from the redox species with subsequent coordination of the redox species to the polymer backbone. Alternatively, and much more frequently, ion-exchange of electro-inactive polymer bound ions for electro-active co-ions in solution is employed to effect functionalisation. Redox cycling has been shown to aid this process.⁵³ Major disadvantages with this approach include the instability of the ion-exchanged moieties as the bound species are in dynamic equilibrium with solution species and the technical difficulty of the preparation procedure.

Examples of post-coating coordination are predominated by the use of the polymer PVP due to the coordination ability of the aromatic nitrogen of the pyridine moiety.^{54,55} The electro-active centres incorporated include $[\text{Ru}(\text{EDTA})]^+$,⁵⁴ $[\text{Ru}(\text{NH}_3)_3]^{2+}$,⁵⁵ and $[\text{Fe}(\text{CN})]^{3-}$.⁵⁶ As these systems tend to be in thermal equilibrium with the solution phase ion, the metal loading may be controlled to some extent.¹⁹ However, these electrodes tend to be more stable than those based on ion-exchange processes.

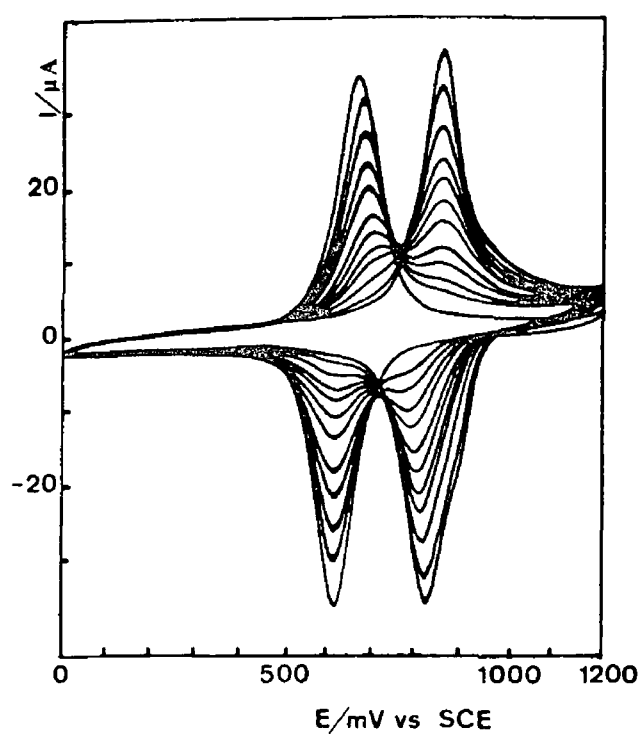


Fig 1 1 Cyclic voltammograms recorded during the photo-substitution of $[\text{Ru}(\text{bipy})_2(\text{PVP})_5\text{Cl}]\text{Cl}$ coated on glassy carbon electrodes The supporting electrolyte was $1.0 \text{ mol dm}^{-3} \text{ HClO}_4$ and the potential sweep rate was 100 mV s^{-1} (Reproduced from O Haas, M Kriens, J G Vos, *J Am Chem Soc*, 1981 103 1318)

Quaternised and/or protonated PVP and Nafion coated onto electrodes have been used extensively for the ion-exchange of redox moieties into polymer films ^{12,57-60} The extent, stability and rate of incorporation depends on the electrostatic interactions between the charged polymer and the redox counter ion In the case of Nafion, the degree of hydrophobicity of the exchanging ion affects the extent of incorporation For these systems the degree of functionalisation is a complex issue, as the system may be under kinetic control as a result of slow polymer solvation or structural changes, rather than equilibrium control Under such circumstances the incorporation, and therefore redox site loading, is difficult to control

1 2 3 2 Simultaneous Polymer Formation and Coating

This approach comprises the principles of electro-polymerisation and plasma initiated polymerisation ⁵⁹ The objectives of this approach are to maintain or augment the reactivity of the monomer during polymerisation Frequently, however, the properties of the film are not intrinsic to the monomer but result from the polymerisation process ⁶⁰

Electro-polymerisation is considered to take place *via* radical intermediates formed in the vicinity of the electrode The rate of initiation of these radicals is controlled by the potential of the electrode and can be measured by the electrode current ¹⁹ This technique allows precise control of the film thickness and in some cases polymer morphology The electro-polymerisation of metal complexes containing vinyl groups has received considerable attention ⁶¹⁻⁶⁴ The vinyl electro-polymerisation process is typically anionic, requiring reductive scanning to initiate the polymerisation process A requirement for a vinyl-containing molecule to undergo electro-polymerisation is that it is conjugated to a more reducible entity, most frequently a bipyridyl or viologen unit ¹⁹ The ease of polymerisation of these materials is intimately related to the number of vinyl groups the monomer contains The linear polymer formed from the monovinyl monomer is obtained with difficulty while di- and trivinyl monomers polymerise easily In order to achieve effective polymerisation, di- or trivinyl monomers are generally required, therefore the polymerisation process is difficult to control and the films tend to be highly cross-linked Due to the intractable nature of the materials they are also

difficult to characterise. In addition, generally only small portions of the films are electro-active and film impermeability is often encountered.

The oxidative electro-polymerisation of a wide range of aromatic monomers, such as pyrrole, aniline and the phenols has been described.⁶⁵ The polymers formed are in an oxidised form and contain charge compensating counter-ions. The counter-ion can affect the mechanism of reactions at the electrode.⁶⁶ Chemically active counter-ions have been incorporated during the electro-polymerisation process to effect specific analytical requirements.⁶⁷ Many analytical applications have been described for these materials and examples of these will be discussed later.

1.3. Electrocatalysis

1.3.1 General Considerations

An electrochemical reaction proceeds at a rate determined by the rate constant for the particular reaction. Electrochemical reactions differ from chemical reactions in that the rate constant for the reaction is dependent on the applied potential of the electrode, this is normally an exponential relationship as described by Butler-Volmer kinetics.⁶⁸ Marcusian theory dictates that electron transfer is iso-energetic (the energy of the electron and donating/accepting orbital are equal), so at a potential where iso-energetic conditions are satisfied, electron transfer should be in equilibrium.⁶⁹ This is the formal potential of the redox couple, E^0 . In real systems, it is often required to apply potentials in excess of that required by thermodynamics to drive a particular electrochemical reaction, this results in a free energy difference between the electron and the donating/accepting orbital. This excess free energy is required to surmount the activation energy barrier for reaction. This is referred to as activation over-potential.^{68,69} The rate constants for electrochemical reactions differ widely, in fact, by many orders of magnitude. The rate of a particular reaction depends to a large extent on the mechanism of the reaction. Many electrochemical reactions involve a simple electron transfer step and proceed at rates predicted by the Marcus theory, without need for the application of an activation over-potential. On the other hand some

reactions have complex multi-step mechanistic sequences involving processes such as adsorption, nuclei coupling, and acid-base chemistry ⁶⁸ Such reactions tend to proceed through high energy intermediates, and are often found to have slow reaction rates. In order to drive these reactions electrochemically at appreciable rates the application of an activation over-potential is required ⁶⁸ The desire to avoid the application of an activation over-potential is great from the perspective of electroanalysis. The application of potential extremes causes an exponential increase in the number of possible interferences which may be encountered, consequently, reducing operational potentials, by even a small amount, may considerably reduce interference ⁷⁰ A lowering in over-potential can be achieved by accelerating the rate of the electrochemical reaction. Such a process is electrocatalysis ⁷¹ In addition, accelerating the rate of the electrochemical reaction may increase the sensitivity and lower limits of detection. With the use of specific electrocatalysts greatly improved selectivity may also be achieved. Electrocatalysis has been reviewed extensively recently in relation to electro-synthesis ⁷¹, electroanalysis ⁷² and modified electrodes ⁷³

It has been shown that for true electrocatalysis the Gibbs free energy, (ΔG), for the electrocatalytic reaction must be negative ⁷¹ (*i.e.* a spontaneous reaction). From thermodynamics we know that

$$\Delta G = -n F \Delta E \quad (1.1)$$

Where n is the number of electrons transferred, ΔE is the potential difference between the electrocatalyst's half-wave potential and the formal potential of the reactant, and F is the energy change as one mole of electrons fall through a potential of one volt. As ΔG must be negative, then ΔE must be positive. This imposes certain limitations on the type of reactions which may occur at modified electrodes. For catalysis of oxidation reactions, the half-wave potential ($E_{1/2}$) of the redox catalyst must be positive of the formal potential of the substrate. For the catalysis of reduction reactions the reverse situation must exist. This thermodynamic control can be used to effect selective detection of target analytes and eliminate interference from co-existing species. To exploit

this, control of the $E_{1/2}$ of the electrocatalyst couple is of paramount importance. This can often only be accomplished by controlled synthetic pathways.

Any electrocatalyst is only effective in the vicinity of the electrode surface⁷, many homogeneous electrocatalysts are known, however, the ability to immobilise the electrocatalyst on the electrode surface provides a cheap, convenient and effective way of confining the material in the electro-active spatial region⁷. Many materials immobilised on electrode surfaces have been used for the electrocatalysis of electrode reactions, these include metallic⁷⁴ and metal oxide micro-particles immobilised in polymer matrices⁷⁵, organic redox polymers⁷⁶ and redox polymers containing coordinated electro-active groups⁷⁷.

For many modified electrodes used as electrochemical sensors, electrocatalysis is accomplished with the use of surface immobilised redox sites which “shuttle” electrons by repeated cycling between the catalytic and pre-catalytic state between the electrode and the electro-active substrate in a process that is known as mediated electrocatalysis⁷³. Saveant has shown that for reactions proceeding at rates approaching those predicted by Marcusian theory, monolayer modification of the electrode with a redox catalyst is ineffective at accelerating the reaction rate and consequently lowering operational potentials⁷⁸. However, with multi-molecular arrangements, considerable current gain can be achieved due to the three dimensional nature of the reaction zone⁷³. For reactions which proceed at sub-Marcusian rates, the modification of the electrode can be expected to result in a potential gain (lowered over-potential) and current gain for even mono-molecular modified electrodes. Several examples of this have been demonstrated^{34,53,79,80}. So, it is expected that modification of electrodes with electron mediators will be effective where the reaction proceeds slowly, or not at all at conventional electrodes, and in situations where the mediated reaction can occur in a three dimensional reaction zone. For these reasons and others mentioned earlier, mediated electrocatalysis is predominantly carried out using polymeric electrode modifiers⁶⁰.

1.3.2 Theory of Mediated Electrocatalysis at Redox Polymers

The theory of mediated electrocatalysis has been studied extensively by many authors and established theories allow mechanistic elucidation and kinetic parameters to be evaluated^{56,81-88}. In the design of modified electrodes for electroanalysis these theories can be used to help to optimise the performance of the sensor.

The fundamental redox reactions which can occur between a solution species Y and a mediating layer containing the redox couple A/B are shown in Fig. 1.2. The mediating process can be described by reactions 1.2 and 1.3:



In this example, the mediation process involves the reduction of the surface bound redox species, A, but for a mediation process based on the oxidation of the surface bound redox species, the same theory applies. Other more complex mediating processes involving reversible mediation reactions, self-exchange reactions, pre-activation steps and charge exchange have been considered by Saveant and co-workers^{79,89-94}. Depending on factors such as film morphology, film thickness, the partition coefficient and diffusion rate of the electro-active species through the film and electron transfer rates, four types of limiting cases can be identified⁸⁹:

- (1) Electron and substrate diffusion (D_E and D_Y respectively) are so fast that the rate-controlling step is the rate, k , of the catalytic reaction

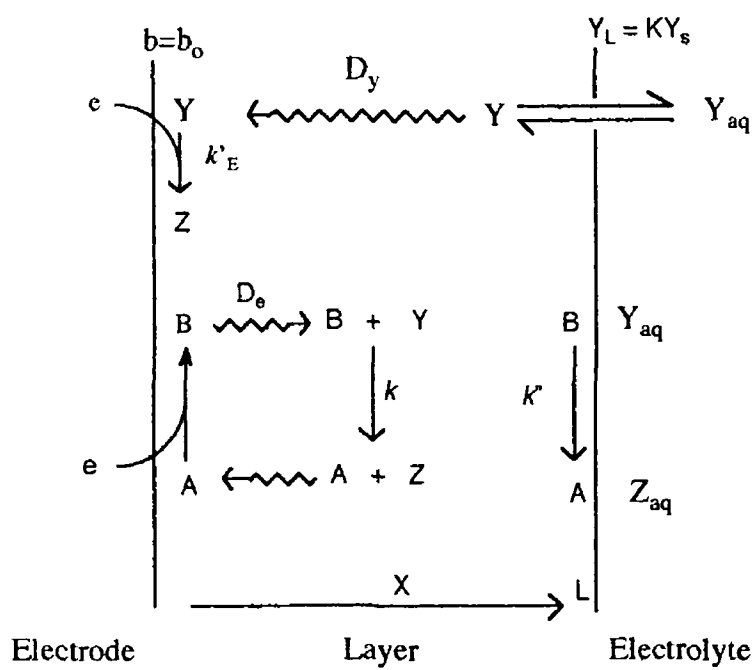


Fig 1 2 Schematic representation of the processes possible at redox polymer modified electrodes

- (2) The catalytic reaction is so fast that the rate is controlled by the two diffusion processes, *i.e.* diffusion of electrons and substrate
- (3) When diffusion of electrons is faster than diffusion of substrate, a pure kinetic situation may arise by mutual compensation of the latter process and the catalytic reaction
- (4) In the opposite case where diffusion of substrate is faster than diffusion of electrons, a pure kinetic situation may again arise resulting in the mutual compensation of electron diffusion and catalytic reaction

The fundamental processes involved in the mediating process are identified as charge introduction at the modifying layer/electrode interface, charge introduction at the layer/electrolyte interface and reaction of the target analyte with the modifying layer. Coupled to these reactions one may observe substrate diffusion into the film as dictated by the partition coefficient, K . If the substrate is capable of penetrating the film, then the diffusion rate of substrate, D_Y , within the layer will, in all but a few cases, be considerably less than the solution value D_S .

The theory presented here is that developed by Alberly and co-workers^{81,94-96}. A similar model describing the mediating processes has been developed by Saveant⁸⁹⁻⁹³. The two theories are essentially equivalent, but differ in that Alberly introduced the concept of "reaction layers" to describe two different reaction zones within the polymer film, (a) a region where permeating Y is converted to product Z , and (b) a region of consumption of an electron or B . These reaction layers are usually located close to the film/electrolyte and electrode/film interfaces respectively. In Saveant's work mediation processes are described in terms of characteristic currents. Alternative models have also been developed⁹⁷⁻⁹⁹.

To analyse the mediating processes for electrocatalytic modified electrodes the following equations, given certain boundary conditions, must be solved,

$$D_E \frac{\partial^2 b}{\partial x^2} - kby = 0 \quad (14)$$

$$D_Y \frac{\partial^2 y}{\partial x^2} - kby = 0 \quad (1.5)$$

These equations describe the concentration profiles of both the fixed redox couple (1.4) and the substrate (1.5) within the film. In these equations b and y are the concentrations in the film of B and Y respectively. The boundary conditions used are

- (1) Assuming Marcusian A/B self-exchange behaviour, it is assumed that charge introduction at the electrode/film interface will be more rapid than charge propagation through the film.⁹ Thus heterogeneous charge transfer is not expected to be rate limiting.
- (2) At $x = 0$ the concentration of B is b_0 , and is controlled by the electrode potential.
- (3) The modifying layer acts in a catalytic manner, such that any substrate that permeates the layer and reaches the underlying electrode will not react there, therefore $(dy/dx)_0 = 0$. This boundary condition is in agreement with the perception of a modified electrode where the substrate is not reacting directly at the underlying electrode, but where the electrochemical process is controlled by the modifying layer. It should be noted here that in Saveants' approach the possibility of reaction at the underlying electrode is included.⁸⁸⁻⁹³
- (4) The partition of the substrate Y, between the solution and the modifying layer is given by,

$$Y_L = K y_s \quad (1.6)$$

where Y_L is the concentration of Y in the polymer film, K is the partition coefficient and y_s is the concentration of Y in solution.

(5) The electron flux at the layer/solution interface is related to the kinetics by equation 1 7,

$$-D_E(\delta b / \delta x)_L = k'' b_L y_s \quad (1\ 7)$$

where b_L is the concentration of B at the interface ($X = L$) and k'' is the rate constant for the cross-exchange reaction. Using these boundary conditions and equations 1 2 and 1 3, the electron flux at the electrode, j_0 , which is proportional to the current, i , has to be obtained

$$j_0 = i / FA = -D_E(\delta b / \delta x)_0 \quad (1\ 8)$$

At this stage an electrochemical rate constant, k'_{ME} , can be introduced⁸¹, which relates the concentration of Y at the layer/solution interface to the electron flux, as in equation 1 9

$$j_0 = k'_{ME} y_s \quad (1\ 9)$$

The rate constant, k'_{ME} can be evaluated from the intercepts of Koutecky-Levich plots using rotating disc electrode voltammetry⁸¹. The observed current at the rotating modified electrode, i_F , is thus related to the sum of the fluxes of direct (j_Y) and mediated (j_B) charge transfer and the concentration gradients at the electrode/film interface by

$$(i_F / nFA) = j_0 = j_B + j_Y = -D_E(\delta b / \delta x)_0 = D_Y(\delta y / \delta x)_0 = k'_{ME} y_s \quad (1\ 10)$$

As discussed earlier an essential concept to be included is that of the “reaction layer”. The first reaction layer X_L , defines the distance which Y

can travel within the film prior to reaction with the reduced form of the mediator catalyst. This distance is given by equation 1.11

$$X_L = (D_Y / kb_L)^{1/2} \quad (1.11)$$

The second reaction layer, X_0 , defines the average distance an electron can diffuse before reacting with Y

$$X_0 = (D_E / ky_0)^{1/2} \quad (1.12)$$

With the concept of the electrochemical rate constant and of the reaction layer introduced, one can now refer to equations 1.4 and 1.5. Depending on the relative importance of electron and substrate diffusion, different approximations for k'_{ME} can be obtained. If $D_E b_0 \gg D_Y k y_s$, i.e. fast electron transport or slow permeation or ineffective partitioning of the substrate, then

$$\frac{1}{k'_{ME}} = \frac{y_s L}{D_E b_0} + \frac{1}{k'' b_0 + kb_0 K X_L \tanh(L/X_L)} \quad (1.13)$$

The first term on the right hand side refers to electron transport within the polymer film while the second term represents the competition of the kinetics of the surface reaction (k'') and the layer reaction (k)

If permeation by the substrate is very fast and/or electron transport is relatively slower, then $D_E b_0 \ll D_Y K y_s$, so

$$\frac{1}{k'_{ME}} = \frac{L}{k D_Y} + \frac{k'' \tanh(L/X_0) + k K X_0}{k K X_0 b_0 [k'' + k K X_0 \tanh(L/X_0)]} \quad (1.14)$$

The first term on the right hand side of this equation describes the transport of Y across the polymer layer while the second term again describes kinetic competition of the surface and layer reactions

From these two equations it can be deduced that the slower contribution to the mediated reaction, which can be either kinetic or diffusional in nature, will determine the magnitude of k'_{ME} . For the limiting case represented in equation 1.13, the reaction flux may be limited by the kinetics of the mediated reactions (right hand term) or alternatively, by electron transport through the film to a value $D_E b_0/L$. The position of the reaction layer is reflected in the equation obtained for k'_{ME} in these limiting cases and will depend on the ratio between the reaction layer thickness X_L , and the layer thickness L . For cases where $X_L \gg L$ the whole layer participates in the mediated reaction, this is called the layer case (L). In the reverse situation the reaction occurs in a thin-layer at the layer/electrolyte interface, the surface (S) case

The position of the reaction layer in the second limiting case as described by equation 1.14 can be obtained by a similar approach. If the layer thickness $L \gg X_0$, then the kinetic term reduces to kKX_0b_0 and the reaction takes place at a layer adjacent to the electrode/layer interface. This is the layer/electrode case (LE). In the reverse situation, when $L \ll X_0$, the reaction takes place at the layer/electrolyte interface, i.e. the layer/surface case (LS). For intermediate values of L and X_0 the reaction takes place throughout the whole film

Another situation may arise in which equations 1.9 and 1.10 are invalid. This occurs when the rate of electron transport and substrate diffusion within the film are of the same magnitude and can be described by the equation

$$\frac{D_E b_0}{K D_Y \gamma_s} \approx \frac{X_0^2}{X_L^2} \approx 1 \quad (1.15)$$

Under such conditions, and if X_0 or X_L is less than L , then the reaction will take place in a region of the film located somewhere between the electrode/layer and layer/electrolyte interfaces. This is called the

layer/reaction zone (LRZ) case For this situation the solution for k'_{ME} is given by

$$\frac{1}{k'_{ME}} = \frac{L}{D_Y K + D_E b_0 / y_s} \quad (1.16)$$

From the above equations it can be seen that the LE, LS and S cases can be controlled by either the transport or by the kinetic term So, depending on the relative importance of these two terms, these cases can be segregated into two sub-classes These sub-classes are either controlled by transport processes, in which cases they are given the label t_e or t_y , depending on whether electron or substrate transport is rate limiting, or by kinetic factors in which case the label is k or k'' Using this notation, LE_k denotes a mediated reaction that takes place at a layer close to the underlying electrode surface and is controlled kinetically, whereas in the LE_{t_y} case the reaction takes place in the same part of the layer but is controlled by substrate diffusion These labels, together with their corresponding rate constants for the various limiting cases, are listed in Table 1.1, A diagram depicting the various reaction zones at redox polymer modified electrodes can be seen in Fig 1.3

The equations given above have been used to construct a kinetic zone diagram An example of such a diagram is given in Fig 1.4 “surface” and “electrode” cases give a third dimension to the diagram, but those cases are not of interest in the search for three dimensional sensor devices and therefore only the layer cases are included These diagrams are useful in predicting the effect of changing experimental variables such as b_0 , L , y_s , D_E , D_Y and k Some of these parameters such as b_0 , y_s and L are easily changed while others like D_E , D_Y and k are not considered so readily variable

The conditions for optimum efficiency of catalytic modified electrodes, that is a high value for the ratio between the electrochemical rate constant for the modified and bare electrodes k'_{ME} / k'_E , have been considered by Alberly *et al* ⁹⁵ In these studies, factors such as layer thickness, L , and limits for the kinetic parameters discussed above have been addressed Where the electrode response has been optimised with

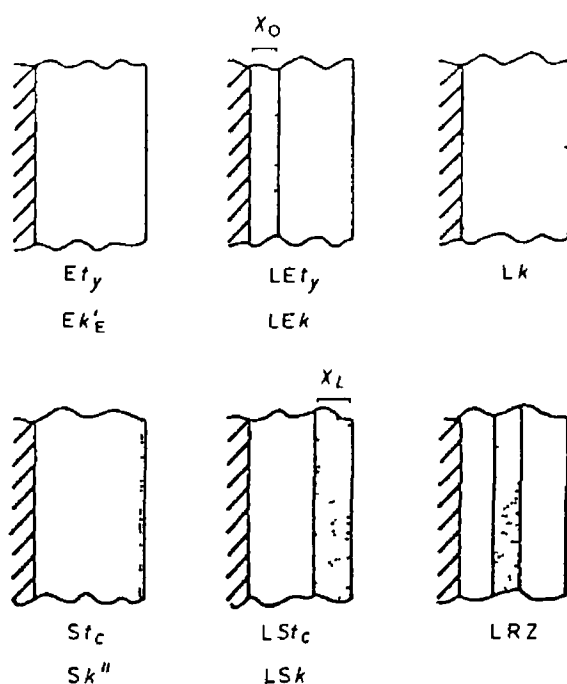


Fig 1 3 The location of the possible reaction zones at redox polymer modified electrodes along with the notation used to distinguish them (Reproduced from P N Bartlett, "*Biosensors, Fundamentals and Applications*", A P F Turner, I Karub, G S Wilson, (Eds), Oxford, University Press, NY, 1987, Ch 13, p 211

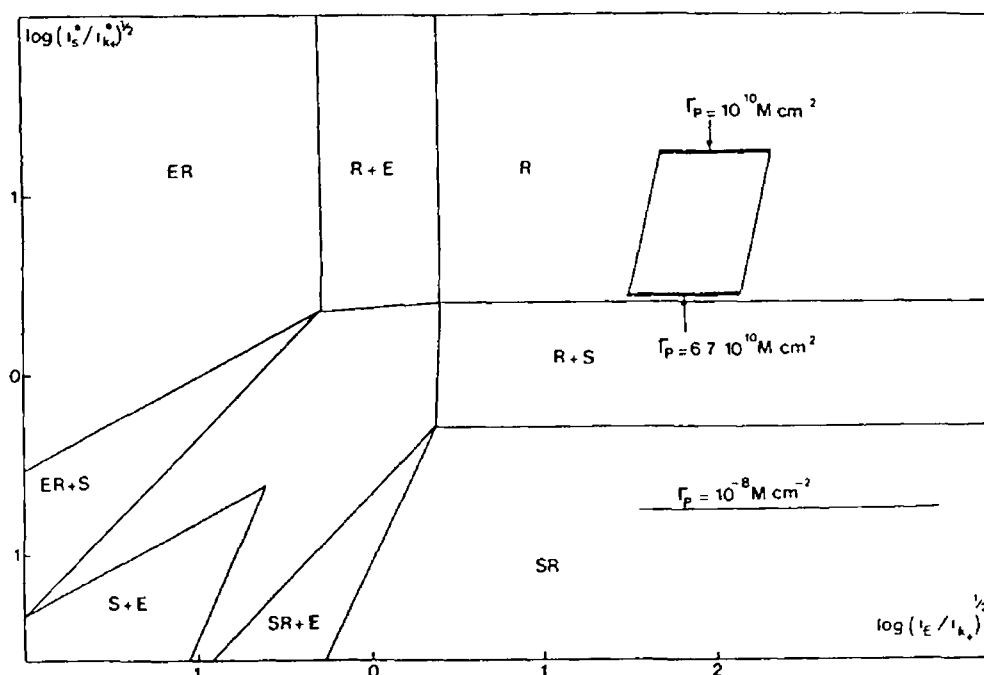


Fig 1 4 Kinetic zone diagram showing the kinetic control of the processes taking place in the polymer film as a function of surface coverage, Γ (Reproduced from C P Andrieux, O Haas, J M Saveant, *J Am Chem Soc*, 1986 108 8175)

Case	A	k_{Me}	Location
Sk	-	$k b_0$	Surface reaction at electrolyte layer interface
St _e	E	$D_e b_0 / L v_s$	
LSk	SR	$k (k b_0 D_v)^{1/2}$	Reaction layer close to electrolyte layer interface
LSt _e	E	$D_e b_0 / L y_s$	
Lk	R	$K k L b_0$	Throughout the layer
LRZ _{1e1y}	S + E	$\frac{D_e b_0}{L v_s} + \frac{K D_v}{L}$	Narrow reaction zone in layer
LEk	ER	$k b_0 (D_e k / y_s)^{1/2}$	Reaction layer close to electrode
LEt _v	S	$K D_v / L$	
Ek _F	-	k_F	Direct reaction on electrode
Et _v	S	$K D_v / L$	

Table 1 1 The ten different kinetic cases possible at redox polymer modified electrodes along with their corresponding rate constants Column (A) refers to Saveants notation (Reproduced from W J Albery, A R Hillman, *J Electroanal Chem*, 1984 170 27)

respect to electron transport and morphology it is usually found that electron diffusion is faster than substrate diffusion and that the concentration of the surface bound redox mediator is larger than that of the substrate

Because of the limitations discussed above, the number of limiting cases to be considered for optimisation of the modified electrode response is limited, with the layer cases showing the most promise. The optimum efficiency cases are LS_k and LE_k . LS_k corresponds to rapid electron transport compared to substrate diffusion through the film, the reaction occurring in a region of polymer close to the layer/electrolyte interface, with the exact position depending on the mediated rate constant, k . For the LE_k the mediated reaction occurs at a region close to the electrode/layer interface. For the layer cases, the magnitude of k'_{ME} will increase with increasing layer thickness (all sites are electro-active and mediate electron transfer under kinetic control), then pass through a maximum before decreasing to transport limitations of the substrate. The ideal case corresponds to a sufficient amount of mediator sites for substrate consumption combined with efficient substrate or charge diffusion. Such a scenario would result in the ideal three dimensional modified electrode, i.e. the LS_k and LE_k situations. For the LS_k case, the catalytic advantage becomes

$$k'_{ME} / k'_E = KX_L / l \quad (1.17)$$

This can be large as the reaction layer thickness can be much greater than l , the distance over which electron transfer can take place. It can be clearly seen that, for reactions which exhibit slow homogeneous kinetics, a layer reaction is required where Y permeates the film rapidly. This requires an open porous structure for the film to allow efficient permeation of B. However, charge transport must also be fast to prevent limitations imposed by charge transfer.

For the two optimum surface and electrode cases, Sk'' and Ek'_E , mediation does not occur throughout the layer, with the reactions taking place at the layer/solution and layer/electrode interfaces, respectively.

These reactions can not be described as three dimensional but this does not necessarily result in limited application in analysis. In the S_k case, a practical application can be envisaged if B is a specific catalyst for the oxidation or reduction of substrate Y, or, if the rate of the cross-exchange reaction and charge transport are sufficiently fast to ensure total consumption of the substrate flux at the layer/solution interface. The electrode case will become applicable when favourable partitioning can be obtained, or by the selective exclusion of interferences. In this case, even as the reaction is taking place at the underlying electrode surface, a catalytic effect can be obtained due to the a high value of the partition coefficient, K. This approach has been used for the development of sensors based on preconcentration and exclusion membranes. Such devices will be described in more detail in a later section.

The experimental determination of parameters involved in the theoretical approach described above relies on the recognition of the appropriate limiting processes. It is the use of rotating disc and rotating ring disc electrodes which provides the means of analysing the kinetics and catalysis at the modified electrode surface. These techniques allow control of the substrate diffusion in solution and thus allow the elucidation of the kinetics and mechanism of the mediated electrode reaction. By controlling the electrode potential, the concentration of the surface species can be reduced to zero and the current response becomes limited by mass transport and is given by the Levich equation ¹⁰⁰

$$i_{Lev} = 1.554 nAF D^{2/3} \nu^{-1/6} \omega^{1/2} \quad (1.18)$$

Where A is the electrode area, D is the diffusion coefficient of the substrate in solution, ν is the kinematic viscosity of the electrolyte and ω is the electrode rotation speed. Rotating disc measurements are ideal for the investigation of mediated electrocatalysis at electrode surfaces as the rate of mass transport can be controlled. This has led to the widespread application of the technique ¹⁰¹⁻¹⁰⁴. It is often found that a rate limiting step other than substrate mass transport control currents is observed at polymer modified electrodes, as a result the Levich equation may not

represent the currents observed. In such cases the limiting current is given by the Koutecky-Levich equation which has the general form ¹⁰⁵,

$$1/i_{Lim} = 1/i_F + 1/i_{Lev} \quad (1.19)$$

or for a redox polymer ⁸¹,

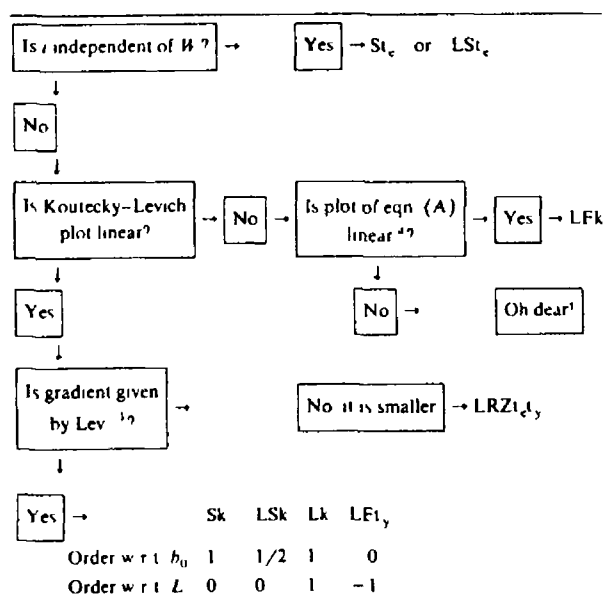
$$1/i_{Lim} = (nFAk'_{ME}y)^{-1} + (1.554nFAD^{2/3}\nu^{-1/6}y\omega^{1/2})^{-1} \quad (1.20)$$

A plot of i_{Lim}^{-1} vs $\omega^{-1/2}$ yields a straight line, with a slope equal to the reciprocal of the Levich slope, and the intercept yielding the value k'_{ME} . Albery and Hillman have published a useful flow chart for the diagnosis of the reaction type based on this mode of analysis ¹⁰⁶, this is shown in Fig 1.5. In this scheme, the functional dependence of k'_{ME} on b_0 , y_s , ω and L allows classification of the current limiting process.

1.4. Analytical Voltammetry and Amperometry

1.4.1 Introduction

Voltammetry involves the measurement of the current flow between a working electrode and an auxiliary electrode as a function of potential applied with respect to a reference electrode in a three electrode cell. A trace of current vs potential is known as a voltammogram and is utilised for the investigation of the analyte species. Many voltammetric techniques have been developed such as linear sweep, square wave, cyclic, potential step and rotating disc voltammetry for the investigation of both organic and inorganic species. Such techniques can also be applied to the fundamental study of polymer modified electrodes. Amperometric measurements are made by recording the current flow at a working electrode as a function of time using a fixed applied potential in a three



* Eqn (A)

$$\left(\frac{nFAi_{\infty}}{i_L} \right)^2 = \frac{nFAi_{\infty}}{i_L} \frac{(Lev^{-1})}{W^{1/2}} + \left(\frac{1}{k_{MT}} \right)^2$$

where $k_{MT} = Kb_0(D_r k / i_{\infty})^{1/2}$ and the remaining symbols are as in eqn (1)

Fig 1 5 Diagnostic chart for the mechanisms at modified electrodes (Reproduced from W J Albery, M G Boutelle, A R Hillman, *J Electroanal Chem*, 1985 182 99

electrode assembly. By their measurement domain, voltammetric techniques are much more informative than amperometric techniques. However, for the development of electrochemical sensors, amperometry is favoured due to the simple electronic circuitry required for measurement and ease of measurement. In addition, operation at a fixed potential reduces charging currents significantly.

Both these techniques are however essential in the development and operation of electrochemical sensors, and will be discussed in the following sections. In addition a brief account of electrode processes will be given.

1.4.2 Electrochemical Processes

Electrochemical reactions which involve the transfer of charge at the electrode/electrolyte interface are classed as heterogeneous processes.⁶⁹ The overall rate of the electrochemical reaction and therefore the magnitude of the resulting current response is dependent on a number of physical and/or chemical processes operating at the interfacial region. For the simple redox reaction,



conversion of the oxidised form to the reduced form of the species involves the following processes.¹⁰⁷

- (1) Transport of Ox from the bulk of solution to the electrode surface
- (2) Electron transfer between the electrode and the species to form Red
- (3) Transport of Red away from the electrode to the bulk of solution

During electrolysis, three modes of mass transfer are generally important, these are¹⁰⁷

- (1) Migration, the movement of a charged species under the influence of an applied DC electric field
- (2) Diffusion, the movement of particles under the influence of a concentration gradient
- (3) Convection, resulting from thermal or density gradients, deliberate stirring or hydrodynamic transport

The Nernst-Planck equation gives a full mathematical description of the effect of these three modes of transport^{69,108} For transport in the x direction only, this equation yields

$$J(x,t) = -D_0 \frac{\delta C_0(x,t)}{\delta x} - \frac{zF}{RT} D_0 C_0(x,t) \frac{\delta \phi(x,t)}{\delta x} + v(x,t) C_0(x,t) \quad (1.22)$$

where $J(x,t)$ is the mass flux, D_0 is the diffusion coefficient of the species O, ϕ is the electrostatic potential, $v(x,t)$ is the hydrodynamic velocity of the solution, z is the charge of the species O and C_0 is the concentration of the species O

The current at the electrode may be limited either by mass transport of the reactant to the electrode surface or by the rate of the electron exchange reaction. The mass transport component can be controlled precisely with techniques such as rotating disc electrode voltammetry^{100,105} but the rate of electron exchange is more difficult to control as this component is a function of the substrate, electrode material, electrolyte and applied potential. In addition, the overall electrode reaction mechanism can involve a homogeneous chemical reaction, either prior to, or immediately after the charge transfer step¹⁰⁹ Furthermore, other heterogeneous processes such as adsorption or desorption of reactants or products may be coupled to the electrode reaction. The overall rate of the electrochemical reaction will therefore be determined by the slowest process involved in the mechanism. This is the rate determining or current

limiting step For electroanalysis it is generally desirable to operate under mass transport controlling conditions

The extraction of analytical information from an experiment depends on the degree of control that can be exerted on experimental parameters such as mass transport, electrode potential, electrolyte and the understanding the electrode reaction ¹⁰⁷ Migration currents can be minimised with the use of electro-inactive electrolytes, and convective currents can be eliminated by avoiding thermal or density gradients within the electrolyte For useful analytical information, the electrode current should be controlled by diffusion of the species of interest from the bulk This gives rise to a faradaic current and a direct relationship between current response and analyte concentration can be established Currents due to non-faradaic processes such as double-layer charging and adsorption, and from impurities, need to be characterised fully The double-layer charging current results from the change in structure of the interfacial region of the electrode with applied potential The electrode surface when in contact with an electrolyte is believed to behave as a capacitor, with the interfacial region comprising of ordered charge particles, the electrical double-layer ⁶⁹ A widely accepted model of this double layer is given in Fig 1 6 ⁷² Most modern electroanalytical techniques are designed to maximise faradaic current and minimise the capacitance current With the use of amperometry, the structure of the double-layer is constant as the potential is held constant, and this allows the charging current to decay to zero ¹¹⁰

The electrochemical behaviour of electro-active species, and consequently the current-voltage response, is a direct result of the mechanism of the electrode reaction Whether a reaction is reversible in an electrochemical sense may depend on the time scale of the experiment ¹¹¹ An electrochemical reaction is considered reversible when the electron transfer reaction (reaction 1 21) is facile in both directions and when the reactants and products are stable over the time scale of the experiment If the rate of electron transfer is slow (*i.e.* when the heterogeneous forward and backward rate constants, k_f and k_b are small), the reaction is said to be quasi-reversible A different situation arises when the product Red is not stable and undergoes a subsequent homogeneous reaction Thus Red

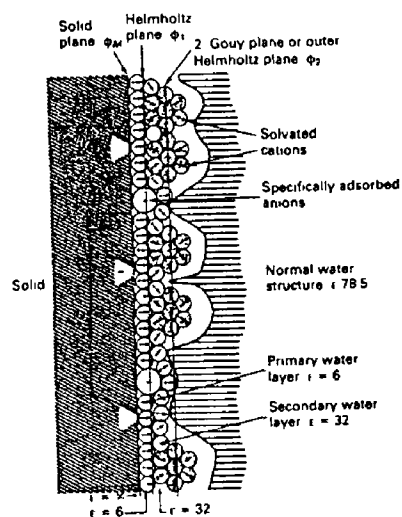


Fig 1 6 Structure of the electrical double-layer at the electrode surface (Reproduced from H B Mark, *Analyst*, 1990 115 667)

may not exist long enough to be re-oxidised and the reaction is therefore irreversible

1 4 3 Voltammetric and Amperometric Techniques

1 4 3 1 Cyclic Voltammetry

Cyclic voltammetry (CV) involves monitoring current as a function of applied potential when a regularly varying potential is applied to the working electrode in quiescent solution ^{112,113} This technique has become popular for mechanistic studies of redox processes and the study of modified electrodes ⁹⁷ The potential wave form applied can be seen in Fig 1 7 In general, the potential sweep is started at a potential where no reaction occurs (E_i), and proceeds to a potential where the species of interest is electro-active, and then to a final or switching potential (E_λ), from where the scan direction is reversed The values of E_i , E_λ , and potential sweep rate, v , can be varied depending on the application envisaged Single or multiple potential cycles can be used

A typical CV for the oxidation-reduction of a solution species can also be seen in Fig 1 7 The important features of a CV include the anodic (E_{pa}) and cathodic (E_{pc}) peak potentials, and anodic (i_{pa}) and cathodic (i_{pc}) peak currents The processes which occur during a typical cyclic voltammetric experiment can be described as follows, when the potential is scanned from an electro-inactive region to a potential where the substrate becomes electro-active the potential results in the reduction of Ox to produce Red according to the Nernst equation

$$E = E^0 + RT / nF \ln ([Ox]/[Red])_{x=0} \quad (1\ 23)$$

As the surface concentration of Ox decreases, Ox begins to diffuse from solution If the potential is swept further the surface concentration of Ox falls and the current decays according to the Cottrell relationship ¹⁰⁸

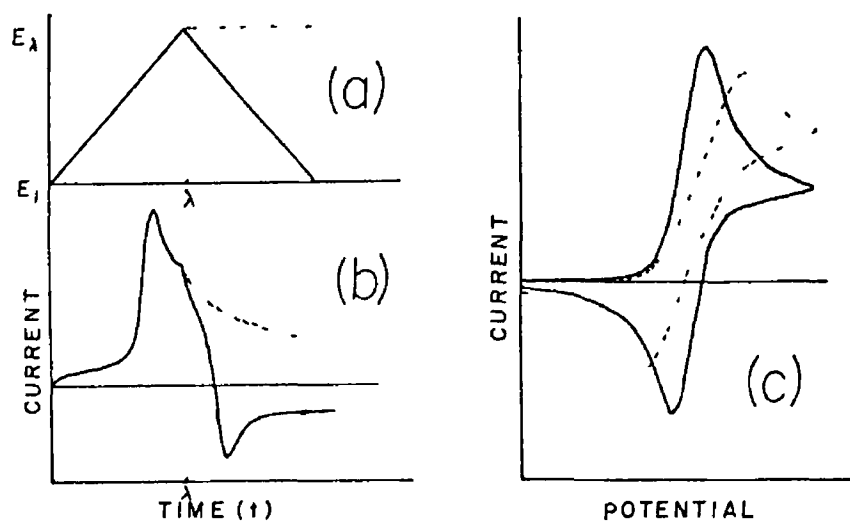


Fig 1 7 Cyclic voltammetry (a) potential profile, (b) current-time profile for a reversible system and (c) current-potential profile for a reversible system (full curve) and a kinetically hindered process (broken curve)

$$i(t) = \frac{nFA D_0^{1/2} C_0^*}{(\pi t)^{1/2}} \quad (1.24)$$

(where t = time) to give a steady-state diffusionally controlled current. This gives rise to the characteristic peak in the current-voltage curve. Before the peak, the current is kinetically controlled and is therefore a function of the electrode potential. The rate of the forward (k_f) reduction reaction can be described by the Butler-Volmer equation,

$$k_f = k^0 \exp[-\alpha n (F / RT) (E - E^0)] \quad (1.25)$$

where k^0 is the standard heterogeneous electron transfer rate constant, α is the symmetry factor describing the symmetry of the energy barrier to reaction and E^0 is the formal potential of the reduction reaction. Similarly the reverse process can be described by

$$k_b = k^0 \exp[(1-\alpha)n (F / RT)(E - E^0)] \quad (1.26)$$

The peak current for a reversible electrode process under a semi-infinite diffusion regime is given by the Randles-Sevcik equation

$$i_p = [0.4463 (nF)^{3/2} A D^{1/2} \nu^{1/2} C_0^*] / (RT)^{1/2} \quad (1.27)$$

While after the peak, the current is diffusionally controlled as predicted by the Cottrell equation

The peak-to-peak separation between the anodic and cathodic processes is equal to $0.0591/n$ V for a reversible electrode reaction. The

separation of peak potentials is independent of sweep rate but is slightly dependent on switching potential and cycle number. Quasi-reversible systems possess peak-to-peak separations greater than $0.0591 / n$ V due to the non-equilibrium conditions encountered at the electrode surface causing deviation from the Nernstian behaviour.

Cyclic voltammetry has been extensively used to characterise the electro-activity of polymer modified electrodes and for the mechanistic elucidation and the evaluation of charge transport rates.¹¹⁴⁻¹¹⁶ This technique gives a wide variety of information over a wide potential range without need for specialised experimental conditions. Much of the CV studies have focussed on qualitative information as well as quantitative data.

Quantitative data regarding charge transport have been largely been obtained from examining the modifying layer at high potential sweep rates, where semi-infinite diffusion conditions prevail. The equation describing the characteristic current for the oxidation or reduction of the immobilised redox species under these conditions is given by a modified Randles-Sevcik equation

$$i_p = [0.4463 (nF)^{3/2} A D_{ct}^{1/2} c v^{1/2}] / [(RT)^{1/2}] \quad (1.28)$$

Where D_{ct} is the charge transport diffusion coefficient and c is the concentration of electro-active sites within the film. In addition, the following conditions prevail¹¹⁷

$$E_p = E_{pa} - E_{pc} = 0.0591/n \text{ V} \quad (1.29)$$

$$i_{pa} / i_{pc} = 1 \quad (1.30)$$

When there is no diffusional limitations such as at low potential sweep rates (surface or thin-layer conditions) , the peak current varies linearly with ν . At higher sweep rates a change over to semi-infinite diffusional control occurs and a $\nu^{1/2}$ dependence is observed. Thus the variation of peak current with sweep rate is a simple diagnostic tool for the charge diffusion behaviour of modified electrodes. Under the finite diffusion conditions the following criteria must be satisfied,

$$i_p = [n^2 F^2 \Gamma_T \nu] / [4 RT] \quad (1.31)$$

$$E_{pa} = E_{pc} \quad (1.32)$$

$$FWHM = 0.0906 n V \quad (1.33)$$

where Γ_T is the total amount of electro-active material on the electrode surface and FWHM is the full width at half height of the CV peak. The quantity Γ_T can be determined using slow sweep rate CV using the relation $\Gamma_T = Q / nFA$, where Q is the total charge passed upon oxidation or reduction of the polymer film.

It is often encountered that the diffusion layer extends to the polymer/electrolyte interface over the timescale of the experiment. This situation, for a finite diffusion space for linear sweep voltammetry, has been examined by Aoki and co-workers¹¹⁶ for reactions with reversible kinetics with the following assumptions

(1) Mass transfer of both species is governed by Fick's second law,

$$\delta C_0^*(x,t) / \delta t = D \delta^2 C_0^*(x,t) / \delta x^2 \quad (1.34)$$

- (2) The solutions initially contains Red of concentration C_0^*
- (3) The diffusion coefficients of the oxidised and reduced forms of the redox couple have a common diffusion coefficient D
- (4) Electro-active species cannot pass through the film/electrolyte interface
- (5) The electrode reaction is sufficiently rapid to ensure Nernstian response

The boundary conditions at the electrode are given by

$$C_0(0,t) / C_r(0,t) = \exp[nF (E_1 + vt - E^0) / RT] \quad (1.35)$$

$$i/nF = D(\delta C_r/\delta x)_{x=0} = -D(\delta C_0/\delta x)_{x=0} \quad (1.36)$$

where C_r and C_0 represents the concentrations of Ox and Red, respectively at time, t . The theta function has been used to evaluate the i - E curve, which is described by

$$i = nFC_0^* [D v (nF/RT)^{1/2} f(w,\xi)] \quad (1.37)$$

where $f(w,\xi) = W^{1/2} \int_0^\infty \theta_2(0/z) e^{Wz-\xi} / (1+e^{Wz-\xi})^2 dz$, and with $W =$

$(nF/RT) v d^2/D$, the square root of which denotes the ratio of the diffusion thickness space, d , to the diffusion-layer thickness. The approximate solution to the finite diffusion space equation is given by Simpson's rule as

$$i_p/nF = (446(C_0^* D/d) W^{1/2} \tanh(0.56W^{1/2} + 0.05W) \quad (1.38)$$

This theory allows the evaluation of the charge transfer diffusion coefficient over large potential sweep ranges simply from a knowledge of surface coverage and the peak current. For solution type behaviour (i.e. when W is large), this equation reduces to the semi-infinite diffusion equation of Randles-Sevcik, while if W is less than 1 the Langmuir surface equation (equation 1.31) is obtained. Aoki has also considered the cases of quasi-reversibility and totally irreversible redox processes using the concept of finite diffusion space.¹¹⁸

1.4.3.2 Chronoamperometry

Chronoamperometry has been used to evaluate D_{ct} values. This technique involves the application of a potential step across the redox couple to a potential where the Red (or Ox) form is stable and monitoring the current response as a function of time. This is depicted in Fig. 1.8. Using the Cottrell equation, (equation 1.24), an estimate for D_{ct} can be obtained.¹⁰⁹ This technique is considered to reflect electron hopping and the additional possible rate determining steps such as counter ion movement and polymer segment motion. Most workers using this technique neglect the finite diffusion equation and manipulate the time scale of the experiment to ensure semi-infinite diffusional behaviour. It is believed that this technique probes a small portion of the film close to the electrode/film interface while the CV techniques are more representative of the bulk structure of the film. This is a reflection of the time scale involved in both experiments. Chronoamperometry measurements are carried out over a millisecond time scale, while CV measurements extend over a much longer time scale, of the order of seconds.

1.4.3.3 Hydrodynamic Amperometry

As stated earlier, amperometry is the measurement of electrode current with respect to time at a fixed applied potential. The amount of

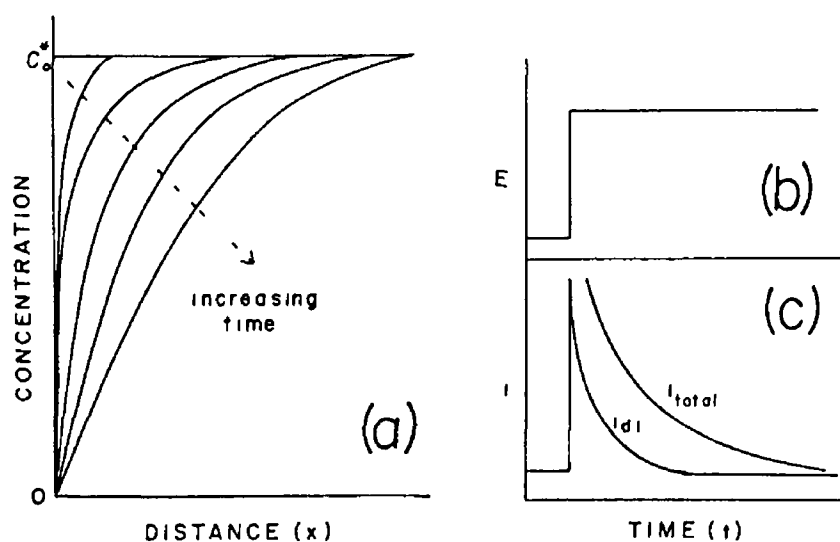


Fig 1.8 (a) Concentration of reactant plotted against distance from electrode surface due to the application of (b) a potential step in a solution of oxidised species (c) The relative currents due to the double layer charging (i_{dl}) and total current (i_{total})

mechanistic data which can be extracted using such a technique is limited. However, the technique is highly valuable in electroanalysis as it allows continuous monitoring during techniques such as flow injection analysis (FIA), HPLC, and coulometric and amperometric titrations. Under hydrodynamic conditions, the current is generally controlled by mass transfer to the electrode surface. Hydrodynamic conditions are produced by electrode rotation, solution stirring or by solution flow in FIA and HPLC.

1.4.3.3.1 *Mass Transfer Processes Under Hydrodynamic Conditions*

The most commonly used theory concerning the kinetics of heterogeneous reactions in stirred solutions is that of Nernst.¹¹⁹ According to this theory, there is a thin-layer of static liquid immediately adjacent to the surface of the electrode through which diffusion of the reacting species must occur. This layer is the diffusion layer of thickness, δ . Within the diffusion layer the solution is believed to be static and the concentration distribution linear. However, experimental observations suggest that the concentration gradient is non-linear and that the solution is non-static in the vicinity of the electrode surface.

The exact treatment of mass transport involving convection and diffusion has been given by Levich.¹⁰⁰ Here it is assumed that mass transport is a function of two processes: diffusion under the influence of a concentration gradient and transport of entrained particles in the moving liquid. The combination of these processes is known as convective diffusion. In the vicinity of the electrode surface both these processes can play a role. The overall concentration distribution relating to a heterogeneous reaction is given as follows,

$$dC_1 = (D_1 \nabla C_1) - V \nabla C_1 + z_1 F \nabla(u_1 C_1 \Phi) + R_1 \quad (1.39)$$

where D_1 is the diffusion coefficient of species 1, C_1 is the concentration of 1, V is the flow velocity vector, z_1 is the charge on 1, u_1 is the ionic mobility, Φ is the electric field strength and R_1 is the rate of the

homogeneous chemical reaction. The first term on the right hand side of this equation relates to the concentration gradient of species 1, the second to the macroscopic fluid flow velocity and the concentration of 1, with the third term relating to the migration and the fourth to the homogeneous chemical reaction. This equation can only be solved in a few cases, usually for systems with very simple electrode geometries. Levich has however solved this equation for a number of electrode geometries including the rotating disc electrode, flat surfaced electrodes, tubular and conical micro-electrodes.¹⁰⁰ The current for the rotating disc electrode is given by the Levich equation (equation 1.18). The diffusion layer thickness, δ , is inversely proportional to the rotation speed (or solvent velocity) of the electrode.

Electroanalysis in flowing streams is one of the fastest growing areas in analytical electrochemistry.¹⁰⁷ The detector design can incorporate a planar electrode in a thin-layer configuration, a tubular, a packed-bed or wall jet electrodes as the working electrode.¹²⁰ These designs can be seen in Fig. 1.9. Electrochemical detectors are classified according to their electrolytic efficiency. Amperometric detectors generally have a low electrolytic efficiencies with generally less than 10% conversion of the analyte. Alternatively, coulombic detectors have close to 100% conversion efficiencies. On this basis, it would appear that coulombic detectors are potentially more sensitive than amperometric sensors. However, due to the large surface area required for the former, larger background currents are observed which limit the LOD that can be obtained. For these electrodes, operating under hydrodynamic conditions, the current response equation can be obtained from equation 1.39. For the thin-layer planar electrode configuration with rectangular electrodes, two equations are available to describe the steady-state current depending on whether laminar flow (1.40) is achieved or not (1.41).^{100,121}

$$i = 1.47 nFC_0^* (AD_0/p)^{2/3} U^{1/3} \quad (1.40)$$

$$i = 0.68 nFC_0^* D_0^{2/3} v^{-1/6} (A/p)^{1/2} U^{1/2} \quad (1.41)$$

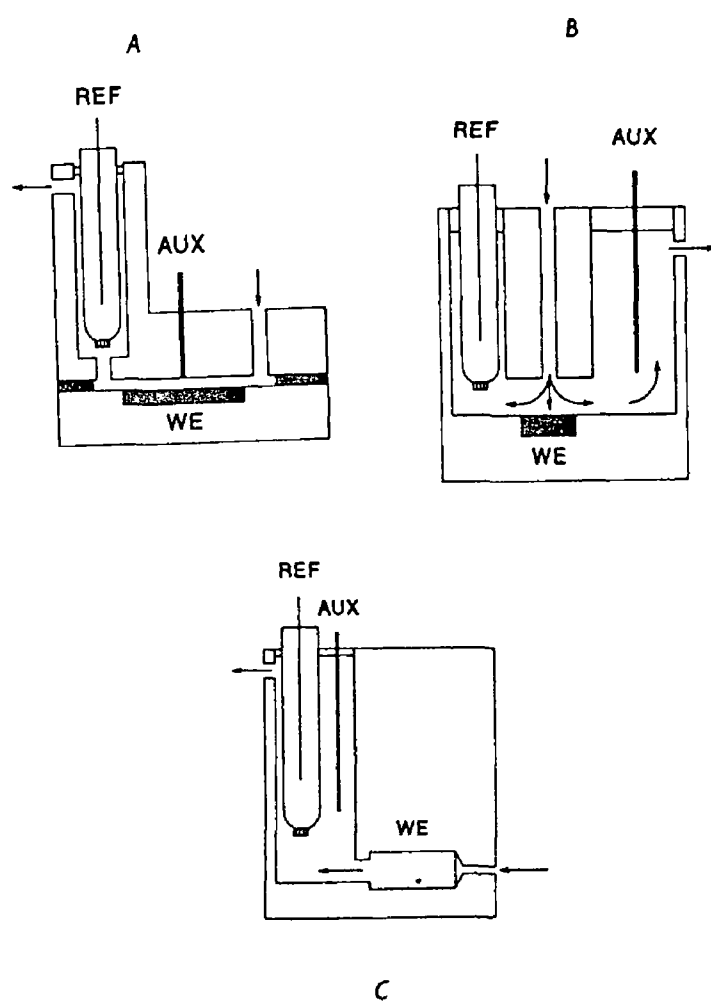


Fig 1 9 Schematic representations of (A) thin-layer, (B) wall-jet and (C) packed-bed flow through electrochemical cells Ref = reference electrode, Aux = auxiliary electrode and WE = working electrode

where U is the volume flow rate, p is the distance from the nozzle to the electrode. It is worth noting here that steady-state is rarely achieved in flow analysis due to the transient nature of the signal. Equation 1.40 has been recently modified to account for steady-state responses at circular electrodes in thin-layer flow cells.¹²²

$$i = 1.234 n F W_L^{5/3} (D/b)^{2/3} (U/W_c)^{1/3} C_0^* \quad (1.42)$$

where W_c is the channel width perpendicular to the fluid flow and W_L the length of the electrode. This equation is valid in situations where the diameter of the circular electrode does not exceed the channel width and where the sample injection volume is much greater than the dead volume between the injector and detector. Recently, a detailed account of thin-layer behaviour taking into account the van Deemter equation in HPLC has been given.¹²³ It is reported that at optimum flow rate small changes in flow rate do not affect the response significantly.

1.5. Analytical Applications of Modified Electrodes

1.5.1 Introduction

Modified electrodes have been widely applied for electroanalysis as these devices display attributes which conventional electrodes do not possess. The attributes which are desirable for sensors constructed from modified electrodes are: a reproducible response which is easily defined and well understood, the response should be linear (but not necessarily) over a large concentration range. The sensor should be sensitive, selective with low background response, fast response time, have a low limit of detection and allow a high analytical throughput. Sensors should be easily prepared (compatible with lithographic technology) and be both physically and chemically stable. In order to achieve some, if not all of these

objectives, considerable creative chemistry will be required to design the electrode/electrolyte interface ¹²⁴

Recently, “ground rules” concerning the design of modified electrodes for electroanalysis have been proposed ¹²⁵ The approach to modified electrode design should be dictated almost exclusively by the analytical requirements The properties of the target analyte, the possible interferences and their expected concentration ranges along with the sample matrix must be considered It is only when these parameters are carefully considered that a judicious approach to sensor design can be achieved

Electrode modification for electroanalysis revolves around the three central themes of preconcentration, perm-selectivity and electrocatalysis ^{8,125} By exploiting any one or combination of these themes, the construction of selective, sensitive operational sensors is possible The design and analytical application of modified electrodes will be discussed along these themes

1 5 2 Preconcentration

The concept of preconcentrating analytes at electrode surfaces is not new The three dimensional nature of the mercury drop poised at an appropriate potential allows for the effective electrolytic scavenging of very dilute solutions to produce high surface concentrations of analyte ¹²⁶ When the potential is swept in the opposite direction a large analytical signal may be obtained Alas, with mercury, only a limited potential region can be exploited and the electrode reaction must be reversible ^{126,127} This severely limits the applicability of the technique With modified electrodes, however, the potential range can be broadened and irreversible reactions can be exploited The principles of ion-exchange, complexometry, and precipitation have been used to preconcentrate analytes at the surface of modified electrodes Chemically reactive sites in polymer films have also been used to effect preconcentration In addition to the sensitivity enhancement which can be obtained, careful design of the modifier can enhance selectivity on the basis of electrostasis, chemical functionality, stereochemistry, selective binding or molecular size In order to obtain maximum benefit from preconcentration, the process should take

place in a three dimensional zone at the electrode surface. For this reason polymeric films have predominated preconcentration at modified electrodes although carbon paste electrodes have also been described for this purpose.

The application of polymers functionalised with coordination sites have been actively investigated by several groups.¹²⁸⁻¹³⁴ The polymer provides the three dimensional network along with physical stability, while judicious choice of ligand controls the selectivity of the sensor. The analyte must be able to permeate the film and coordinate to the polymer bound ligand(s). The formation constant of the complex, k_f , is of fundamental importance as it affects the operational performance of the sensor. Large k_f values favour increased sensitivities and lowered LOD. The use of ligands with large k_f values can be used to effect very selective binding thus discriminating against possible interferents with smaller formation constants. Large k_f values may be also disadvantageous, as the surface concentration of ligand sites is low, typically 10^{-8} mol cm⁻², then saturation of the sites may occur at low analyte concentrations if the complexation reaction is too favourable. As the modifier participates in a dynamic chemical reaction prior to electrolysis, the time for the reaction to reach equilibrium should be as short as possible for practical application. Unfortunately this is seldom the case. In general, equilibrium times can be controlled by careful choice of electrode size, polymer film thickness, polymer permeability and morphology and k_f .

An elegant example of this type of electrode modification has been demonstrated by Abruna *et al.*¹³¹ In this work a poly(4-vinyl pyridine) polymer containing the ligand, 2,2'-bipyridyl, was found to be effective at sequestering Fe(II) from solution. The incorporated Fe(II) was then oxidised by linear sweep voltammetry to give an analytical signal (charge). The problem with response saturation was also addressed. By incorporating an "internal standard" into the polymer film, in this case a ferrocene moiety, which can be determined *in situ* using slow sweep rate CV, the total interfacial quantity of coordination sites can be evaluated, with a knowledge of the coordination number of the metal complex from solution studies, the response (charge) from a saturated film can then be estimated. Sufficient mobility of the polymer bound coordination sites is of paramount importance in order to form stable multi-dentate complexes. It is recognised that ligand mobility within the film may be restricted due to

steric or other factors, as a result multiple coordination to a metal centre may not take place. As the $E_{1/2}$ of the metal centre is a function of its coordination sphere then this may have serious implications for analytical applications. For the Fe(II) coordination, a tris complex was formed (as expected from solution studies) within the polymer, so no restrictions on ligand mobility was evident. In situations where ligand mobility may be problematic, it has been suggested that thin polymer films may alleviate this problem. In another study it was found that only 0.1 to 1.0 % of actual analyte incorporated into a chelating film was subsequently detected electrochemically.¹³⁰ This suggests that mass and/or charge transport restrictions within the polymer film is detrimental to sensor response. For this reason such polymers should exhibit fast charge and mass transport properties in order to exploit the preconcentration effect fully. A major problem associated with these type of electrodes is that they may be used for a single determination only. This may be a result of irreversible binding or very slow release of the electrolytic product. It has however been demonstrated that the use of ligands with formation constants strongly influenced by the oxidation state of the metal centre this can be alleviated.¹³²

It is fortuitous that selectivity trends for metal/ligand interaction exhibited in solution can be extrapolated to the electrode surface. With a wide body of information concerning such interactions in solution, along with the huge number of ligands available, considerable scope exists for the development of novel electrochemical sensors from these materials.

The use of ion-exchange materials for electrode modification was recognised early in the development of CMEs. Some of the first polymer modified electrodes described were based on electrostatic incorporation of charged redox sites into oppositely charged polymer films.⁶⁰ The ability to preconcentrate electro-active material in a film close to the electrode surface using the inherent thermodynamic driving force for the ion-exchange reaction resulted in several applications of this process for electroanalysis.¹³⁵ The most widely studied materials for ion-exchange preconcentration are protonated PVP, quaternised PVP, both of which are polycationic¹³⁶, and Nafion, which is an anionic ionomer.

The fundamental behaviour of ion-exchange processes which can occur at Nafion and other ion-exchange materials have been investigated

extensively ^{137,138} For any ion-exchange material, the extent of preconcentration depends on the ion-exchange selectivity coefficient, K_{ex} . Preconcentration occurs when the selectivity for the analyte is greater than that for the competing counter ion. For Nafion, ion-exchange selectivity coefficients depend on the charge and structure of the exchangeable ion. In general, selectivity coefficients increase with increasing charge and hydrophobicity of the ion. ¹³⁷ The bulk structure of Nafion in aqueous electrolyte is thought to be composed of a hydrophilic domain containing $-\text{SO}_3^-$ groups and a hydrophobic domain comprised of the carbon fluoride polymer framework. It is this structure which results in high selectivity for large hydrophobic cations. For PVP-based ion-exchange modifiers the greater the charge on the competing ion the more effectively it will be scavenged from solution. ¹³⁹ Due to the general nature of ion-exchange processes, and as the extent of preconcentration is determined by the molecular properties of the analyte and any competing co-ion in the sample, considerable matrix effects can be encountered in real analytical situations using these types of materials. Some control over ion-exchange selectivity can be achieved however, by careful control of electrolyte pH, as this affects the ionisation of weak acids and bases and consequently their availability for ion-exchange. Also, the ionic strength of the electrolyte should be kept as low as possible to minimise competition from electrolyte co-ions. However, due to the general nature of ion-exchange processes, ion-exchange preconcentration is inherently less selective than coordination processes.

One of the major disadvantages of ion-exchange preconcentration is the lengthy time intervals required for the ion-exchange process to reach equilibrium. ¹³⁷ The equilibrium time depends on the size, charge, structure and concentration of analyte, the ionic strength of the electrolyte, geometric dimensions of the electrode, and the thickness of the polymer film. ¹³⁵ It is usually found that the rate determining step in reaching equilibrium is the rate of ionic diffusion within the film. ¹³⁷ For this reason polymers must be designed for maximum mass transfer rates. It has also been observed that ion-exchange isotherms are linear only over a small concentration range, therefore these electrodes may be easily saturated and have a limited response range. As the ion-exchange process is thermodynamically driven, the regeneration of the polymer for multiple determinations is difficult. ¹³⁵ The use of high ionic strength electrolytes to remove the analyte is impractical and unacceptable in continuous

monitoring situations. In a very elegant example of the power of synthetic control, it has been demonstrated that by incorporating a ferrocene moiety into the Nafion modifier, oxidation of the ferrocene unit then allows the ferrocenium ion to act as the counter ion, charged analytes acting as counter ions are then expelled from the film to maintain electro-neutrality.¹³⁵

Probably the most popular application of ion-exchange preconcentration is the determination of dopamine.^{140,141} Dopamine, a neuro transmitter, is found at low concentration in the synapse. Dopamine is cationic at physiological pH, and can be selectively incorporated into the anionic Nafion. This preconcentration step along with the exclusion of ascorbic acid, allows the determination to be carried out *in vivo*. In another example, a styrene sulphonate-containing polymer containing ferrocene as an internal standard, was found to preconcentrate protonated aromatic amines. The internal standard was used to normalise responses with respect to surface coverage of polymer.¹⁴²

Analytes can be preconcentrated by reaction with chemically reactive groups at the electrode surface. This approach may result in considerable selectivity enhancement due to the specific nature of the chemical reaction. It is also possible that stereospecific reactions may be used to distinguish between optical isomers. Price and Baldwin modified a platinum electrode with unsaturated primary amine by adsorption.¹⁴³ The surface immobilised amine was capable of a condensation reaction with carbonyl-containing analytes. The selectivity power of this electrode was demonstrated by the selective determination of ferrocenecarboxaldehyde in the presence of ferrocene in 100-fold excess.

The precipitation of analytes at polypyrrole modified electrodes has been demonstrated recently.⁶⁷ The principle is based on the incorporation of chemically active counter ions during the electro-polymerisation process. These counter ions are selected according to their ability to precipitate the analyte of interest. It was found that Ag^+ precipitated when Cl^- was the counter-ion, the precipitation process occurred while the electrode was held at open circuit. The subsequent oxidation of Ag could be used analytically.

1.5.3 Perm-selectivity

The use of polymeric perm-selective films on electrode surfaces provides a elegant approach for discriminating the species of interest from co-existing interferences. Perm-selective membranes provide an *in situ* separation process directly at the electrode surface resulting in an increase in selectivity and provides protection of the electrode surface.¹⁴⁴ This is achieved by controlling mass transport through the polymer film. The target analyte must be able to permeate the polymer film, if this process is active (*i.e.* thermodynamically driven), such as by ion-exchange, then preconcentration of the analyte may also occur. If the transport process is not active, then the analyte passes through the film by simple diffusion without accumulation. In the latter case, diffusional constraints imposed by the polymer film generally results in less analyte reaching the underlying electrode, consequently lowering sensitivity. It should be emphasised here that the *focus* of perm-selective film design are to optimise the rejection of interferences and to allow distribution of the analyte into and transport through the polymer film.¹⁴⁵ Obviously, perm-selective films need not preconcentrate analytes. It is, however, advantageous to provide such an effect, as this may offset the lowering in sensitivity due to hindered mass transport. Usually the polymer films employed are electro-inactive but examples of permeation control of electro-active polymers have also been demonstrated.¹⁴⁶ Selective discrimination of interferences are based on molecular properties such as charge, size, shape and polarity.

Cellulose acetate has been a very successful electrode modifier for the exclusion of interferences based on molecular size.^{147,148} The porosity of cellulose acetate can be controlled by time-controlled base hydrolysis of the film on the electrode surface.¹⁴⁸ This treatment results in uniform holes in the polymer film through which small analytes can diffuse passively and prevent the passage of larger electro-active ions such as proteins and organic surfactants. This treatment results in simplified chromatograms and freedom from surface fouling effects due to protein precipitation. These effects are demonstrated in Fig. 1.10. Polyaniline, polyphenol and polypyrrole have also been used as selective membranes. The perm-selectivity of these materials was found to be dependent on the electro-polymerisation time and the concentration of the monomer.¹⁴⁶ From the results of a fundamental study, the selective permeabilities of

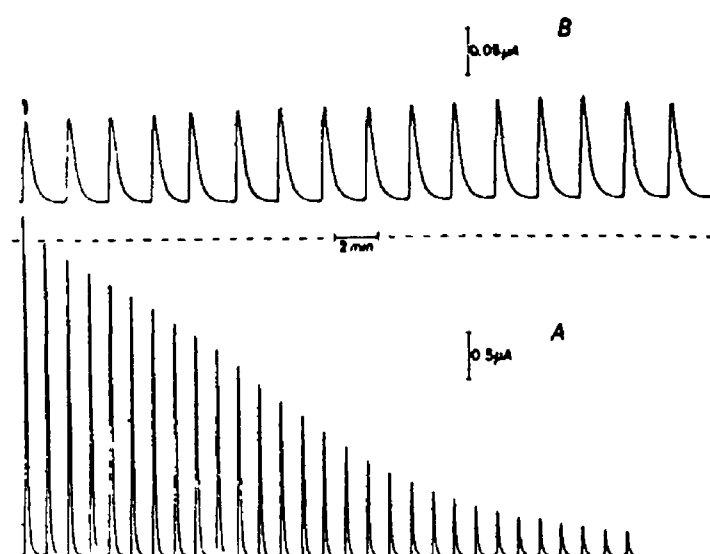


Fig 1 10 Amperometric detection of $1.0 \times 10^{-4} \text{ mol dm}^{-3}$ phenol at (A) bare glassy carbon and (B) at a cellulose acetate coated electrode (Reproduced from J Wang, L D Hutchins, *Anal Chem*, 1985 57 1536)

polyphenolic and polyaniline can be explained approximately on the basis of the Stokes radii of the permeating ion ⁶⁵ However, the degree of selectivity of the films can not be explained by the differences in Stokes radii alone ¹⁴⁹ It has been proposed that this may be due to chemical interaction between the permeating species and the modifier

It was stated earlier that coulombic association could be used to preconcentrate analytes in polymeric films through ion-exchange The opposite force, coulombic repulsion, can be used to prevent interferences from reaching the electrode surface This is based on the principle that charged polymer films tend to reject ions of the same charge (co-ions) ¹³⁵ The extent of rejection depends on the net charge on the co-ion and on the polymer film, degree of polymer swelling, thickness of film, type and concentration of electrolyte and electrolyte pH Unfortunately, a small amount of diffusion of co-ions through charged polymer films is quite a common phenomenon resulting in non-zero permeabilities ^{53,145} The extent of this process must be assessed to allow application of these materials for electroanalysis

The response time of perm-selective polymer coated electrodes is important in many applications such as FIA and HPLC The diffusional resistance imposed by the polymer film can result in prolonged response times and band broadening of the eluting sample plug Such an effect can lower the analytical through-put in FIA procedures and seriously affect resolution in HPLC It has been shown theoretically that band broadening increases with increasing polymer film thickness and is inversely related to the diffusion coefficient of the analyte in the polymer film ¹⁵⁰ The current response of a perm-selective film is given by the equation ¹⁴⁸,

$$i_d = i_L [1 / 1 + (P_s/P_m)] \quad (1.43)$$

where i_L is the current at the bare electrode, and P_s and P_m are the permeability of the substrate in the solution and the film respectively It is well known that the electrode current is effectively independent of flow rate for perm-selective electrodes ¹²¹ From the above equation, under

sufficiently low or high flow rates, the current becomes either solution or film controlled respectively

1 5 4 Electrocatalysis

The theoretical considerations concerning electrocatalysis have been dealt with in section 1 3 In this section some of the applications of electrocatalysis for the development of electrochemical sensors will be described

Amperometric detection of a solute species is dependent on the analyte of interest undergoing a redox reaction Frequently, however, the electrode kinetics are such that the species of interest will not react or only react very slowly at the electrode without the application of potential extremes ^{8,65,139,144} As discussed earlier, surface modification with electron transfer mediators can accelerate the rate of electrochemical reaction and in so doing, lower activation over-potentials ⁷⁸ This is of particular advantage as it may bring the reaction into a potential domain where the species of interest can be determined free from interferences ¹⁹ In addition, the electrocatalysis of the electrode reaction may result in enhanced sensitivity and lowered background currents As LOD is a function of sensor sensitivity and noise, these effects may result in significant lowering in LOD

The nature of modifying layers for electrocatalysis differ greatly depending on the application The most frequently encountered modification involve deposited metallo-polymers ⁷⁷, polymer immobilised metallic micro-particles ¹⁵¹ and inorganic films on electrodes ¹²⁷

Probably the most widely exploited form of electrocatalysts are the metallo-polymers These materials possess a strongly bound mediator site in a three dimensional network at high surface concentrations ¹⁹ and the mediators can be chosen from a knowledge of solution based homogeneous kinetics In addition, theory describing the transport processes and kinetics at these type of electrodes are firmly established as discussed earlier, and may be used for the optimisation of sensor response ^{81,94-96,107} In addition, these theories allow a detailed understanding of the physical and chemical processes which control the electrode behaviour and response Many applications have been described for polymer-bound

metal complexes, most notably ruthenium, iron and iridium. These metal centres are particularly useful for a number of reasons, their complexes exhibit facile reversible kinetics at a variety of electrode materials, their complexes are stable in a number of oxidation states, the $E_{1/2}$ of the metal centre is easily controlled by controlling the coordination sphere and their electrochemistry is well documented. Geraty *et al.* ¹⁵² have utilised ruthenium-containing polymeric materials for the determination of Fe(II) and obtained a linear range from 5×10^{-6} to 1×10^{-2} mol dm⁻³. Electrodes modified with this polymer also exhibited lower operational potential and improved sensitivities for the oxidative determination of nitrite and nickel bis(2-hydroxyethyl)dithiocarbamate in flow systems. ¹⁵³ The use of this material in flow systems is, however, restricted due to the loss of electro-active material from the electrode surface caused by abrasion by the carrier electrolyte flow. This has been alleviated by the application of a second polymer (bi-layer arrangement) such as the conducting polymer poly-3-methylthiophene, or non-conducting polymer *e.g.* poly-N ethyltyramine on top of this mediating film. ¹⁵⁴ In a recent study it has been found that the electro-deposition of this ruthenium polymer resulted in films of superior stability compared to the drop coated films. ¹⁵⁵ The use of ruthenium and osmium bridged dimers $[(bipy)_2(H_2O)M^{3+}]_2O_4^{4-}$ immobilised in a cation-exchange resin (p-chlorosulphonated polystyrene) has been demonstrated to give catalytic currents for Cl⁻ oxidation. ¹⁵⁶ This system was applied to the determination of Cl⁻ using RDE voltammetry. Other metallo-polymer coatings used to perform electrocatalysis include the poly(vinylferrocene)-4-methyl-4'-vinyl-2,2'-bipyridyl co-polymer. This material was deposited onto Pt wire and used to determine Fe²⁺ at pH 2.1 with a linear range of 50 nM—5 μ M Fe. Poly(vinylferrocene) coated electrodes have been prepared for the electrocatalytic determination of ascorbic acid, these electrodes exhibited a linear range extending from 6×10^{-6} to 6×10^{-2} mol cm⁻³. ¹⁵⁷⁻¹⁵⁹ Pickup and Mao have used a series of electronically conducting anion-exchange polymers based on polypyrrole for the electrostatic binding of ferrocyanide. ¹⁵⁷ The ferrocyanide moiety was subsequently used for the electrocatalytic oxidation of ascorbic acid. The electrostatic binding of $[IrCl_6]^{3/4-}$ into quaternised PVP has been demonstrated, and these electrodes have been shown to mediate the oxidation of nitrite in flow injection analysis. ¹⁶⁰ The electrode has a linear range extending from 10^{-3} to 10^{-5} mol dm⁻³ nitrite and a limit of

detection of 0.072 ppm. Surface poisoning due to SCN^- is prevented and interference from Pb(II) , Mn(II) , and Fe(II) is attenuated. Further work on $[\text{IrCl}_6]^{2/3-}$ in the same polymer matrix extended the linear range from $8 \times 10^{-6} \rightarrow 4 \times 10^{-3} \text{ mol dm}^{-3}$.¹⁶¹ The electrocatalyst, cobalt phthalocyanine, has been used extensively for the modification of carbon paste electrodes (*vide infra*).¹²⁷ In a recent publication, the compound Co-4,4',4'',4'''-tetra-aminophthalocyanine has been electro-polymerised onto glassy carbon electrodes.¹⁶² The polymer was found to exhibit electrocatalytic properties similar to the monomeric compound. The electrodes were however found to be much more stable than carbon paste and compatible with organic solvents such as those commonly used for HPLC. The electrodes were found to detect picomole quantities of thiol compounds at low operational potentials.

Purely inorganic modifications of the electrode surface were amongst the first to be used for electroanalysis. This area has been reviewed recently by Cox *et al*.¹²⁷ Electrodes modified with inorganic films generally belong to one of the following categories, metal phthalocyanines,¹⁶³ and metal porphyrins,¹⁶⁴ polynuclear transition metal cyanides,¹⁶⁵ (Prussian Blue and its analogues), metal oxides,¹⁶⁶ or clay/zeolite structures.¹⁶⁷

Metal phthalocyanines and porphyrins are macrochemical species of high chemical stability.¹²⁷ Phthalocyanic compounds have been shown to exhibit electrocatalytic properties towards the oxidation of sulfhydryl groups.¹⁶⁸ Zagal has demonstrated the efficacy of cobalt phthalocyanine (CoPC) as an electrocatalyst for the oxidation of 2-mercaptoethanol and cysteine, both of which involve oxidation of the thiolate anions to radicals which then undergo dimerisation.¹⁶⁹ Zagal and co-workers used CoPC to lower the over-potential for the oxidative determination of hydrazine with FIA.¹⁷⁰ The mechanism by which CoPC promotes electrochemical reactions is little understood. However, many of the oxidations appear to involve mediation, *i.e.* the primary electrode reaction is the oxidation of Co(II) to Co(III) , which subsequently oxidises the analyte present at the electrode/solution interface.¹⁷¹ The selectivity towards mercaptans, α -keto acids and certain carbohydrates suggests that the electrode process is related to at least one other factor. In this regard, catalysis appears to be related to the highest occupied *d* orbital of the metal centre.¹²⁶ Prussian Blue compounds, although popular modifiers, have not received

widespread attention for analysis. However, Ni(II) hexacyanoferrate has been used for the detection of Fe(III) in a liquid chromatography system¹⁷² and Prussian Blue for the oxidation of ascorbic acid.¹⁷³ The sensitivity for ascorbic acid detection was greater by factor of 28 compared to the unmodified electrode. The flow injection determination of hydrazine by electrocatalytic oxidation at Prussian blue modified electrode has been reported recently.^{165,174} In this study the stability of the coating was improved by overlaying with Nafion. The detection limit was 0.6 ng. The modification of glassy carbon electrodes with CuCl deposits have been used for the detection of carbohydrates following anion-exchange chromatography.¹⁷⁵⁻¹⁷⁹ The electrodes were stable in NaOH solution and could be used for detection without the need for cleaning wave forms as is required for unmodified electrodes. The electrode showed wide applicability to polyhydroxyl compounds and the LOD was at the picomole level. It appears that the activity of the electrode is related to the Cu(II) and/or Cu(III) states even though the modification is in the form CuCl. This system was further extended by incorporating the CuCl in a Nafion matrix. This further enhanced the stability of the electrode response and provides discrimination against hydroxy acids.¹⁷⁵

Polymer immobilised micro-particles have been used for electrocatalytic detection of certain analytes. Platinum particles have been deposited in Nafion by potential cycling in chloroplatinic acid.¹⁸⁰ These electrodes have been used in flow cells and give rise to an electrocatalytic response to H₂O₂. H₂O₂ is an important analyte as it is the product of many enzyme reactions used for sensor development. The response is linear from 1 µM — 50mM where the Pt particle density is greater than 150 µg cm². The electrode was found to be very stable and was applied to the detection of H₂O₂ generated at a glucose oxidase electrode. The sensor was applied to the determination of glucose in blood.¹⁵¹ The electrodeposition of palladium, iridium, ruthenium and platinum from acidic solution of the metal complexes into PVP films has been reported.⁷⁴ Cross-linking the polymer with 8 mol % of 1,1,6-dibromohexane was found to stabilise the films effectively. The modified electrodes were found to be effective electrocatalysts for hydrogen evolution from acidic solution. A film containing palladium and iridium deposited directly onto glassy carbon electrodes has been used for the sensitive electrocatalytic reduction of H₂O₂.¹⁸¹ The response was linear over the range 0.2 to 1.8 mmol L⁻¹. Oxygen however, interfered with the response. The use of redox

polymers for the electro-deposition of silver micro-particles has been described recently ¹⁸² The polymer immobilised electro-active sites appeared to nucleate the deposition process under certain conditions Such devices may prove useful analytically

1.6. Conclusion

Through the unique properties of modified electrodes, many potential applications for these devices have been proposed Undoubtedly, chemical sensor development is the most prolific area of research in the field of modified electrodes The ultimate goal of sensor development is the production of an operational device which is cheap, simple to construct and operate The response from the sensor must be well defined and be simply calibrated Such attributes are easily conferred to amperometric sensors Finally, and most importantly, the device must be selective, and herein lies the challenge In order to control the reactivity of the electrode, control over the electrode potential ($E_{1/2}$ of the electrocatalyst) and transport (inhibited or promoted) to the electrode must be established Many elegant examples of such control are available and no doubt many more will follow These can only be achieved by chemical “engineering” on the molecular level

1.7. Scope of Thesis

The purpose of the work described in this thesis is, the development of novel electrochemical sensors from electrodes modified with osmium and ruthenium containing metallo-polymers Several novel detection systems for the electroanalysis of commercially important analytes will be described The physical stabilisation of the redox polymer films by manipulation of the polymer back-bone and by chemical cross-linking is also described Finally, the kinetics and transport processes occurring at the modified electrodes for a number of electro-active substrates are analysed using conventional theory of mediated electrocatalysis Some of the results presented here have appeared in the literature ¹⁸³⁻¹⁸⁶

1.8. References

- 1 J Heyrovsky, *Chemické Listy*, 1922 16 256
- 2 S J Updick, C P Hicks, *Anal Chem*, 1966 38 726
- 3 R F Lane, A T Hubbard, *J Phys Chem*, 1973 77 1401
- 4 R F Lane, A T Hubbard, *J Phys Chem*, 1973 77 1411
- 5 R W Murray, *Ann Rev Mater Sci*, 1984 14 145
- 6 G J Patriarche, *J Pharm Biomed Anal*, 1986 4 789
- 7 L R Faulkner, *Chem Eng News*, 1984 62 28
- 8 R W Murray, A G Ewing, R A Durst, *Anal Chem*, 1987 59 379A
- 9 F C Anson, *J Phys Chem*, 1980 84 3336
- 10 D A Buttry, F C Anson, *J Am Chem Soc*, 1984 106 59
- 11 D C Bookbinder, M S Wrighton, *J Am Chem Soc*, 1980 102 5123
- 12 H D Abruna, A J Bard, *J Am Chem Soc*, 1981 103 6898
- 13 H Akahoshi, S Toshima, K Itaya, *J Phys Chem*, 1982 85 818
- 14 Z Zhang, W R Seitz, *Anal Chim Acta*, 1984 160 47
- 15 C K Chiang, *Polymer*, 1981 22 1454
- 16 T Ohsaka, K Naoi, S Ogano, S Nakamura, *J Electrochem Soc*, 1987 134 2096
- 17 P G Pickup, R W Murray, *J Am Chem Soc*, 1983 105 4510
- 18 C E D Chidsey, R W Murray, *J Phys Chem*, 1986 90 1479
- 19 R J Forster, J G Vos in *Comprehensive Analytical Chemistry*, Vol XXVII, M R Smyth, J G Vos, (Eds), Elsevier, Amsterdam, 1992, Ch 7
- 20 D G Davis, R W Murray, *Anal Chem*, 1977 49 194
- 21 P R Moses, L Weir, R W Murray, *Anal Chem*, 1975 47 1882
- 22 K K Kanazawa, A F Diaz, R H Geiss, W D Gill, J F Kwak, J A Logan, J F Rabolt, G B Street, *J Chem Soc Chem Commun*, 1979 854
- 23 J M Clear, J M Kelly, C M O'Connell, J G Vos, *J Chem Res*, (M) 1981 3037
- 24 V S Srinivasan, W J Lamb, *Anal Chem*, 1977 49 1639

- 25 A F Diaz, U Hetzler, E Kay, *J Am Chem Soc* , 1977 99 6780
- 26 P R Moses, L M Weir, J C Lennox, H O Finklea, J R Lenhard, R W Murray, *Anal Chem* , 1978 50 576
- 27 J R Lenhard, R W Murray, *J Am Chem Soc* , 1978 100 7870
- 28 N Oyama, F C Anson, *J Am Chem Soc* , 1979 101 1634
- 29 O Haas, H R Zumbrennen, *Helv Chim Acta* , 1981 64 854
- 30 K Oyata, A J Bard, *Anal Chem* , 1978 50 1487
- 31 M S Wrighton, M C Palazzotto, A B Bocarsly, J M Bolts, A B Fischer, L Nadj, *J Am Chem Soc* , 1978 100 7264
- 32 T Osa, M Fujihira, *Nature*, 1977 268 226
- 33 I Haller, *J Am Chem Soc* , 1978 100 8050
- 34 A Beetleheim, R J H Chan, T Kuwana, *J Electroanal Chem* , 1980 110 93
- 35 J F Evans, T Kuwana, *Anal Chem* , 1977 49 1632
- 36 J F Evans, T Kuwana, *Anal Chem* , 1979 51 358
- 37 N Oyama, K B Yap, F C Anson, *J Electroanal Chem* , 1979 100 233
- 38 C E D Chidsey, R W Murray, *Science*, 1986 231 25
- 39 M S Wrighton, *Science*, 1986 231 32
- 40 W J Albery, M J Eddowes, H A O Hill, A R Hillman, *J Am Chem Soc* , 1981 103 3904
- 41 N Oyama, A P Brown, F C Anson, *J Electroanal Chem* , 1978 87 435
- 42 R Nowak, F A Schultz, M Umana, H D Abruna, R W Murray, *J Electroanal Chem* , 1978 94 219
- 43 S Mazur, T Matusinovic, K Cammann, *J Am Chem Soc* , 1977 99 3888
- 44 M Sharp, M Petersson, K Edstrom, *J Electroanal Chem* , 1979 95 123
- 45 K S V Santhanam, N Jespersen, A J Bard, *J Am Chem Soc* , 1977 99 274
- 46 I Rubenstein, *J Electroanal Chem* , 1985 195 431
- 47 A P Brown, F C Anson, *J Electroanal Chem* , 1977 83 203
- 48 A P Brown, F C Anson, *J Electroanal Chem* , 1976 72

- 49 K Pool, R P Buck, *J Electroanal Chem* , 1979 95 303
- 50 S M Geraty, J G Vos, *J Chem Soc Dalton Trans* , 1987 3073
- 51 R J Forster, J G Vos, *Macromolecules*, 1990 23 4372
- 52 O Haas, M Kriens, J G Vos, *J Am Chem Soc* , 1981 103 1318
- 53 N Oyama, F C Anson, *Anal Chem* 1981 53 1192
- 54 N S Scott, N Oyama, F C Anson, *J Electroanal Chem* , 1980 110 303
- 55 N Oyama, F C Anson, *J Am Chem Soc* , 1979 101 3450
- 56 K Shigehara, N Oyama, F C Anson, *J Am Chem Soc* , 1981 103 2552
- 57 N Oyama, T Ohsaka, T Ushiroguchi, *J Phys Chem* , 1984 88 5274
- 58 N Oyama, T Ohsaka, H Yamamoto, *Anal Chem* , 1983 55 1429
- 59 M D Ryan, G S Wilson, *Anal Chem* , 1982 54 20R
- 60 A R Hillman, in *Electrochemical Science and Technology of Polymers*, R G Linford, (Ed), Elsevier, Amsterdam, 1987 Ch 5
- 61 O K KIm, *J Polym Sci Polym Lett* , Ed , 1982 20 663
- 62 P Denisevich, H D Abruna, C R Leidner, T J Meyer, R W Murray, *Inorg Chem* , 1983 21 2153
- 63 P K Ghosh, T G Spiro, *J Electrochem Soc* , 1981 128 1281
- 64 J M Calvert, R H Schmehl, B P Sullivan, J S Facci, T J Meyer, R W Murray, *Inorg Chem* , 1983 22 2151
- 65 N Oyama, in *Chemical Sensor Technology*, T Seigama, (Ed), Elsevier, Tokyo, Vol 2, 1989
- 66 M E G Lyons, W Breen, J F Cassidy, *J Chem Soc Faraday Trans 1*, 1990 86 2095
- 67 G G Wallace, Y P Lin, *J Electroanal Chem* , 1988 247 145
- 68 A J Bard, L R Faulkner, *Electrochemical Methods*, Wiley, NY 1980 Ch 3
- 69 J O'M Bockris, A K N Reddy, *Modern Electrochemistry*,

- Plenum, NY, 1977, Vol 1, Ch 1
- 70 P T Kissinger, *Anal Chem* , 1977 49 445A
- 71 J M Saveant, *Acc Chem Res* , 1980 13 323
- 72 H B Mark, *Analyst*, 1990 115 667
- 73 R W Murray, *Phil Trans R Soc Lond* , 1981 302 253
- 74 K M Kost, D E Bartak, B Kazee, T Kuwana, *Anal Chem* , 1990 62 151
- 75 D Leech, J Wang, M R Smyth, *Electroanalysis*, 1991 3 37
- 76 O Haas, H R Zumbrennen, *Helv Chim Acta* , 1981 64 854
- 77 R J Forster, J G Vos, *J Chem Soc , Faraday Trans, 1*, 1991 87 1863
- 78 C P, Andrieux, J M Saveant, *J Electroanal Chem* , 1978 93 163
- 79 D C S Tse, T Kuwana, *Anal Chem* , 1978 50 1315
- 80 R D Rocklin, R W Murray, *J Electroanal Chem* , 1979 100 271
- 81 W J Albery, A R Hillman, *Ann Rep Prog Chem* , 1981 C 78 377
- 82 G Inzelt, G Horanyi, J Q Chambers, *J Electroanal Chem* , 1987 218 297
- 83 F C Anson, J M Saveant, K Shigihara, *J Phys Chem* , 1983 87 214
- 84 J Leddy, A J Bard, J T Maloy, J M Saveant, *J Electroanal Chem* , 1985 187 205
- 85 R D Rocklin, R W Murray, *J Phys Chem* , 1981 85 2104
- 86 D A Buttry, F C Anson, *J Electroanal Chem* , 1981 130 333
- 87 J M Saveant, K B Su, *J Electroanal Chem* , 1984 171 431
- 88 C P Andrieux, J M Dumas-Bouchiat, F M'Halla, J M Saveant, *J Electroanal Chem* , 1980 113 19
- 89 C P Andrieux, J M Dumas-Bouchiat, J M Saveant, *J Electroanal Chem* , 1982 131 1
- 90 C P Andrieux, J M Dumas-Bouchiat, J M Saveant, *J Electroanal Chem* , 1984 169 9
- 91 C P Andrieux, J M Saveant, *J Electroanal Chem* , 1984 171 65
- 92 C P Andrieux, J M Saveant, *J Electroanal Chem* , 1982

- 93 C P Andrieux, J M Saveant, *J Electroanal Chem* , 1982 134 163
- 94 W J Albery, A W Foulds, K J Hall, A R Hillman, *J Electrochem Soc* , 1980 127 654,
- 95 W J Albery, A R Hillman, *J Electroanal Chem* , 1984 170 27
- 96 W J Albery, W R Bowen, F S Fisher, A W Foulds, K J Hall, A R Hillman, R G Edgell, A F Orchard, *J Electroanal Chem* , 1980 107 37
- 97 K Aoki, K Tokuda, H Matsuda, *J Electroanal Chem* , 1986 199 69
- 98 M Lovric, *Electrochim Acta* , 1981 26 1639
- 99 M Delamar, M C Pham, P C Lacaze, J E Dubois, *J Electroanal Chem* , 1980 108 1
- 100 V G Levich, *Physicochemical Hydrodynamics*, Prentice Hall, Englewood Cliff, NY, 1962, p 68
- 101 T Ikeda, C R Leidner, R W Murray, *J Electroanal Chem* , 1982 138 343
- 102 T Ikeda, R Schmehl, P Denisevich, K Willman, R W Murray, *J Am Chem Soc* , 1982 104 2683
- 103 Y Ohnuki, H Matsuda, T Osaka, N Oyama, *J Electroanal Chem* , 1983 158 55
- 104 F C Anson, J M Saveant, K Shigehara, *J Electroanal Chem* , 1983 145 423
- 105 J Koutecky, V G Levich, *Zh Fiz Khim* , 1958 32 1565
- 106 W J Albery, M G Boutelle, A R Hillman, *J Electroanal Chem* , 1985 182 99
- 107 J F Cassidy, in *Comprehensive Analytical Chemistry*, M R Smyth, J G Vos, (Eds), Elsevier, Amsterdam, 1992, Ch 1
- 108 N Ibl, in *Comprehensive Treatise in Electrochemistry*, E Yeager, J O'M Bockris, B E Conway, S Sarangapani, (Eds), Plenum, NY, 1983, Vol 6
- 109 A J Bard, L R Faulkner, *Electrochemical Methods*, Wiley, NY, 1980, p 507
- 110 Y Xu, H B Halsall, W R Heineman, *Electroanalysis*, 1992 4 33
- 111 A A Saaman, P Bergveld, *Sensors and Actuators*, 1985 7

- 112 S Nicholson, I Shain, *Anal Chem* , 1964 36 706
- 113 S Nicholson, I Shain, *Anal Chem* , 1965 37 178
- 114 E Laviron, L Roullier, C Degrand, *J Electroanal Chem* , 1980 146 417
- 115 E Laviron, *J Electroanal Chem* , 1980 112 1
- 116 K Aoki, K K Tokuda, H Matsuda, *J Electroanal Chem* , 1983 146 417
- 117 D M Mohilner, *J Electroanal Chem* , 1966 1 241
- 118 K Aoki, K Tokuda, H Matsuda, *J Electroanal Chem* , 1984 160 33
- 119 W Nernst, *Z Phys Chem* , 1904 47 52
- 120 J N Barisci, P J Riley, G G Wallace, in *Comprehensive Analytical Chemistry*, M R Smyth, J G Vos, (Eds), Elsevier, Amsterdam, 1992, Ch 2
- 121 J M Elbicki, D M Morgan, S G Weber, *Anal Chem* , 1984 56 978
- 122 T Ou, J L Anderson, *J Electroanal Chem* , 1991 302 1
- 123 S Prabhu, J L Anderson, *Anal Chem* , 1987 59 157
- 124 A J Bard, *Anal Chem* , 1987 59 347A
- 125 M D Imisides, G G Wallace, E A Wilke, *Trends Anal Chem* , 1988 7 143
- 126 J Bassett, R C Denney, G H Jeffery, J Mendham, *Vogels Textbook of Quantitative Inorganic Analysis* , Edition 4, Longman, London, 1978 p 664
- 127 J A Cox, R K Jaworski, P J Kulesza, *Electroanalysis*, 1991 3 869
- 128 P Ugo, F C Anson, *Anal Chem* , 1989 61 1799
- 129 D M T O'Riordan, G G Wallace, *Anal Proc* , 1986 23 14
- 130 M D Imisides, D M T O'Riordan, G G Wallace, *Anal Lett* , 1988 20 1969
- 131 A R Guadalupe, H D Abruna, *Anal Chem* , 1985 57 142
- 132 L M Wier, A R Guadalupe, H D Abruna, *Anal Chem* , 1985 57 2011
- 133 M J Gehron, A Brajter-Toth, *Anal Chem* , 1986 58 1488
- 134 Y Kurauchi, E Tsurumori, K Ohga, *Bull Chem Soc Jpn* , 1989 62 1341
- 135 M W Espenscheid, A R Ghatak-Roy, R B Moore(III), R M

- Penner, M N Szentirmay, C R Martin, *J Chem Soc Faraday Trans 1*, 1986 82 1051
- 136 R W Murray, in *Electroanalytical Chemistry*, A J Bard (Ed), Marcel Dekker, NY, 1984 Vol 13 pp 191-397
- 137 M N Szentirmay, C R, Martin, *Anal Chem* , 1984 56 1898
- 138 R B Moore(III), J E Wilkerson, C R Martin, *Anal Chem* , 1984 56 2572
- 139 S Dong, Y, Wang, *Electroanalysis*, 1989 1 99
- 140 L A Coury, E W Huber, E M Birch, W R Heineman, *J Electrochem Soc* , 1989 136 1044
- 141 E W Kristensen, W G Kuhr, M R Wrightman, *Anal Chem* , 1987 59 1752
- 142 A R Guadalupe, H D Abruna, *Anal Lett* , 1986 18 1613
- 143 J F Price, R P Baldwin, *Anal Chem* , 1980 52 1940
- 144 J Wang, *Electroanalysis*, 1991 3 255
- 145 J Wang, T Golden, P Tuzhi, *Anal Chem* , 1987 59 740
- 146 J Wang, S P Chen, M S Lin, *J Electroanal Chem* , 1989 273 231
- 147 G Sittampalam, G S Wilson, *Anal Chem* , 1983 55 1608
- 148 J Wang, L D Hutchins, *Anal Chem* , 1985 57 1536
- 149 Y Ohnuki, H Matsuda, T Ohsaka, N Oyama, *J Electroanal Chem* , 1983 158 64
- 150 W T Kok, A J Tudos, H Poppe, *Anal Chim Acta* , 1990 228 39
- 151 H Gunasingham, C B Tan, *Analyst*, 1989 114 695
- 152 S M Geraty, D W M Arrigan, J G Vos, in *Anal Chem Symp Ser* , 25, M R Smyth, J, G Vos (Eds), Elsevier, 1986 pp 303
- 153 N Barisci, E Wilke, G G Wallace, M Meaney, M R Smyth, J G Vos, *Electroanalysis*, 1989 1 245
- 154 G G Wallace, M Meaney, M R Smyth, J G Vos, *Electroanalysis*, 1989 1 357
- 155 J N Barisci, G G Wallace, *Anal Lett* , 1991 24 2059
- 156 W J Vinning, T J Meyer, *Inorg Chem* , 1986 25 2023
- 157 Z Lu, S Dong, *Acta Chim Sinica* , 1986 44 32
- 158 H Mao, P G Pickup, *J Electroanal Chem* , 1989 265 127
- 159 Z Lu, S Dong, *Huaxue Yeubao*, Vol 44, pp 32
- 160 J A Cox, K R Kulkarni, *Analyst*, 1986 111 1219

- 161 J A Cox, P J Kulesza, *J Electrochem Soc* , 1984 175 105
- 162 X Qi, R P Baldwin, H Li, T F Guarr, *Electroanalysis*, 1991, 3 119
- 163 A M Tolbert, R P Baldwin, L M Santos, *Anal Lett* , 1989 22 683
- 164 J Wang, T Golden, *Anal Chim Acta* , 1989 217 343
- 165 W Hou, E Wang, *Anal Chim Acta* , 1992, 257 275
- 166 M E G Lyons, C H Lyons, D E McCormack, T McCabe, W Breen, J F Cassidy, *Anal Proc* , 1991 28 104
- 167 M D Baker, C Senaratne, *Anal Chem* , 1992 64 700
- 168 J H Zagal, C Fierro, R Rozas, *J Electroanal Chem* , 1981 119 403
- 169 J H Zagal, C Paez, *Electrochim Acta* , 1989 34 243
- 170 J H Zagla, E Monoz, S Ureta-Zanarta, *Electrochim Acta* , 1982 27 1373
- 171 L M Santos, R P Baldwin, *Anal Chem* , 1987 59 1766
- 172 P J Kulesza, K Brajter, I, Uchida, *Anal Chem* , 1987 59 2776
- 173 F Li, S Dong, *Electrochim Acta* , 1987 32 1511
- 174 C Lin, A B Bocarsly, *J Electroanal Chem* , 1991 300 345
- 175 S Mannino, M Rossi, S Ratti, *Electroanalysis* , 1991 3 711
- 176 J Zhou, E Wang, *Electroanalysis*, 1992 4 183
- 177 S V Prabhu, R P Baldwin,, *Anal Chem* , 1989 61 2258
- 178 L M Santos, R P Baldwin, *Anal Chem* , 1986 58 848
- 179 P Luo, V Prabhu, R P Baldwin, *Anal Chem* , 1990 62 752
- 180 B T Tay, K P Ang, H Gunasigham, *Analyst*, 1988 113 617 179
- 181 J A Cox, R K Jaworski, *Anal Chem* , 1989 61 2176
- 182 R Wang, R J Forster, A Clarke, J G Vos, *Electrochim Acta* , 1990 35 985
- 183 A P Doherty, R J Forster, M R Smyth, J G Vos, *Anal Chem* , 1992 64 572
- 184 A P Doherty, R J Forster, M R Smyth, J G Vos, *Anal Chim Acta* , 1991 25 45

- 185 A P Doherty, J G Vos, *J Chem Soc , Faraday Trans ,1*,
1992, in press
- 186 M M Malone, A P Doherty, M R Smyth, J G Vos, *Analyst*,
1992, in press

Chapter 2

The Development of a Sensor for Nitrite based on $[\text{Os}(\text{bipy})_2(\text{PVP})_{10}\text{Cl}]\text{Cl}$ Modified Electrodes

2.1. Introduction

Nitrite is an important analyte for a variety of reasons. Nitrite salts are frequently used in meat curing processes and are also common additives in processed meat.¹ It is known that nitrite can react with primary amines to form N-nitrosamines and that this reaction is facilitated by the acidic conditions found in the stomach.^{2,3} It has long been suspected that these N-nitrosamine compounds may be carcinogenic.³ Nitrite is an important primary intermediate in the nitrogen cycle.² Many studies have been carried out recently in an attempt to mimic the enzymatic conversion of molecular nitrogen to ammonia.^{4,5} Nitrite is also a common pollutant from agricultural and industrial sources. As this species is involved in the nitrogen cycle, the environmental impact of such pollution (e.g. algae blooms) may be considerable.⁶ In addition, nitrite is the species through which the environmentally important oxides of nitrogen (NO_x)⁷ and nitrate^{8,9} are usually determined. It is clear from these examples that nitrite is an extremely important analyte from the perspective of industry, agriculture, medicine and environmental protection. This importance is reflected in the number of publications concerning the determination of nitrite, in a variety of sample matrices, which have appeared in the last decade.¹⁰

It has been stated that, as a rule, the properties of anions make it difficult to find suitable reagents for the development of sensitive and selective analytical methods for these species covering the concentration ranges normally encountered.^{9,10} Nitrite is no exception to this rule. In a recent review of methods for the determination of nitrite, the overwhelming majority were based on spectrophotometric methodology.¹⁰ These techniques are based on well known azo dye formation reactions involving nitrite.¹¹ The predominance of a single approach is a result of the difficulty encountered in determining this anion. Under the acidic conditions prescribed by spectrophotometric procedures, nitrite undergoes a diazotisation reaction with compounds such as sulphanilamide, the product of this reaction is subsequently coupled to N-(1-naphthyl)-ethylenediamine dihydrochloride to form the corresponding azo dye for the spectrophotometric determination.¹⁰ Although sulphanilamide appears almost a universal diazotisation reagent, many different reagents have been proposed for the coupling step, which include

1-naphthamine and 1-naphthylamine-7-sulphonic acid¹ Although popular, spectrophotometric techniques for nitrite suffer from a number of distinct disadvantages, including limited linear ranges, poor limits of detection, complicated experimental protocols and low analytical throughput. In addition, many of the procedures involve long reaction times and unstable colorimetric reactions and products.¹² Flow injection (FIA) spectrophotometric methods have recently been introduced to alleviate some of these problems.¹³⁻¹⁵ However, these techniques still suffer from interferences such as ascorbic acid.¹⁶ Ascorbic acid is known to interfere with the colour forming reactions.¹⁷ Due to the biological nature of many of the samples encountered and the use of ascorbic acid as an antioxidant in many processed food products, this interference is a severe limitation of the spectrophotometric procedures.

Electrochemical methods for the analysis of nitrite have also been proposed. The direct reduction potential of nitrite is extremely negative (≈ -1.0 V vs SCE)¹⁸, therefore it is difficult to detect nitrite directly using its reductive behaviour.¹⁹ However, the use of differential pulse polarography has been reported for the direct and indirect determination of nitrite. Direct determination is based on the reduction of nitrous acid.²⁰ This is of limited applicability due to the instability of this species.²¹ The use of catalytic polarography for the indirect determination of trace amounts of nitrite is now well established.¹⁹ These techniques involve the use of electrolytes containing certain polyvalent metal cations such as Mo^{5+} ,²² Cr^{3+} ,²³ Co^{2+} ,²⁴ Y^{3+} ,²⁵ and V^{5+} ,²⁶ in the presence of complexing groups such as thiocyanate²⁷ and glycine.²³ In some of these systems, nitrite appears to complex to the metal centre as nitric oxide^{19,27}, this complex is subsequently reduced (metal based) upon potential scanning. In one example, the product of the electrode reaction reacts with dissolved oxygen in a catalytic cycle to regenerate the analytical species at the electrode surface resulting in enhancement in peak current.¹⁹ Alternatively, with metals such as Mo^{6+} , complex formation does not occur. The mechanism in this situation involves reduction of Mo^{6+} at the electrode to Mo^{5+} , this species subsequently undergoes a redox reaction with NO_2^- to regenerate Mo^{6+} at the electrode surface in a catalytic cycle, resulting in significant current enhancement.²² The detailed chemistry of these catalytic polarographic techniques is complex and is still not fully understood²⁸, but they have been successfully applied to the determination of nitrite in many situations. Many of these

techniques suffer from nitrate interference ^{22,23} In an alternative polarographic approach, the azo dyes formed by the colorimetric reactions discussed above have been used to indirectly determine nitrite electrochemically ²⁹ The reduction reactions in this approach are based on azo dyes This mode of detection does not have a catalytic component, and sensitivities are therefore limited

These polarographic techniques are highly sensitive and are useful for the trace determination of nitrite However, due to the nature of polarographic methods, *i.e.* they are difficult to automate, are subject to metal cation interference and the reduction reactions occur at potentials close to the discharge potential of electrolytes, these techniques have limited applicability in routine analysis

Because of the limitations of the polarographic and spectrophotometric techniques discussed above, the oxidation of nitrite at conventional platinum ³⁰, glassy carbon ¹⁶ and carbon paste ³¹ electrodes has been investigated The oxidation at platinum is severely restricted due to the presence of surface oxides groups on the electrode surface ^{30,32,33} and passivation caused by intermediates involving the oxidation of nitrite occurs ³⁴ With glassy carbon, the most serious difficulties associated with this material is the extreme dependence of the rate of many electrochemical reactions on the surface state of the electrode ³⁵ At these electrodes, large over-potentials are required for the oxidation reaction to proceed at useful rates, typically in excess of 1.1 V vs SCE At such potentials, considerable interference from species such as Cl⁻, thiocyanate and ascorbic acid have been reported ¹⁶ The use of electrochemically pre-treated glassy carbon electrodes for the oxidation reaction was subsequently studied and was found to lower the oxidation potential by about 200-300 mV ³⁵ It was also noted that without pre-treatment, the direct oxidation of nitrite at glassy carbon causes a slow loss in electrode sensitivity due to passivation ³⁴ The common anion thiocyanate was also found to severely passivate the electrode upon oxidation ³⁵ In order to reduce the over-potential further, the application of redox polymer modified electrodes has been introduced The earliest example of the mediated oxidation of nitrite involved [IrCl₆]^{2-/3-} electrostatically incorporated in quaternised PVP ³⁴ The mediation reaction was found to occur at the polymer surface (S_k'') In a subsequent study, the mediator [IrCl₆]^{3-/4-} was found to improve electrode performance by extending the

linear range ³⁶ For both of these modified electrodes, ascorbic acid and thiocyanate caused interference due to mediated oxidation, although the passivation effect of nitrite and thiocyanate was eliminated This suggests that reactive intermediates formed during the oxidation of these species are prevented from adsorbing at the underlying electrode surface Recently, the $[\text{Ru}(\text{bipy})_2(\text{PVP})_5\text{Cl}]\text{Cl}$ redox polymer modified electrode was used for the detection of nitrite in FIA ³⁷ These electrodes were effective in reducing the over-potential for the oxidation by *ca* 300-400 mV, however, electrode stability was limited ³⁸ For all oxidation-based sensors, interference from signals due to the oxidation of ascorbic acid and thiocyanate however remain problematic

It is evident from this discussion that the analysis of nitrite has received considerable attention recently The major limitations of the procedures developed previously involve interferences Therefore the objectives for the development of an electrochemical sensor for the determination of nitrite are, a) prevention of ascorbic acid interference, b) absence of thiocyanate oxidation and resulting passivation, c) prevention of electrode passivation by nitrite oxidation, and d) operation at moderate potentials to ensure minimum interferences The construction of a sensor fulfilling these objectives would constitute a major advance in this area

In this chapter, a novel electrochemical sensor for the detection of nitrite will be described In order to prevent some of the previously reported oxidative interference, the sensor is based on the mediated reduction of nitrite by electrodes modified with the electrocatalytic polymer, $[\text{Os}(\text{bipy})_2(\text{PVP})_{10}\text{Cl}]\text{Cl}$ The possible mechanism of the electrode reaction is described along with the kinetic parameters and transport processes occurring at the modified electrode The characteristics of the sensor under operational conditions are assessed and the application of the sensor for the determination of nitrite in saliva is demonstrated

2.2. Experimental

2.2.1 Materials and Reagents

2.2.1.1 Synthesis of High Molecular Weight Poly(4-Vinylpyridine)

High molecular weight material is desirable to ensure maximum physical stability of the resulting redox polymer. The monomer, 4-vinylpyridine (Aldrich), was purified by vacuum distillation at 70 °C. Next 12.2 cm³ of the purified monomer was degassed using oxygen-free nitrogen. The monomer was then bulk polymerised at 80 °C under nitrogen for 4 h. The polymerisation process was initiated with the free radical initiator, 2,2'-azobisisobutyronitrile (AIBN) at a mole ratio of 500:1 (monomer: initiator). The resulting glassy polymer was dissolved in methanol for subsequent molecular weight fractionation. The bulk fractionation of polymers by the addition of non-solvent is widely practiced.³⁹ The methanol was evaporated to produce a concentrated viscous polymer solution. To this solution, toluene was added drop-wise to cloud point while stirring vigorously. The suspension was then heated slowly to 40 °C and that fraction of polymer remaining undissolved (the high molecular weight portion) was collected. This portion of polymer was then redissolved in methanol and precipitated in diethylether twice for purification. The polymer fraction was then dried thoroughly *in vacuo* at 80 °C. 5.02 g of fractionated polymer was recovered which corresponds to 40% of total the expected yield.

2.2.1.2 Determination of Poly(4-Vinylpyridine) Molecular Weight

The use of hydrodynamic techniques such as viscometry for the molecular weight determination of polymers is well established.³⁹ The empirical formula relating polymer solution viscosity to molecular weight, (Mark-Houwink equation), $[\eta] = K' M^a$, where $[\eta]$ is the intrinsic viscosity of polymer solutions at infinite dilution, K' and a are constants for a particular polymer and solvent and M is the molecular weight of the polymer, is frequently used. This approach is valid only for linear polymers such as PVP. The values K' and a have been evaluated for PVP in dry ethanol previously at 25 °C to be 2.5×10^{-4} and 0.68 respectively.⁴⁰

Polymer solutions in the concentration (c) range 1.0 to 0.2 g / 100 cm³ in dry ethanol were prepared accurately. The efflux time for each solution and solvent between the graduations of an Ubbelohde suspended level viscometer were determined at 25 ± 0.2 °C. Polymer solutions were allowed to equilibrate at this temperature for 15 min prior to measurement. A plot of η_{sp}/c vs c was prepared and extrapolation to infinite dilution reveals $[\eta]$ to be 2.08 ± 0.03 dL g⁻¹. Using the Mark-Howink equation, this reveals a viscosity average molecular weight of 580,000 g mol⁻¹ for the high molecular weight fraction.

2.2.1.3 Synthesis of [Os(bipy)₂Cl₂]

This compound was synthesised by heating 3 mmol OsCl₃ · 3H₂O with 6 mmol of 2,2'-bipyridyl in 40 cm³ of DMF under reflux for 0.5 h. This solution, containing [Os(bipy)₂Cl₂]Cl was then added dropwise into a solution of 2 g Na₂S₂O₄ in 200 cm³ water and stirred for 1 h. After cooling to 0 °C, the black microcrystalline [Os(bipy)₂Cl₂] was filtered off, washed with water and dried *in vacuo* at 80 °C.

2.2.1.4 Preparation of [Os(bipy)₂(PVP)₁₀Cl]Cl

This material was synthesised according to the procedure described by Forster *et al.*⁴¹ with the exception that 2-methoxyethanol was used as the solvent instead of ethanol. A metal loading of 1 metal centre per 10 VP units was chosen as this loading exhibits optimum charge transfer characteristics.⁴² 100 mg of PVP was dissolved in 40 cm³ 2-methoxyethanol. 54.6 mg of [Os(bipy)₂Cl₂] was dissolved in a similar amount of 2-methoxyethanol, both solutions were combined and added to a 150 cm³ round bottomed flask. This reaction mixture was held under reflux at 125 °C for 72 h. The reaction was monitored by UV/visible spectroscopy and CV. The appearance of a redox wave at 0.250 V vs SCE due to the formation of the polymer complex⁴¹ and the complete disappearance of the redox wave at 0.0 V vs SCE due to the [Os(bipy)₂Cl₂] starting material indicated completion of the reaction. The solvent was then evaporated to dryness and the redox polymer redissolved in methanol. The polymer was then precipitated in diethylether, collected

and dried *in vacuo* at 80 °C. The structure of the redox polymer can be seen in Fig. 2.1.

2.2.1.5 Electrolytes and Solutions

All electrolyte solutions were prepared from Milli-Q water. The electrolyte used throughout was 0.1 mol dm⁻³ Na₂SO₄ containing 0.05 mol dm⁻³ H₂SO₄. The pH of this electrolyte was adjusted, where necessary, using 1.0 mol dm⁻³ H₂SO₄ and 1.0 mol dm⁻³ NaOH. The pH was measured using a Corning 240 pH meter calibrated using pH 4 and pH 7 buffer solutions. Nitrite solutions were prepared freshly each day from sodium nitrite in neutral electrolyte. Nitrite is unstable at low pH²¹, therefore, solutions under these conditions were prepared immediately prior to use and measurements made as quickly as possible. Low pH nitrite solutions were prepared by dilution of an appropriate quantity of neutral nitrite solution with an acidic electrolyte to give the desired pH and nitrite concentration.

2.2.2 Procedures

2.2.2.1 UV/Visible Spectroscopy

UV/visible spectroscopy was carried out using a Shimadzu UV 240 spectrophotometer linked to a Shimadzu OPI 1 programmable interface. 1 cm matched quartz cells were used. UV/visible spectra were recorded in the region 900 nm to 190 nm. A scan speed of 10 nm s⁻¹ and a slit width of 2 nm was used. Spectra were recorded on methanolic polymer solutions. Methanol was used in the reference beam.

2.2.2.2 Luminescence Spectroscopy

Luminescence spectroscopy was carried out using the Perkin Elmer LS50 luminescence spectrophotometer interfaced to an Epson AX2e PC. For the room temperature (RT) luminescence measurements a 1 cm fluorescence cell was used while at -196 °C, a quartz tube and holder were employed. The excitation and emission slit widths were 10 nm for all

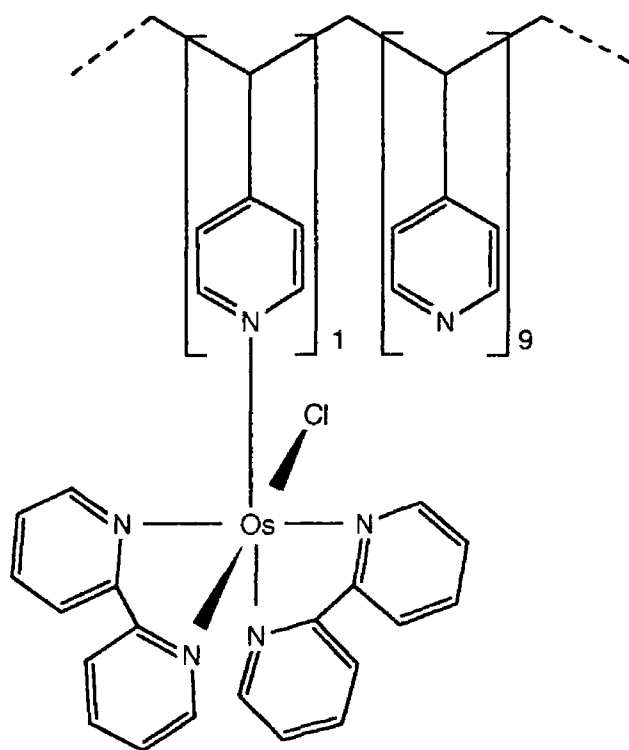


Fig 2 1 Structure of the metallo-polymer, $[\text{Os}(\text{bipy})_2(\text{PVP})_{10}\text{Cl}]\text{Cl}$

experiments. No evidence of luminescence was observed for the redox polymer at both RT and -196 °C.

2.2.2.3 Cyclic Voltammetry and Rotating Disc Electrode Voltammetry

Cyclic voltammetry (CV) and rotating disc electrode (RDE) voltammetry were carried out using a conventional three electrode assembly. The potentiostat used was the EG&G Princeton Applied Research Model 362. The rotating disc assembly was the Metrohm Model 629-10. Voltammograms were recorded on a Linseis X-Y recorder. The working electrodes were 3 mm diameter glassy carbon discs shrouded in Teflon (Metrohm). The counter electrode was 1 cm² platinum gauze placed parallel to the working electrode at a distance of ≈ 1 cm. The reference electrode was the saturated KCl calomel electrode. All potentials are quoted with respect to the SCE without regard to liquid junction potentials. All measurements, unless otherwise stated, were carried out at room temperature.

Modified electrodes were prepared by polishing the glassy carbon electrodes with 5 μ m alumina as an aqueous slurry on a felt cloth. The electrodes were rinsed thoroughly with distilled water and methanol. The electrodes were then treated with chlorosulphonic acid to promote the formation of surface oxide functional groups. The electrodes were again rinsed with distilled water and dried *in vacuo* at room temperature. The electrodes were modified by drop coating using a 1% w/v solution of the polymer. The electrodes were allowed to dry slowly in air and allowed to cure overnight *in vacuo* before use.

2.2.2.4 Flow Injection Apparatus

The flow injection apparatus consisted of a Gilson Miniplus 3 peristaltic pump, a six port Rheodyne injector valve fitted with a 20 μ L fixed volume sample loop, a EG&G Princeton Applied Research Model 400 electrochemical detector connected with Teflon HPLC tubing, and a Philips X-t chart recorder. In the flow cell, an Ag/AgCl electrode acted as the reference. The working electrodes were 3 mm diameter glassy carbon shrouded in a Teflon block. Modified electrodes were prepared as

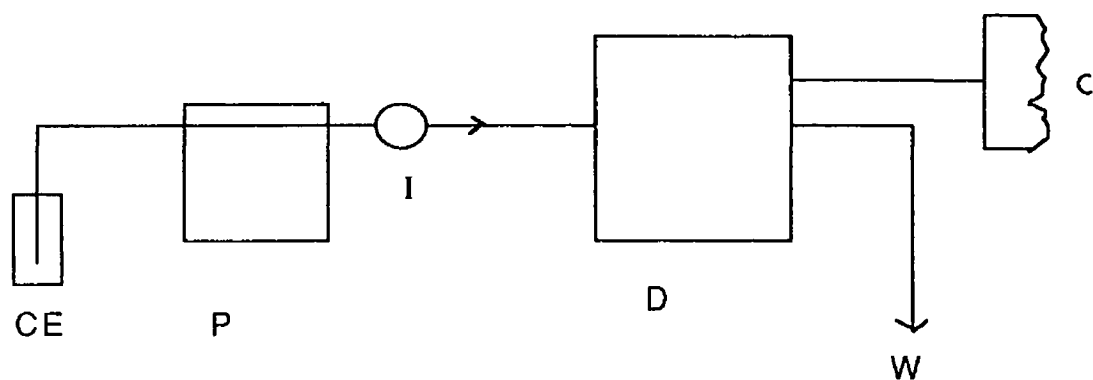


Fig 2 2 Schematic diagram of the Flow Injection Apparatus,
CE = carrier electrolyte, P = peristaltic pump, I = injection port,
D = detector, C = chart recorder and W = waste

described above. All potentials are quoted after numerical conversion to the SCE scale. Sample injections were made using a 2 cm³ glass syringe fitted with a Rheodyne injection needle. The carrier electrolyte used was 0.1 mol dm⁻³ Na₂SO₄ / 0.05 mol dm⁻³ H₂SO₄. A schematic diagram of the FIA apparatus can be seen in Fig. 2.2. Electrode responses were monitored as a function of carrier electrolyte flow rate, applied potential, polymer surface coverage and electrolyte pH.

2.2.2.5 Determination of Nitrite in Saliva

This analysis was carried out using a conventional electrochemical cell with a 3 electrode assembly. 10 cm³ of 0.1 mol dm⁻³ Na₂SO₄ / 0.05 mol dm⁻³ H₂SO₄ electrolyte was placed in the electrochemical cell and the electrolyte was stirred slowly using a magnetic stirrer and follower. A potential of 0.12 V vs. SCE was applied to the working modified electrode. The current response was recorded continuously using a Philips X-t chart recorder. Saliva was collected (with great difficulty!) and sonicated for *ca.* 15 min. 1.0 cm³ aliquots of the saliva were then added to the 10.0 cm³ of electrolyte and the current change to nitrite reduction was recorded. Responses due to standard solutions were recorded in an identical fashion. The calibration curve had a slope of 0.19 $\mu\text{A } \mu\text{g}^{-1} \text{ cm}^3$ and an intercept of 2.23 nA, and a correlation coefficient, $r = 0.997$. Responses were corrected for dilution. Two sub-samples of a single saliva sample were analysed in duplicate.

2.3. Results and Discussion

2.3.1 General Electrochemistry

A CV for the electrocatalytic polymer [Os(bipy)₂(PVP)₁₀Cl]Cl, coated on glassy carbon electrodes is shown in Fig. 2.3. The $E_{1/2}$ of the osmium redox centre in the sulphate electrolyte is 0.25 V vs. SCE. This value indicates that the coordination sphere of the metal centre is [Os(N)₅Cl] as expected from the synthetic strategy.⁴² From UV/visible spectra, λ_{max} values for the polymer complex were found to be 730 nm,

490 nm, 430 nm and 360 nm ⁴¹ The molar extinction coefficients at these wavelengths were also in close agreement with those previously reported for the material. These results again indicate that the redox polymer has the coordination sphere [Os(N)₅Cl] and that the metal loading is 1.10.

The CV of the redox polymer exhibits a number of features characteristic of surface bound redox sites ⁴³ The peak-to-peak separation between the oxidation and reduction waves is close to zero at low potential sweep rates. A plot of peak current vs. potential sweep rate is linear up to about 50 mV s⁻¹, indicating the finite diffusion behaviour of charge transport at the modified electrode ⁴⁴ At higher sweep rates, onset of semi-infinite diffusional behaviour becomes evident and a change over to a square root dependence on potential sweep rate occurs. This can be seen in Fig. 2.4a and 2.4b. In addition, the ratio i_{pa} / i_{pc} is 1, which indicates that the kinetics for the forward and reverse waves are similar. These results demonstrate the almost ideal surface behaviour of this redox polymer ⁴² The rate of charge transport through this redox polymer has been the subject of active investigation recently ⁴⁵⁻⁴⁷ This material exhibits rapid charge transport rates in sulphate electrolytes. For the electrolyte used in this study, the charge transport diffusion coefficient, D_{ct} , was estimated to be 1.3×10^{-11} cm² s⁻¹ using high sweep rate cyclic voltammetry and the Randles-Sevcik equation. This rate may be considered rapid on the CV timescale and ensures rapid regeneration of the electrocatalytic sites in the film. Such rapid D_{ct} values are desirable to ensure sensor responses are not limited by electron transport through the polymer. In addition, optimum polymer modified electrode performances are obtained when the cross-exchange reaction occurs in considerable portions of the film, i.e. the LS_k and LE_k kinetic cases, these kinetic regimes exist only when charge transport (and mass transport) is rapid.

It is expected from thermodynamics, considering the $E_{1/2}$ of this redox polymer, that the electrocatalytic redox centre will mediate reduction reactions with formal potentials, (E°), more positive than 0.250 V vs. SCE ⁴⁸ The reduction of nitrite at glassy carbon is thermodynamically favourable, since the six proton, four electron reaction,

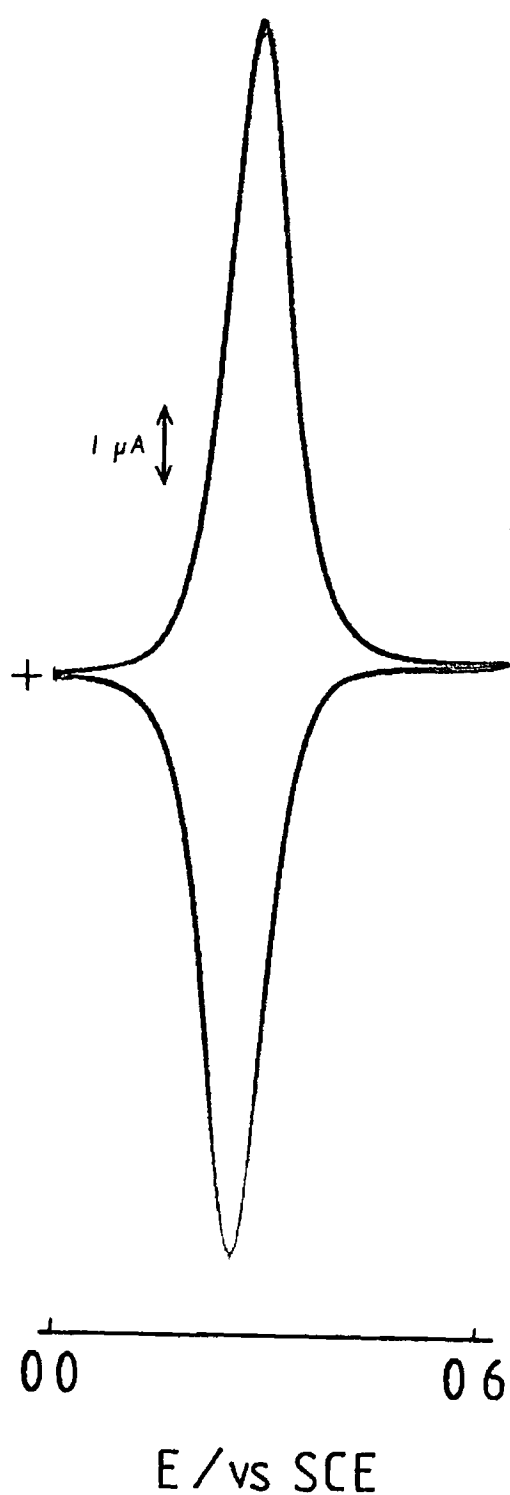


Fig 2.3 A CV of $[\text{Os}(\text{bipy})_2(\text{PVP})_{10}\text{Cl}]\text{Cl}$ coated on a glassy carbon electrode. Polymer surface coverage = $1.0 \times 10^{-8} \text{ mol cm}^{-2}$, electrolyte = $0.1 \text{ mol dm}^{-3} \text{ Na}_2\text{SO}_4 / 0.05 \text{ mol dm}^{-3} \text{ H}_2\text{SO}_4$, potential sweep rate = 2 mV s^{-1}

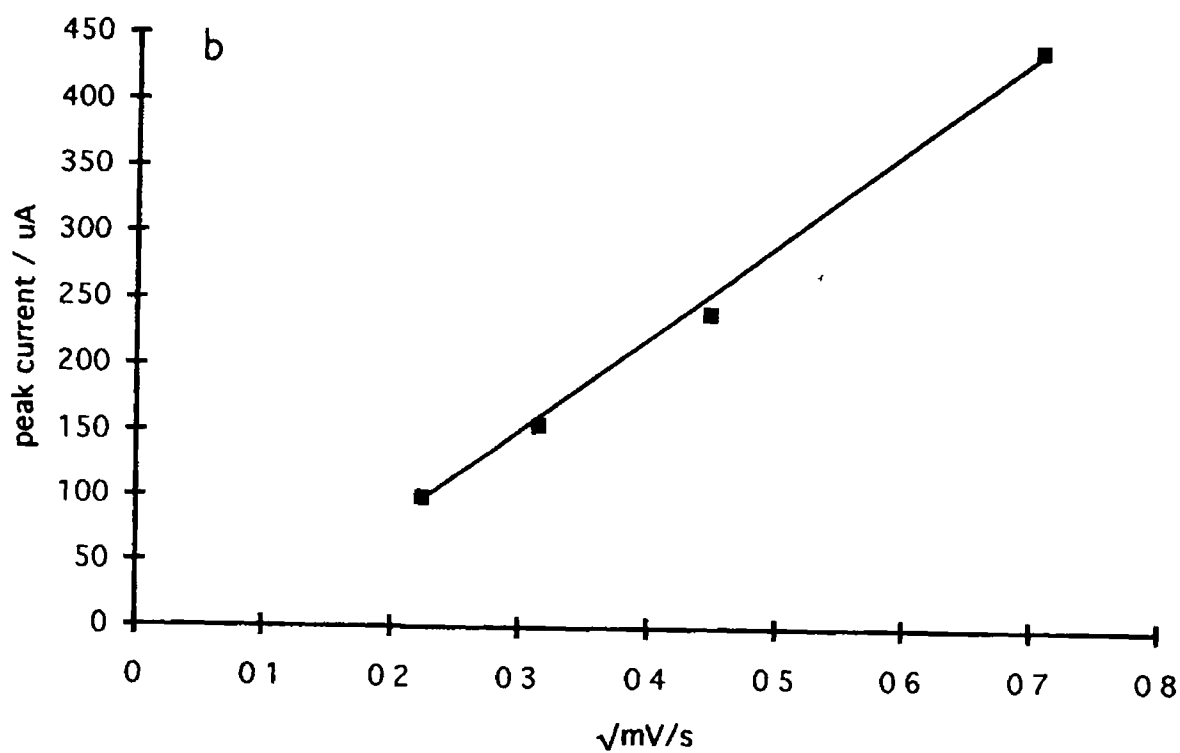
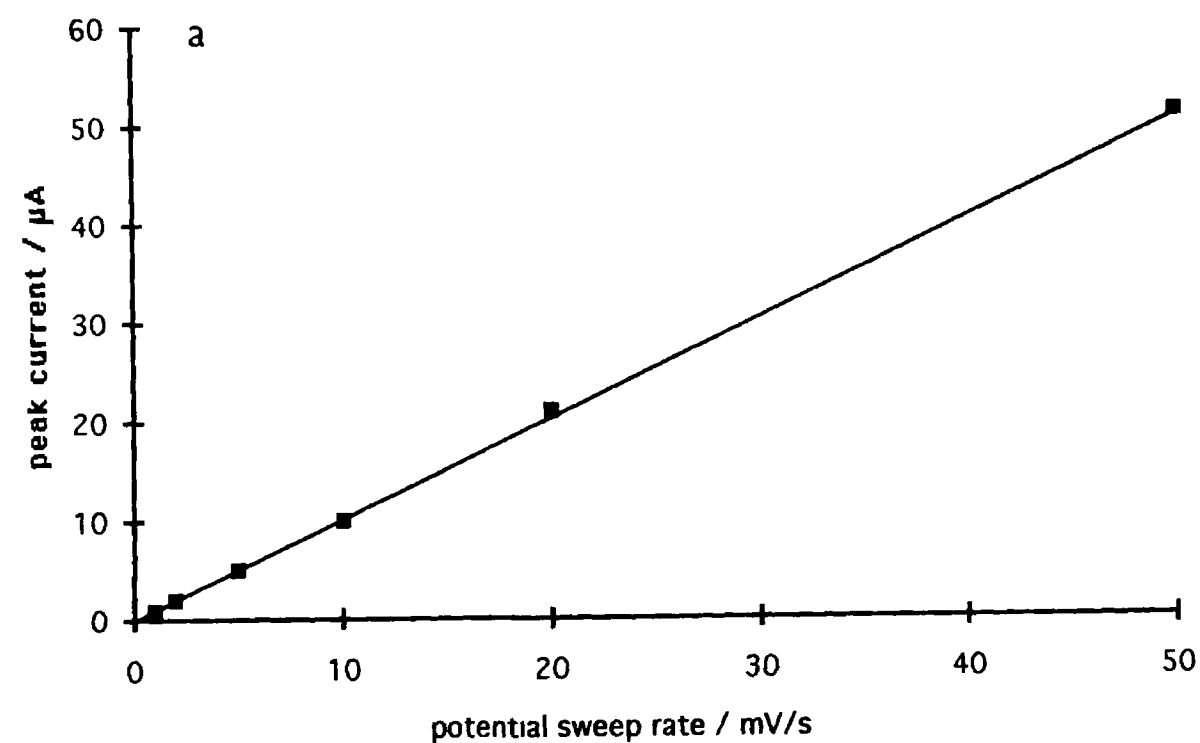
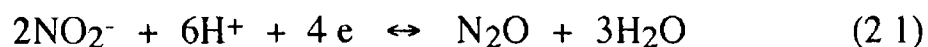


Fig 2.4 (a) Plot of peak current vs potential sweep rate (v) over the range $1 - 50 \text{ mV s}^{-1}$ and (b) plot of peak current vs \sqrt{v} from $50 - 500 \text{ mV s}^{-1}$



has a formal potential of 1.2 V vs SHE. On this basis, it was expected that nitrite reduction may be mediated by the osmium redox couple within the polymer film. Although thermodynamically favourable, the reduction of nitrite at glassy carbon electrodes is known to be kinetically very slow.²⁸ In addition, reduction of nitrite at gold and glassy carbon electrodes is known to cause severe surface passivation, with the electrode response dropping dramatically after several potential cycles.⁵⁰ With the use of the polymeric electrode modifier studied here it may be possible to eliminate these effects, in a similar fashion to that observed for polymer modifiers preventing electrode passivation caused by nitrite and thiocyanate oxidation.^{34,36}

A CV for the reduction of nitrite at a bare glassy carbon electrode can be seen in Fig. 2.5a. Two distinct reduction processes can be observed. The first wave has an $E_{1/2}$ of 0.25 V vs SCE. This reduction wave is very ill-defined and plateaus rather than forms a peak. This suggests that mass transport is not controlling the current flux at potentials past the anodic peak maximum, (E_{pa}), indicating the kinetics of the reaction are very slow. The ill-defined wave shape is indicative of an irreversible electrode reaction. No reverse wave is observed for this electrochemical process, also indicating irreversibility. The second reduction process occurs at a potential of -0.50 V vs SCE. Again, this wave is ill-defined, does not have a reverse wave and therefore appears to be irreversible. Such CV's could only be obtained in very acidic electrolyte (pH 1.0) and at slow potential sweep rates ($< 10 \text{ mV s}^{-1}$). These observations suggest that the electrode reaction is proton dependent and the kinetics of the reaction are sluggish. Fig. 2.5b shows a typical rotating disc electrode voltammogram for nitrite reduction at glassy carbon. Again the curves are ill-defined. The magnitude of the limiting currents are $0.5 \mu\text{A}$ at 0.25 V vs SCE and $4.5 \mu\text{A}$ at -0.50 V vs SCE. Considering the concentration of the nitrite solutions, the magnitude of currents generated at the bare electrode may be considered small. These results confirm previous observations that the reduction of nitrite at glassy carbon is thermodynamically favourable but the charge transfer kinetics are poor.²⁸ Because of this, and the negative potentials

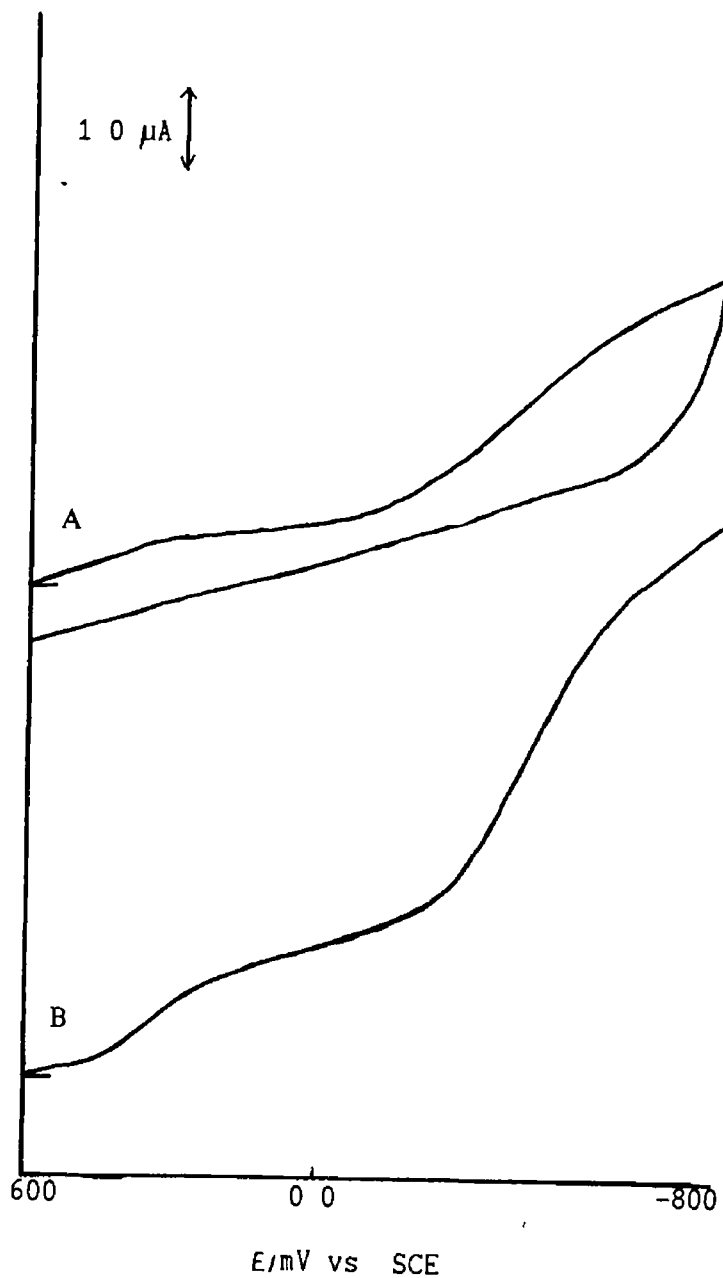


Fig 2.5 (A) A CV for the reduction of nitrite at a bare glassy carbon electrode and (B) current-potential curve for the reduction of nitrite at glassy carbon at a rotation speed of 500 rpm. Nitrite concentration for both was 0.01 mol dm^{-3} and electrolyte as for Fig 2.3

required for significant reaction rates these electrochemical processes can be considered of little analytical utility. It was also observed that after several potential sweeps, the electrode response to nitrite diminished presumably due to adsorption of reactive intermediates. This observation is in direct agreement with that reported previously.

CV has been extensively used to demonstrate electrocatalysis as this technique allows visualisation of the current-potential behaviour of the electrochemical system.⁵¹ In Fig 2.6, a CV for the reduction of nitrite at a modified electrode is presented. The shape of this wave is significant. On inspection it can be seen that the wave is significantly elongated along the current axis. This is indicative of an electrocatalytic reaction occurring at the electrode surface. The onset of mediation can be seen to occur at the onset of Os(II) generation within the polymer film, so the electrode is “switched on” at about 0.4 V vs. SCE in the negative scan direction. In the reverse wave, the electrode is “switched off” at about the same potential. The shoulders on the forward and reverse waves can be attributed to the Os(II)/Os(III) redox couple. As the rate of reduction and re-oxidation of the osmium centres⁵² is significantly faster than the rate of the cross-exchange reaction (*vide infra*), the applied potential causes a rapid redox of osmium sites resulting in a large transient electron flux, transient due to the finite reservoir of osmium sites available for redox reaction. The hysteresis on the wave can be attributed to nitrite depletion at the (static) electrode surface. These results clearly demonstrate mediated charge transfer by redox cycling of surface bound Os(III)/Os(II) sites to a solution species. The steepness of the reduction wave indicates that the kinetics of the mediated reaction are considerably improved in comparison to the reaction at the unmodified electrode (Fig 2.5). The mediation process can be further demonstrated with RDE voltammetry. In Fig 2.7, current potential curves for the mediated reduction of nitrite at the modified electrode can be seen. Again, the onset of mediation occurs at the onset of Os(II) generation in the film. In addition, the plateau currents are well defined and the currents generated are a function of nitrite concentration. This demonstrates the possible utility of the redox polymer for the construction of a nitrite sensor.

It was stated earlier that nitrite reduction at conventional electrodes causes severe surface passivation, For the mediated reaction studied here, no passivation of the electrode was observed over many potential cycles.

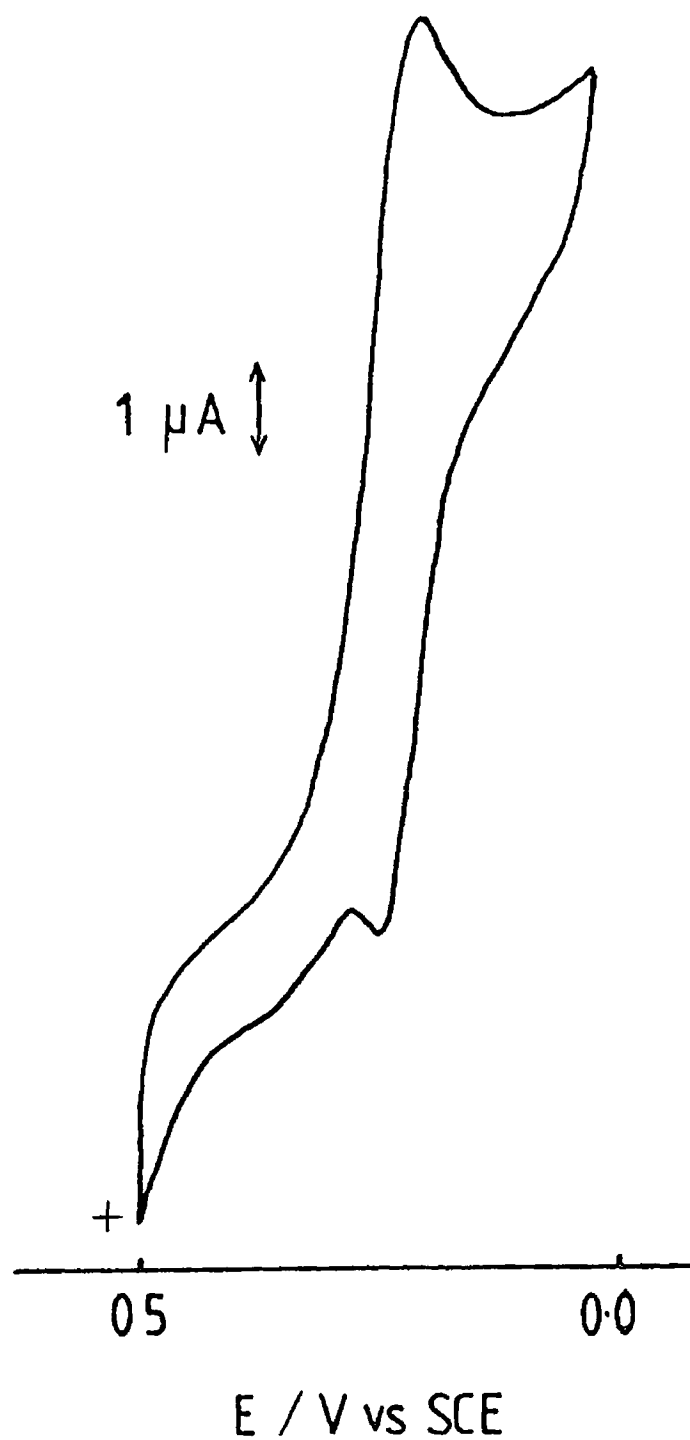


Fig 2.6 A CV for the reduction of $5.0 \times 10^{-3} \text{ mol dm}^{-3}$ nitrite at a modified electrode, Surface coverage = $1.0 \times 10^{-9} \text{ mol cm}^{-2}$, sweep rate = 5 mV s^{-1} , electrolyte as in Fig 2.3

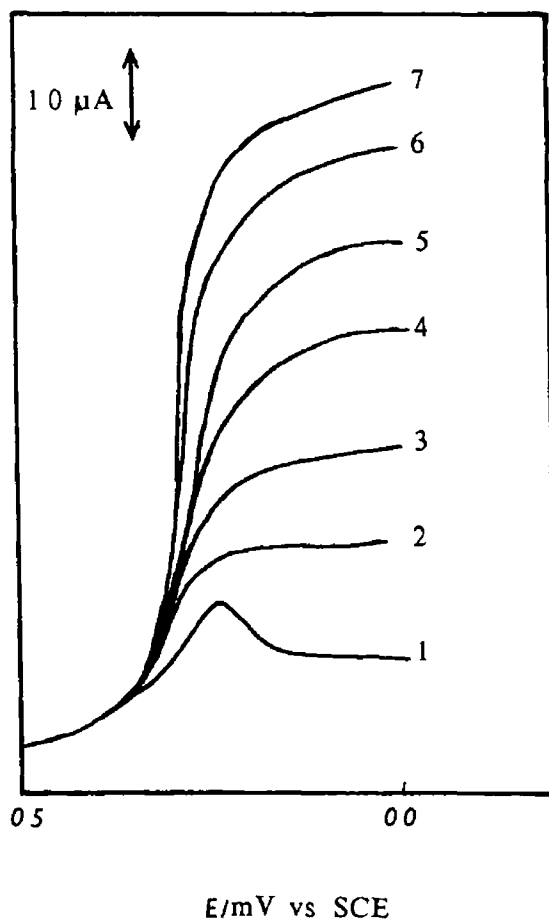


Fig 2 7 Current potential curves for nitrite reduction at a modified electrode Curve 1 shows the reduction wave of the Os(III) centres and curves 2 to 7 show the reduction of $1, 2, 3, 4, 5$ and $6 \times 10^{-3} \text{ mol dm}^{-3}$ nitrite Sweep rate = 2 mV s^{-1} , rotation speed = 500 rpm Electrolyte as for Fig 2 3

This behaviour is encouraging for the development of sensors capable of multiple determinations. Many modified electrodes proposed in the literature are not re-useable.⁵³

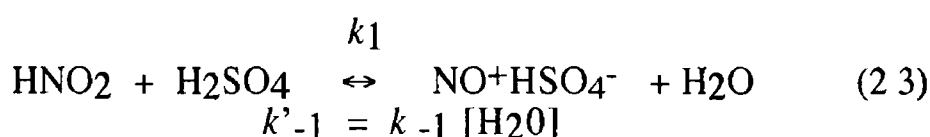
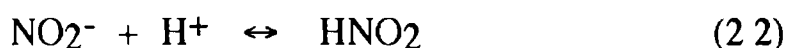
2.3.2 Mechanism for the Mediated Reduction of Nitrite

In trying to establish a mechanism for the mediated reduction reaction, previously reported observations must be considered. The reduction of nitrite at platinum electrodes involves a two step process in the potential range 0.0-0.7 V. The first step results in the generation of nitric oxide (NO), and in the second step, nitrous oxide (N₂O) is liberated.^{35,54} A third step observed at more negative potentials is due to the formation of hydroxyl amine (NH₂OH). It has been observed that at glassy carbon a single reduction wave is observed at positive potentials corresponding to the first two reduction processes. A single reduction wave has also been observed for polyaniline-coated electrodes but the exact process responsible has not been elucidated.⁵⁰ For the unmodified electrode severe passivation of the surface due to the adsorption of reactive intermediates was observed.⁵⁰

Considerable effort has recently been directed at the interconversion of nitrate and nitrite to ammonia *via* the lower oxides of nitrogen such as nitric oxide and nitrous oxide to mimic the action of nitrogen fixation enzymes.^{4,5,55-57} This has been achieved using metal complexes of osmium, ruthenium and iron. The main conclusion from this work is that the chemistry is complex and little understood. However, it appears that nitrite is coordinated to the metal centres in the form of the nitrosonium ion, NO⁺, and that the initial site for the multi-electron reduction reaction is this ligand. This species is also involved with the enzymatic conversion of nitrogen to ammonia.⁵⁸ In both cases the product of the initial reduction is nitric oxide.

It is known that the direct reduction potential of nitrite is more negative than -1.0 V, so in order to produce the reduction behaviour seen here and by other workers, nitrite must be converted in acidic electrolyte to a species more readily reduced. It is accepted that nitrite, in acidic solution, exists predominantly as the nitrosonium ion.^{59,60} In sulphuric acid electrolyte, the nitrosonium ion is not thought to exist in isolation but

as the ion association species, $\text{NO}^+\text{HSO}_4^-$ ⁶⁰ It is reasonable to assume under the conditions used here that this species is formed. The pK_a of nitrous acid is 3.4, consequently, nitrite is in the protonated form in the electrolytes studied here ⁶¹ The nitrosonium ion is generated by the following acid-base equilibria ³⁹



This acid-base equilibria has the effect of removing one of the oxide atoms from the nitrogen centre and creating low lying energy levels, mainly π^* (NO) in character, creating a possible initial site for reduction ⁵ The reduction of nitrite coordinated to osmium, iron and ruthenium centres involved adduct formation and inner sphere electron transfer. For the reaction studied here, the mediated reaction is centred at 0.25 V vs SCE, at the $E_{1/2}$ of the electrocatalytic centre in the polymer film. The limiting current plateau for the mediated reaction was found to be very flat, (Fig 2.8b). Both of these features are indicative of a purely outer sphere electron transfer process which is indeed expected for this electrocatalytic material ⁶² This has been confirmed by UV/visible spectroscopy, no change in the UV/visible spectrum of the polymer complex is observed in the presence of nitrite under acidic conditions over the range 200 nm to 900 nm, clearly demonstrating that no change occurs to the coordination sphere of the metal centre. In addition, the potential of the Os(II)/Os(III) redox couple does not change in the presence of nitrite. Armed with this information, it is likely that the mediated reaction involves a simple cross-exchange reaction between the mediator sites and the nitrosonium ion according to reaction 2.4,

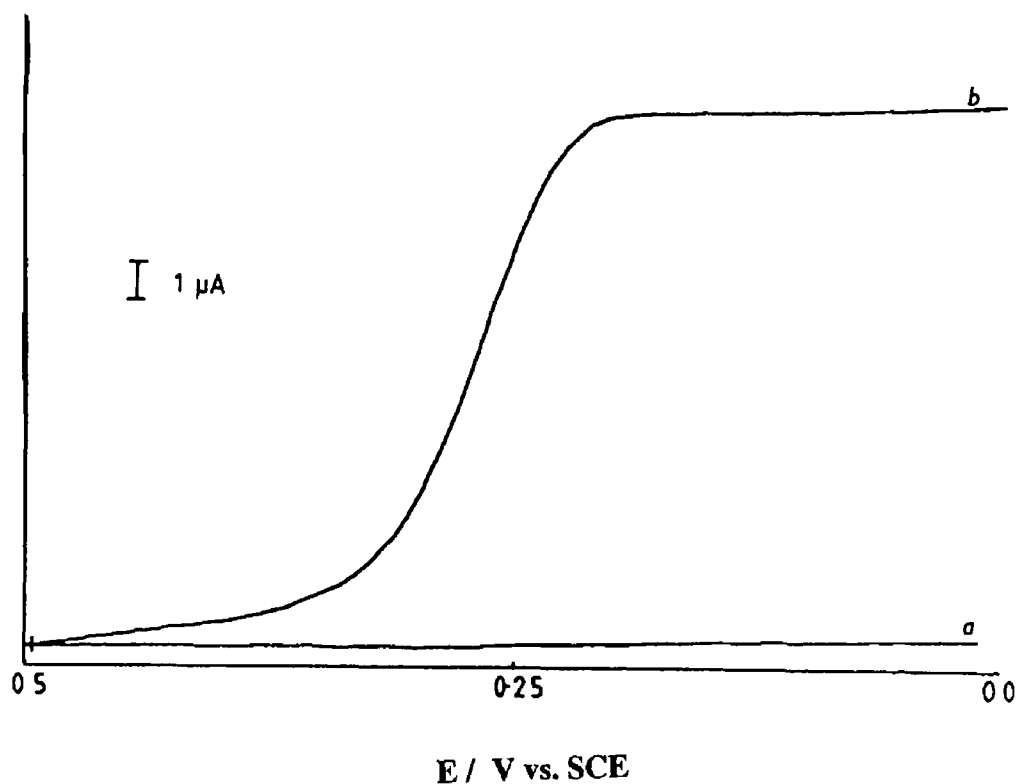
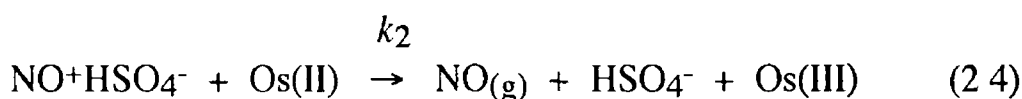


Fig 2 8 Current-potential curves for the reduction of $5.0 \times 10^{-3} \text{ mol dm}^{-3}$ nitrite at a glassy carbon (a) and at a modified electrode (b) Sweep rate = 5 mV s^{-1} , rotation speed = 500 rpm, electrolyte as for Fig 2 3



to liberate nitric oxide where k_2 is the second order rate constant for the cross-exchange reaction. This corresponds to the first reduction step observed at conventional electrodes and for the reduction of nitrite as a bound species. We believe that this is the only electrochemical process occurring in the polymer film under the conditions of RDE experiments. To verify this proposed mechanism, a theoretical kinetic equation defining the current flux at steady-state can be derived and compared to the experimental results.

For a mediating redox polymer, which exhibits a through layer reaction and with efficient partitioning of substrate into the film (*vide infra*), the flux of electrochemical reaction, J_Σ , is given by ⁶³,

$$J_\Sigma = \Gamma K k_2 [\text{NO}^+] \quad (2.5)$$

where Γ is the surface coverage of the electro-active centres, K is the partition coefficient of the substrate between the electrolyte and the polymer film and k_2 is the second order rate constant for the cross-exchange reaction. The terms NO^+ and H^+ will be used in the following argument instead of $\text{NO}^+\text{HSO}_4^-$ and H_2SO_4 for convenience. The quantity, $[\text{NO}^+]$, may be approximated using the steady-state approximation

$$d[\text{NO}^+]/dt = k_1[\text{HNO}_2][\text{H}^+] - \{k'_{-1}[\text{NO}^+] + \Gamma K k_2[\text{NO}^+]\} = 0 \quad (2.6)$$

Solving for $[\text{NO}^+]$

$$[\text{NO}^+] = k_1[\text{HNO}_2][\text{H}^+] / k'_{-1} - k_2 \Gamma K \quad (2.7)$$

Combining with equation 2.5 we obtain

$$j_\Sigma = \Gamma K k_2 \{k_1 [\text{HNO}_2][\text{H}^+] / k'_{-1} + k_2 \Gamma K\} \quad (2.8)$$

Assuming that $k_2 \ll k'_{-1}$ the second term can be neglected and the total interfacial flux is given by

$$j_\Sigma = k_2 \Gamma K \{k_1 [\text{HNO}_2][\text{H}^+] / k'_{-1}\} \quad (2.9)$$

As $k_1 / k'_{-1} = K'_{\text{eq}}$ then

$$j_\Sigma = \Gamma K k_2 (K'_{\text{eq}} [\text{HNO}_2][\text{H}^+]) \quad (2.10)$$

So, the current at steady-state is given by

$$i_\Sigma = n F A K \Gamma k_2 K'_{\text{eq}} [\text{HNO}_2][\text{H}^+] \quad (2.11)$$

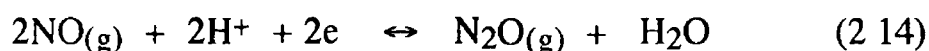
Consequently, the current for the mediated reduction of nitrite, at steady-state, should be first order with respect to $[\text{HNO}_2]$, $[\text{H}^+]$ and Γ

To check the validity of equation 2.11 and the proposed mechanism, the reaction orders with respect to $[\text{HNO}_2]$, $[\text{H}^+]$ and Γ were investigated experimentally. The reaction order for solution species may be evaluated using the following equation ⁶⁴

$$m_j = d \log i_{Lim} / d \log c_j \quad (2.13)$$

Where m_j and c_j are the reaction order with respect to species j and the concentration of j , respectively. A plot of $\log i_{Lim}$ vs $\log c_j$ should be linear with a slope equal to the reaction order for the species. The reaction order plot for $[HNO_2]$ can be seen in Fig. 2.9. This plot is linear and the slope is 1.0 ± 0.02 . This clearly suggests that the mediated reaction is first order with respect to $[HNO_2]$ as expected from the proposed reaction mechanism. In Fig. 2.10 the reaction order plot for $[H^+]$ can be seen, where the slope is 0.90 ± 0.03 . This indicates the first order dependence on proton concentration, again in agreement with the proposed mechanistic sequence. In Fig. 2.11, a plot of $\ln \Gamma$ vs $\ln i_{Lim}$ for modified electrodes at various surface coverages can be seen. The slope of this plot is 0.90 ± 0.05 . This indicates that the current flux due to the mediated reduction of nitrite is first order with respect to surface coverage.

These observations indicate that the reaction mechanism is a simple cross-exchange process from Os(II) to NO^+ to form $NO_{(g)}$. Knowing the complexity of the chemistry of oxides of nitrogen in acidic media^{59,60}, the simplicity of the mediated reaction is somewhat surprising. The second possible step, the liberation of $N_2O_{(g)}$, does not appear to occur at the redox polymer modified electrode under these conditions. The generation of $N_2O_{(g)}$ at conventional electrodes²⁸ occurs *via* a proton coupled reduction of $NO_{(g)}$ according to reaction 2.12



This reaction is thermodynamically favourable with an E° of 1.39 V vs SCE⁴⁹, and on the basis of free energy differences, should be mediated by the redox polymer⁴⁸. A possible explanation why this step does not occur at the modified electrode is that with the electrocatalytic polymers used here, the inter-site distance is of the order of 2.5 nm along the polymer chain⁶⁵ and each redox site provides a single electron. It is then unlikely that two nitric oxide molecules will be close enough to undergo

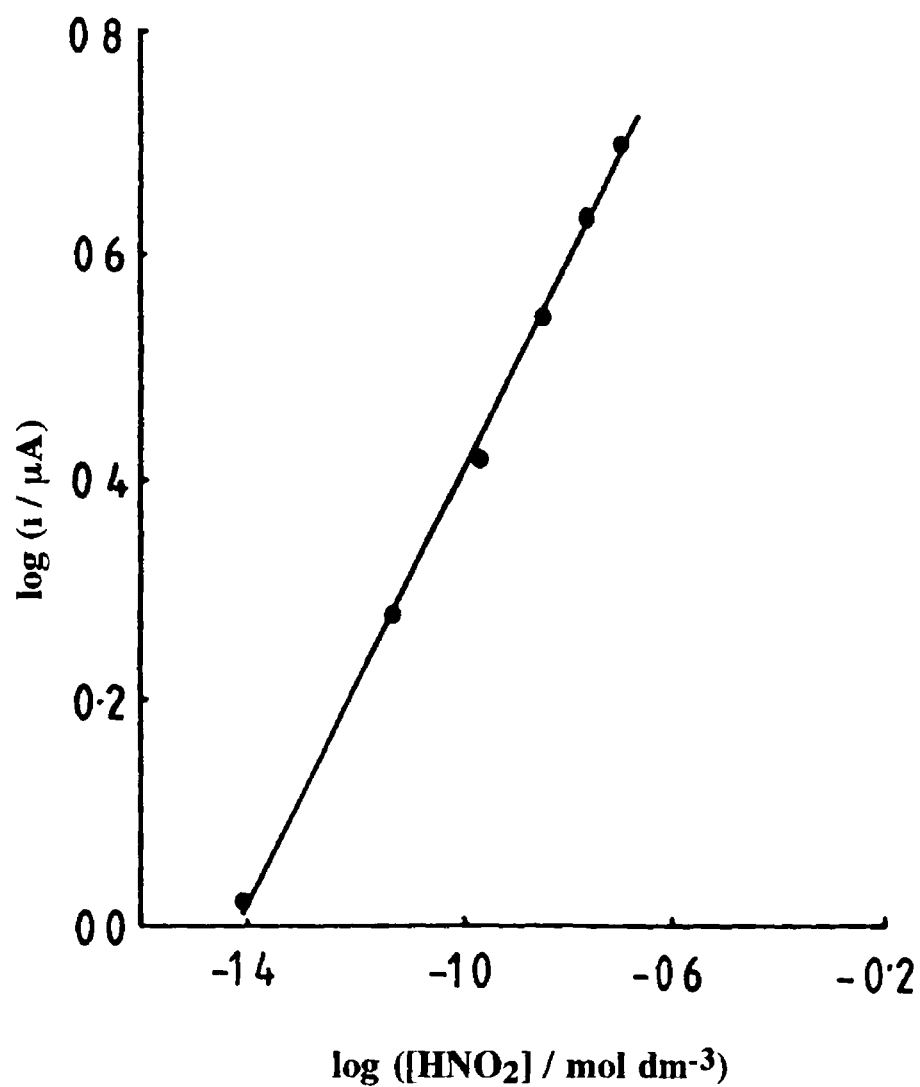


Fig 2.9 Reaction order plot for $[HNO_2]$, data obtained at a rotation speed of 500 rpm and sweep rate of 2 mV s^{-1} , the electrolyte was that for Fig 2.3 ($\text{pH} = 1.0$)

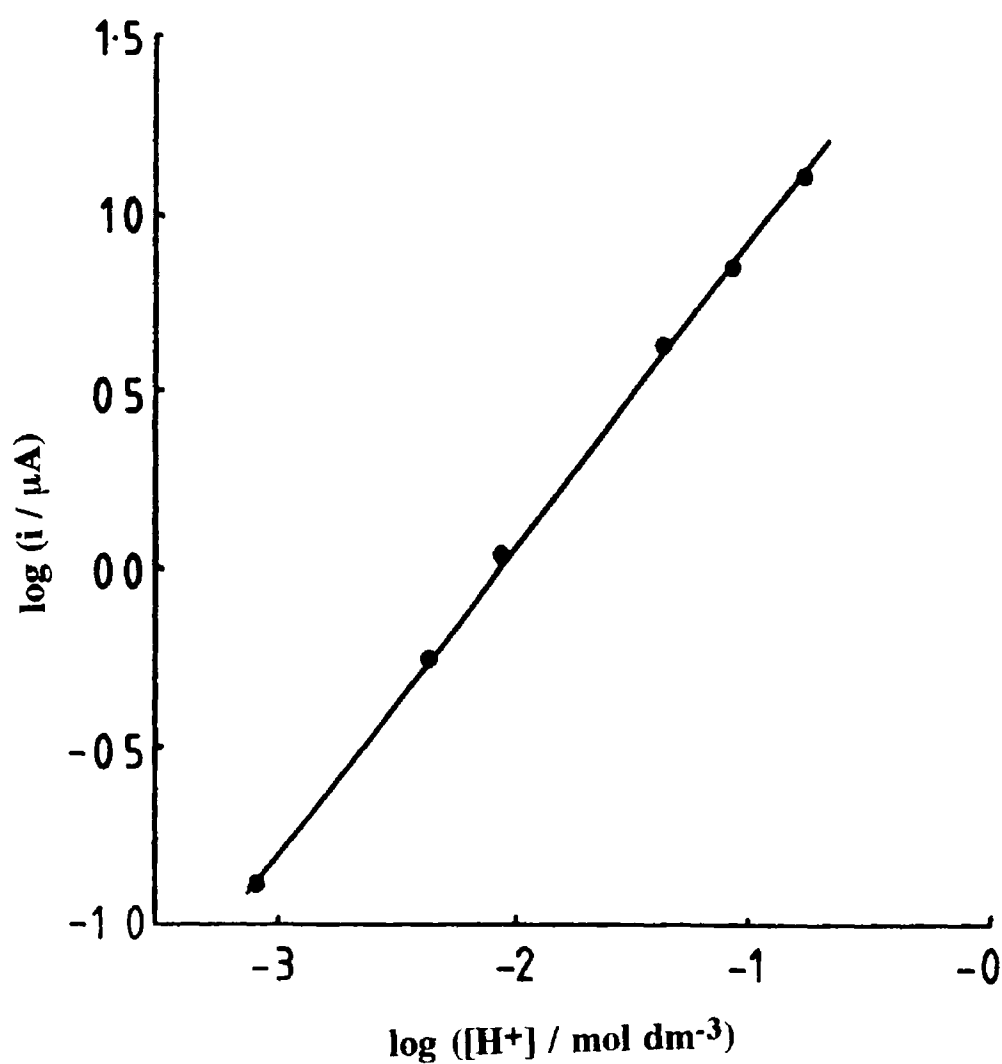


Fig 2 10 Reaction order plot for $[H^+]$, data obtained at a rotation speed of 500 rpm and sweep rate of 2 mV s^{-1} and the electrolyte as for Fig 2 3 $[HNO_2] = 0.02 \text{ mol dm}^{-3}$

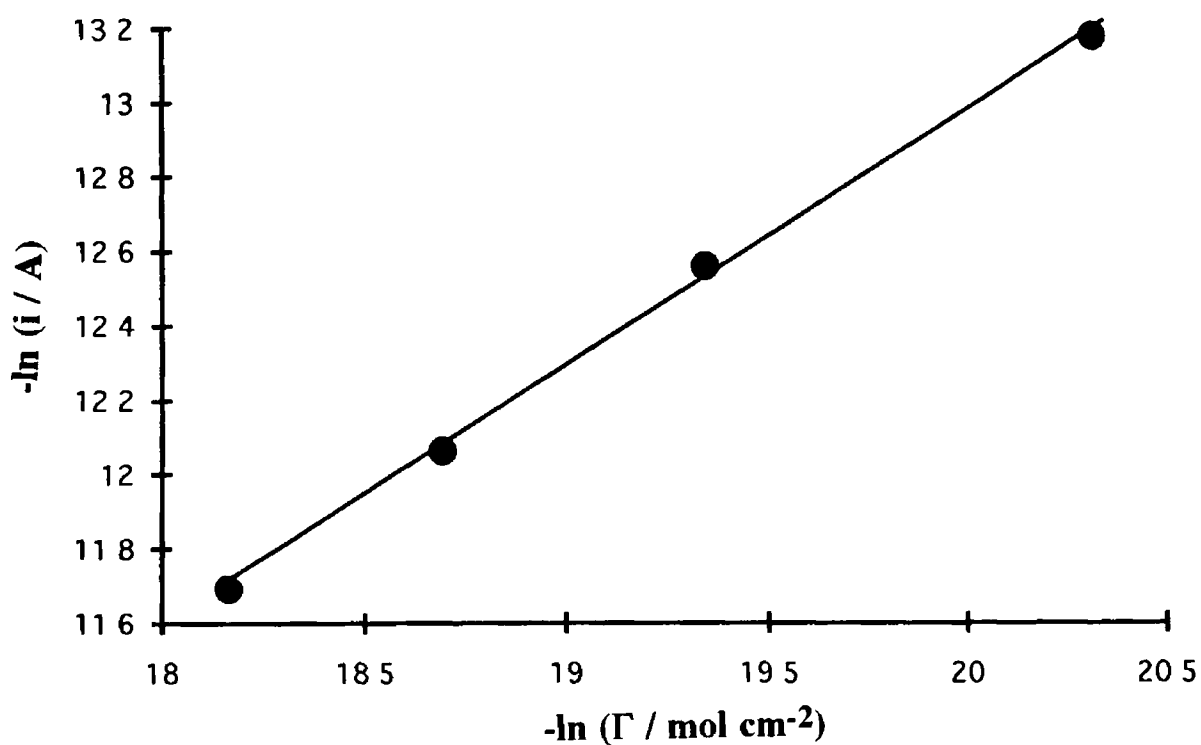


Fig 2.11 Reaction order plot with respect to Γ $[\text{HNO}_2] = 2.0 \times 10^{-3} \text{ mol dm}^{-3}$ in the usual electrolyte at a rotation speed of 500 rpm and a sweep rate of 5 mV s^{-1}

electron transfer and nuclei coupling simultaneously. At solid electrodes there would be an increased probability of such an event occurring due to the immobilisation of intermediates by adsorption. It is this type of multi-step reaction which exhibit sub-Marcusian electron transfer rates for which many electrocatalytic electrode surfaces are currently being developed. If such reactions require *a priori* a chemical linkage step, then polymer-bound mediator electrocatalysts may not offer the best approach. From the perspective of electroanalysis, whether this behaviour is an advantage or disadvantage depends on the application envisaged for the sensor and the possible interferences which may be encountered. The development of the redox polymers studied here is directed towards the acceleration of outer-sphere electron transfer reactions. As many reactions cannot occur *via* this route, this allows a certain degree of selectivity to be obtained compared to bare electrodes operating at the same potential.

Tafel analysis is also useful for delineating kinetic aspects of electrochemical reactions.⁶⁶ A Tafel plot constructed from data extracted from the rising portion of curves such as curve 2.8b is shown in Fig. 2.12. Tafel analysis was carried out with the knowledge that interfacial dynamics control electrode currents rather than mass transport (*vide infra*). The plot is linear, which under these conditions is indicative of irreversible electrode kinetics. Such plots reveal an average Tafel slope of -84 ± 5 mV decade⁻¹. This slope suggests a symmetry factor of 0.70 ± 0.05 which indicates considerable asymmetry of the energy barrier for reaction. This is hardly surprising given the gaseous nature of the reaction product and the irreversibility of the reaction. The experimentally obtained kinetic data concerning the mediated reaction are tabulated in Table 2.1.

2.3.3 Modified Electrode Kinetics

Theoretical treatments of the kinetics and transport limitations of electrocatalytic reactions at redox polymer modified electrodes have been proposed in order to delineate the precise kinetic regime pertaining at the modified electrode and to optimise electrode performance.^{63, 67-77} These theories have been discussed in detail in Chapter 1. The kinetic analysis presented here is based on the use of Koutecky-Levich plots.

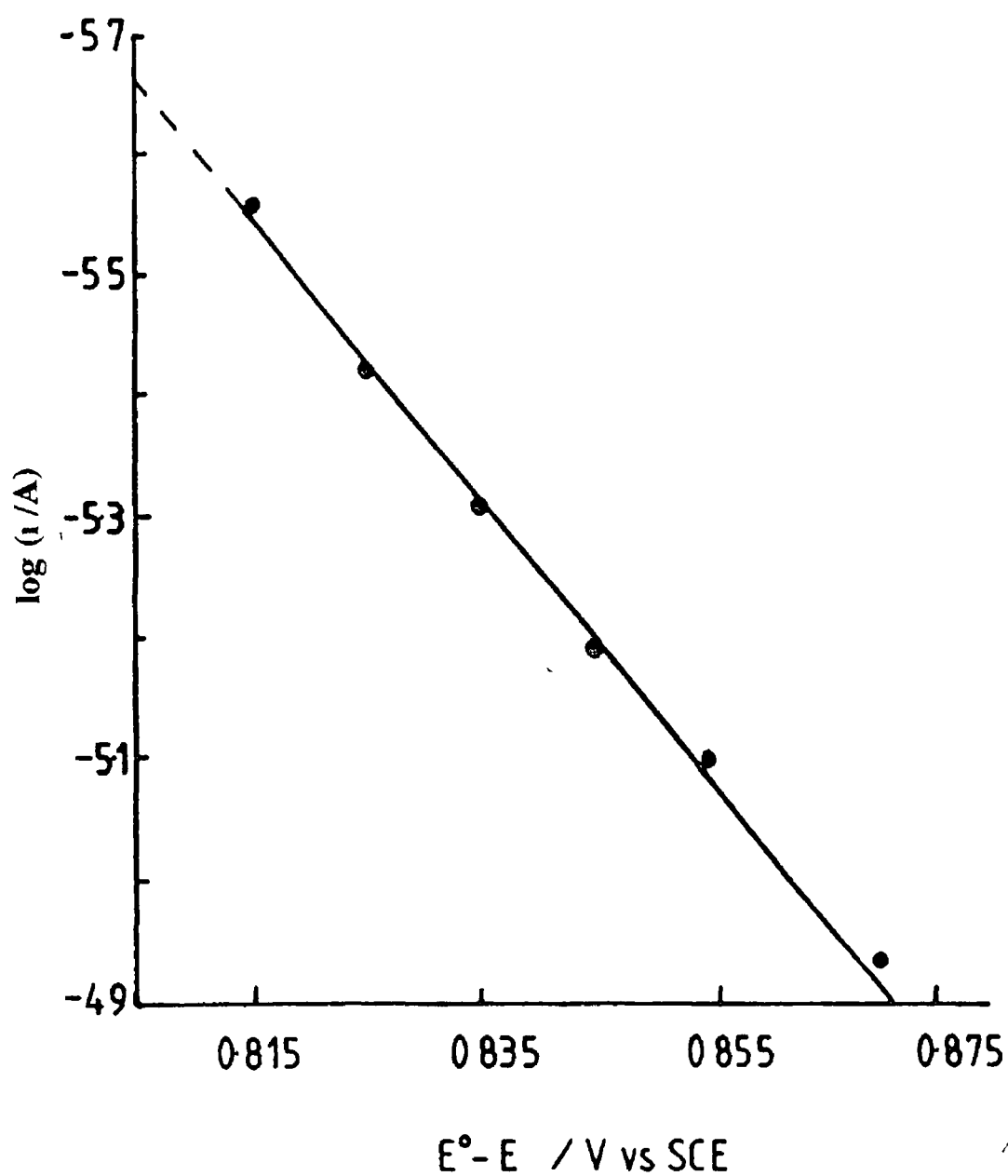


Fig 2 12 Tafel plot for the reduction of nitrite at a modified electrode, conditions as for Fig 2 6

Parameter	Experimental Value
Tafel slope/ mV decade ⁻¹	-84 ± 5
Symmetry factor, α	0.7 ± 0.05
Reaction order w r t [H ⁺]	0.9 ± 0.03
Reaction order w r t [NO ₂ ⁻]	1.0 ± 0.02
Reaction order w r t Γ	0.9 ± 0.05
rate constant, $k_2 / \text{dm}^3 \text{ mol}^{-1} \text{ cm s}^{-1}$	$9.4 \pm 2 \times 10^{-1}$

Table 2.1 Experimentally obtained kinetic parameters for the reduction of nitrite at the modified electrode

Levich plots obtained for the reduction of nitrite at modified electrodes with various polymer surface coverages can be seen in Fig 2 13 It is evident that the currents generated at the modified electrodes are independent of electrode rotation speed and therefore independent of the rate of substrate diffusion It seems likely that this unusual behaviour is a result of a slow rate of cross-exchange between the Os(II) and the nitrosonium ion

In Fig 2 14 typical Koutecky-Levich plots for various surface coverages of redox polymer can be seen These plots have zero slopes as expected from the Levich plots It can also be seen that the intercepts of these plots are inversely proportional to polymer surface coverages Increasing the surface coverage of the polymer results in an increase in the number of possible electrocatalytic sites at the electrode surface where the mediated reaction can take place In Table 2 2, values for k'_{ME} at various surface coverages are shown A plot of $\ln k'_{ME}$ vs $\ln L$ yield slopes of 0.9 ± 0.5 which demonstrates the first order relationship between layer thickness and the modified electrode rate constant ⁷⁷ These results indicates that the mediated reaction occurs throughout the entire polymer film, i.e. the L_k situation according to the notation of Alberly and Hillman and the equivalent situation, R, according to Saveant's notation ^{72,73} This kinetic regime corresponds to a situation where mass and electron transport within the film are fast in comparison to the rate of the cross-exchange reaction ⁶³ This supports the rapid charge transport rates observed for the polymer and the assumption that the rate of the cross-exchange reaction is slow

The reciprocals of the intercepts of the Koutecky-Levich plots yield the apparent modified electrode rate constant, k'_{ME} for the mediated reaction (see Table 2 2) ⁶⁸ The analytical expression relating k'_{ME} for the L_k kinetic regime to the second order rate constant, k_2 , for the cross-exchange reaction is given by ⁶³

$$k'_{ME} = k_2 K b_0 L \quad (2.15)$$

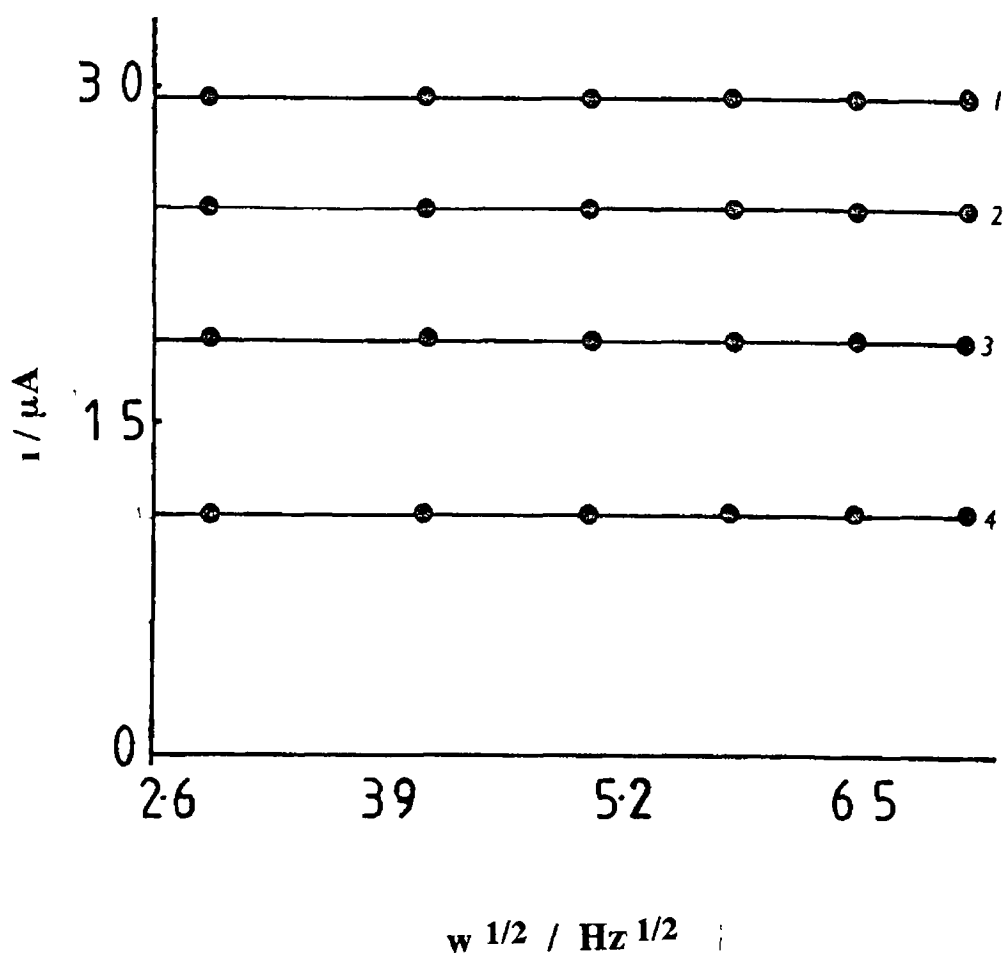


Fig 2.13 Levich plot for the reduction of nitrite at a modified electrode. Curves 1 – 4 represent $4.0, 3.0, 2.0$ and $1.0 \times 10^{-3} \text{ mol dm}^{-3}$ nitrite respectively in the usual electrolyte, surface coverage = $1.5 \times 10^{-9} \text{ mol cm}^{-2}$, sweep rate = 5 mV s^{-1}

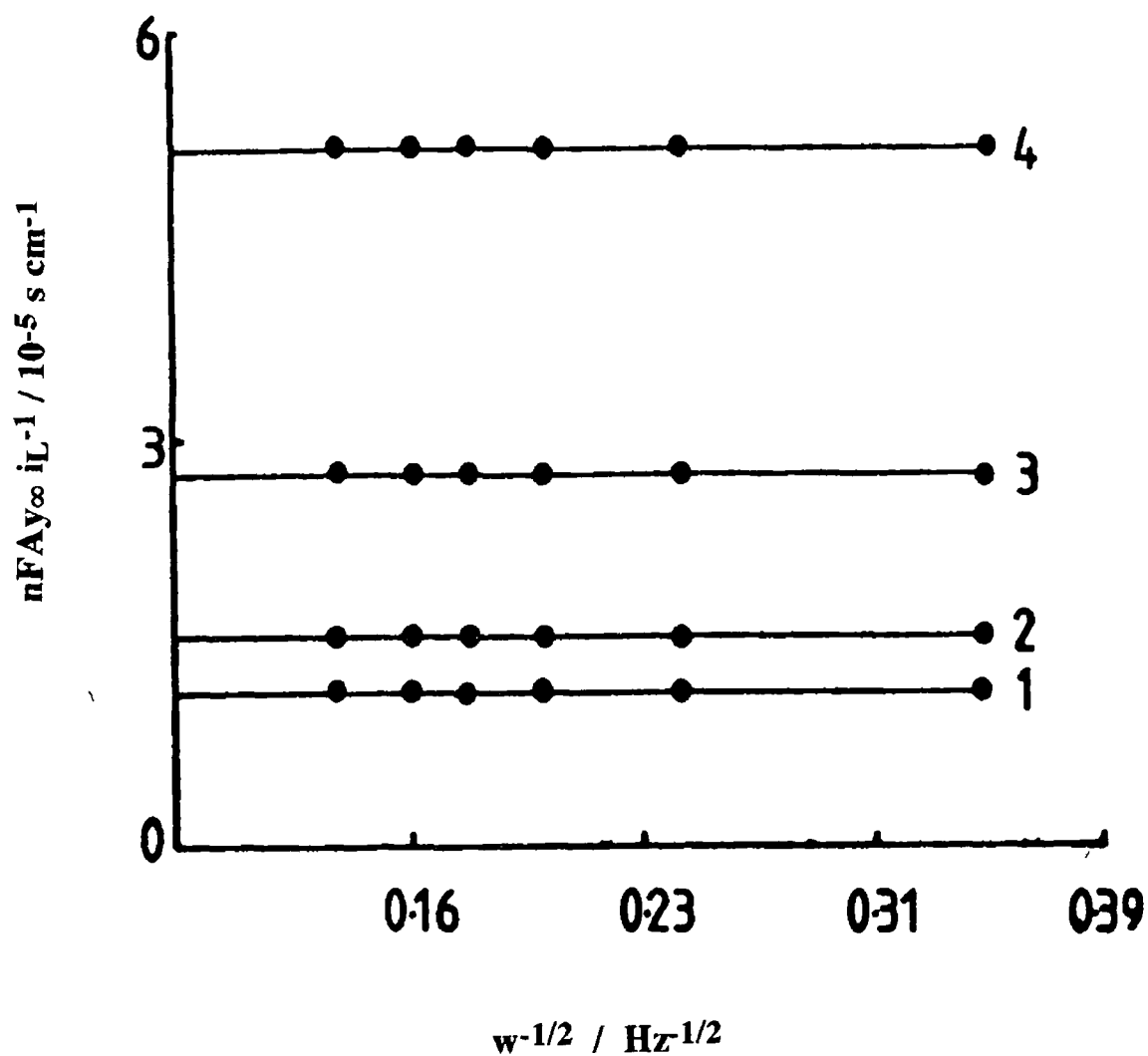


Fig 2 14 Koutecky-Levich plots for the reduction of $2.0 \times 10^{-3} \text{ mol dm}^{-3}$ nitrite at the modified electrode. Curves 1 – 4 represent surface coverages of 1.8×10^{-8} , 6.2×10^{-9} , 4.0×10^{-9} and $1.5 \times 10^{-9} \text{ mol cm}^{-3}$ respectively in the usual electrolyte, sweep rate = 5 mV s^{-1} .

The concentration of the electro-active centres in the redox polymer has been estimated from the dry density of the material determined by flotation in non-swelling solvents ⁴¹ to be, $b_0 = 0.7 \times 10^{-3} \text{ mol cm}^{-3}$. Swelling of the polymer by electrolyte has not been taken into account in this study although considerable swelling in sulphuric acid electrolyte is likely.

To obtain an estimate of the penetration of nitrite into the polymer film, the oxidation of nitrite at an electrode with a similar thickness of polymer was investigated. The currents obtained for the oxidation of nitrite at such electrodes were found to be almost equal to those obtained at bare glassy carbon electrodes, $10.9 \mu\text{A}$ vs $11.8 \mu\text{A}$ for the modified and unmodified electrode respectively. Since the oxidation of nitrite cannot be mediated by the osmium redox centres, oxidation occurs solely at the underlying glassy carbon. Therefore the concentration of nitrite within the film is equivalent to that in solution. As a result, we concluded that the partition coefficient, K , is likely to be close to 1, with rapid penetration and diffusion of substrate within the film. With this in mind, the second order rate constant k_2 was estimated to be $9.4 \pm 2 \times 10^{-1} \text{ dm}^3 \text{ mol}^{-1} \text{ cm s}^{-1}$ using a layer thickness calculated from the dry density of the polymer. This rate constant may be considered small when compared to the value $2.8 \times 10^3 \text{ dm}^3 \text{ mol}^{-1} \text{ cm s}^{-1}$ obtained for the reduction of $[\text{Fe}(\text{H}_2\text{O})_6]^{3+}$ with the same electrocatalyst ⁷⁸. This small value for k_2 along with the rapid D_{ct} and favourable partition ($K \approx 1$) is entirely consistent with the through film nature of the mediated reaction.

The PVP has a $\text{pK}_a \approx 3.3$ ⁷⁹. Therefore at pH 1.0, the polymer is fully protonated and swollen to give a polycationic chain network. The cation $[\text{Fe}(\text{H}_2\text{O})_6]^{3+}$ is known to penetrate the polymer film under similar conditions with a partition coefficient, $K \approx 0.2$. This level of penetration is surprising considering the considerable coulombic repulsion forces which exist. In fact, several successful perm-selective electrode modifiers have been developed on this principle ⁸⁰. It is interesting that the cationic nitrosonium ion can penetrate the polymer film very favourably with $K \approx 1$. This is likely to be a result of the formation of the ion association species, $\text{NO}^+\text{HSO}_4^-$, in the sulphuric acid electrolyte. As this species is neutral, no coulombic repulsion forces exist to hinder partition. It is, therefore, likely that it is the ion association species which penetrates the

k'_{ME} / $10^{-6} \text{ cm s}^{-1}$	L / nm	k_2 $\text{dm}^3 \text{ mol}^{-1} \text{ cm s}^{-1}$
1.9	25	0.110
3.5	65	0.076
6.2	90	0.098
11.5	180	0.091

Table 2.2 Dependence of k'_{ME} on polymer layer thickness
 $[\text{HNO}_2]$ was $2.0 \times 10^{-3} \text{ mol dm}^{-3}$ and $[\text{H}^+]$ was 0.1 mol dm^{-3}

polymer film and undergoes subsequent reaction. In addition, the apparent rapid transport of the species may be a result of the highly swollen nature of the polymer which promotes the diffusion of the species through the polymer.

It was seen in Fig. 2.8 that the current due to the mediated reduction of nitrite is significantly larger than the response obtained at bare glassy carbon. In this example, approximately a sixty-fold amplification in electrode response compared to the bare electrode was observed. Using equation 2.14, the catalytic advantage of a modified electrode compared to an unmodified electrode can be calculated.⁶³ The upper limit for stable surface coverage for the redox polymer investigated is about $1 \times 10^{-7} \text{ mol cm}^{-2}$ which corresponds to a film thickness of $\approx 2 \text{ }\mu\text{m}$. For such modified electrodes, with a substrate concentration of 5.0 mol dm^{-3} , the value for the kinetic current defined by Saveant^{69,70}, i_k , is $4.8 \times 10^{-5} \text{ A cm}^{-2}$. Under the same conditions, the current for the reduction of nitrite at a bare electrode (i_b) found experimentally at a freshly polished glassy carbon electrode was, $i_b \approx 0.10 \times 10^{-6} \text{ A cm}^{-2}$. This gives a catalytic advantage of

$$i_k / i_b \approx 4.8 \times 10^{-5} / 0.1 \times 10^{-6} \approx 480 \quad (2.16)$$

The magnitude of this catalytic advantage is considerable and is an impressive demonstration of the power of these modified electrodes. The use of such a thick polymer film (up to $\approx 2 \text{ }\mu\text{m}$) is possible but these are, however, subject to stability problems.

Using the diagnostic scheme of Alberly and Hillman⁷⁷, the initial observation that the limiting currents were independent of the rotation speed of the modified electrode would indicate that the kinetic regime was either S_{te} or LS_{te} , as in both cases electron transport would limit observed currents. In such situations, discrimination between these kinetic cases can be accomplished by lowering substrate concentration sufficiently to allow change over from S_{te} to S_k'' or LS_{te} to LS_k . For both the latter possible cases, the modified electrode rate constants, k'_{ME} would be independent of layer thickness, but S_k'' would have a first order

relationship with respect to the concentration of electro-active species within the film, b_0 , while LS_k would have a reaction order of $1/2$ ⁶³ It is quite clear from the observations made that the kinetic regime for the mediated reduction of nitrite is of the L_k type Applying the diagnostic scheme rigidly would lead to erroneous interpretation of the experimental data A discrepancy therefore exists in the diagnostic scheme between the independence of limiting current on electrode rotation speed and the possible causes of this independence This discrepancy can be accounted for as follows Alberly and Hillman considered that only the S_{te} or LS_{te} kinetic cases would result in i_{Lim} being independent of ω , i.e. the electron flux through the polymer becomes rate limiting at sufficiently high substrate concentration, so increasing the rate of substrate transport to the electrode surface is ineffective at increasing the current flux In the situation here the rate of the cross-exchange reaction, k , is current limiting, increasing the rate of substrate arriving at the electrode surface should increase the current response according to the Levich equation

$$i_{Lev} = 1.554 n A F D^{2/3} \nu^{-1/6} \gamma \omega^{1/2} \quad (2.17)$$

It is however possible that in situations where the rate of substrate transport to the electrode surface greatly exceeds the rate of electrolytic consumption, the limiting current will become independent of ω In the present study, such a situation appears to exist This can be described quantitatively, from the magnitudes of currents generated for nitrite reduction at the modified electrode (about $1 \mu A / mmol cm^{-2}$), the flux of substrate reacting at the electrode, J As given by Ficks first law, J is about $2 \times 10^{-10} mol cm^{-2} s^{-1}$ (depending on Γ and ω), therefore only a small portion of NO^+ arriving at the electrode is consumed and consequently the surface concentration of NO^+ is essentially equal to that in bulk of solution Effectively, the rate of the cross reaction is sufficiently slow to prevent concentration polarisation at the electrode surface, as a result the diffusion layer thickness, $\delta \rightarrow 0$ Under these conditions, increasing mass transport to the electrode surface does not result in the corresponding increase in electrode current as predicted by the Levich equation

In addition to the implications for kinetic diagnostics, the independence of mass transport control on modified electrode currents have important consequences for the development of electrochemical sensors. The inverse of the slope of the Koutecky-Levich plot is the Levich constant, Lev , which is given by ⁶³

$$Lev = 1.554 D^{2/3} \nu^{-1/6} \quad (2.18)$$

As the electrode currents are independent of ω (see Fig. 2.14), the two controlling mass transfer terms, D , the diffusion coefficient of the substrate in solution and ν , the kinematic viscosity of the electrolyte, do not exert any control over the limiting currents observed at the modified electrode. The significance of this is that the modified electrode may be applied for analysis in situations where the reactant flux is difficult to control precisely and in situations where the diffusion coefficient of the reactant may be variable due to variations in the sample matrix. This is of considerable advantage for nitrite sensors constructed from these electrodes, as in real analytical situations, the control of mass transport is frequently cited as one (*sic*) of the major limitations of amperometric sensors ⁸¹

When mass transport does not influence limiting currents, it can be shown that limiting currents under moderate hydrodynamic conditions can be related to known and easily measurable parameters. The pK_a for nitrous acid is 3.4 ⁶¹, therefore reaction 2.2 would lie completely to the right at pH 1.0. The Koutecky-Levich equation for nitrite reduction at the polymer modified electrode therefore is of the form

$$1/i_{Lim} = 1/nFA(K'_{eq}[HNO_2][H^+])k'_{ME} + 1/Lev \cdot nFA\omega^{1/2}(K'_{eq}[HNO_2][H^+]) \quad (2.19)$$

Since the right hand term does not influence limiting currents, this term can be eliminated. With $k'_{ME} = k_2 K \Gamma$ then the limiting current under the experimental conditions used here is given by

$$i_{Lim} = n F A k_2 K \Gamma (K'_{eq}[HNO_2][H^+]) \quad (2.20)$$

Since the terms $n F$, A , k_2 , K , Γ , K'_{eq} and $[H^+]$ are known and constant at constant pH, a measurement of the limiting current can be used directly to estimate the concentration of nitrite in solution without requirement for external calibration of the sensor

A difficulty concerning the investigation of redox polymer modified electrodes is the swelling encountered when immersed in electrolyte. This is caused by the mutual repulsion of fixed charged sites on the polymer chain. Such swelling may lead to stability problems and also present difficulties in fundamental investigations where the polymer film thickness needs to be known precisely. For the through film reaction studied here, any changes in surface coverage due to stripping of the polymer from the electrode surface will result in lowering of the sensor response. However, for a nitrite sensor based on the osmium polymer, a measurement of Γ *in situ* can account for such effects. In addition, differences in the degree of swelling which may occur depending on the sample matrix composition do not affect sensor response as Γ is the product $b_0 L$, and as L increases (or decreases) by swelling (contraction) then b_0 changes inversely, *i.e.* the value Γ remains constant irrespective of the degree of swelling.

2.3.4 Amperometry and Sensor Characterisation

The use of constant potential (amperometric) detection for electroanalysis has a number of advantages compared to voltammetric techniques. These include the absence of charging currents due to changing applied potential, continuous monitoring of solution species (real time analysis and information) and the ability to manipulate the signal for background correction and signal averaging. For the modified electrodes used here, the analytical signal is superimposed on the Os(II)/Os(III) redox wave in voltammetric techniques. Difficulty therefore exists in delineating the analytical signal especially at low concentrations of analyte. However, operation in the amperometric mode, according to the Nernst equation,

ensures that the Os(II)/Os(III) ratio is constant and the current required to establish this equilibrium is incorporated into the background signal. For these reasons, amperometry is best suited to the analytical application of redox polymer modified electrodes. Amperometry can be carried out in conventional electrochemical cells under hydrodynamic conditions (solution stirring or electrode rotation). Recently however, the introduction and widespread adoption of electrochemical flow cells for FIA and HPLC detection has resulted in a predominance of amperometric sensors being used in flowing solutions.⁸² The electrochemical flow cell used here is a planar flow-through electrochemical cell. The parameters which control the performance of the modified electrode for the amperometric analysis of nitrite will be discussed below.

2.3.4.1 Effect of Applied Potential

A hydrodynamic voltammogram showing the effect of applied potential over the range 0.075 V to 0.345 V vs. SCE on the sensor response in a thin-layer electrochemical flow cell to a 1.0×10^{-3} mol dm⁻³ solution of nitrite can be seen in Fig. 2.15. At a potential of 0.345 vs. SCE, the redox sites are predominantly in the pre-catalytic Os(III) state and therefore electrode currents are close to zero. As the potential moves closer to the $E_{1/2}$ of the redox couple an increased population of the catalytic Os(II) sites are generated within the film resulting in an increase in response to the test solution. As the potential moves more negative of the $E_{1/2}$, the redox sites are predominantly in the Os(II) state and the response begins to level off as the number of catalytic sites reaches a maximum. From these results, the optimum operational potential for detection of nitrite was found to be ca. 0.12 V vs. SCE. In the theories of mediated electrocatalysis^{63,72,73}, the concentration of electro-active sites within the polymer, (b_0) is assumed to be controlled by electrode potential according to the Nernst equation. In addition, for the kinetic regime L_k , the electrode response should be first order with respect to b_0 , which results in an increase in response as a function of applied potential.⁶³ The behaviour observed here is entirely in agreement with the predictions of the theoretical models.

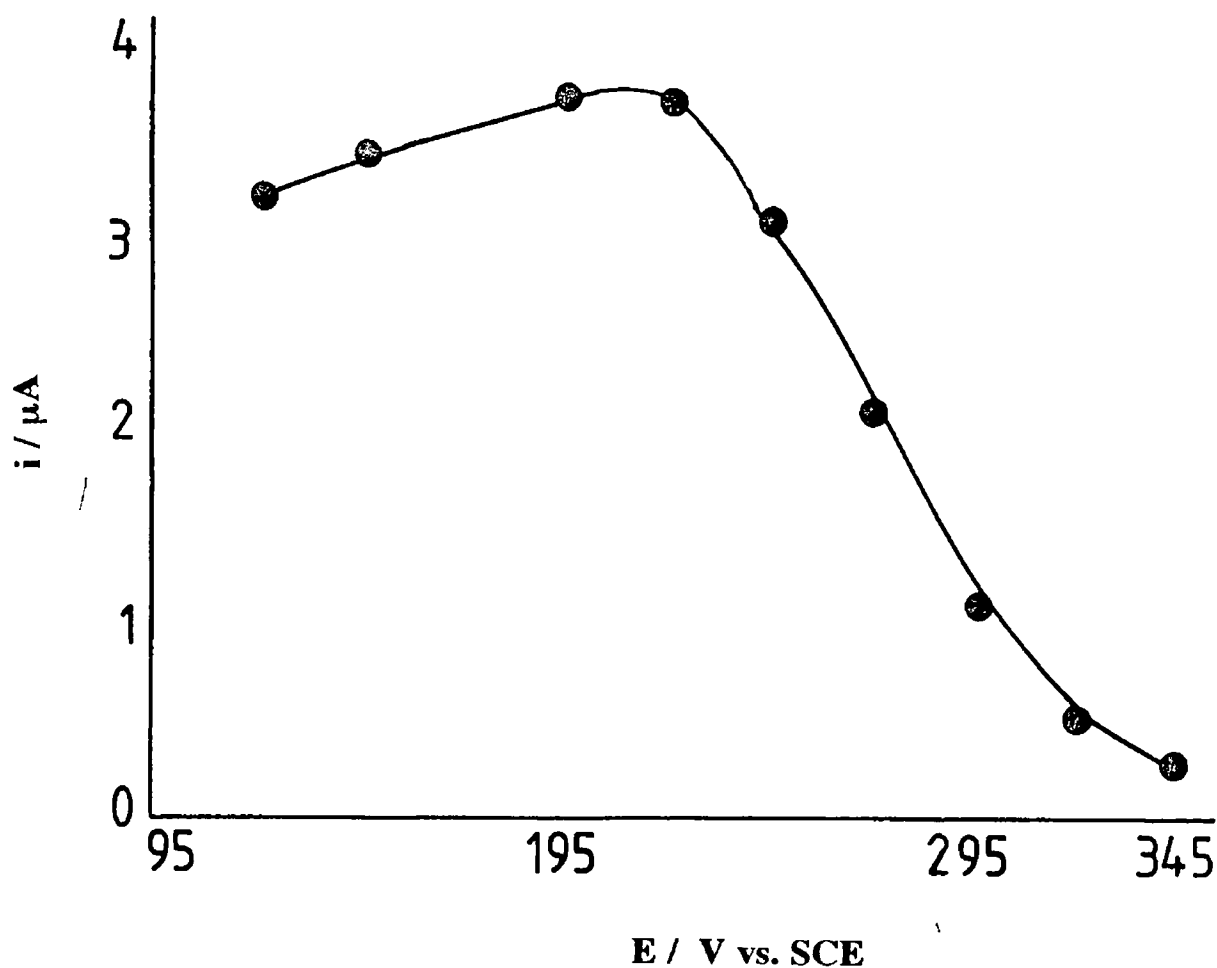


Fig 2 15 Hydrodynamic voltammogram for the reduction of nitrite at the modified electrode in the thin-layer electrochemical flow-cell Flow rate of the usual electrolyte was $0.5 \text{ cm}^3 \text{ min}^{-1}$ and nitrite concentration was $5.0 \times 10^{-3} \text{ mol dm}^{-3}$

2.3.4.2 Sensor Response Characteristics

Typical FIA traces for the detection of nitrite at the modified electrode in the thin-layer flow cell can be seen in Fig. 2.16a. At a flow rate of $1.0 \text{ cm}^3 \text{ min}^{-1}$ the peaks are sharp and well defined. Such peaks are ideal for the purposes of quantitative analysis. These traces also show the rapid response of the sensor to changes in nitrite concentration. The commonly used response time parameters are listed in Table 2.3. The time constant, τ , ($0.0 \rightarrow 63\%$ of maximum response) for the sensor was 1.7 s , while the rise time ($10 \rightarrow 90\%$ of maximum response) was 1.6 s . The response time ($0.0 \rightarrow 98\%$ maximum response) was found to be 2.4 s . Such rapid responses are important for a number of reasons. Firstly, the analytical through-put of the FIA procedure is a direct function of the speed of response of the monitoring devices. The theoretical analytical through-put for the sensor described here is $720 \text{ samples h}^{-1}$ based on the value for response time assuming a Gaussian peak profile. In reality, slight tailing of the peak is evident and this limits the actual through-put of $120 \text{ samples h}^{-1}$. This is still quite a large through-put. Fast response times are also required to maintain peak integrity in chromatographic applications. This is of particular importance in closely eluting analytes.⁸³ The precision of sensor response was also found to be excellent with a relative standard deviation (RSD) of 0.82% ($n=8$). This shows that the rapid passivation effect observed at bare glassy carbon electrodes for nitrite reduction is not problematic at the modified electrode. No deterioration in electrode response was observed over hundreds of determinations. This allows continuous re-use of the modified electrode. Many proposed modified electrodes are useful for only single determinations, therefore direct calibration is impossible under such restraints. For the sensor described direct calibration with standard solutions is possible.

A typical calibration plot in the concentration range 5.0×10^{-6} to $1.0 \times 10^{-2} \text{ mol dm}^{-3}$ nitrite can be seen in Fig. 2.17. The sensor response obeys a linear relationship with respect to nitrite concentration over this concentration range. The sensitivity (slope of calibration curve) of the modified electrode in the flow cell, at a flow rate of $0.1 \text{ cm}^3 \text{ min}^{-1}$, is $0.050 \mu\text{A mg}^{-1} \text{ cm}^3$ which is approximately equivalent to the sensitivity found for the batch procedure, which has a sensitivity of $0.06 \mu\text{A mg}^{-1} \text{ cm}^3$ (normalised with respect to Γ). Equivalent sensitivity in both procedures is probably due to the absence of mass transport control for

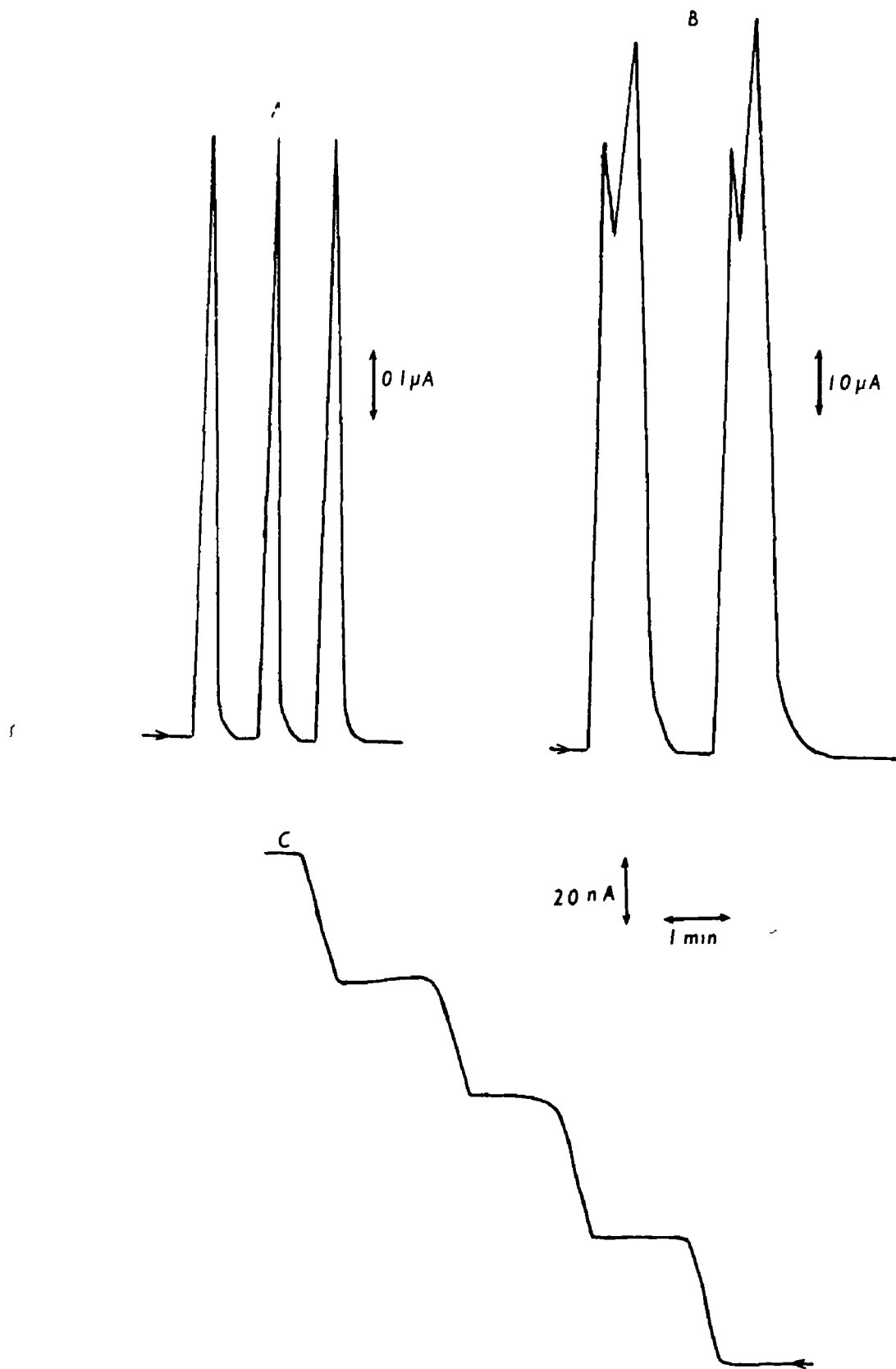


Fig 2 16 Typical modified electrode ($\Gamma = 1.0 \times 10^{-8} \text{ mol cm}^{-2}$) responses for the detection of $1.0 \times 10^{-2} \text{ mol dm}^{-3}$ nitrite in a thin-layer flow-cell at flow rates of (A) $1.0 \text{ cm}^3 \text{ min}^{-1}$ and (B) $0.1 \text{ cm}^3 \text{ min}^{-1}$. Trace (C) represent modified electrode ($\Gamma = 1.0 \times 10^{-9} \text{ mol cm}^{-2}$) response in a conventional electrochemical cell to $1.0 \times 10^{-3} \text{ mol dm}^{-3}$ nitrite. Electrolyte for both as for Fig 2 3. Applied potential for both was 0.12 V vs SCE.

Parameter	Value
Sensitivity Batch	0.19 $\mu\text{A } \mu\text{g}^{-1} \text{ cm}^3$
FIA	0.05 $\mu\text{A } \mu\text{g}^{-1} \text{ cm}^3$
Linearity	5.0 $\times 10^{-6}$ to 1.0 $\times 10^{-2} \text{ mol dm}^{-3}$
LOD (S/N = 2/1) Batch	0.023 ng cm^{-3}
FIA	0.23 ng cm^{-3}
Precision (n=8)	0.83 % RSD
Response Time	2.4 s
Rise Time	1.6 s
Time Constant (τ)	1.7 s
Sample Through-put	720 h^{-1} * 129 h^{-1} #

* through-put calculated on the basis of response time
assuming Gaussian peak profile

actual measured through-put

Table 2.3 Table of sensor parameters. All parameters were estimated in usual electrolyte and at a flow rate of 1.0 $\text{cm}^3 \text{ min}^{-1}$

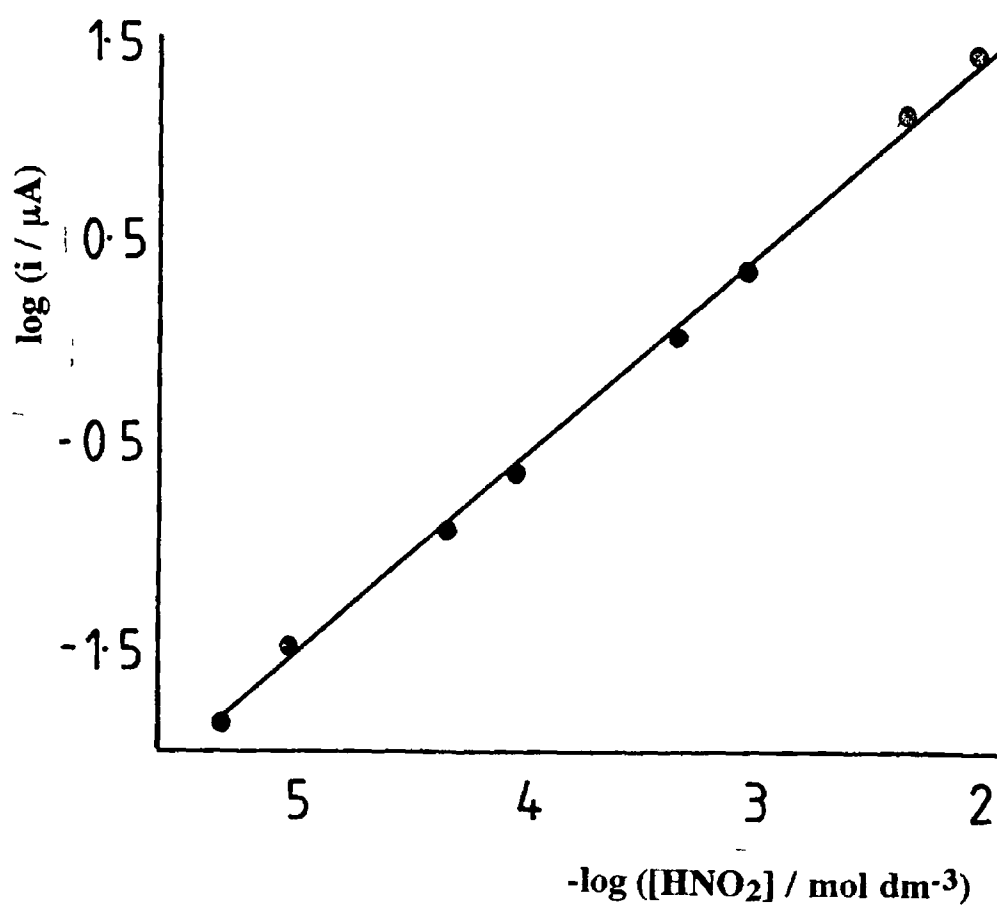


Fig 2 17 Typical calibration plot for FIA responses towards nitrite The flow rate of the usual electrolyte was $0.2 \text{ cm}^3 \text{ min}^{-1}$ and the applied potential was 0.12 V vs SCE

both modes of operation. Correlation coefficients, r , were typically ≥ 0.999 for the sensor responses in the flow system. The linearity extends to $1 \times 10^{-1} \text{ mol dm}^{-3}$, however the polymer film is unstable at these concentrations. The polymer is quickly stripped from the electrode surface presumably due to large quantities of gas (nitric oxide) being generated within the polymer film. Fortunately, instability is not encountered at lower nitrite concentrations. Integration of the charge passed for the response for a $1 \times 10^{-2} \text{ mol dm}^{-3}$ solution in the thin-layer flow cell at a flow rate of $1.0 \text{ cm}^3 \text{ min}^{-1}$ suggests that less than 0.1% of the nitrite in the sample plug undergoes conversion. This is somewhat less than normally encountered with amperometric sensors. This again is due to the slow kinetics of the reaction. This level of conversion would generate 6×10^{-11} moles of nitric oxide, which at standard temperature and pressure, (STP), would occupy a volume of $4.5 \times 10^{-6} \text{ cm}^3$. For a typical $1 \times 10^{-8} \text{ mol cm}^{-2}$ surface coverage, the volume of gas produced would be significantly greater than the volume of the polymer (calculated from dry density of the unswollen polymer) film, $1 \times 10^{-6} \text{ cm}^3$. As the mediated reaction occurs within the film, it is therefore not surprising that at high nitrite concentrations polymer stability problems are encountered. The linear range of this sensor is impressive when compared to existing spectrophotometric and electrochemical procedures.^{1,10-15} This large linear range is a function of the kinetic control of the sensor response. The limit of detection for the sensor was found to be $0.23 \text{ } \mu\text{g cm}^{-3}$ in the FIA system and $0.023 \text{ } \mu\text{g cm}^{-3}$ in conventional electrochemical cells. These LOD's are generally better than those observed for spectrophotometric procedures.¹⁰

It was mentioned earlier that amperometry can be performed in conventional electrochemical cells under hydrodynamic conditions. In Fig 2.16c traces for the amperometric detection of nitrite under such conditions can be seen. The sensitivity of the sensor under these conditions is $0.06 \text{ } \mu\text{A mg}^{-1} \text{ cm}^3$, similar to that obtained under flow conditions. These results again demonstrate the fast response time of the sensor. In addition they show the stability of response at steady-state and the additive nature of the responses, features which are prerequisites for the development of successful sensors.

At lower carrier electrolyte flow rates, ($\leq 0.1 \text{ cm}^3 \text{ min}^{-1}$), the FIA peaks were found to be broad and in the form of a doublet (Fig 2.16b).

Depending on the flow rate of the electrolyte, the resolution of the two peak components can be varied. Such peaks have limited utility for analytical application. The origin of the doublet behaviour however gives some confirmation to the proposed mechanism of the mediated reaction (*vide supra*). In order to verify that the doublet was an intrinsic property of the mediated reduction of nitrite rather than an artifact of the flow system, different concentrations of Fe(III) were injected under identical experimental conditions and single sharp peaks for the reduction to Fe(II) were recorded. Also nitrite and ascorbic acid were oxidised at 1.0 V vs SCE and single sharp peaks were observed in both cases. This clearly showed that splitting of the sample plug was not occurring. By plotting hydrodynamic voltammograms for both components of the peak, (Fig 2.18a and 2.18b), two waves corresponding to two distinct time resolved electrode processes can be observed. The first component wave (Fig 2.18a) is identical to that found at higher flow rates (Fig 2.15) and is centred at the $E_{1/2}$ of the electrocatalyst *i.e.* 0.25 V vs SCE. This demonstrates that this process is mediated by the osmium sites in the polymer film. The wave for the second process is centred more negative at 0.20 V vs SCE, indicating that the osmium sites are not mediating this process. When it is considered that the two processes are time resolved and that the charge passed for the secondary process is $\approx 20\%$ of the charge passed for the first process and mediation is not occurring, it seems likely that the secondary process occurs at the underlying glassy carbon surface and the substrate for the secondary process is that product formed close to the electrode/polymer interface by the film (first) reaction. In order to confirm the possibility that the product formed by the mediated reduction of nitrite is electro-active at the applied potential used, a second bare glassy carbon electrode was placed down stream of the working electrode and of a bare glassy carbon electrode. This down stream electrode acts as a collector electrode akin to the ring in rotating ring disc electrode experiments,⁸⁴ It was found that currents at the collector electrode were 10-30% larger when a modified electrode was up-stream compared to an up-stream unmodified electrode showing the formation of an electro-active product. From this we believe that the first process under these conditions is the outer sphere electron transfer process from the Os(II) sites in the film to the nitrosonium ion forming nitric oxide, reaction 2.4, and the secondary process is the subsequent reduction of nitric oxide generated at the electrode/polymer interface to form nitrous oxide,

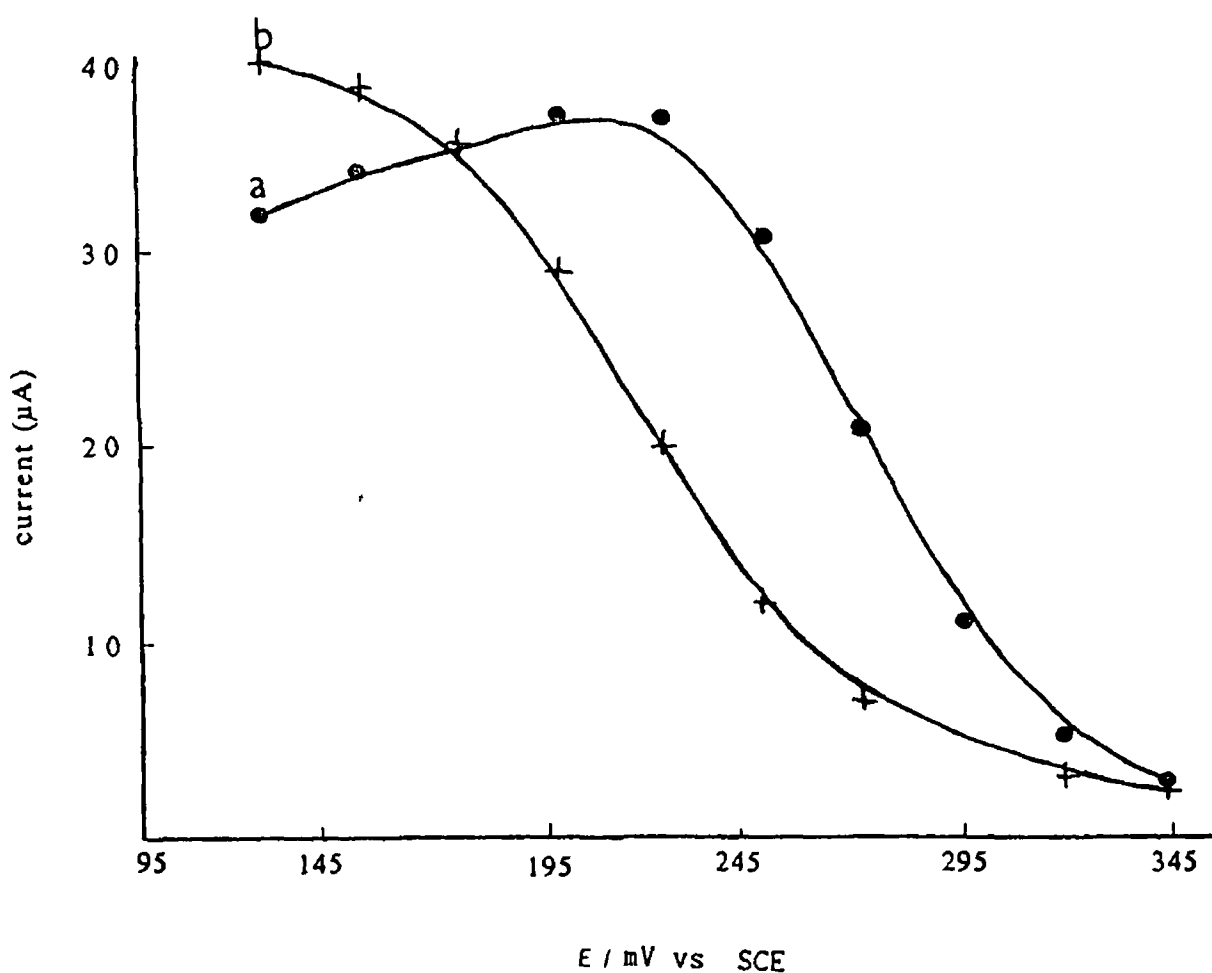


Fig 2 18 Hydrodynamic voltammogram for the two-step reduction of $5.0 \times 10^{-3} \text{ mol dm}^{-3}$ nitrite in the thin-layer flow-cell. Curve 1 represents the initial mediated reaction while curve 2 shows the subsequent reaction at glassy carbon. Surface coverage = $1.0 \times 10^{-8} \text{ mol cm}^{-2}$, flow rate = $0.05 \text{ cm}^3 \text{ min}^{-1}$, applied potential = 0.12 V vs SCE , electrolyte as for Fig 2 3.

reaction 2.13. This overall proposed reaction process involves six protons and four electrons, which is the stoichiometry known to exist for nitrite reduction at conventional electrodes.¹⁹ These results are consistent with the proposed reaction mechanism and the belief that nitric oxide does not undergo reduction within the polymer film. It must be stressed that this behaviour has only been observed for electrodes placed in thin-layer flow cells at very low carrier electrolyte flow rates, and therefore does not constitute an operational problem.

2.3.4.3 Effect of Carrier Electrolyte Flow Rate

A graph of sensor response vs. carrier flow rate is shown in Fig. 2.19. It can be seen that an increase in flow rate causes an exponential decrease in sensor response. Low flow rates are therefore required for maximum sensor responses but significant peak broadening is evident which would limit the analytical throughput. Electrochemical detectors can be classified as mass rate detectors, i.e. the response is a function of the quantity of analyte passing through the detector per unit time ($i = \partial Q / \partial t$).⁸² In addition, increasing the flow rate decreases the diffusional layer thickness at the electrode surface.⁸⁵ Both of these processes should result in an increase in electrode response with increasing flow rate. This has been observed for the oxidation of nitrite at a ruthenium analogue modified electrode.⁸⁶ Inverted behaviour as observed for the reduction of nitrite, has been observed for other modified electrodes^{87,88} and in the case of a copper modified electrode⁸⁷, it was attributed to slow reaction kinetics. The behaviour observed here can also be attributed to slow reaction kinetics. The nitrite samples are introduced into the flow system as a neutral solution, whereupon they mix with acidic carrier electrolyte forming $\text{NO}^+ \text{SO}_4^-$. The residence time in the pre-detector mixing tubing will be different at each flow rate and therefore the extent of conversion may be different. It is the kinetics of this step or possibly the actual rate of the cross-exchange reaction which may be responsible for the trend observed. As acid-base reactions are known to be fast, it seems probable that the rate of the mediated reaction is responsible for the response decrease. At rotating disc electrodes, the electrode response was independent of the hydrodynamic conditions employed. It would therefore be expected that in the thin-layer flow cell variation in the electrolyte flow

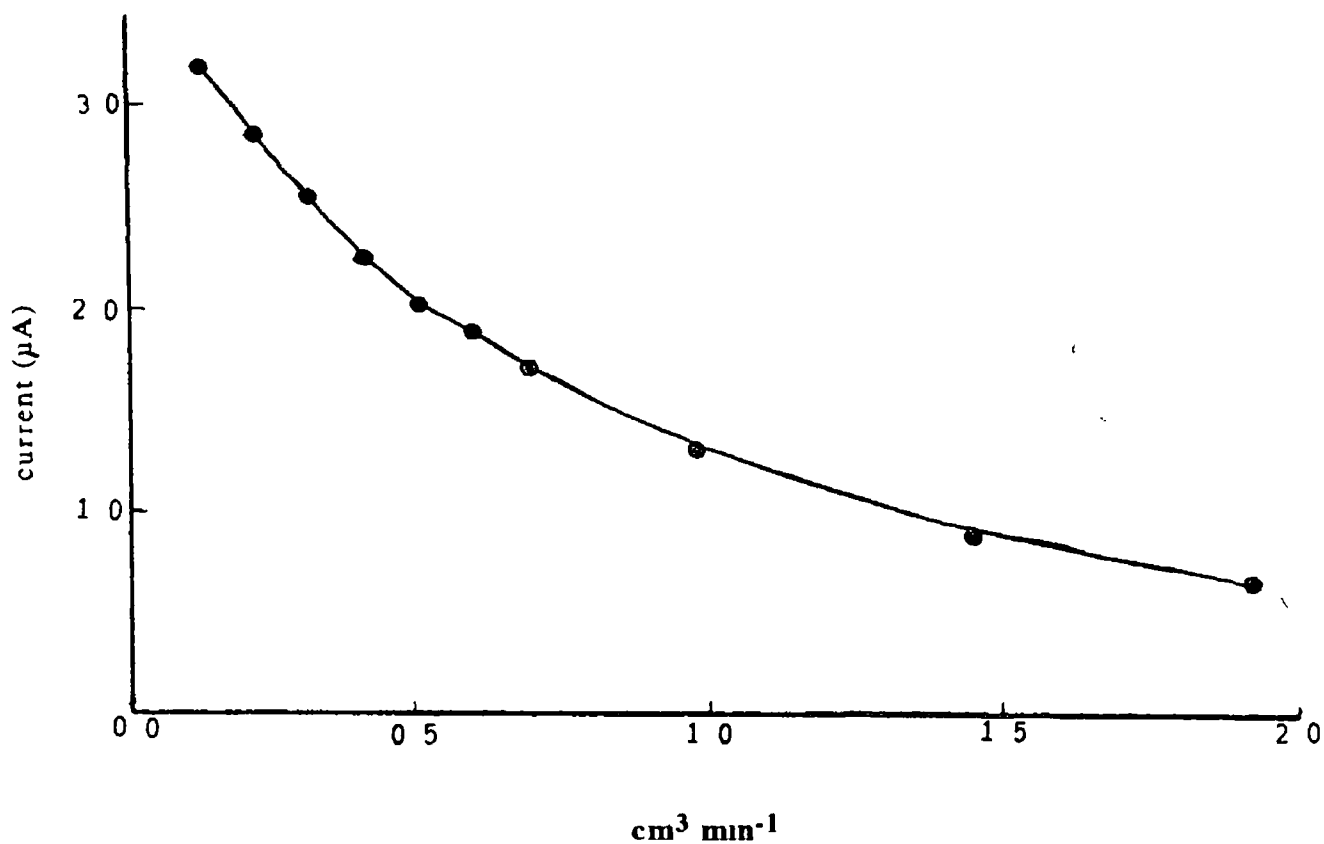


Fig 2 19 The effect of electrolyte flow rate on modified electrode response The nitrite concentration was $1.0 \times 10^{-3} \text{ mol dm}^{-3}$ and the surface coverage was $2.0 \times 10^{-8} \text{ mol cm}^{-2}$

rate should have minimal influence on sensor response. The reason why this is not the case is due to the transient nature of the FIA signal compared to the steady-state response from the rotating disc electrode. It should be noted that at a flow rate of $0.1 \text{ cm}^3 \text{ min}^{-1}$ the electrode sensitivity is similar to that observed for batch type experiments. This may indicate, at this flow rate, near steady-state conditions in the flow-cell. One significant disadvantage of the marked dependence on flow rate is the need to provide stable reproducible flow conditions under operational conditions.

2.3.4.4 Effect of Carrier Electrolyte pH

The electrochemical reaction was seen to have a first order relationship with respect to proton concentration, as this determines the population of NO^+ available for detection. It is therefore expected that the pH of the carrier electrolyte would significantly influence the response of the sensor. In these experiments, the ionic strength of the electrolyte was kept constant as pH was varied. It was found that at pH 4.0 the response of the sensor to a $2 \times 10^{-3} \text{ mol dm}^{-3}$ solution of nitrite was $0.063 \mu\text{A}$, while at pH 1.0 the response rises dramatically to $2.8 \mu\text{A}$. For this reason, low pH electrolytes are required to ensure maximum sensitivity. These results are in agreement with the behaviour observed in the conventional macro-electrochemical cell.

2.3.4.5 Effect of Polymer Surface Coverage

In Fig. 2.20 a plot of $\ln i$ vs $\ln \Gamma$ for the modified electrode in the thin-layer flow cell is given. It is evident that this plot is linear and the slope is 0.93 ± 0.3 which indicates a first order relationship between sensor response and the surface coverage of the redox polymer. These results indicate that the entire polymer film is electro-active in the flow cell. Considering the residence time of the sample plug in the flow cell is $\approx 15 \text{ s}$ this also indicates that the partition and diffusion of the analyte in the film is rapid. For a surface coverage of $2 \times 10^{-9} \text{ mol cm}^{-2}$, the response to a $5 \times 10^{-3} \text{ mol dm}^{-3}$ solution of nitrite was $14.1 \mu\text{A}$ while at the unmodified electrode the response was $0.2 \mu\text{A}$, representing a seventy fold

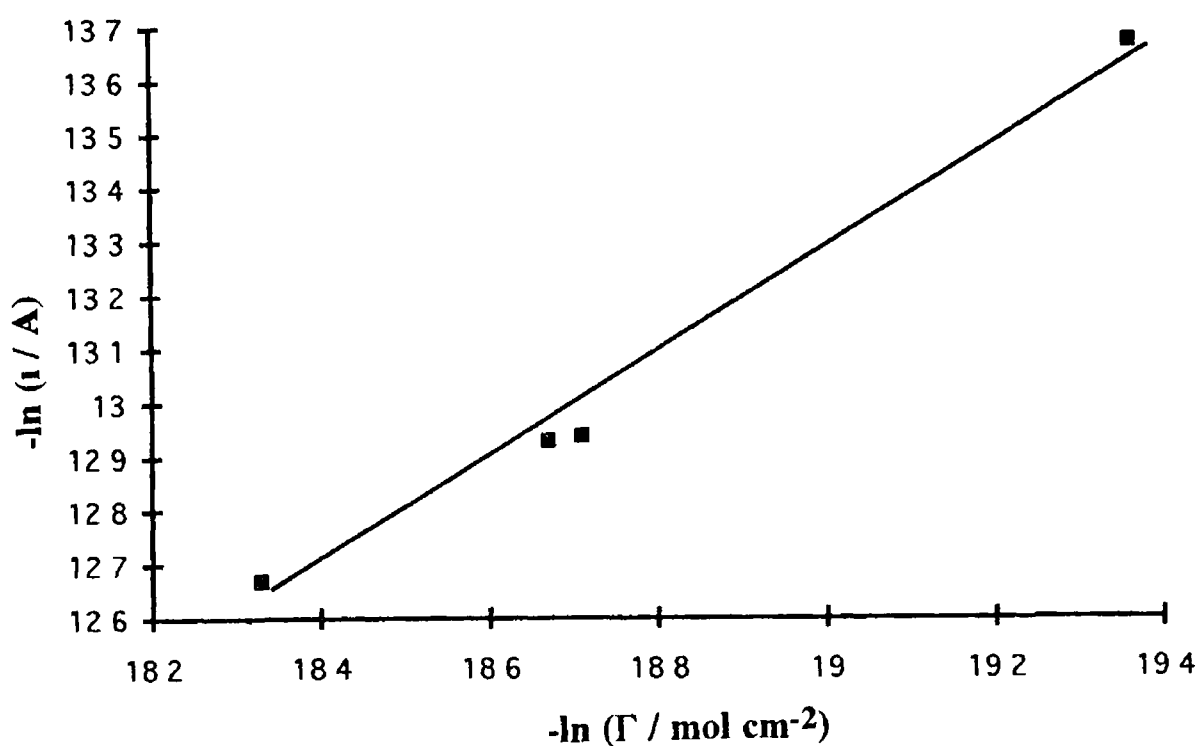


Fig 2 20 The effect of surface coverage on electrode response to nitrite in the thin-layer flow-cell. The usual electrolyte was used at a flow rate of 0.2 cm min^{-1} , nitrite concentration was $1.0 \times 10^{-3} \text{ mol dm}^{-3}$ and the applied potential was 0.120 V vs SCE .

amplification in electrode response Both these observations are in agreement with those observed in the conventional electrochemical cell

2.3.5 Analysis of Nitrite in Saliva

The nitrite content of a human saliva sample was determined using a batch type experiment with the modified electrode The saliva samples were introduced to the electrochemical cell directly following sonication to remove air bubbles Two sub-samples ($n=2$) of a single sample were analysed and the concentration found to be 5.54 ± 0.01 and 5.53 ± 0.01 $\mu\text{g cm}^{-3}$ for each sub-sample Although the nitrite content of saliva is variable, these results are comparable with those reported in the literature^{89,90} Saliva contains appreciable quantities of protein which is notorious for passivation of electrode surfaces This was, however, not observed for the analysis carried out here This may be attributed to the lack of adsorptive properties of the redox polymer and possibly to the size exclusion effects preventing transport of the protein to the electrode surface The acidic conditions used also induced a visible precipitation of proteins which prevents passage to the electrode surface In addition, the viscosity changes in the electrolyte due to the added sample did not appear to affect sensor sensitivity This property was predicted on the basis of the kinetic results where the rate of mass transport did not affect limiting currents Another advantage of the analytical approach developed here is the minimal sample preparation required Usual methodology involve protracted extraction procedures The effect of interferences such as ascorbic acid, Fe(III) and Cu(II) will be discussed in detail in chapter 6

2.4. Conclusions

It has been shown in this chapter that the electrochemical reduction of nitrite in acidic electrolyte at conventional electrodes is kinetically slow, causes surface passivation and is therefore of little use analytically It has also been shown that the redox polymer $[\text{Os}(\text{bipy})_2(\text{PVP})_{10}\text{Cl}]\text{Cl}$ is an effective electrocatalyst for the reduction of nitrite under acidic conditions It was observed that the rates of charge transport and substrate transport

within the polymer film are rapid and that the rate of the cross-exchange reaction is comparatively slow. Experimentally, this leads to the kinetic regime L_k , which is in agreement with the theoretical models describing mediated electrocatalysis at redox polymer modified electrodes. It is also evident that these kinetic models are very useful in predicting the behaviour of modified electrodes in thin-layer flow cells. Although the rate of cross-exchange can be considered slow, the kinetics of this reaction are considerably improved compared to the unmodified electrode. The catalytic advantage for a 1 μm film of ≈ 480 is large and is a clear demonstration of the catalytic activity of these materials.

The mechanism of the mediated reaction appears simple in comparison to the complex electrochemistry known to exist at conventional electrodes. The reaction is likely to involve simple electron transfer to the nitrosonium ion in the form of $\text{NO}^+\text{HSO}_4^-$. This allows the reaction to proceed cleanly in a single one electron step without adsorption of intermediates and the absence of passivation effects normally seen at conventional electrodes. The huge catalytic advantage and the clean charge transfer process allows the construction of sensors which are sensitive and can be directly calibrated and used for multiple determination.

It was also observed that the nuclei coupling reaction forming N_2O is not mediated by the osmium redox sites, although this is thermodynamically favourable. This is probably related to the non-adsorptive properties of the polymer and considerable inter-site distance. This suggests that only simple electron transfer reactions are feasible at these electrodes, so, those substrates requiring more involved reaction pathways are excluded from reaction. This is advantageous as it excludes many possible reactions which may interfere with the sensor response at any possible operational potential.

The independence of the modified electrode response on the hydrodynamic conditions employed in the RDE experiments conveys distinct advantages to the sensor described here. The sensor can be applied in situations where the viscosity of the electrolyte is variable and consequently the diffusion coefficient of the analyte is variable. In addition, the need for precise control of hydrodynamic conditions is not of great importance in conventional cells. As the mass transport term of the Koutecky-Levich equation can be eliminated, the response of the sensor

1

can be directly related to nitrite concentration without need for direct calibration. It is generally accepted that rapid electrochemical kinetics are important for the development of sensitive and selective electrochemical sensors. However, as shown here slow reaction kinetics can have some desirable properties which may make operation and construction of this sensor simple. Because of these advantages and as nitrite is an important analyte, (NO_3^- and NO_x are determined following conversion to NO_2^-), this sensor may be commercially attractive.

2.5. References

- 1 R J Elliot, A G Porter, *Analyst*, 1972 96 522
- 2 T Ohta, Y Arai, S Takitani, *Anal Chem* , 1986 58 3132
- 3 H Ohshima, M Friesen, I O'Neill, H Bartsch, *Cancer Lett* , 1983 20 183
- 4 M R Rhodes, T J Meyer, *Inorg Chem* , 1988 27 4772
- 5 W R Murphy, K Takeuchi, M H Barley, T J Meyer, *Inorg Chem* , 1986 25 1041
- 6 A Trojanek, F Opekar, *J Electroanal Chem* , 1986 214 125
- 7 L Guanghan, H Zhike, L Yuling, *Talanta*, 1992 39 123
- 8 A Otsuki, *Anal Chim Acta* , 1978 99 375
- 9 M Okada, H Miyata, K Toei, *Analyst*, 1979 104 1195
- 10 D Chen, M D Luque de Castro, M Valcarcel, *Analyst*, 1991 116 1095
- 11 F C Snell, C T Snell, *Colorimetric Methods of Analysis*, Princeton, 1936, p 644
- 12 H Barnes, A R Folkard, *Analyst*, 1951 76 599
- 13 T P Lynch, *Analyst*, 1988 113 1597
- 14 S Nakashima, M Yagi, M Zenki, A Takahashi, K Toei, *Anal Chim Acta* , 1983 155 263
- 15 F Canete, A Rios, M D Luque de Castro, M Valcarcel, *Analyst*, 1988 113 739
- 16 J E Newbery, M P Lopez de Haddad, *Analyst*, 1985 110 81
- 17 G Norwitz, P Keliher, *Analyst*, 1987 112 903
- 18 D L Ehman, D T Sawyer, *J Electroanal Chem* , 1963 16 541
- 19 Z Zhao, X Cai, *J Electroanal Chem* , 1988 252 361
- 20 J A Cox, A F Brajter, *Anal Chem* , 1979 51 2230
- 21 J A Cox, P J Kulesza, M A Mbugwa, *Anal Chem* , 1982 54 787
- 22 D T Chow, R J Robinson, *Anal Chem* , 1953 25 1493
- 23 R E Hamm, C D Withrow, *Anal Chem* , 1955 27 1913
- 24 A Saito, S Himeno, *J Electroanal Chem* , 1979 98 181
- 25 S W Boese, V S Archer, J W O'Loughlin, *Anal Chem* , 1977

- 26 F Baumann, *J Electroanal Chem* , 1963 6 245
- 27 P Li, Z Zhao, Z Gao, *Electroanalysis*, 1992 4 199
- 28 S M Chen, Y O Su, *J Electroanal Chem* , 1990 280 189
- 29 S Sabharwal, *Analyst*, 1990 115 1305
- 30 J E Harrar, *Anal Chem* , 1971 43 143
- 31 M Sarwar, G G Willems, *J Chem Soc Pak* , 1980 2 123
- 32 E Julien, M Comtat, *Rev Chem Miner* , 1969 6 885
- 33 G Schmid, M A Lobeck, *Ber Bunsenges Phys Chem* , 1969 73 189
- 34 J A Cox, P J Kulesza, *J Electroanal Chem* , 1984 175 105
- 35 A Y Chamsi, A G Fogg, *Analyst*, 1988 113 1723
- 36 J A Cox, K R Kulkarni, *Analyst*, 1986 111 1219
- 37 J N Barsci, E Wilke, G G Wallace, M Meaney, M R Smyth, J G Vos, *Electroanalysis*, 1989 1 245
- 38 G G Wallace, M Meaney, M R Smyth, J G Vos, *Electroanalysis*, 1989 1 357
- 39 F W Billmeyer, "Textbook of Polymer Chemistry", Wiley-Intersciences, NY, 1984, Chs 7 and 8
- 40 J B Berkowitz, M Yamin, R M Fuoss, *J Polym Sci* , 1958 28 69
- 41 R J Forster, J G Vos, *Macromolecules*, 1990 23 4372
- 42 R J Forster, A J Kelly, J G Vos, M E G Lyons, *J Electroanal Chem* , 1989 270 365
- 43 A R Hillman, in *Electrochemical Science and Technology of Polymers*, R G Linford, (Ed), Elsevier, Amsterdam, 1987 Ch 5
- 44 P N Bartlett, "Biosensors, Fundamentals and Applications", A P F Turner, I Karube, G S Wilson, (Eds), Oxford, University Press, 1987, Ch 13
- 45 R J Forster, M E G Lyons, J G Vos, *J Chem Soc Faraday Trans* , 1991 87 3761
- 46 R J Forster, M E G Lyons, J G Vos, *J Chem. Soc Faraday Trans* , 1991 87 3769
- 47 R J Forster, J G Vos, *Electrochimica Acta*, 1992 37 159
- 48 E Laviron, *J Electroanal Chem* , 1982 131 61
- 49 W M Latimer, "Oxidation Potentials", 2nd Edition, Prentice Hall, NJ, 1952

- 50 G Mengoli, M M Musiani, *J Electroanal Chem* , *J Electroanal Chem* , 1989 269 99
- 51 K Aoki, K Tokuda, H, Matsuda, *J Electroanal Chem* , 1986 199 69
- 52 R J Forster, Ph D Thesis, Dublin City University, 1990
- 53 A R Guadalupe, H D Abruna, *Anal Chem* , 1985 57 142
- 54 R R Gadde, S Brukenstein, *J Electroanal Chem* , 1974 50 163
- 55 M S Thompson, T J Meyer, *J Am Chem Soc* , 1981 103 5577
- 56 D W Pipes, M Bakır, S E Vitols, J Hodgson, T J Meyer, *J Am Chem Soc* , 1990 112 5507
- 57 M H Barley, K J Takeuchi, T J Meyer, *J Am Chem Soc* , 1986 108 5876
- 58 M J Losada, *Mol Catal* , 1975 1 245
- 59 A F Wells, *Structural Inorganic Chemistry*, 4th Edition, Clarendon, Oxford, 1975, p 653
- 60 V F Wolf, S Yao-Dzen, *Z Anorg Allg Chem* , 1967 354 12
- 61 R C Weast, (Ed), *Handbook of Physics and Chemistry* 66th Edition, CRC Press, Florida, 1986 Table D-163
- 62 R Jaing, F C Anson, *J Electroanal Chem* , 1991 305 171
- 63 W J Albery, A R Hillman, *Ann Rep Prog Chem* , 1981 C 78 377
- 64 M E G Lyons, W Breen, J F Cassidy, *J Chem Soc Faraday Trans, 1*, 1990 86 2095
- 65 M Tomoi, Y Akada, H Kakiuchi, *Macromol Chem, Rapid Commun* , 1982 3 537
- 66 A J Bard, L R Faulkner,, “*Electrochrmical Methods*”, Wiley, NY, 1980, p 106
- 67 J M Saveant, K B Su, *J Electroanal Chem* , 1984 171 431
- 68 C P Andrieux, J M Dumas-Bouchiat, F M'Halla, J M Saveant, *J Electroanal Chem* , 1980 113 19
- 69 C P Andrieux, J M Dumas-Bouchiat, J M Saveant, *J Electroanal Chem* , 1982 131 1
- 70 C P Andrieux, J M Dumas-Bouchiat, J M Saveant, *J Electroanal Chem* , 1984 169 9

- 71 C P Andrieux, J M Saveant, *J Electroanal Chem* , 1984 171 65
- 72 C P Andrieux, J M Saveant, *J Electroanal Chem* , 1982 142 1
- 73 C P Andrieux, J M Saveant, *J Electroanal Chem* , 1982 134 163
- 74 W J Albery, A W Foulds, K J Hall, A R Hillman, *J Electrochem Soc* , 1980 127 654,
- 75 W J Albery, A R Hillman, *J Electroanal Chem* , 1984 170 27
- 76 W J Albery, W R Bowen, F S Fisher, A W Foulds, K J Hall, A R Hillman, R G Edgell, A F Orchard, *J Electroanal Chem* , 1980 107 37
- 77 W J Albery, M G Boutelle, A R Hillman, *J Electroanal Chem* , 1985 182 99
- 78 R J Forster, J G Vos, *J Chem Soc , Faraday Trans* , 1991 87 1863
- 79 P Ferruti, R Barbucci, *Adv Polym Sci* , 1984 58 55
- 80 M W Espenscheid, A R Ghatak-Roy, R B Moore(III), R M Penner, M N Sztetirmay, C R Martin, *J Chem Soc Faraday Trans 1*, 1986 82 1051
- 81 W J Albery, P N Bartlett, A E G Cass, D H Craston, G D Haggett, *J Chem Soc , Faraday Trans 1*, 1986 82 1033
- 82 P T Kissinger, *Anal Chem* , 1977 49 445A
- 83 W T Kok, A J Tudos, H Poppe, *Anal Chim Acta* , 1990 228 39
- 84 S Brukenstein, B Miller, *Acc Chem Res* , 1977 10 54
- 85 *Electrochemical Detection in HPLC, a Practical Primer*, Hewlett-Packard, Avondale, PA, 1989 pp 3-5
- 86 D P Leech, Ph D Thesis, Dublin City University, 1991
- 87 S V Prabhu, R P Baldwin,, *Anal Chem* , 1989 61 2258
- 88 J Wang, T Golden, P Tuzhi, *Anal Chem* , 1987 59 740
- 89 T Ohta, Y, Arai,, S Takitani, *Anal Chem* , 1986 58 3132
- 90 S R Tannenbaum, A J Sinskey, M Weisman, W Bishop, *J Natl Cancer Inst* , 1974 53 79

Chapter 3 (Part A)

Development of a Dual Sensor for the Speciation Analysis of Fe(II) / Fe(III)

3.1. Introduction

The speciation analysis of an element has been defined by Florence¹ as the determination of the concentrations of the individual physio-chemical forms of the element in a sample, that together constitute its total concentration. The use of speciation analysis has been particularly widespread in the field of ecotoxicology^{2,3}. It is known that the biological activity of an element can vary widely from one chemical species to another⁴. The total concentration of a metal therefore generally does not correlate well with its impact on life forms, rather, the speciation of the metal may determine its ecological significance and, in particular, the availability of the metal to organisms⁵. The relationship between the free, uncomplexed metal concentration and its toxicity is well known^{5,6}. Complexation results in detoxification by removing the metal from bioavailability^{2,7}. Since the Minimata disaster, resulting from mercury poisoning, it has become clear that metal speciation is an essential step in the study of the significance of priority metal pollutants during discharge, mobilisation or transformation in natural waters. In addition, the growing awareness of the need for environmental protection resulted in the widespread interest in the determination of individual chemical species in the environment. It has been recommended for some time that routine environmental monitoring programs should involve speciation analysis⁸. The term “speciation” has therefore become closely connected with environmental analysis. Speciation studies have also found importance in areas such as geology⁹, metallurgy¹⁰ and process analysis¹¹.

The development of techniques for speciation has become one of the major research areas in analytical chemistry and is currently one of the most challenging tasks facing analytical chemists¹². In fact, it has been stated that “metal speciation is at best a difficult task”⁸. As many forms of the element with similar physio-chemical properties may co-exist, often in dynamic equilibrium and at widely differing individual concentrations, the difficulty lies in the selective discrimination of the individual species without perturbing the distribution of the chemical species in the sample¹³. To overcome these difficulties, traditional speciation procedures often involve a complex scheme of operations to simplify the analytical protocol as much as possible to ensure reliable quantitative data¹⁴.

The speciation analysis of Fe(II)/Fe(III) has received considerable attention recently ¹⁵⁻¹⁷ In order to discriminate between the two ionic forms of this metal, chromatographic ¹⁸, spectrophotometric ^{19,20} and electrochemical ^{6,9,11} techniques have been proposed For the spectrophotometric methods, several strategies have been developed in order to differentiate between the two redox states, these often involve multi-step analytical protocols Generally the Fe(II) concentration of the sample is initially determined colorimetrically using complexing reagents such as 1,10-phenanthroline and acetohydroxamic acid ^{21,10} Following this, the total iron is estimated by techniques such as atomic absorption spectroscopy (AAS) ²⁰ and the Fe(III) concentration found by difference Alternatively, the remaining Fe(III) can be reduced to Fe(II) using the Jones reductor column ^{16,22} followed by estimation of the total concentration of the two ionic forms using the colorimetric reagent In the reverse approach, the iron concentration can be determined with reagents which form stable complexes with Fe(III), for example, thiocyanate ²³ and sodium 1,2-dihydroxybenzene-3,5-disulphonate ¹⁹ Again total iron is subsequently determined by AAS or following oxidation of Fe(II) Fe(II) is then found by difference Examples of differential kinetic methods have been reported for this speciation analysis ¹⁹ This is accomplished by aerial oxidation of Fe(II) and recording the exponential absorbance-time profile Quantitation was based on non-linear least squares fitting of the experimental data

Chromatography is useful in the analysis of closely related species and has been recently applied to the analysis of metal ions High performance liquid chromatography (HPLC) has been applied to speciation analysis of Fe(II)/Fe(III) ^{18,24} Normally, reversed-phase columns have been used for separation In this mode, complexing agents such as 8-hydroxyquinoline and 1,10-phenanthroline ²⁶ and ion pairing reagents such as hexanesulphonic acid ²⁷ have been used to effect separation These organic moieties act to retain the analyte on the column by hydrophobic interaction By using complexing groups selective to a particular ionic form, good selectivity can be obtained The complexes however tend to be unstable under the chromatographic conditions employed, thus limiting the applicability of the procedure In addition, conventional UV/visible HPLC detection systems results in complex chromatograms The use of element specific in-line AA and atomic

emission (AES) detection systems have been successful in simplifying the chromatograms, but the interfacing of the chromatographic and spectrophotometric instrumentation remains problematic ¹⁴

Electrochemical methods predominate in the speciation analysis of Fe(II)/Fe(III) ⁶ Polarographic techniques such as DC, AC, differential pulse and stripping voltammetry (ASV,CSV) have been exploited As the Fe(II)/Fe(III) redox couple is reversible at mercury electrodes ($k^0 > 1 \text{ cm s}^{-1}$) ⁹, the use of reagents to separate the oxidation and reduction waves is necessary Reagents such as pyrophosphate, 3-(N-morpholino)-1-propanesulphonic acid and N-(2-hydroxyethyl)piperazine-N'-(2-ethanesulphonic acid) have been used for this purpose ²⁸ Providing the oxidation and reduction potentials are well separated, the analytical strategy for the polarographic techniques generally involves determining Fe(II) in a potential sweep in the positive direction and Fe(III) in a negative sweep In a multiplexed system, AC voltammetry was used to determine total Fe(II)/Fe(III) in a single potential sweep (as the technique does not discriminate between cathodic and anodic current) while the ratio of the ferric/ferrous forms was determined by DC polarography ⁹ The detection of Fe(II) and Fe(III) at solid electrodes has also been reported At glassy carbon the kinetics of the redox process are slow and the reaction is therefore irreversible and ill-defined ²⁹, while at platinum electrodes, fouling of the surface occurs ³⁰ For these reasons solid electrodes are of limited application for this speciation analysis

From the brief discussion above, it is evident that speciation of Fe(II)/Fe(III) using conventional techniques requires considerable effort This involves either the use of selective complexing reagents, inter-conversion of the redox states or the use of more than one detection system Such approaches are therefore operator, reagent and instrument intensive, difficult to automate and the chemical manipulation of the analytes involves a significant risk of disturbing the Fe(II)/Fe(III) ratio These are major drawbacks for the routine speciation analysis of Fe(II)/Fe(III)

The use of polymer modified electrodes for the determination of metal ions in solutions has been subject of active investigation recently Modified electrodes for the detection of Fe(II), Cu(II) and Pb(II) have been described ^{34,35,36,37} Given the unique properties of modified electrodes

³⁸, such as the inherent selectivity attainable in the design of modifier, it is likely that these devices will find application for the selective discrimination of closely related chemical species such as the various redox states of metals. Mercury electrodes modified with Nafion and cellulose acetate have been demonstrated for the selective discrimination of metal complexes on the basis of charge and size respectively ³⁹. In a significant paper ⁴⁰, Abruna *et al* described the determination of Cu(II) at an electrode modified with poly(4-vinylpyridine) (PVP) containing electrostatically incorporated ligands with formation constants with copper which vary over a broad range. Excellent correlation between the electrode response and the formation constant of the ligand was found, mimicking the solution behaviour of the incorporated ligand. The presence of other competing ligands (as in real aquatic samples), such as oxalate and humic acid, caused a diminution in the electrode response. By simple measurement of the electrode current, the fraction of metal present in a coordination environment of a given strength could be ascertained, and from this, inference about the chemical form in which this fraction is present could be made. Furthermore, as only small amounts of analyte are required to perform the analysis, the system was minimally disturbed ¹³. These are attributes which are desirable for speciation analysis.

In this chapter, the principle of a dual electrode constructed from glassy carbon electrodes modified with the electrocatalytic polymers $[M(bipy)_2(PVP)_{10}Cl]Cl$ (where $M = Os$ and Ru) for the speciation analysis of Fe(II)/Fe(III) is described. The development, operation and analytical performance of the dual sensor is described. The relative merits of this approach for the discrimination of Fe(II)/Fe(III) are discussed in relation to existing speciation methodology for this and other redox couples. Some of the possible applications of this approach are highlighted.

3.2. Experimental

3.2.1 Materials and Reagents

3.2.1.1 Synthesis of $[\text{Ru}(\text{bipy})_2\text{Cl}_2] \cdot 2\text{H}_2\text{O}$

7.8 g (29.8 mmol) of commercial $\text{RuCl}_3 \cdot 3\text{H}_2\text{O}$ (Johnson Matthey), 9.36 g (60 mmol) of 2,2'-bipyridyl and 0.8 g (2 mmol) LiCl were heated under reflux in 50 cm^3 of reagent grade dimethylformamide for 8 hours. The reaction mixture was stirred continuously during reflux. The reaction mixture was then cooled to room temperature, 250 cm^3 of acetone was added, the resulting solution cooled and left standing at 0 $^\circ\text{C}$ overnight. The resulting green-black microcrystalline product was then filtered and washed with three 25 cm^3 portions of distilled water followed by three 25 cm^3 portions of diethylether. The product was found to have UV/visible λ_{max} at 365 nm and 525 nm which corresponds well to the reported values for $[\text{Ru}(\text{bipy})_2\text{Cl}_2] \cdot \text{H}_2\text{O}$.⁴¹

3.2.1.2 Synthesis of $[\text{Ru}(\text{bipy})_2(\text{PVP})_{10}\text{Cl}]\text{Cl}$

A metal loading of 1/10 (metal centre : monomer) was chosen as this loading exhibits optimum charge transport properties for the osmium-based redox polymers.⁴² This metal loading was obtained by the reaction of stoichiometric amounts of high molecular weight PVP polymer and $[\text{Ru}(\text{bipy})_2\text{Cl}_2] \cdot 2\text{H}_2\text{O}$. 100 mg of the polymer was weighed accurately and dissolved in 40 cm^3 of 2-methoxy ethanol (BDH). This solution was then transferred to a 150 cm^3 round bottomed flask. Next 49.5 mg of $[\text{Ru}(\text{bipy})_2\text{Cl}_2] \cdot 2\text{H}_2\text{O}$ was dissolved in 40 cm^3 of 2-methoxy ethanol, this solution was then added and mixed with the polymer solution in the round bottomed flask. The resulting mixture was held under reflux at 125 $^\circ\text{C}$ for 48 h. The reaction was monitored by UV/visible spectroscopy and electrochemically by CV. The formation of a product with a redox wave at 0.75 V vs. saturated calomel electrode (SCE) indicated the formation of the redox polymer. When the starting material redox wave had disappeared completely, the redox polymer was precipitated twice from 2-methoxy ethanol in diethylether. The precipitate was dried *in vacuo* at 80 $^\circ\text{C}$ for 24 h. 110 mg of product was recovered which corresponds to a 73% yield. Light was excluded at all times during synthesis and use to

prevent the photo-substitution of the labile chloride ligand ^{43,44} The synthesis of high molecular weight PVP and the osmium redox polymer were described in chapter 2

3 2 1 3 Electrolyte and Solutions

Due to the formation of insoluble $[\text{Fe}(\text{OH})_3]$ at pH's > 4, the electrolyte used through-out this study was $0.2 \text{ mol dm}^{-3} \text{ Na}_2\text{SO}_4 / 0.05 \text{ mol dm}^{-3} \text{ H}_2\text{SO}_4$ (pH = 1.0). The low pH ensured solubility of the iron redox species and also prevents inter-conversion of the redox states. All Fe(II) and Fe(III) solutions were prepared in this electrolyte. This electrolyte also acted as the carrier for flow injection analysis experiments. The salts $(\text{NH}_4)_2[\text{Fe}(\text{SO}_4)_2] \cdot 6\text{H}_2\text{O}$ and $\text{NH}_4[\text{Fe}(\text{SO}_4)_2] \cdot 12\text{H}_2\text{O}$ were used for the preparation of Fe(II) and Fe(III) solutions respectively.

3 2 2 Procedures

3 2 2 1 UV/Visible Spectroscopy

UV/visible spectroscopy was carried out using a Shimadzu UV 240 spectrophotometer. 1 cm matched quartz cells were used. UV/visible spectra were recorded in the region 900 nm to 190 nm. A scan speed of 10 nm s^{-1} and a slit width of 2 nm was used. Spectra were recorded on methanolic polymer solutions. Methanol was used in the reference beam.

3 2 2 2 Luminescence Spectroscopy

Luminescence spectroscopy was carried out using the Perkin Elmer LS50 luminescence spectrophotometer interfaced to an Epson AX2e PC. For the room temperature luminescence measurements a 1 cm fluorescence cell was used while at -196°C , a quartz tube was employed. The excitation and emission slit widths were 10 nm for all experiments.

3 2 2 3 Cyclic Voltammetry and Rotating Disc Electrode Voltammetry

CV and RDE voltammetry were carried out using a conventional three electrode assembly. The potentiostat used was the EG&G Princeton Applied Research Model 362. The rotating disc assembly was the Metrohm Model 629-10. Voltammograms were recorded on a Linseis X-Y recorder. The working electrodes were 3 mm diameter glassy carbon discs shrouded in Teflon (Metrohm). The counter electrode was 1 cm² platinum gauze placed parallel to the working electrode at distance of ≈ 1 cm. The reference electrode was the saturated KCl calomel electrode. All potentials are quoted with respect to the SCE without regard to liquid junction potentials. All measurements, unless otherwise stated, were carried out at room temperature.

Modified electrodes were prepared by polishing the glassy carbon electrodes with 5 μ m alumina as an aqueous slurry on a felt cloth. The electrodes were rinsed thoroughly with distilled water and methanol. The electrodes were then treated with chlorosulphonic acid to promote the formation of surface oxide functional groups. The electrodes were again rinsed with distilled water and dried *in vacuo* at room temperature. The electrodes were modified by drop coating using a 1% w/v solution of the polymer. The electrodes were allowed to dry slowly in air and allowed to cure overnight *in vacuo* before use.

3 2 2 4 Flow Injection Apparatus

The flow injection apparatus consisted of a Gilson Miniplus 3 peristaltic pump, a six port Rheodyne injector valve fitted with a 20 cm³ fixed volume sample loop, an EG&G Princeton Applied Research Model 400 electrochemical detector connected with Teflon HPLC tubing, and a Philips X-t chart recorder. In the flow cell, an Ag/AgCl electrode acted as the reference. The stainless steel cell body opposing the working electrodes acted as the auxiliary electrode. The two working electrodes were 3 mm diameter glassy carbon discs shrouded in a single Teflon block. One electrode was modified with the osmium polymer while the other electrode was modified with the ruthenium polymer. The dual electrode was then placed in the flow-cell parallel to the flow direction. This is shown

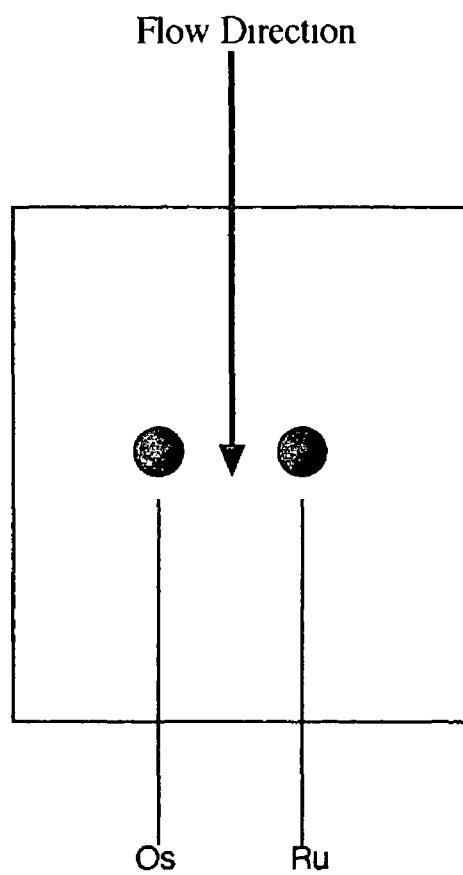


Fig 3 1 Schematic diagram representing the carrier electrolyte flow direction with respect to position of sensors

in Fig 3 1 Modified electrodes were prepared as described above All potentials are quoted after numerical conversion to the SCE scale Sample injections were made using a 2 cm³ glass syringe fitted with a Rheodyne injection needle Electrode responses were monitored as a function of carrier electrolyte flow rate, applied potential, polymer surface coverage and electrolyte pH

The recoveries of Fe(II) and Fe(III) from “spiked” drinking water samples was assessed The water sample was firstly acidified to pH 1.0 with conc H₂SO₄, Aliquots of standard Fe(II) and Fe(III) solutions were then added to give the desired concentration of each redox species Mixed calibration solutions were used to construct calibration curves for each species over the desired concentration ranges No difference in response was observed between mixed or separate calibration solutions The recovery of each species was assessed using the calibration curves The amount recovered was compared to the known analytical concentration

3.3 Results and Discussion

3.3.1 Characterisation of [Ru(bipy)₂(PVP)₁₀Cl]Cl

The synthesis and characterisation of this redox material and its analogues is well documented ⁴³⁻⁴⁵ A detailed discussion of the electronic spectroscopy of this type of compounds is beyond the scope of this thesis Therefore, the results described in this section is for the purpose of confirming the structure of the material used for the development of the speciation sensors The characterisation of [Os(bipy)₂(PVP)₁₀Cl]Cl was detailed in chapter 2

3.3.1.1 Absorption and Emission Spectroscopy

The electronic spectra of 2,2'-bipyridyl complexes of ruthenium have been well documented and has been useful in the characterisation of such compounds ⁴³⁻⁴⁶ In particular, the energy of the lowest absorption maxima and the wavelength of emission are characteristic of a particular

ruthenium moiety. According to the literature⁴¹, the visible absorption spectrum of Ru(II)-diimine compounds is assigned to a spin allowed metal-to-ligand charge transfer transition (¹MLCT) from the metal d-orbital to the π^* -orbital of the bipyridyl ligand, while the emission is thought to originate from a ligand-based triplet state (³MLCT).

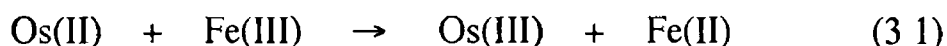
The electronic spectra for the redox polymer in methanol show strong overlapping bands at 215 ± 5 nm, 250 ± 5 nm and 290 ± 5 nm resulting from $\pi \rightarrow \pi^*$ transitions of the aromatic electrons of the pyridine moieties of the polymer backbone. Two transitions in the visible region occurring at 356 ± 5 nm and 502 ± 5 nm were observed. These bands are due to the $d \rightarrow \pi^*$ transitions. These λ_{max} are consistent with the belief that the coordination sphere of the metal centre is $[\text{Ru}(\text{N})_5\text{Cl}]$.⁴³⁻⁴⁶ The magnitude of the molar extinction coefficient of the lowest energy band is useful for confirming the metal centre to monomer unit ratio. For a 1.0×10^{-4} mol dm⁻³ solution of the redox polymer, the molar extinction coefficient, ϵ , of the 502 nm band was found to be 8500 ± 250 mol⁻¹ dm³ cm⁻¹. An extinction coefficient for the lowest energy ¹MLCT band of 8500 mol⁻¹ dm³ cm⁻¹ for the monomeric model compound has been reported.⁴⁷ The value obtained for the polymeric material confirms that the metal loading is 1/10.

Upon excitation at 500 nm an intense emission maxima at 720 ± 10 nm was observed at room temperature. At -196 °C, the emission occurred at 675 ± 10 nm. These observations confirm the coordination sphere as $[\text{Ru}(\text{N})_5\text{Cl}]$.⁴⁷

3.3.2 Mediated Oxidation/Reduction of Fe(II) and Fe(III) by Ruthenium- and Osmium-Containing Metallo-Polymers

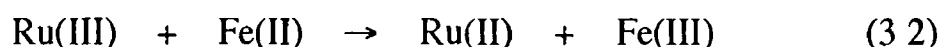
The redox chemistry of the Fe(II)/Fe(III) couple is poor at conventional electrodes.^{29,30} However, the polymer-bound electrocatalysts used here have the potential of improving the kinetics of the Fe(II)/Fe(III) redox. The following description of the electrocatalysis of the redox chemistry of the Fe(II)/Fe(III) is based on the results of kinetic studies by Saveant *et al.*⁴⁸ and Forster *et al.*⁴⁹

The electrocatalytic reduction of Fe(III) by the redox polymer [Os(bipy)₂(PVP)₁₀Cl]Cl in sulphuric acid electrolyte has been reported recently ⁴⁹, and is given by reaction 3 1



It was found that this redox material lowered the over-potential of Fe(III) by 200-300 mV and therefore is a very effective electrocatalyst for this reduction reaction. The substrate was found to partition into the film well ($K \approx 0.2$) and for surface coverages up to $1 \times 10^{-8} \text{ mol cm}^{-2}$ the reaction occurs throughout the polymer film *i.e.* the L_k kinetic regime. At higher surface coverages total catalysis is obtained and a change over to the LS_k mechanism occurs. The rate of the cross-exchange reaction between the osmium sites and the Fe(III) was found to be rapid with $k = 2.8 \times 10^3 \text{ mol}^{-1} \text{ dm}^3 \text{ cm s}^{-1}$. The mediated reduction of Fe(III) at the osmium modified electrode can be seen in Fig 3 2 along with the reduction the bare glassy carbon under identical conditions. It is evident from this diagram that significant improvement in the kinetics of the reduction of Fe(III) is obtained by simple modification of the electrode. In this case, an amplification in response by a factor of about nine was obtained for a surface coverage of $1.5 \times 10^{-8} \text{ mol cm}^{-2}$. In addition to the current gain, a significant potential gain is obtained by the operation of the electrodes at less extreme potentials. These features are characteristic of mediated electrocatalysis ⁵⁰. This results in enhanced responses and less potential electrochemical interferences compared to conventional solid electrodes.

The oxidation of Fe(II) at a ruthenium polymer modified electrode in acidic electrolyte has been investigated recently ⁴⁸ and is given by reaction 3 2



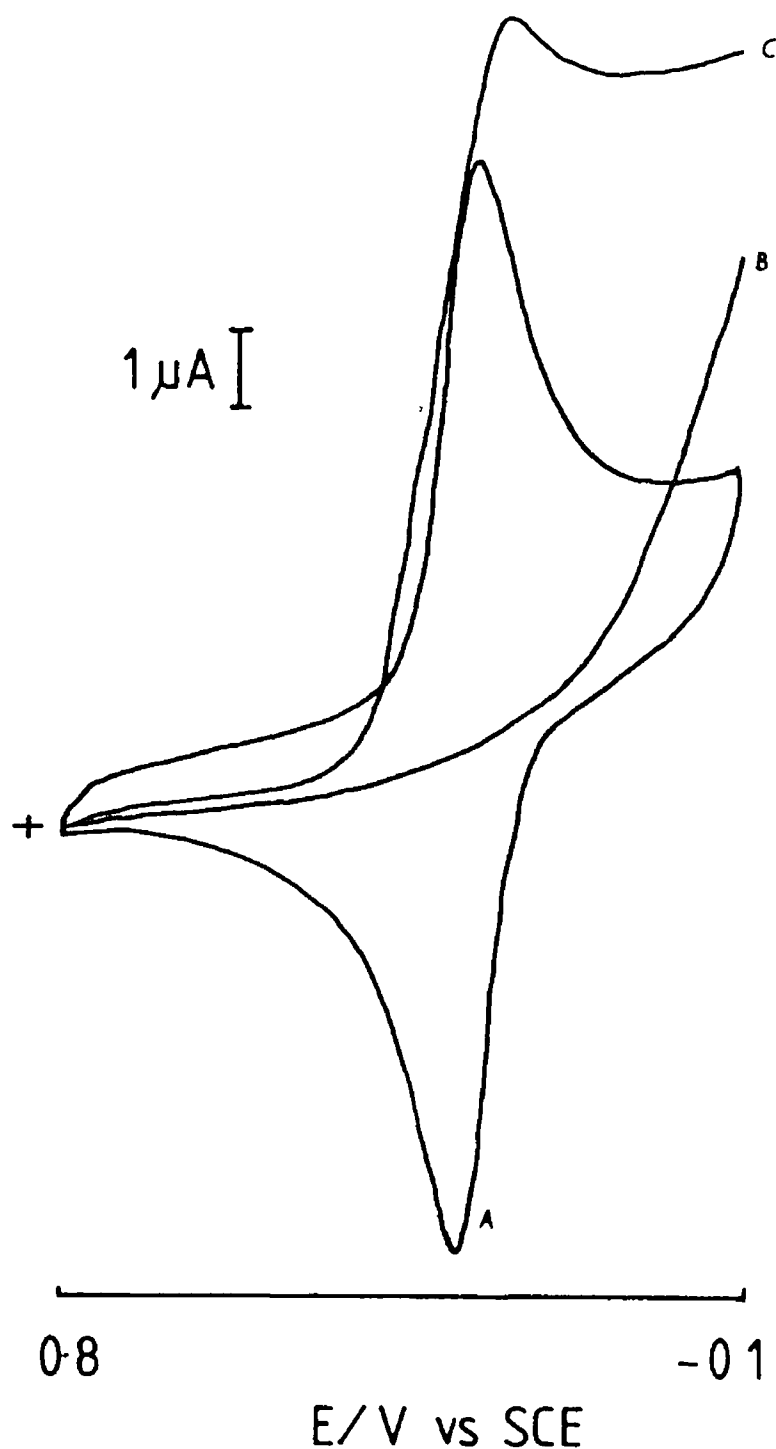


Fig 3 2 (A) a CV of the polymer $[\text{Os}(\text{bipy})_2(\text{PVP})_{10}\text{Cl}]\text{Cl}$ coated on a glassy carbon electrode at a sweep rate of 10 mV s^{-1} (B) a current-potential curve for the reduction of $8.0 \times 10^{-4} \text{ mol dm}^{-3}$ $\text{Fe}(\text{III})$ at a bare glassy carbon electrode and (C) at a redox polymer modified electrode. Conditions $\omega = 500 \text{ rpm}$, $\nu = 2 \text{ mV s}^{-1}$ in $0.05 \text{ mol dm}^{-3} \text{H}_2\text{SO}_4$

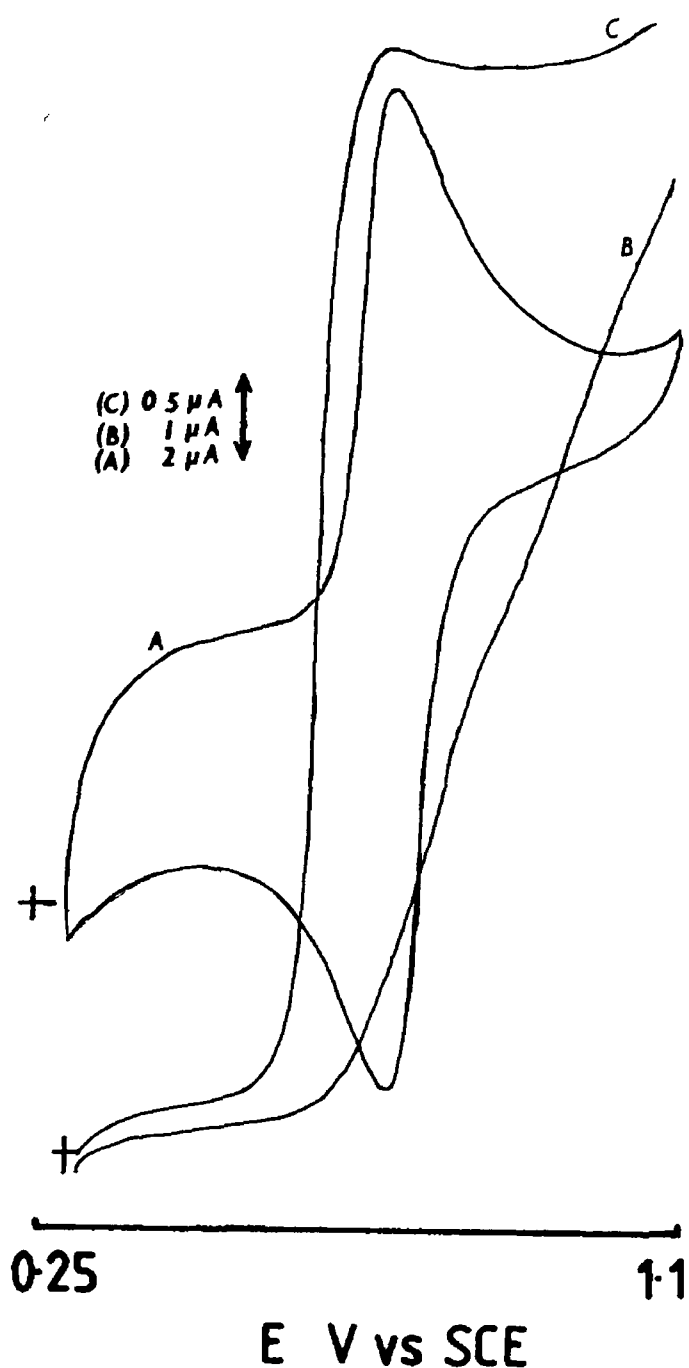


Fig. 3.3 (A) a CV of the polymer $[\text{Ru}(\text{bipy})_2(\text{PVP})_{10}\text{Cl}]\text{Cl}$ coated on glassy carbon electrode at a sweep rate of 10 mV s^{-1} (B) a current-potential curve for the reduction of $8.0 \times 10^{-4} \text{ mol dm}^{-3}$ $\text{Fe}(\text{III})$ at a bare glassy carbon electrode and (C) at a redox polymer modified electrode. Conditions. $\omega = 500 \text{ rpm}$, $\nu = 2 \text{ mV s}^{-1}$ in $0.05 \text{ mol dm}^{-3} \text{H}_2\text{SO}_4$

Again the substrate was found to partition into the polymer film effectively and the cross-exchange reaction occurred in considerable portions of the polymer film. At surface coverages less than $1 \times 10^{-8} \text{ mol cm}^{-2}$ the kinetic regime was L_k , while at thicker polymer films total catalysis was evident and change over to the LS_k mechanism occurred. The rate of the cross-exchange reaction was estimated and found to be fast, with $Kk = 4.5 \times 10^4 \text{ mol}^{-1} \text{ dm}^3 \text{ cm s}^{-1}$. Making the assumption that the permeation coefficient, K , is equal to that for Fe(III) , then $k \approx 2.3 \times 10^5 \text{ mol}^{-1} \text{ dm}^3 \text{ cm s}^{-1}$ which is a value close to that observed for the solution based cross-exchange reaction. The mediated oxidation of Fe(II) at a $[\text{Ru}(\text{bipy})_2(\text{PVP})_{10}\text{Cl}]\text{Cl}$ modified electrode can be seen in Fig. 3.3. These traces clearly show lowering in discharge potential by 200-300 mV and a current gain of by a factor of ten compared to the glassy carbon electrode. These features are again indicative of efficient electrocatalysis.⁵⁰

From the above discussion, it is evident that the electrochemistry of the Fe(II)/Fe(III) redox couple is kinetically slow at bare glassy carbon electrodes. Simple modification of the electrodes with osmium and ruthenium redox polymers greatly enhances the current responses and results in lowered operational potentials. These features suggest that these modified electrodes may be useful for the construction of electrochemical sensors for Fe(II) and Fe(III) .

3.3.3 Principle of Operation of Speciation Dual Sensor

In order to carry out a speciation analysis, discrimination of the different forms of the element must be achieved. Various approaches have been adopted to effect such discrimination. If the thermodynamics of mediated electrocatalysis are considered then it is conceptually possible to discriminate between Fe(II) and Fe(III) using free energy differences between the analyte and the appropriate electrocatalyst. In Fig. 3.4, the formal potentials of the iron, osmium and ruthenium redox couples are shown. It can be seen that the formal potentials of the electrocatalysts envelop the formal potential of the Fe(II)/Fe(III) redox couple. This results in a 210 mV electrochemical driving force for the mediated reduction reaction and a 290 mV driving force for the mediated oxidation reaction. It has been discussed in chapter 1 that for electrocatalysis, the Gibbs free

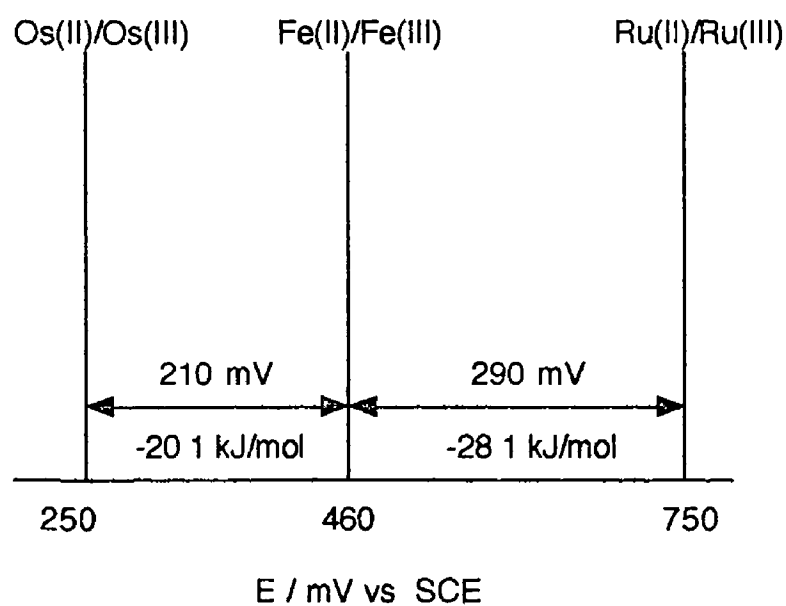


Fig 3 4 Schematic representation of the enveloped position of the Fe(II)/Fe(III) formal potential with respect to the $E_{1/2}$ values of the osmium and ruthenium electrocatalysts. The free energy differences are also shown.

energy, (ΔG), for the electrocatalytic reaction must be negative (i.e. a spontaneous reaction) ⁵¹ From thermodynamics we know that

$$\Delta G = -n F \Delta E \quad (3.3)$$

Where n is the number of electrons transferred, ΔE is the potential difference between the oxidant and reductant and F is the energy change as one mole of electrons fall through a potential of one volt. This results in a free energy difference of $-20.2 \text{ kJ mol}^{-1}$ for reaction 3.1 and $-28.1 \text{ kJ mol}^{-1}$ for reaction 3.2. These reactions will therefore occur spontaneously. The possible reverse oxidation reaction of Fe(II) with Os(III) sites in the polymer results in a ΔE of -210 mV and a ΔG of $+20.2 \text{ kJ mol}^{-1}$.

Obviously, this reaction is thermodynamically impossible. Similarly, for the possible reverse reduction reaction of Fe(III) with the Ru(II) centres within the polymer is impossible as ΔG is $+28.1 \text{ kJ mol}^{-1}$. This situation provides a means of differentiating between the redox pair and allows the design of a dual sensor where an osmium polymer modified electrode detects Fe(III) and the ruthenium polymer modified electrode senses Fe(II), with the thermodynamics of mediated electrocatalysis ensuring the absolute selectivity of each sensory element to its corresponding iron species.

The dual sensor is constructed from two modified electrodes placed in parallel in a thin-layer flow-cell. One of the electrodes is modified with the osmium polymer while the other is modified with the ruthenium polymer. As the electrodes are positioned in a parallel arrangement, the sample plug reaches each electrode simultaneously for detection.

3.3.4 Operational Performance of the Dual Sensor

3.3.4.1 Sensor Response Attributes

Typical dual sensor responses for the detection of Fe(II) and Fe(III) ($1.0 \times 10^{-3} \text{ mol dm}^{-3}$) in a single sample aliquot can be seen in Fig. 3.5. It can be seen that the detection of both redox species occurs simultaneously in the flow cell. The responses of both sensors are sharp and well defined.

Such responses are useful for quantitative analysis. In Table 3.1 the parameters describing the sensor responses are tabulated. The speed of response of both sensors are fast. The time constant, τ , was found to be 1.2 s and 1.3 s for the Fe(III) and Fe(II) sensors respectively. The rise time for the Fe(II) sensor was 1.3 s and 1.4 s for the Fe(III) sensor. The response time was found to be 2.0 s and 2.2 s for the oxidised and reduced species respectively. These values indicate that the sensor response are very rapid, which may be attributed to the facile kinetics of the cross-exchange reactions. Such rapid responses are desirable to ensure high sample throughput. On the basis of the response time, a theoretical throughput of 800 samples / h is possible. However, slight tailing of the Fe(III) response was observed, and as a result, this limited the actual experimental throughput to 180 samples / h. This through-put is still impressive compared to existing speciation procedures for Fe(II)/Fe(III).

The linearity of both sensors was assessed in the thin-layer flow cell. The linear range for both electrodes was found to extend over five orders of magnitude from 1.0×10^{-7} mol dm⁻³ to 1.0×10^{-2} mol dm⁻³ Fe(II) and Fe(III). Typical correlation coefficients, r , over this concentration range, were ≥ 0.9999 for both sensors, which demonstrates the linearity of response. The limit of detection (LOD) was found to be 5×10^{-8} mol dm⁻³ Fe for both sensors at a S/N of 2/1. The sensitivity of both sensors was good. The Fe(II) sensor was found to have a sensitivity (slope of calibration line) of 6.419 ± 0.004 μ A mmol⁻¹ (1.14 μ A mg⁻¹ cm³). A sensitivity of 3.080 ± 0.004 μ A mmol⁻¹ (0.55 μ A mg⁻¹ cm³) was found for the Fe(III) sensor. It has been proposed that the kinetics of electrocatalytic reactions at redox polymer modified electrode generally reflect the thermodynamic driving forces governing the reaction.^{52,53} It is therefore likely that the lower sensitivity for the Fe(III) sensor compared to the Fe(II) sensor may be a result of the difference in ΔG between the analytes and their respective electrocatalysts. The precision of the sensor responses was found to be excellent with relative standard deviations of 0.52% and 1.32% for the Fe(III) sensor ($n=8$) and the Fe(II) sensor ($n=7$), respectively. No memory effects were encountered for both sensors. The electron transfer step proceeds cleanly without adsorption or accumulation of electrolytic products within the film. These observations are consistent with purely outer-sphere electron-transfer processes with fast diffusion of reactants and products within the films.

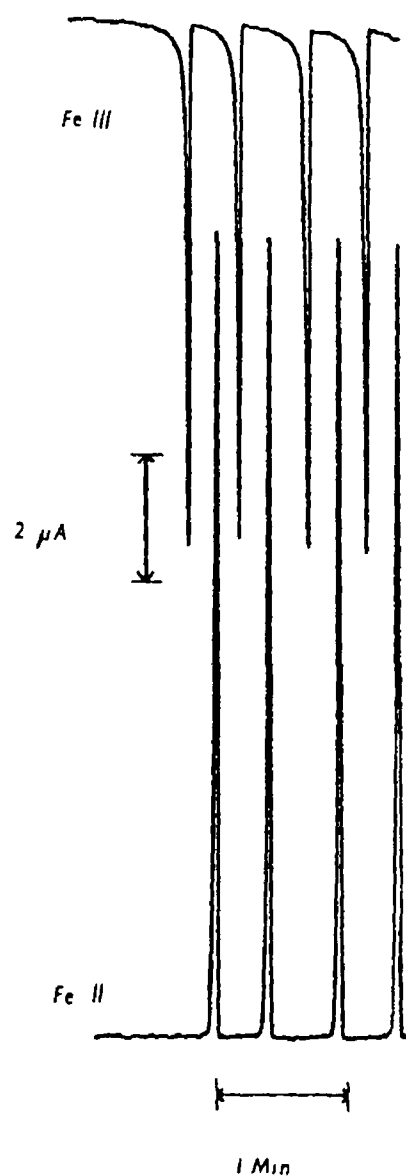


Fig 3 5 Typical recorder traces for the detection of Fe(II) and Fe(III) The electrolyte was $0.2 \text{ mol dm}^{-3} \text{ Na}_2\text{SO}_4 / 0.05 \text{ mol dm}^{-3} \text{ H}_2\text{SO}_4$ The concentration of Fe(II) and Fe(III) was $1.0 \times 10^{-3} \text{ mol dm}^{-3}$ and the electrolyte flow rate was $1.0 \text{ cm}^3 \text{ min}^{-1}$

Parameter	Value	
	Fe(II)	Fe(III)
Sensitivity $\mu\text{A mmol}^{-1} \text{ dm}^3$	$6\,419 \pm 0\,004$	$3\,080 \pm 0\,004$
Linear Range (mol dm^{-3})	$1\,0 \times 10^{-7} -$ $1\,0 \times 10^{-2}$	$1\,0 \times 10^{-7} -$ $1\,0 \times 10^{-2}$
LOD (2/1) (mol dm^{-3})	$5\,0 \times 10^{-8}$	$5\,0 \times 10^{-8}$
Precision (% RSD)	1.32 (n=7)	0.52 (n=8)
Time constant, τ (s)	1.3	1.2
Response time, (s)	2.2	2.0
Rise time, (s)	1.3	1.4
Analytical through-put		
Theoretical*	800 h^{-1}	800 h^{-1}
Experimental	180 h^{-1}	180 h^{-1}

* Based on Gaussian peak profile

Table 3.1 Table of sensor attributes. All parameters were estimated in usual electrolyte and at a flow rate of $1.0 \text{ cm}^3 \text{ min}^{-1}$

3 3 4 2 Effect of Carrier Electrolyte Flow Rate

The effect of carrier electrolyte flow rate in FIA is an important parameter from a number of view points. Firstly, the flow rate determines the sample through-put of the analytical procedure. In addition, flow rate can affect the sensitivity of the sensor response. Electrochemical detectors can be classified as mass rate detectors, *i.e.* the current response is a function of the quantity of analyte passing through the detector per unit time ($i = \partial Q / \partial t$). In addition, increasing the flow rate decreases the diffusional layer thickness at the electrode surface.⁵⁴ Both of these processes should result in an increase in electrode response with increasing flow rate.⁵⁵ It is therefore important to operate FIA experiments at optimum flow rates to ensure maximum sensitivity and analytical throughput. In Fig. 3 6, the effect of carrier electrolyte flow rate on the response of the Fe(II) and Fe(III) sensors can be seen. It is evident from trace B that increasing the carrier flow rate causes an increase in the electrode response for the Fe(III) sensors, with optimum responses recorded at flow rates $\geq 1.0 \text{ cm}^3 \text{ min}^{-1}$. Similar behaviour is observed for the Fe(II) sensor but the increase is less pronounced. The optimum flow for the Fe(II) sensor is obtained at $0.5 \text{ cm}^3 \text{ min}^{-1}$. A flow rate of $1.0 \text{ cm}^3 \text{ min}^{-1}$ was used for all experiments unless specified otherwise.

3 3 4 3 Effect of Applied Potential

A hydrodynamic voltammogram showing the effect of applied potential over the range 0.075 V to 0.345 V vs. SCE on the Fe(III) sensor response in a thin-layer electrochemical flow-cell to a $1.0 \times 10^{-3} \text{ mol dm}^{-3}$ solution can be seen in Fig. 3 7a. At a potential of 0.345 V vs. SCE, the redox sites are predominantly in the pre-catalytic Os(III) state and therefore electrode currents are close to zero. As the potential moves closer to the $E_{1/2}$ of the osmium redox couple an increased population of the catalytic Os(II) sites are generated within the film resulting in an increase in response to the test solution. As the potential moves more negative of the $E_{1/2}$, the redox sites are predominantly in the catalytic Os(II) state and the response begins to level off as the number of catalytic sites reaches a maximum. From these results, the optimum operational potential for detection of Fe(III) is *ca.* 0.12 V vs. SCE. This potential was used unless otherwise stated for all experiments.

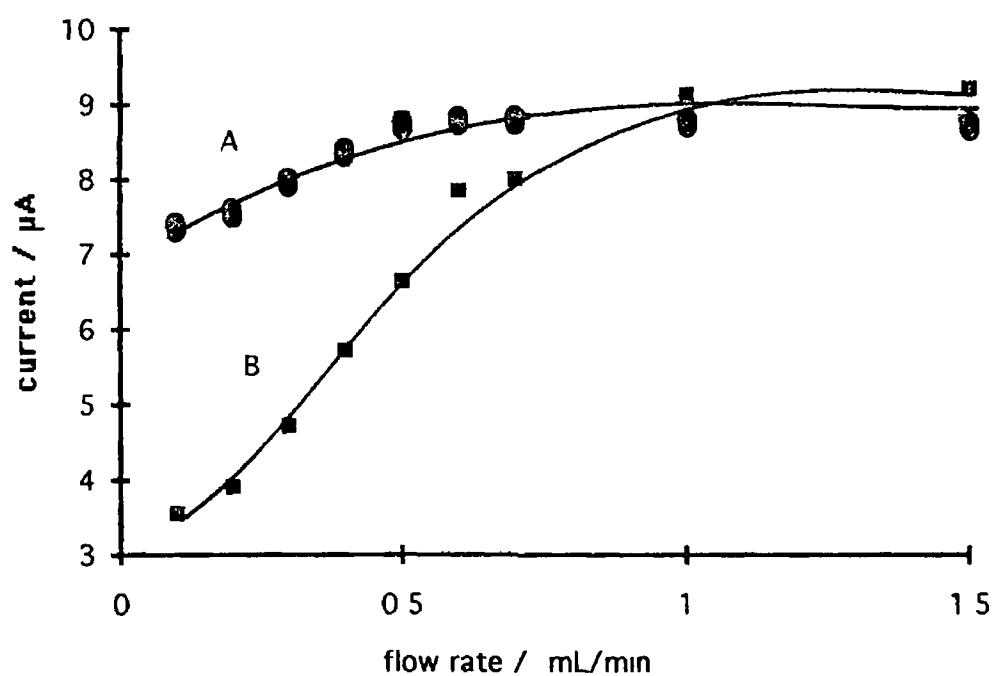


Fig 3.6 Effect of carrier electrolyte flow rate on sensor responses
 The electrolyte was $0.2 \text{ mol dm}^{-3} \text{ Na}_2\text{SO}_4 / 0.05 \text{ mol dm}^{-3} \text{ H}_2\text{SO}_4$
 The concentration of Fe(II) and Fe(III) was $1.0 \times 10^{-3} \text{ mol dm}^{-3}$

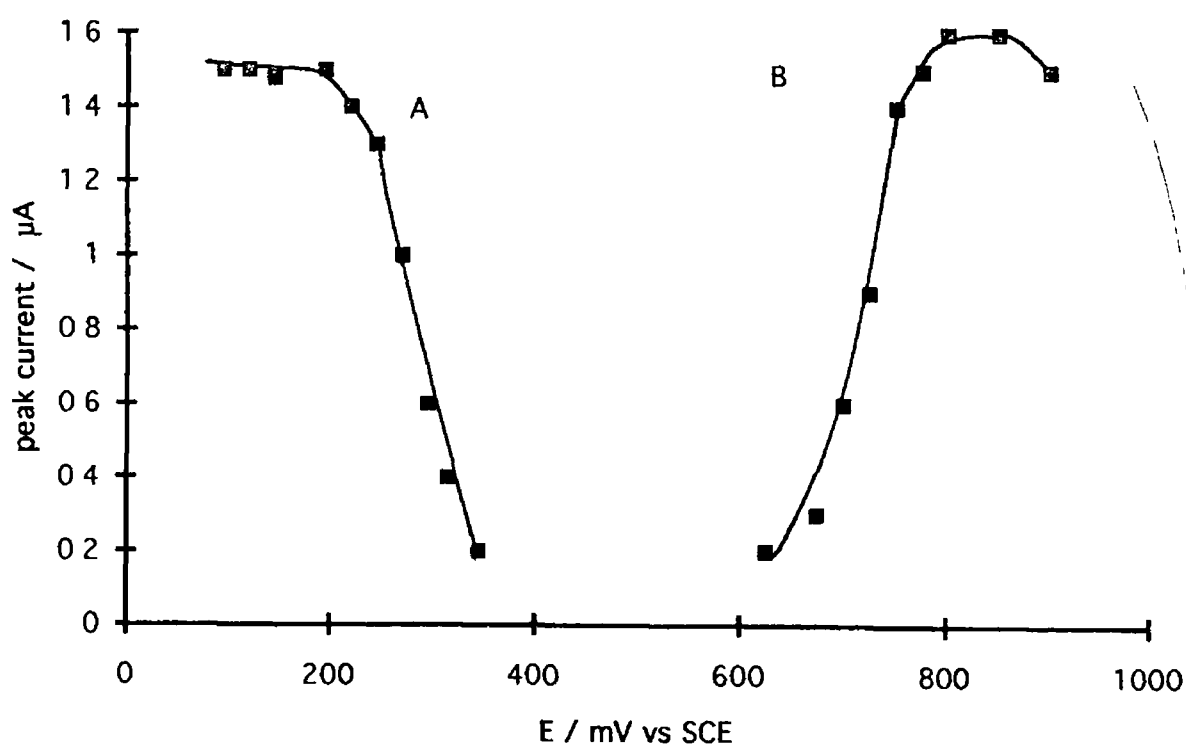


Fig 3.7 Hydrodynamic voltammograms for the reduction of Fe(III) (A) at an osmium polymer modified electrode and the oxidation of Fe(II) (B) at a ruthenium modified electrode. The usual electrolyte was used at a flow rate of $1.0 \text{ cm}^3 \text{ min}^{-1}$. The Fe(II) and Fe(III) concentrations were $1.0 \times 10^{-4} \text{ mol dm}^{-3}$.

Fig 3 7b shows a hydrodynamic voltammogram for the oxidation of Fe(II) at the ruthenium polymer modified electrode. In a similar fashion to the osmium electrode, at potentials favouring the pre-catalytic Ru(II) state, electrode responses are small, while at potentials more positive than the $E_{1/2}$ of the ruthenium centres, where the Ru(III) form is favoured, electrode responses reach a maximum. The optimum applied potential for the Fe(II) sensor was 0.85 V vs SCE. This potential was used through-out this study unless otherwise stated.

In the theories of mediated electrocatalysis, the concentration of electro-active sites within the polymer, (b_o) is assumed to be controlled by electrode potential according to the Nernst equation.⁵⁰ In addition, for the kinetic regime L_k , which pertains at both of the modified electrodes studied here, the electrode response should be first order with respect to b_o , which results in an increase in response as a function of applied potential. The behaviour observed here is entirely in agreement with the predictions of the theoretical models.

3.3.4.4 Effect of Electrolyte pH

The effect of pH of the electrolyte on the response of the Fe(II) and Fe(III) sensors was investigated. It is known that the pH of electrolytes can affect the kinetics of proton coupled electrocatalytic reactions⁵⁶ and also the rate of heterogeneous reactions at electrodes.⁵⁷ For both sensors studied here, the response of the sensors was found to be independent of electrolyte pH over the range pH 1.0 to pH 4.0. This is consistent with the outer sphere nature of the electron transfer reactions which occur for Fe(II)/Fe(III) redox. Higher pH were not examined as Fe(III) precipitates as $[\text{Fe}(\text{OH})_3]$ at pH > 4.

3.3.4.5 Effect of Polymer Surface Coverage

In Fig 3 8, a plot of $\ln i$ vs $\ln \Gamma$ shows the effect of polymer surface coverage on electrode response for the Fe(III) sensor. It is clear that increasing the polymer layer thickness results in an increase in electrode response for this sensor. Similar behaviour was observed for the Fe(II) sensor. For the L_k kinetic regime, the electrode response should obey a

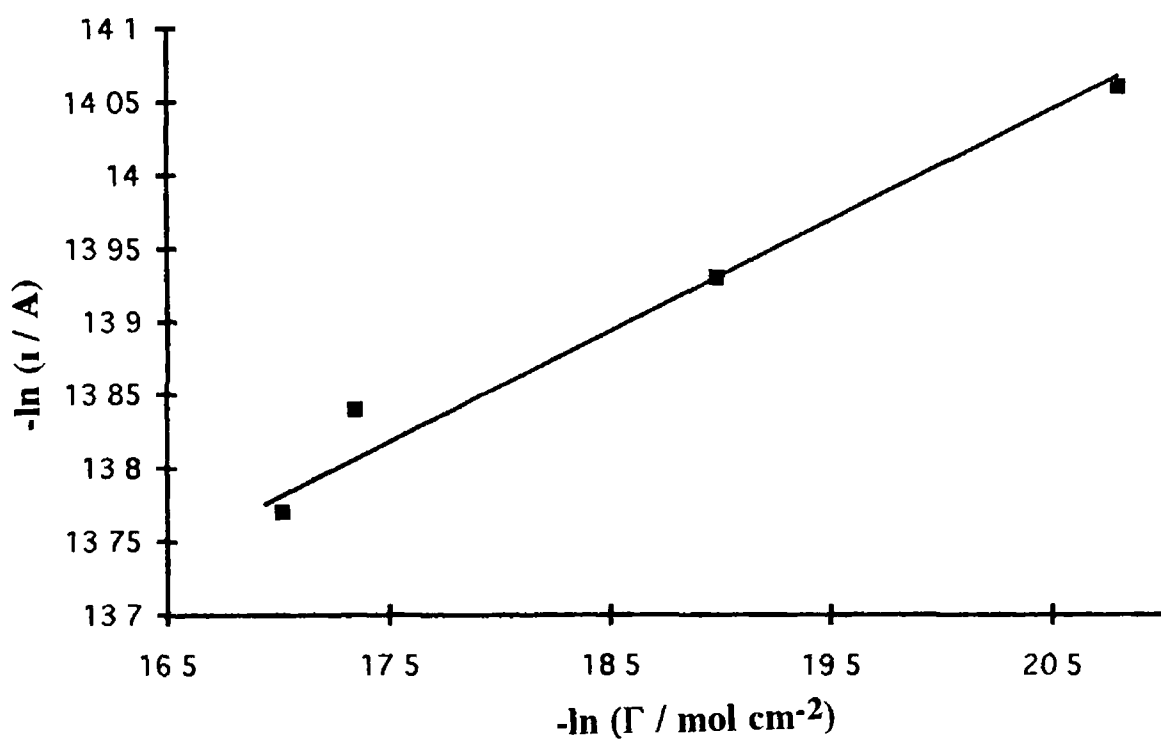


Fig 3 8 Effect of polymer surface coverage, Γ , on the Fe(III) sensor response in the thin-layer flow cell. $[\text{Fe(III)}] = 1.0 \times 10^{-3} \text{ mol dm}^{-3}$ and the electrolyte flow rate was $1.0 \text{ cm}^3 \text{ min}^{-1}$

first order relationship with respect to Γ , so the slope of the above plot should be 1.0. Slopes for both Fe(II) and Fe(III) responses with respect to surface coverage are however considerably less than that expected from theory. Slopes for the Fe(III) and Fe(II) responses were found to be of the order $\approx 0.2 \pm 0.1$. Considerable variability in the slopes were observed for all repetitions of this experiment, but the general trend of increasing response with increasing Γ was observed in all cases. The general trend appears to indicate that in the thin-layer electrochemical flow cell, the analytes partition into the polymer films quickly and that the mediated reactions occurs throughout the polymer film (L_k). However, as the slope $\ll 1.0$, the responses appear to be far from the steady-state behaviour observed and expected for the rotating disc electrode. These differences may be attributed to the different modes of mass transport and the short residence time of the substrate in the flow-cell given the high flow rate of the electrolyte and the low cell volume.

3.3.4.6 Electrode “Cross Talk”

“Cross talk” between electrodes in electrode array devices has been reported. For the dual electrode under investigation, two possible forms of “cross talk” can be identified. Firstly, electronic cross talk is observed. This behaviour occurs because the counter and reference electrode are common to both working electrodes. When a large depolarisation of a sensor occurs, with respect to the adjacent sensor, a shift in the background current (non-faradaic) at the adjacent sensor occurs. This behaviour becomes important when the $[\text{Fe(II)}]/[\text{Fe(III)}]$ ratio becomes greater than 1000 or less than 0.001. At less extreme concentration ratios, the shift in baseline is insignificant in comparison to the magnitude of responses, typically less than 0.1% of the current response of the lower concentration redox species. This limits the safe use of the dual sensor to Fe(II)/Fe(III) concentration ratios in the range 100–0.01. So, samples with Fe(II)/Fe(III) concentration ratios within two orders of magnitude of each other can be applied to this detection system. In situations where the relative concentrations of both redox species are very different, splitting of the sample plug followed by detection at individual thin-layer cells would circumvent this possible limitation.

The second form of “cross talk” which may be problematic at the dual electrode is chemical cross talk. It is recognised that the electrolytic product formed at each sensor is capable of producing a faradaic response at the adjacent sensor. It is possible that this may be a source of chemical cross talk between the sensors. It was however found that at flow rates as low as $0.1 \text{ cm}^3 \text{ min}^{-1}$ (where diffusion in the flow-cell may be problematic), no detection of the electrolytic product of each sensor at the adjacent sensor was apparent. This observation is not surprising as the parallel arrangement of the electrodes allows simultaneous measurement of both species in the sample plug and the continuous forward flow of the electrolyte ensures that the electrolytic products are swept swiftly from the cell. In addition to cell design, the physical constraints on diffusion would prevent diffusional processes from causing chemical cross talk. Under the assumptions of the worst case situation where the system is under static conditions, the diffusion coefficient of the Fe(II) and Fe(III) species is $2.0 \times 10^{-6} \text{ cm}^2 \text{ s}^{-1}$, there is total consumption of all the iron species reaching the electrode, and the peak width is 8 s, then the diffusional layer thickness at each electrode would be $7.0 \times 10^{-3} \text{ cm}$, which is smaller by a factor of 14 compared to the inter-electrode distance of 0.1 cm. Under these conditions, the time interval required for the diffusion of the product from one sensor to the adjacent sensor would be of the order 1600 s. It is obvious that the design of the thin-layer cell used here along with the constraints on diffusion prevent chemical cross talk even at very low flow rates.

3.3.4.7 Recoveries from Analytical Samples

In order to test the applicability of the dual sensor for the speciation of Fe(II)/Fe(III) in real analytical samples, the recovery of these redox species from “spiked” drinking water samples was determined. The results are given in Table 3.2. Due to the presence of electronic “cross talk”, only solutions with $[\text{Fe(III)}]/[\text{Fe(II)}]$ ratios in the range 100-0.01 were examined. From the results presented in Table 3.2 it can be seen that good recoveries are obtained in the concentration range 1.0×10^{-4} to $1.0 \times 10^{-6} \text{ mol dm}^{-3}$ at different concentration ratios. It can also be seen that solutions of equal concentration of both redox species show good recoveries over the concentration range $1.0 \times 10^{-2} \text{ mol dm}^{-3}$ to 1.0×10^{-6}

Ratio [F(III)] / [Fe(II)]	[Fe(II)] / mol dm ⁻³		[Fe(III)] / mol dm ⁻³	
	Anal	Recovered	Anal	Recovered
100	1.0 x 10 ⁻⁶	1.05 x 10 ⁻⁶ (± 5 x 10 ⁻⁸)	1.0 x 10 ⁻⁴	1.04 x 10 ⁻⁴ (± 3 x 10 ⁻⁶)
0.01	1.0 x 10 ⁻⁴	1.02 x 10 ⁻⁴ (± 2 x 10 ⁻⁶)	1.0 x 10 ⁻⁶	1.0 x 10 ⁻⁶ (± 2 x 10 ⁻⁸)
1	1.0 x 10 ⁻⁶	1.0 x 10 ⁻⁶ (± 2 x 10 ⁻⁸)	1.0 x 10 ⁻⁶	1.0 x 10 ⁻⁶ (± 2 x 10 ⁻⁸)
1	1.0 x 10 ⁻⁴	9.8 x 10 ⁻⁵ (± 2 x 10 ⁻⁶)	1.0 x 10 ⁻⁴	1.0 x 10 ⁻⁴ (± 2 x 10 ⁻⁶)
1	1.0 x 10 ⁻²	9.98 x 10 ⁻³ (± 3 x 10 ⁻⁴)	1.0 x 10 ⁻²	1.01 x 10 ⁻² (± 3 x 10 ⁻⁴)

9.

Table 3.2 Analytical recoveries for various concentration ratios of Fe(III)/Fe(II) from spiked drinking water samples. The concentrations recovered are an average of five repeat determinations and the standard deviation for the measurement is given in the parentheses. The usual electrolyte was used at a flow rate of 1.0 cm³ min⁻¹ and the polymer surface coverage for both electrodes was 1.0 x 10⁻⁹ mol cm⁻².

mol dm⁻³ These results demonstrate the applicability of this sensor system for the speciation analysis of aquatic samples

3 3 4 8 General Considerations

From the results presented, it is clear that the principle upon which the dual sensor for speciation is developed is useful for the selective detection of redox pairs such as Fe(II) and Fe(III) The straight forward approach upon which the dual sensor is based conveys considerable advantages to this device compared to existing methods for the speciation In this section, these advantages will be highlighted Interferences will be dealt with in chapter 6

Some of the main advantages of the detection system described include the speed of sample through-put which can be attained and the simplicity of the analytical procedure It has been pointed out by many authors that the simplification of any speciation analysis is of great importance as it allow analysis with minimum intervention and consequently provides more reliable data concerning the actual identity and quantity of particular chemical entities in the sample It also results in faster and more prolific data acquisition, which is extremely important as the current knowledge of the environmental levels of many toxic species is limited

The sensors operate using the simple DC amperometric detection mode, and as a result there is no requirement for potential scanning or elaborate pulse sequences to be used which are prerequisites of existing electrochemical procedures for this analysis This mode of operation requires only simple, cheap and portable instrumentation This favours the development of sensor systems for field analysis or remote sensing applications Another feature of this device is the principle upon which detection and selectivity is obtained This ensures that each sensor has absolute selectivity for its corresponding redox species As a result, there is no requirement either for inter-conversion from one redox species to another, nor for the use of colorimetric complexing agents or for reagents to separate the $E_{1/2}$ potentials for the oxidation-reduction processes Again greatly improved simplification of the analytical protocol This approach also allows rapid and simultaneous determination of both redox species in

the sample in a single sample aliquot. Time-dependent changes in the concentration ratio of the redox pair during analysis is therefore eliminated. Fast reliable extraction procedures (in the second time scale) for Fe(II) and Fe(III) from complex matrices have been developed, however, time dependent interconversion of the redox states during the analytical step is problematic, therefore rapid detection may improve the reliability of such methods.

Another feature of this electroanalytical system is that the electrode responses are independent of pH up to pH 4.0, therefore rigorous control of pH is not necessary for this approach, whereas, chromatographic, spectrometric and polarographic methods require precise pH control. In a recent publication⁵⁸, a “double acidification method” was proposed, the concentration of electrochemically labile (uncomplexed) metal at different pH's was used to assess the toxicity of water samples. As the pH was lowered the concentration of free metal species (toxic portion) increased due to release from the complexed state. In the experimental protocol, it was required to strongly acidify the samples before the anodic stripping step. This led to uncertainties in the measurement. With the electrodes described here, the free metal at each pH may be determined from a single measurement without need for further acidification during the analytical procedure. This would increase the reliability of the data obtained.

Since its inception, FIA has become one of the most important developments in analytical chemistry due to the advantages associated with this technique. With the use of FIA procedures, only small sample aliquots (20 μ L) are required for satisfactory sensor responses. Many speciation studies involve small scale laboratory experiments such as the uptake and release of metal ions from biological materials such as ferritin. For the purposes of speciation analysis using this device, small samples may be obtained with minimum disturbance of the system under study. Also, the FIA procedure used allows the analytical system to be easily automated, this can include automated in-line sample extraction and preparation steps. There is also no requirement for an in-line separation process and only one simple detection system is required. These practical attributes are of considerable advantage compared to existing techniques which require relatively large sample sizes and are conducted using batch type operator and instrument intensive procedures.

In addition to the simplicity of the analysis, there is considerable improvement in the performance of the analytical method. The concentration of chemical species in the environment is variable depending on the sampling location and degree of transformation. The linear range extending over five orders of magnitude is significantly greater than that reported for existing methods. This wide detection window allows analysis of samples with widely differing concentrations without dilution of concentrated samples or preconcentration of dilute samples. The LOD of 3 ppb is also impressive compared to the spectrometric, chromatographic and existing electrochemical methods. The sample solutions in the acidic electrolyte were also found to be stable for at least 24 h. No inter-conversion from one redox state to another was evident. This is significant as it is recognised that many speciation procedures affect the concentration of the individual chemical species considerably.

3.4. Conclusions

Probably the most attractive feature of the synthetic strategy employed for the synthesis of the electrocatalytic materials used in this study is the ability to control the $E_{1/2}$ of the catalytic redox centres. When the $E_{1/2}$ is controlled then the catalytic properties of the electrode are also under control. In this chapter, it has been shown that manipulation of the $E_{1/2}$ potentials of two electrocatalysts can be achieved such that an analyte redox (reversible) formal potential can be enveloped between the $E_{1/2}$'s of two electrocatalysts. When this situation has been achieved, the thermodynamic limitations on the nature of electrocatalytic reactions which are permissible at these types of modified electrodes allow the development of sensors which have absolute specificity for its corresponding redox species. This approach has considerable advantage with regard to simplicity, speed and operational performance.

The principle of operation of the speciation sensor developed here was demonstrated by the Fe(II)/Fe(III) redox couple as the analytes. It is conceivable that this approach may also be applied to the FIA speciation analysis of other environmentally important redox couples such as

Cr(III)/Cr(VI), Cu(II)/Cu(I) and Mn(VII)/Mn(IV) with the use of appropriately designed electrocatalysts. In addition, with the current developments in electrode array devices, it may also be possible to use arrays of modified electrodes with systematically controlled $E_{1/2}$ values for the simultaneous analysis of several redox species or several redox states of the same element. Such advances would result in considerable simplification of speciation analysis which would result in more reliable data and accelerate the rate of data acquisition.

Another possible commercial application of the device demonstrated is its use in detection in the ion chromatography of metal cations. Current detection systems involve monitoring the conductivity of the eluant following ion suppression (removal of highly conducting H^+) which is technically difficult, expensive and limits the eluant composition which can be used. The detection system described here may be used without need for ion suppression prior to detection. In addition, the separation of the individual forms of each redox pair is not necessary as speciation is a function of the detection principle. This is of particular advantage, for example, the redox pair Cr(III)/Cr(VI) are almost impossible to separate by ion chromatography. However, with the detection principle outlined here, separation would not be required as discrimination may be possible on the basis of appropriately designed electrocatalytic properties of the modified electrodes. These advantages again would allow simplification of the analytical protocol and allow more control and flexibility of the chromatographic conditions.

3.5. References

- 1 T M Florence, *Talanta*, 1982 29 354
- 2 G M Morrison, C Wei, *Anal Proc* , 1991 28 70
- 3 G M Morrison, G E Batley, T M Florence, *Chem Br* , 1989 791
- 4 O Abollino, E Mentasti, C , Sarzanini, V Porta, C M G van den Berg, *Anal Proc* , 1991 28 72
- 5 C M G van den Berg, *Anal Proc* , 1991 28 58
- 6 T M Florence, *Analyst*, 1986 111 489
- 7 L E Brand, W G Sunda, R R L Guillard, *J Mar Exp Biol Ecol* , 1986 96 225
- 8 J C van Loon, *Anal Chem* , 1979 51 1139
- 9 M E Beyer, A M Bond, R J W McLaughlin, *Anal Chem* , 1975 47 479
- 10 A T Senior, J D Glennon, *Anal Chim Acta* , 1987 196 333
- 11 E P Parry, D P Anderson, *Anal Chem* , 1973 45 459
- 12 Y K Chau, *Analyst*, 1992 117 571
- 13 *Analytical Aspect of Environmental Analysis*, D F S Natusch, P K Hopke, (Eds), Wiley, NY, 1983 p 6
- 14 J C van Loon, R R Barefoot, *Analyst*, 1992 117 563
- 15 M D Luque de Castro, *Talanta*, 1986 33 45
- 16 A T Faizullah, A Townshend, *Anal Chim Acta* , 1985 167 225
- 17 J A Cox, S Al-Shakshir, *Anal Lett* , 1988 21 1757
- 18 M Connor, T O'Shea, M R Smyth, *Anal Chim Acta* , 1989 224 65
- 19 S Abe, T Salto, M Suda, *Anal Chim Acta* , 1986 181 203
- 20 J L Burguera, M Burguera, *Anal Chim Acta* , 1984 161 375
- 21 J Mortatti, F J Krug, L C R Pressenda, E A G Zagatto, S S Jorgensen, *Analyst*, 1982 107 659
- 22 E G Sarantonis, A Townshend, *Anal Chim Acta* , 1986 184 311
- 23 T P Lynch, N G Kernoghan, J N Wilson, *Analyst*, 1984 109 843

- 24 M Meaney, M Connor, C Breen, M R Smyth, *J Chromatography*, 1988 449 241
- 25 A M Bond, Y Nagaosa, *Anal Chim Acta* , 1985 178 197
- 26 J W O'Loughlin, R S Hanson, *Anal Chem* , 1980 52 2236
- 27 I S Krull, K W Panaro, *Appl Spectrosc* , 1985 39 960
- 28 C D Kennedy, *Analyst*, 1990 115 1067
- 29 J W Dieker, W E van der Linden, *Anal Chim Acta* , 1980 114 267
- 30 K Stulik, V Hora, *J Electroanal Chem* , 1976 70 253
- 31 A R Guadalupe, H D Abruna, *Anal Chem* , 1985 57 142
- 32 L M Wier, A R Guadalupe, H D Abruna, *Anal Chem* , 1985 57 2011
- 33 D M T O'Riordan, G G Wallace, *Anal Proc* , 1986 23 14
- 34 S M Geraty, D W M Arrigan, J G Vos, "Electrochemistry, Sensors and Analysis" M R Smyth, J G Vos, (Eds), Elsevier, Amsterdam, 1986 p 303
- 35 M D Imisides, D M T O'Riordan, G G Wallace, *Anal Lett* , 1988 20 1969
- 36 Y Kurauchi, E Tsurumori, K Ohga, *Bull Chem Soc Jpn* , 1989 62 1341
- 37 M D Baker, C Senarante, *Anal Chem* , 1992 64 697
- 38 R J Forster, J G Vos in *Comprehensive Analytical Chemistry*, Vol XXVII, M R Smyth, J G Vos, (Eds), Elsevier, Amsterdam, 1992, Ch 7
- 39 G M Morrison, T M Florence, *Electroanalysis*, 1989 1 485
- 40 S K Cha, H D Abruna, *Anal Chem* , 1990 62 274
- 41 F E Lytle, D M Hercules, *J Am Chem Soc* , 1969 91 253
- 42 R J Forster, A J Kelly, J G Vos, M E G Lyons, *J Electroanal Chem* , 1989 270 365
- 43 J M Clear, J M Kelly, J G Vos, *Makromol Chem* , 1983 184 613
- 44 J M Clear, J M Kelly, C M O'Connell, J G Vos, *J Chem, Res, (M)*, 1981 3039
- 45 S M Geraty, J G Vos, *J Chem Soc, Dalton Tans* , 1987 3073
- 46 O Haas, J G Vos, *J Electroanal Chem* , 1981 20 139
- 47 B A Moyer, T J Meyer, *Inorg Chem* , 1981 20 444

- 48 C P Andrieux, O Haas, J M Saveant, *J Am Chem Soc* , 1986 108 8175
- 49 R J Forster, J G Vos, *J Chem Soc , Faraday Trans* , 1, 1991 87 1863
- 50 W J Albery, A R Hillman, *Ann Rep Prog Chem* , 1981 (C) 78 377
- 51 J M Saveant, *Acc Chem Res* , 1980 13 323
- 52 A R Hillman, in *Electrochemical Science and Technology of Polymers*, R G Linford, (Ed), Elsevier, Amsterdam, 1987 Ch 5
- 53 C R Leidner, R W Murray, *J Am Chem Soc* , 1984 106 1601
- 54 *Electrochemical Detection in HPLC, a Practical Primer*, Hewlett-Packard, Avondale, PA, 1989 pp 3-5
- 55 J Wang, T Golden, P Tuzhi, *Anal Chem* , 1987 59 740
- 56 G E Cabaniss, A A Diamantis, W R Murphy, R W Linton, T J Meyer, *J Am Chem Soc* , 1985 107 1845
- 57 M R Deakin, K J Stutts, R M Wightman, *J Electroanal Chem* , 1985 182 113
- 58 T M Florence, *Analyst*, 1992 117 551

Chapter 3 (Part B)

Electroanalysis of Nitrate using a Cu/Cd Reductor Column and a $[\text{Ru}(\text{bipy})_2(\text{PVP})_{10}\text{Cl}]\text{Cl}$ Polymer Modified Electrode

3.6. Introduction

The determination of nitrate is considered to be one of the most frequent measurements in environmental analysis, as nitrate is a common aquatic pollutant ¹ The source of nitrate pollution in aquatic environments is predominantly from nitrate fertilisers used by the agricultural sector ² Nitrate is suspected to be toxic and has been implicated in “blue baby syndrome” Nitrate is also involved in the nitrogen cycle and is known to accelerate algae blooms and the eutrophication of lakes ³ Due to the toxicity of this species, and its detrimental effect on the environment, strict limits on the permissible levels of nitrate in water are enforced by EC regulations The extent of nitrate pollution is currently so widespread that large scale nitrate removal from potable water supplies have been introduced in the UK and Europe to bring levels in municipal supplies within EC limits Also, the analysis of atmospheric NO_x's is carried out by trapping these compounds as nitrate ⁴ Nitrate is therefore an important analyte Due to the difficulty in determining this species, nitrate is normally converted to a more readily detectable species prior to analysis ⁵

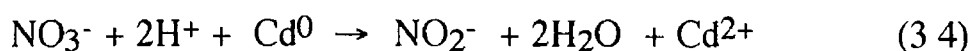
Traditionally, nitrate has been determined by the Kjeldahl method for nitrogen ⁶ In this method, nitrate is reduced to ammonia using Devardas alloy (50% Cu 45% Al, 5% Zn) The ammonia is then steam distilled and trapped in dilute boric acid solution and the ammonia is determined by titration with standard H₂SO₄ Nitrate has also been determined directly by nitration of chromotropic acid ⁷, phenol disulphonic acid ⁸, 2,6-xyleneol ⁹, 3,4-xyleneol ¹⁰ or by the oxidation of nitrate by brucine ¹¹, diphenylamine ¹² and strychnine ¹³ These procedure are, however, very slow, relatively insensitive, operator and reagent intensive and often unreliable in many applications, As a result, more sensitive and reliable alternative methods of analysis have been developed ⁵

Several examples of the electrochemical determination of nitrate have been proposed Catalytic polarography, in the presence of polyvalent cations such as La(III), Yb(III) and Ce(III) has been investigated ¹⁴ Although the detailed chemistry of these procedures is little understood, it appears that the lower oxidation state of the cation reduces nitrate and the cation is regenerated at the electrode surface in a catalytic cycle Rotating

disc electrodes have also been used for the determination of nitrate. Davenport and Johnson used a rotating cadmium electrode for nitrate determination in the concentration region $\approx 10^{-4} \text{ mol dm}^{-3}$.^{15,16} Coating of the cadmium electrode with metallic copper was found to improve the analytical performance of the electrode.¹⁷ In another study, the reduction of nitrate was catalysed by the simultaneous bulk deposition of cadmium and copper at pyrolytic graphite electrodes. Pletcher and Poorabedi have shown that nitrate can be detected amperometrically at copper electrodes.¹⁸ Albery *et al.* used this theme with packed-bed wall-jet copper electrodes for the determination of nitrate, however, after several determinations, severe poisoning of the electrode surface was evident.^{19,20} Renewal of the copper surface was necessary between measurements. In a recent study, nitrate has been reduced to nitrite at the disc of a rotating ring disc electrode.¹⁴ The disc consisted of a gold electrode coated with an under-potential deposition of cadmium. The nitrite was subsequently detected oxidatively at the collector ring electrode. A linear range extending over three orders of magnitude was found. Fogg *et al.*²¹ have described the direct reductive determination of nitrate at a copper electrode formed *in situ* in a capillary-fill sensor device. Again, the copper surface had to be renewed after each determination. The use of a silver electrode for the reduction of nitrate has also been described.² In this work, nitric oxide was formed at the silver electrode and is subsequently detected at a gold plated porous collector electrode placed down stream in the detector. All these reductive techniques require highly acidic conditions for the reduction reaction to proceed, and as a result, such conditions are not useful for routine analysis. The reduction of nitrate under moderate acidic conditions at a polyaniline modified electrode has recently been reported.²² The modified electrodes were also free from surface passivation effects prevalent with conventional electrode surfaces. Major limitations of all the reductive techniques is the potential extremes required where many sources of interference may be problematic, for example, hydrogen evolution, oxygen reduction and the discharge of metal cations. This has prevented the adoption of electrochemical techniques for the determination of nitrate.

Current methods for the determination of nitrate involves prior reduction to nitrite, followed by determination of the nitrite.⁵ The reduction to nitrite can be accomplished with the use of heterogeneous reductors prepared from zinc, cadmium, cadmium amalgams, or

copperised cadmium or by homogeneous reagents such as hydrazine ²³ The use of hydrazine is known to be unreliable and is not amenable to automation ²⁴ For the heterogeneous reduction, the use of cadmium and copperised cadmium materials have been prominent due to the efficiency of the reduction to nitrite Cadmium in the form of wire, powder, granules electrolytic cadmium, amalgamated cadmium and “spongy cadmium” have been used The formation of nitrite from nitrate *via* these routes is simple and well established The mechanism for reduction of NO₃⁻ to NO₂⁻ is believed to occur as follows ²⁵



The presence of metallic copper deposited at the cadmium surface appears to catalyse the above reaction, and as a result copperised cadmium is most frequently used The formed nitrite is normally determined using the conventional spectrophotometric techniques involving diazotisation reactions such as those outlined in chapter 2 Although popular, spectrophotometric techniques for nitrite suffer from a number of distinct disadvantages, these include limited linear ranges, poor limit of detection (LOD), complicated experimental protocols and relatively low analytical through-put In addition, many of the procedures often involve long reaction times and unstable colorimetric reactions and products The nitrate reduction and subsequent colorimetric reaction has recently been automated using flow injection (FIA) methods This has been found to alleviate some of the problems associated with the batch type procedures However, the spectrophotometric techniques still suffer from interferences such as ascorbic acid and chloride In addition, the FIA procedure requires in-line mixing with colorimetric reagent following the reduction step Given the absence of suitable alternative methods for the detection of nitrite, the spectrophotometric procedures have been established as the standard analytical method for the determination of nitrate following reduction to nitrite ²⁶ A number of commercial auto-analysers have been developed to carry out this analysis

It is clear from the above discussion that attempts to directly detect nitrate electrochemically are futile due to the highly acidic condition and

extremes of potential required for reduction. The advantage of prior reduction to an easily detectable species is clearly evident. The analytical difficulties with the standard spectrophotometric procedures are associated with the colorimetric reaction following the formation of nitrite. The use of a redox polymer modified electrode for the direct detection of nitrite may be useful in increasing the analytical performance of such analytical protocols. In this section, the use of a $[\text{Ru}(\text{bipy})_2(\text{PVP})_{10}\text{Cl}]\text{Cl}$ modified electrode for the determination of the nitrate following reduction to nitrite by a copperised cadmium column is described. This study is intended to demonstrate the applicability of redox polymer modified electrodes to existing analytical strategies and to highlight some of the advantages associated with the application of the modified electrode.

3.7. Experimental

3.7.1 Materials and Reagents

The synthesis of the redox material $[\text{Ru}(\text{bipy})_2(\text{PVP})_{10}\text{Cl}]\text{Cl}$ was described in part A of this chapter. The solutions used throughout were prepared from Milli-Q water. The salts NaNO_3 , KNO_3 and NH_4NO_3 were used to prepare nitrate solutions for comparative purposes. These solutions were prepared in 0.1 mol dm^{-3} NaCl . The components of the copperisation solutions were dissolved in the following order, firstly NaCl (where present), then disodium ethylenediaminetetraacetic acid (EDTA) followed by $\text{CuSO}_4 \cdot 5\text{H}_2\text{O}$. Details of concentrations are given in the appropriate section.

3.7.2 Procedures

3.7.2.1 Construction of Copperised Cadmium Reductor Column

Commercial reductor columns are normally constructed from narrow bore ($< 0.3 \text{ cm}$ internal diameter (i.d.)) glass or plastic tubing. The Cu/Cd reductor column used here was constructed from 0.2 cm i.d. silicone tubing. The length of the reductor column was varied from 0.25

cm to 2.0 cm. The cadmium was prepared from high purity (99.9 %) cadmium wire (0.1 cm diameter) by cutting small portions of the wire (≈ 0.1 cm long) to form cadmium chips. The surface area of these chips were $\approx 1 \times 10^{-3} \text{ cm}^2$. The cadmium chips were then packed tightly into the silicone tubing and the chips were held in place by inserting glass wool at both ends of the column. This also had the effect of reducing “dead volume” in the column to a minimum. The packed column was then placed in-line between the injector and detector in the FIA apparatus described below.

3.7.2.2 *In Situ* Copperisation of Cadmium Chips

As copperised cadmium appears to be more effective reducing agent for nitrate than cadmium alone, the cadmium chips were copperised. The cadmium chips were washed for 5 min with 0.1 mol dm^{-3} nitric acid to remove surface oxides. This was accomplished by passing the nitric acid solution over the cadmium chips in the column using the peristaltic pump at a flow rate of $0.5 \text{ cm}^3 \text{ min}^{-1}$. The cadmium chips were then rinsed with Milli-Q water for several minutes. The chips were copperised using two different protocols. The first method was that described by Otsuki²⁷, this involved passing an aqueous solution (by peristaltic pump) containing $12.5 \text{ g CuSO}_4 \cdot 5\text{H}_2\text{O} / \text{dm}^3$ and $30.0 \text{ g} / \text{dm}^3$ EDTA over the cadmium chips for 1 min. The copperised chips were then rinsed with Milli-Q water for 5 min.

The alternative copperisation protocol involved passing a solution containing 0.1 mol dm^{-3} NaCl, $10 \text{ g} / \text{dm}^3$ EDTA and $0.413 \text{ g} / \text{dm}^3$ $\text{CuSO}_4 \cdot 5\text{H}_2\text{O}$ continuously over acid washed cadmium chips. This solution was also used as the carrier for the subsequent FIA experiments.

3.7.2.3 Flow Injection Apparatus

The flow injection apparatus consisted of a Gilson Miniplus 3 peristaltic pump, a six port Rheodyne injector valve fitted with a $50 \mu\text{L}$ fixed volume sample loop, a EG&G Princeton Applied Research Model 400 electrochemical detector connected with Teflon HPLC tubing, and a Philips X-t chart recorder. In the flow-cell, a Ag/AgCl electrode acted as

the reference electrode. All potentials are quoted after numerical conversion to the SCE scale. The working electrodes were 3 mm diameter glassy carbon shrouded in a Teflon block. Modified electrodes were prepared by polishing the glassy carbon electrodes with 5 μm alumina as an aqueous slurry on a felt cloth. The electrodes were rinsed thoroughly with distilled water and methanol. The electrodes were then treated with chlorosulphonic acid to promote the formation of surface oxide functional groups. The electrodes were again rinsed with distilled water and dried *in vacuo* at room temperature. The electrodes were modified by drop coating using a 1% w/v solution of the polymer. The electrodes were allowed to dry slowly in air and allowed to cure overnight *in vacuo* before use. Surface coverages of $1.0 \times 10^{-8} \text{ mol cm}^{-2}$ were used throughout. The stainless steel cell body acted as the counter electrode. Sample injections were made using a 2 cm^3 glass syringe fitted with a Rheodyne injection needle. The optimum carrier electrolyte composition was 0.1 mol dm^{-3} NaCl containing 10 g dm^{-3} EDTA and 0.413 g dm^{-3} $\text{CuSO}_4 \cdot 5\text{H}_2\text{O}$. The reductor column length was normally 1.2 cm and a flow rate of the carrier was usually 0.5 $\text{cm}^3 \text{ min}^{-1}$. The applied potential was generally 0.95 V vs SCE.

3.7.2.4 Analysis of Nitrate in Commercial Fertiliser Using the Modified Electrode

The fertiliser sample (1 g) was ground using a mortar and pestle. 42.75 mg of the ground fertiliser was then placed in a 100 cm^3 beaker with 50 cm^3 of 0.1 mol dm^{-3} NaCl. The sample was dissolved by sonication for 15 min. The resulting solution was transferred quantitatively to a 100 cm^3 volumetric flask and made up to the mark with the 0.1 mol dm^{-3} NaCl solution. This solution was used for the subsequent analysis. A stock nitrate solution was prepared by dissolving 0.8522 g NaNO_3 in 0.1 mol dm^{-3} NaCl and making up to 100 cm^3 . No difference in analytical response between NaNO_3 , KNO_3 or NH_4NO_3 was evident. This stock solution was used to prepare a calibration series in the concentration range 1.0×10^{-3} to $1.0 \times 10^{-2} \text{ mol dm}^{-3} \text{ NO}_3^-$. The responses from the calibration solutions and the sample solution were recorded at an applied potential of 0.95 V vs SCE. Blank responses were also recorded by replacing the Cu/Cd reductor column with a glass wool packed column.

The FIA carrier was 0.1 mol dm⁻³ NaCl, 10 g / dm³ EDTA and 0.413 g / dm³ CuSO₄ · 5H₂O at a flow rate of 0.5 cm³ min⁻¹. The copperised cadmium column was 1.2 cm in length. The concentration of NO₃⁻ in the sample was then estimated from the calibration curve. The analysis was carried out in triplicate.

3.7.2.5 Potentiometric Determination of Nitrate in Commercial Fertiliser

The Orion model 93-07 nitrate ion selective electrode in conjunction with the Universal PT 16 high impedance volt meter was used to determine nitrate in the fertiliser sample. The sample solution was prepared in an identical fashion to that for the modified electrode determination. The Nernstian slope (0.058 V) for the ion selective electrode was measured using a series of standard NO₃⁻ solutions prepared as described above. The method of standard addition for the potentiometric determination of nitrate was applied using the following equation²⁸

$$C_x = (C_s + V_s)/(V_x + V_s) [10^{(nF\Delta E / 0.058)} - V_x/(V_x + V_s)]^{-1} \quad (3.5)$$

Where C_x , V_x and C_s , V_s are the concentration and volumes of the unknown and standard solutions respectively, ΔE is the change of electrode potential upon standard addition, 0.058 is the experimentally determined Nernstian slope, and where n and F have their usual meaning. 40.0 cm³ of the sample solution was placed in a 100 cm³ beaker. The electrode was then immersed in the solution and the solution was stirred slowly with a magnetic stirrer. After stabilisation, the electrode potential was recorded. Then 2.0 cm³ of a standard 1.0 mol dm⁻³ solution of NO₃⁻ was added by pipette to the original solution. The potential was allowed to stabilise and the change in the potential was recorded. This was carried out in duplicate. The concentration of nitrate in the solution was then estimated from the above equation.

3.8. Results and Discussion

3.8.1 Mediated Oxidation of Nitrite by [Ru(bipy)₂(PVP)₁₀Cl]Cl Modified Electrode

In conventional methods for the analysis of nitrate, the stream containing nitrite generated at the Cu/Cd reductor (distilled water or a borate buffer solution) column is mixed with the reagent stream containing sulphanilamide and N-(1-naphthyl)-ethylenediamine dihydrochloride whereupon the colorimetric reaction occurs. With the use of electrochemical detection, direct detection of the nitrite can be accomplished without need for post column mixing and the associated colorimetric reagents. The use of electrochemical detection therefore may result in simplified analytical protocols. The oxidative detection of nitrite in FIA applications using ruthenium-containing redox polymer modified electrodes has been investigated by several workers recently.^{29,30} The ruthenium redox material reduces the over-potential for nitrite oxidation by 200-300 mV compared to glassy carbon and improves the sensitivity of the oxidative detection of nitrite. The surface passivation of carbon resulting from nitrite oxidation is also eliminated. The mediated oxidation reaction appears to be that shown in reaction 3.6.³¹



This reaction has a formal potential of 0.59 V vs SCE and therefore the cross-exchange reaction has a 0.160 V electrochemical driving force. For the [Ru(bipy)₂(PVP)₁₀Cl]Cl modified electrode, the mediated reaction occurs in the entire film (L_k) up to a surface coverage of 8.0×10^{-9} mol cm⁻². At higher surface coverages, total catalysis is observed and the LS_k kinetic regime is obtained.³¹ For this reason, surface coverages of 1.0×10^{-8} mol cm⁻² were used throughout this study. The approach adopted here for the detection of nitrite involves placing the ruthenium polymer modified electrode directly after the Cu/Cd reductor column in the flow system for the simple detection of the generated electro-active species. The optimisation of carrier electrolyte composition, applied potential,

electrolyte flow rate and the reductor column length will be described in the following sections

3.8.2 Optimisation of Carrier Electrolyte

As the electrochemical detection system requires an electrolyte for operation, the composition of the carrier must be compatible with the Cu/Cd reduction step. When using simply $0.1 \text{ mol dm}^{-3} \text{ NaCl}$ as the carrier with reductor columns copperised according to the procedure of Otsuki²⁷, rapid de-activation of the columns was observed. The responses declined by $\approx 50\%$ over approximately 20 injections of $1.0 \times 10^{-3} \text{ mol dm}^{-3} \text{ NO}_3^-$. The reactivity of the electrode was assessed by injecting nitrite samples in the absence of the reductor column, then no loss in modified electrode activity was evident. It was concluded that the loss in response originated with the Cu/Cd reductor column. On inspection, a white precipitate in the reductor column was observed, which is likely to be $[\text{Cd}(\text{OH})_2]$. Such precipitation has been previously observed^{23,32}. Removal of the column contents followed by washing in dilute nitric acid and distilled water was found to reactivate the Cu/Cd reductor. It appears likely that the precipitate physically blocks the metal surface from reaction with NO_3^- in solution, and therefore reduces conversion efficiency and consequently sensitivity. Such reactivation procedures were very inconvenient and therefore this approach was not pursued further.

In an attempt to eliminate the effect of the $[\text{Cd}(\text{OH})_2]$ precipitate, EDTA was added to the electrolyte. Addition of 10 g / dm^3 EDTA to the $0.1 \text{ mol dm}^{-3} \text{ NaCl}$ resulted in considerable improvement in the performance of the reductor column. No white precipitate was found to form in the reductor column. This is likely to be a result of complexation of Cd(II) with EDTA to form the soluble complex, $[\text{Cd}(\text{EDTA})]$ which is removed by the carrier flow. A steady decline in activity of the reductor column was however evident. The loss in sensitivity was accompanied by a gradual blackening of the copperised surface of the cadmium chips. The black compound is likely to be CuO. This appears to be a result of Cu oxidation by dissolved oxygen³². Again, this is likely to block surface cadmium sites from reducing solution phase nitrate. No evidence of decline in modified electrode activity was observed over the same time period. Removal of the cadmium chips followed by nitric acid washing and

re-copperisation restored the original activity of the reductor column. The steady decline in activity of copperised cadmium reductor columns is normal and has been reported extensively^{27,32}. As a result, frequent (daily) regeneration of the copperised surface or replacement of the entire column is necessary. The life time for the reductor columns with this carrier electrolyte was 1-2 days, which corresponds to about 200 sample injections of $1.0 \times 10^{-3} \text{ mol dm}^{-3}$ nitrate. Again, this carrier electrolyte was abandoned due to the inconvenience of frequent regeneration of the reductor column.

It was observed that very strict conditions were required for copperisation according to the method of Otsuki²⁷. Exposure of the Cd chips to the copperisation solution for prolonged time periods ($> 2 \text{ min}$) resulted in a rough, highly copperised black surface layer. The black compound is again probably CuO, possibly resulting from the oxidation of metallic copper deposited on the cadmium surface by dissolved oxygen^{27,32}. Such columns were found to be completely inactive. In order to simplify and standardise the copperisation procedure and to attempt to achieve continuous *in situ* regeneration of the copperised cadmium column, thus negating the requirement for frequent column changes or direct regeneration, the composition of the carrier was modified to include Cu(II). It was conceived that the presence of Cu(II) in the carrier electrolyte could copperise and subsequently maintain the active surface of the Cd after oxidation by nitrate and also be compatible with the electrochemical detection system.

The carrier electrolyte found to achieve the objectives outlined above was comprised of 0.1 mol dm^{-3} NaCl containing 10 g / dm^3 EDTA and 0.413 g / dm^3 CuSO₄ · 5H₂O. The NaCl acts as the electrolyte (also copperisation in the presence of chloride is known to eliminate chloride interference in the nitrate reduction process³³). The function of EDTA is to complex Cd(II) and the CuSO₄ is required to copperise and maintain the active cadmium surface. Fresh nitric acid washed cadmium chips were copperised with this carrier electrolyte at a flow rate of $0.5 \text{ cm}^3 \text{ min}^{-1}$. The pristine metallic copper layer developed on the cadmium chips slowly in comparison to the previous procedure, probably due to the more dilute Cu(II) solution. Throughout the lifetime of the column, the copper surface was highly lustrous and no CuO blackening was evident over prolonged exposure to this solution (2 weeks). This copperisation procedure resulted

in stable reductor columns giving reproducible responses to nitrate after \approx 1 h of flow. The resulting reductor columns were extremely stable, these columns were used continuously for up to two weeks without requirement for direct regeneration.

As Cd is lost in the reduction reaction (reaction 3.4) a slow unavoidable decline in response was observed over the two week period. This is probably due to the gradual decrease in the surface area of the cadmium chips. No deterioration due to CuO or $[\text{Cd}(\text{OH})_2]$ formation was evident. As the homemade reductor column used here did not achieve 100 % conversion of nitrate to nitrite (*vide infra*), consequently, any change in active surface area of the Cd results in a corresponding decrease in conversion. With the use of commercial high surface area Cu/Cd reductor columns, where 100 % conversion is possible, the decline in sensitivity due to decrease in surface area should not be problematic.

The simple procedure developed resulted in very stable Cu/Cd reductor columns, which, by virtue of the flow of the carrier electrolyte, are regenerated continuously *in situ*. Due to the high stability of these reductor columns, this procedure was used for all subsequent copperisation and the solution was also used for the carrier electrolyte.

3.8.3 FIA System Responses

Having established a carrier electrolyte compatible with the copperisation procedure, the maintenance of an active cadmium surface and the reduction of nitrate to nitrite, the behaviour of the analytical system was assessed. In Fig. 3.9 typical modified electrode responses to nitrite generated by the reduction of nitrate at the Cu/Cd reduction column in the optimised electrolyte can be seen. These responses are due solely to nitrite oxidation. This has been established since nitrate solutions and pure electrolyte injections, in the absence of the Cu/Cd column, do not produce responses at the modified electrode, and increasing the nitrate concentration results in the corresponding increase in electrode response. The electrode responses are well defined, near symmetrical and can be considered useful for analytical purposes. At an electrolyte flow rate of $0.5 \text{ cm}^3 \text{ min}^{-1}$, the peak widths at the peak base is approximately 1.0 min. Such broad peaks are normal for the spectrophotometric FIA.

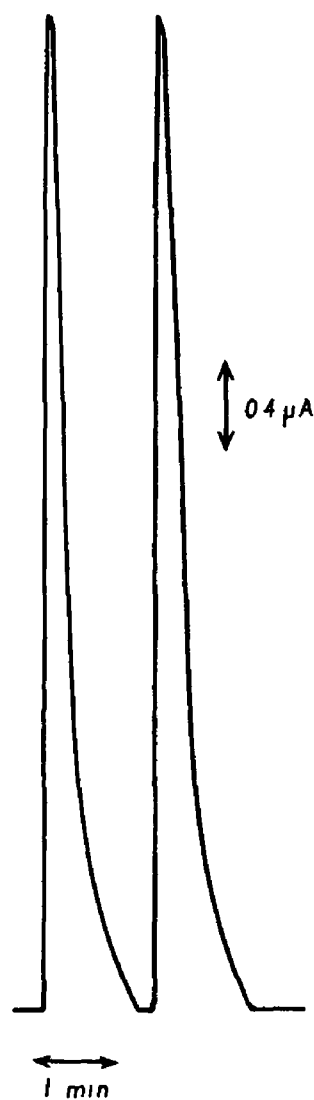


Fig 3.9 Typical FIA responses to $1.0 \times 10^{-3} \text{ mol dm}^{-3}$ nitrate after reduction to nitrite using a 1.2 cm Cu/Cd reductor column. The applied potential was 0.95 V vs SCE and the carrier was 0.1 mol dm^{-3} NaCl containing 10 g dm^{-3} EDTA and 0.413 g dm^{-3} $\text{CuSO}_4 \cdot 5\text{H}_2\text{O}$ at a flow rate of $0.5 \text{ cm}^3 \text{ min}^{-1}$.

determination of nitrate.³⁴ The broad nature of the peak is due to the slow flow rate of the electrolyte, and also the considerable dead volume in the reduction column contributes significantly to the broadening of the analytical peak. When it is considered that the reduction column is 0.2 cm i.d. compared to 0.05 cm for the HPLC tubing used in the rest of the FIA apparatus, considerable peak broadening is not surprising. Dead volume can be kept to a minimum by tightly packing the cadmium chips and inserting glass wool into the column ends. Based on the peak width under these operational conditions, an analytical through-put of 60 samples h⁻¹ can be achieved which is comparable to the spectrophotometric procedures.³⁵ The precision of response was assessed by repeat determinations of 5.0×10^{-4} mol dm⁻³ nitrate solutions. The relative standard deviation (RSD) was found to be 2.0 % for n=8. This again is comparable to the spectrophotometric procedures.³⁵

In Fig. 3.10 a typical calibration plot over the concentration range 1.0×10^{-6} to 1.0×10^{-2} mol dm⁻³ nitrate can be seen. The linear range extends from 1.0×10^{-5} mol dm⁻³ (0.15 ppm N as NO₃⁻) to 1.0×10^{-2} mol dm⁻³ (620 ppm) with typical correlation coefficients, $r \geq 0.999$. The linear range therefore extends over a concentration range of three orders of magnitude. This linear range is significantly greater than that observed for spectrophotometric procedures which are normally linear only over very narrow concentration ranges (typically < 20 ppm). The linear range also encompasses the normal nitrate levels found in environmental water samples, typically ≈ 1 –40 ppm NO₃⁻. For the spectrophotometric approach judicious dilution of samples with high levels of nitrate is required, while for the electrochemical approach no dilution is required. The limit of detection was estimated at S/N of 2/1 to be 5.0×10^{-6} mol dm⁻³ or 0.07 ppm N as nitrate. Normally, special precautions such as experimental correction for light scattering are required to achieve similar LOD using spectrophotometry compared to the electrochemical approach.³⁶ The LOD achieved is therefore a considerable improvement in comparison to the spectrophotometric procedures.

These results indicate that the analytical performance of the electrochemical determination of nitrate after Cu/Cd reduction to nitrite is comparable to the conventional spectrophotometric procedures with respect to analytical through-put and precision but is superior with respect to linear range and LOD. These are the main limitations of the

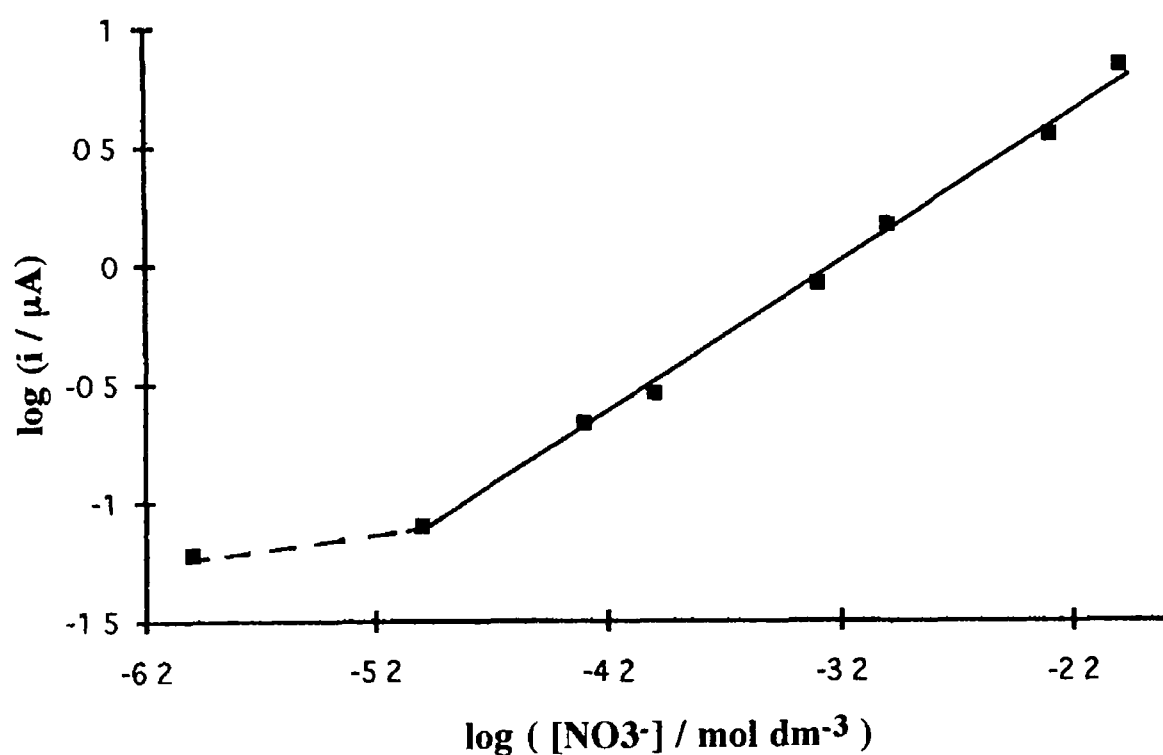


Fig 3.10 Typical calibration plot for the determination of nitrate using a 1.2 cm Cu/Cd reductor column. The applied potential was 0.95 V vs SCE and the carrier was 0.1 mol dm⁻³ NaCl containing 10 g / dm³ EDTA and 0.413 g / dm³ CuSO₄ · 5H₂O at a flow rate of 0.5 cm³ min⁻¹.

spectrophotometric procedures. The application of the alternative electrochemical detection system appears to overcome the problems of limited dynamic range and LOD.

3.8.4 Effect of Applied Potential

In Fig. 3.11 a hydrodynamic voltammogram for the oxidation of $1.0 \times 10^{-2} \text{ mol dm}^{-3}$ solution of nitrite at the modified electrode is shown. At a potential of 0.60 V vs. SCE, no response to nitrite oxidation is evident. At this potential, the electrocatalytic sites are in the Ru(II) oxidation state and therefore can not mediate the oxidation of nitrite. Increasing the applied potential results in the generation of catalytic Ru(III) sites within the polymer and the onset of mediated oxidation of nitrite is evident. It can be seen from this plot that the optimum responses for nitrite oxidation are obtained at an applied potential of $\approx 1.0 \text{ V}$ vs. SCE. However, at this potential excessive background current was observed ($\approx 1 \mu\text{A}$), therefore a lower operating potential of 0.95 V vs. SCE was used for detection in all studies. The background at this potential was $\approx 0.5 \mu\text{A}$.

3.8.5 Effect of Carrier Electrolyte Flow Rate

In Fig. 3.12 a plot of electrode response vs. carrier electrolyte flow rate can be seen. It is evident that increasing the flow rate of the electrolyte from $0.075 \text{ cm}^3 \text{ min}^{-1}$ to $0.3 \text{ cm}^3 \text{ min}^{-1}$ results in a non-linear decrease in the response from the modified electrode. At flow rates higher than $0.3 \text{ cm}^3 \text{ min}^{-1}$, the response levels off to a constant value. Injections of nitrite standard solution instead of nitrate, at various flow rates results in an increase in electrode response with increasing flow rate which indicates the mass rate behaviour of the electrochemical detection system. This has also been observed by Leech.³¹ The decrease in sensor response for nitrate is clearly due to the decreased rate of conversion of nitrate to nitrite by the Cu/Cd reductor column. Increasing the flow rate of the electrolyte decreases the residence time of the sample plug in the reduction column and therefore the extent of nitrate conversion. It is likely that this is responsible for the reduced sensitivity observed with increasing electrolyte flow rate. Optimum responses are therefore obtained at very low flow

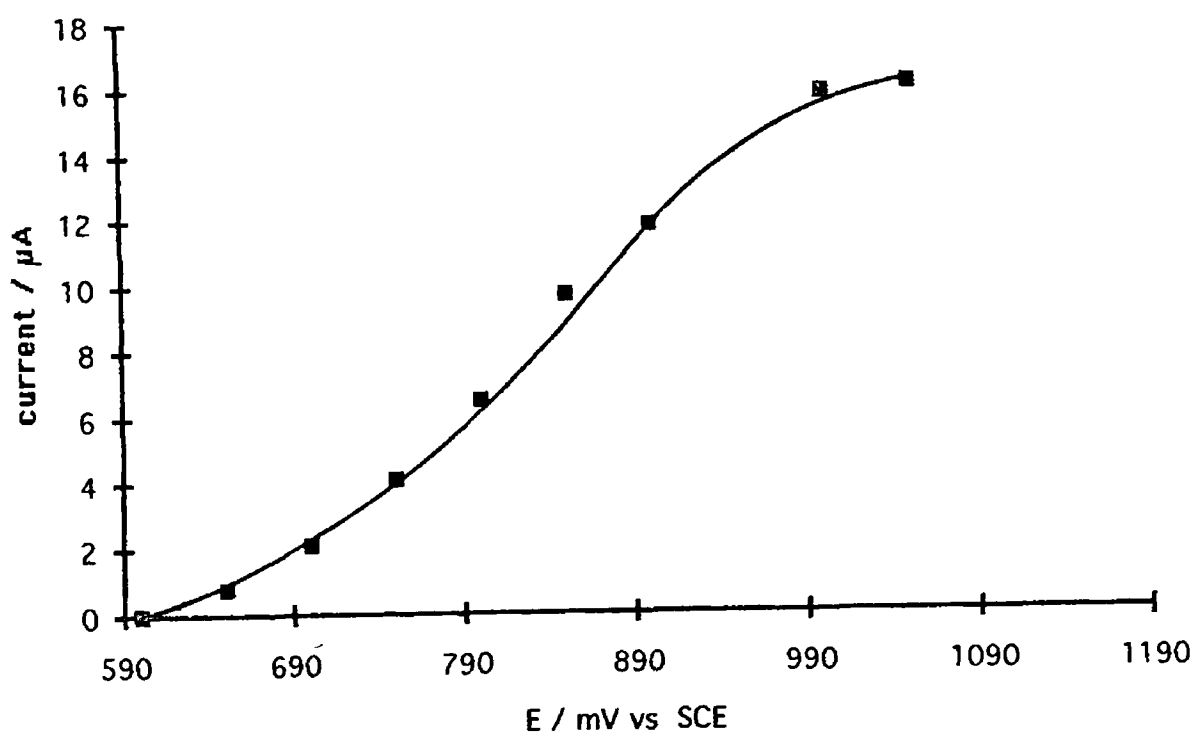


Fig 3 11 Hydrodynamic voltammogram for the detection of nitrite at the ruthenium polymer modified electrode. A 1.2 cm Cu/Cd reductor column was used and the carrier was 0.1 mol dm^{-3} NaCl containing 10 g / dm^3 EDTA and 0.413 g / dm^3 $\text{CuSO}_4 \cdot 5\text{H}_2\text{O}$ at a flow rate of $0.5 \text{ cm}^3 \text{ min}^{-1}$.

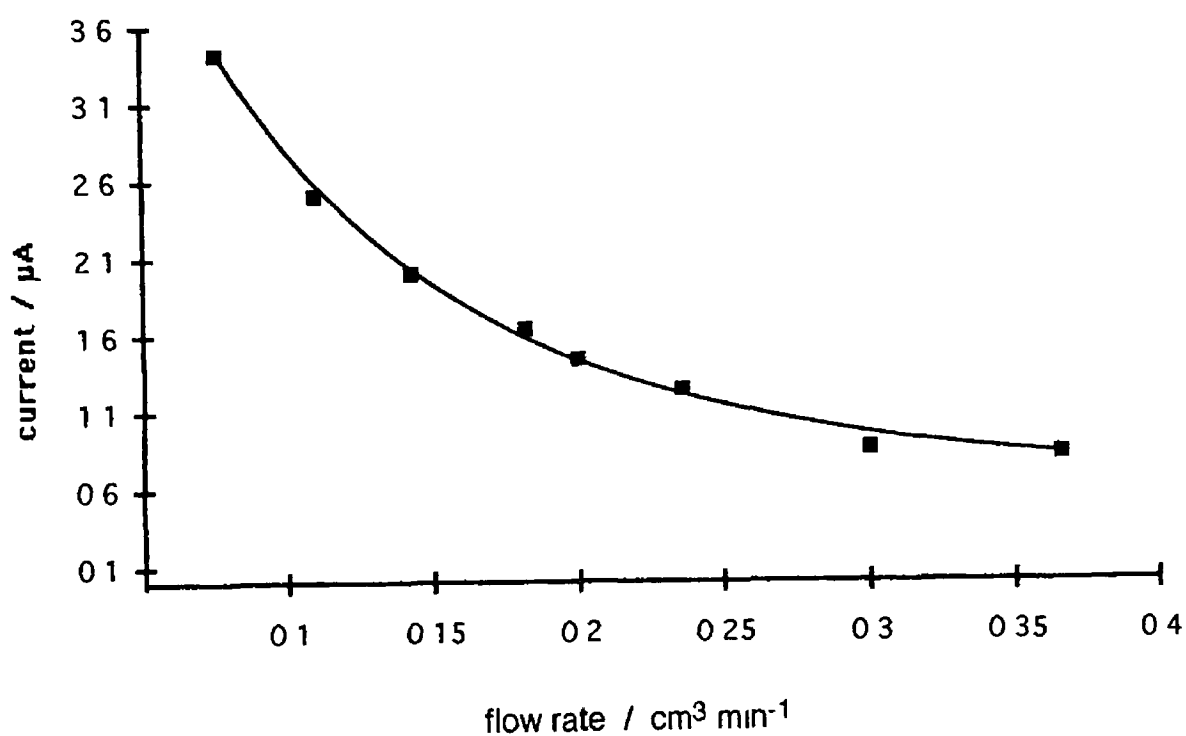


Fig 3 12 The effect of carrier electrolyte flow rate on the FIA response to nitrate. A 1.2 cm Cu/Cd reductor column was used and the carrier was 0.1 mol dm^{-3} NaCl containing 10 g dm^{-3} EDTA and 0.413 g dm^{-3} $\text{CuSO}_4 \cdot 5\text{H}_2\text{O}$. The nitrate concentration was $1.0 \times 10^{-3} \text{ mol dm}^{-3}$ and the applied potential was 0.95 V vs SCE .

rates but, in order to minimise sample plug dispersion and provide reasonable sample through-put rates, a flow rate of $0.5 \text{ cm}^3 \text{ min}^{-1}$ was used. This was found to give sample through-put rates and precision comparable to the spectrophotometric procedures and also greatly superior linear ranges and LOD.

3.8.6 Efficiency of Nitrate to Nitrite Conversion

Given the low surface area of the copperised cadmium chips, which is about $0.2 \text{ cm}^2 / \text{cm}$ of reduction column (calculated from the total quantity of cadmium chips / cm and their approximate surface area), it was expected that total conversion of nitrate to nitrite was unlikely. In Fig 3.13 a plot of % conversion vs. reduction column length at various flow rates can be seen. The extent of conversion was calculated by comparing the area of FIA peaks for $1.0 \times 10^{-3} \text{ mol dm}^{-3}$ nitrate solution and for a nitrite solution of the same concentration. As the concentration of nitrite and nitrate are within the linear response range, a direct comparison between the sensor responses at constant flow rate can be made and this used to estimate conversion efficiencies. Direct comparison between different flow rates can not be made accurately as the residence time of the analyte plug in the electrochemical cell are different, therefore, the extent of nitrite oxidation and hence peak area is different at each flow rate.

It can be seen from these plots that increasing the Cu/Cd column length results in increased conversion efficiencies. This is an expected result because of the increasing surface area of the Cd available for reduction. It can also be seen that lower flow rates favour optimum conversion rates. Optimum conversion is therefore obtained at longer column lengths and lower flow rates. As a reasonable analytical through-put is required along with adequate sensitivity a column length of 1.2 cm at an electrolyte flow rate of $0.5 \text{ cm}^3 \text{ min}^{-1}$ was used for most experiments described.

The most striking aspects of these results is the low levels of nitrate to nitrite conversion obtained. A maximum of 16 % conversion at a flow rate of $0.25 \text{ cm}^3 \text{ min}^{-1}$ with a 2 cm reduction column for a $1.0 \times 10^{-3} \text{ mol dm}^{-3}$ nitrate solution. Decreasing the nitrate concentration to 1.0×10^{-4}

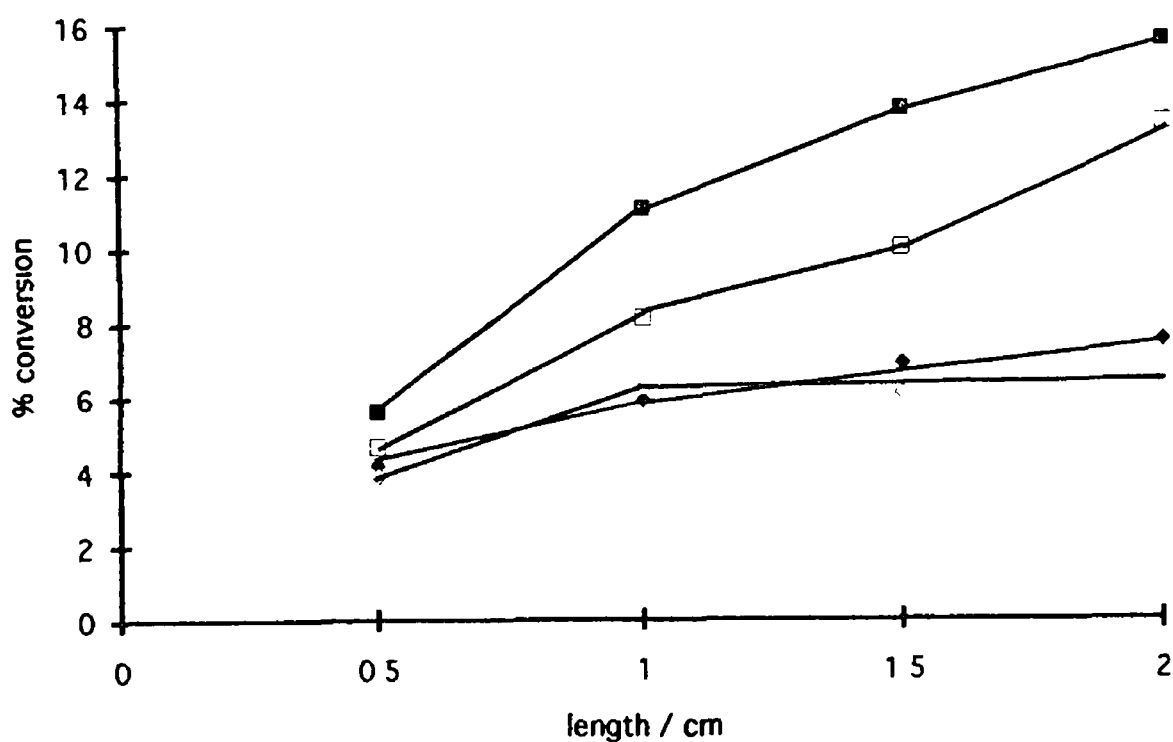


Fig 3 13 The effect of reductor column length on the conversion of nitrate to nitrite The carrier was 0.1 mol dm^{-3} NaCl containing 10 g / dm^3 EDTA and 0.413 g / dm^3 $\text{CuSO}_4 \cdot 5\text{H}_2\text{O}$ The nitrate concentration was $1.0 \times 10^{-3} \text{ mol dm}^{-3}$ and the applied potential was 0.95 V vs SCE The traces ■, □, ◆ and ◇ represents flow rates of 0.25 , 0.50 , 0.75 and $1.0 \text{ cm}^3 \text{ min}^{-1}$ respectively

mol dm⁻³ has a marginal effect with an increase to 26 % conversion. The possibility exists that the Cu/Cd reductor column reduces nitrate to lower oxidation states than nitrite. This can be discounted as the response to standard nitrite solutions remains constant irrespective of whether Cu/Cd is present in the column or solely glass wool. As commercial Cu/Cd reduction columns obtain 100 % conversion efficiency, the column used here may be considered very inefficient. It is conceivable that increasing the conversion efficiency may increase the linear range and lower the LOD of the electroanalytical procedure developed here. The low level of conversion also supports the view stated earlier that the slow decline in sensitivity is a result of decreasing surface area of the cadmium with use. It is likely that the use of Cu/Cd columns with large conversion efficiencies may eliminate the slow decrease in sensitivity.

3.8.7 Analysis of Nitrate in a Commercial Fertiliser

Having established reductor column specifications and electrolyte conditions conducive for the determination of nitrate following reduction to nitrite, the nitrate concentration in a commercial fertiliser sample was determined by the Cu/Cd amperometric method and also by potentiometry.

For the amperometric FIA method a calibration plot was constructed over the concentration range 1.0×10^{-3} mol dm⁻³ to 1.0×10^{-2} mol dm⁻³ nitrate. Plots of $\log_{10} [\text{NO}_3^-]$ vs. current responses were found to be linear over this concentration range with $r = 0.9995$. Blank injections of 0.1 mol dm⁻³ NaCl did not produce measurable responses. The average response for $n=3$ determinations (comprising of three replicate injections for each n) for the dissolved sample was 4.466 ± 0.020 μA . A blank response, in the absence of the copperised cadmium chips, was found to be 0.287 ± 0.005 μA . The sample response was adjusted for the blank response. The blank response is probably due to interferences in the fertiliser sample such as nitrite. These results yield a concentration of 46.1 ± 0.5 % w/w NO_3^- in the fertiliser sample. For comparative purposes, the analysis was carried out using an alternative analytical method. The potentiometric method utilising the standard addition approach yielded ΔE values of $13.4 \text{ mV} \pm 0.1 \text{ mV}$ ($n=2$) for the addition of 2.0 cm^3 1.0 mol dm⁻³ NO_3^- to 40.0 cm^3 of the sample solution. Using

equation 3.5, the concentration of NO_3^- in the sample solution was estimated and the original concentration in the fertiliser sample calculated to be 45.2 ± 0.2 % w/w NO_3^- . These results indicate that the amperometric FIA procedure for the determination of nitrate is both accurate and precise.

3.9. Conclusions

There is a currently great need for improvements in the performance of analytical methods for the conventional spectrophotometric techniques for the determination of nitrate. This is especially important with respect to increasing the linear range and lowering limits of detection. As nitrate analysis is one of the most frequent analysis, any improved methods must also be compatible with automation. The simple electroanalytical procedure investigated was found to address these problems. This approach improves the performance of the Cu/Cd reductor column methodology by significantly reducing the LOD and extending the linear range considerably. The FIA system is also convenient to automate. In addition, the reductor columns were stable over protracted time periods, due to *in situ* regeneration, which is a significant improvement in current methodology where reductor columns need daily regeneration. These attributes confer considerable advantages to the electrochemical approach compared to the conventional spectrophotometric methods. It is possible that the application of redox polymer modified electrodes to current analytical strategies for other analytes may also prove successful.

3.10. References

- 1 A Hulanicki, W Matuszewski, M Trojanowicz, *Anal Chim Acta* , 1987 194 119
- 2 A Trojanek, F Opekar, *J Electroanal Chem* , 1986 214 125
- 3 M A Koupparis, K M Walczak, H V Malmstadt, *Anal Chim Acta* , 1982 142 119
- 4 L Guanghan, H Zhike, L Yuling, *Talanta*, 1992 39 123
- 5 D Chen, M D Luque de Castro, M Valcarcel, *Analyst*, 1991 116 1095
- 6 J Bassett, R C Denny, G H Jeffery, J Mendham, *Vogel's Textbook of Quantitative Inorganic Chemistry*, Edition 6, Longman, 1978, pp 312-314
- 7 P W West, G L Lyles, *Anal Chim Acta* , 1960 23 227
- 8 F B Hora, P J Webber, *Analyst*, 1960 85 567
- 9 D W W Andrews, *Analyst*, 1964 89 730
- 10 H Barnes, *Analyst*, 1950 75 388
- 11 F L Fisher, E R Ibert, H F Beckman, *Anal Chem* , 1958 30 1972
- 12 A V Trofimov, *Z Phys Chem* , 1935 9 756
- 13 O Deniges, *Z Anal Chem* , 1912 51 158
- 14 X Xing, D A Scherson, *Anal Chem* , 1987 59 962
- 15 R J Davenport, D C Johnson, *Anal Chem* , 1973 45 1979
- 16 R J Davenport, D C Johnson, *Anal Chem* , 1974 46 1979
- 17 G A Sherwood, D C Johnson, *Anal Chim Acta* , 1981 129 87
- 18 D Pletcher, Z Poorabedi, *Electrochim Acta* , 1979 24 1253
- 19 W J Albery, B G D Haggett, C P Jones, M J Pritchard, L R Svanberg, *J Electroanal Chem* , 1985 188 257
- 20 W J Albery, P N Bartlett, A E G Cass, D H Craston
B G D Haggett, *J Chem Soc , Faraday Trans 1*, 1986 82 1033
- 21 A G Fogg, S P Scullion, T E Edmonds, B J Birch, *Analyst*, 1991 116 573

- 22 G Mengoli, M M Musiani, *J Electroanal Chem* , 1989 269 99
- 23 A Henriksen, A R Selmer-Olsen, *Analyst*, 1970 95 514
- 24 A J Kempers, A G Luft, *Analyst*, 1988 113 1117
- 25 W Davidson, C Wolf, *Analyst*, 1979 104 385
- 26 American Public Health Association, American Waterworks Association, Water Pollution Control Federation, *Standard Methods for the Examination of Water and Waste Water*, 15th Edition, American Public Health Association, New York, 1980
- 27 A Otsuki, *Anal Chim Acta* , 1978 99 375
- 28 J Bassett, R C Denny, G H Jeffery, J Mendham, *Vogel's Textbook of Quantitative Inorganic Chemistry*, Edition 6, Longman, 1978, p 589
- 29 J N Barisci, E Wilke, G G Wallace, M Meaney, M R Smyth, J G Vos, *Electroanalysis*, 1989 1 245
- 30 J N Barasci, G G Wallace, *Anal Lett* , 1991 24 2059
- 31 D P Leech, Ph D Thesis, Dublin City University, 1991
- 32 N Nydahl, *Talanta*, 1976 23 349
- 33 R L Lambert, R J DuBois, *Anal Chem* , 1971 43 955
- 34 R B Willis, *Anal Chem* , 1980 52 1377
- 35 J F van Staden, *Anal Chim Acta* , 1982 138 403
- 36 L Anderson, *Anal Chim Acta* , 1979 110 123

Chapter 4

Physical Stabilisation of Electrode Surfaces Modified with [Os(bipy)₂(PVP)₁₀Cl]Cl Using Cross-linking Agents

4.1. Introduction

Since the first examples of modified electrodes, much criticism concerning the physical and chemical stability of the modifying species has been voiced, and in many cases, justifiably ¹⁻³ Through the course of their development, many examples of modified electrodes with improved stability have been reported ^{4,5} However, the purpose of these studies are seldom concerned with improving stability, rather exerting control over mass/transport properties or the electrocatalytic activity of the redox polymer As a result, strategies for polymer film stabilisation have no systematic theme, and the procedures adopted hitherto include a diversity of approaches, mostly based on principles borrowed from polymer science

The early examples of adsorbed monolayer modified electrodes were subject to severe stability problems as the adsorption processes were often in dynamic equilibrium with solution species, resulting in desorption of the modifier in electrolytes devoid of the redox species ^{2,6,7} The covalently attached redox sites, such as those studied by Murray and co-workers,^{8,9} based on surface condensation reactions, were often easily hydrolysed, again, resulting in the loss of redox component from the electrode surface Although elegant, such modified electrodes were of limited application due to their instability Adsorbed polyelectrolyte polymers presented an attractive and stable means of immobilising redox species at electrode surfaces by electrostatic incorporation or attachment by coordination ¹⁰⁻¹⁵ The desorption of such adsorbed polymers is known to be a slow process ¹⁶ Consequently, redox polymers exhibited enhanced stability in comparison to the monolayer modified electrodes ^{2,11} Although electrodes coated with polyelectrolytes loaded with redox reactants have been exploited in a variety of applications, the number of useful polyelectrolyte systems that are available is limited as all commonly available materials lack one or more of the essential properties required for use as an electrode modifier ⁵ These include strong irreversible adsorption of the modifier to the electrode surface, rapid charge and mass transport properties, retention of the electro-active redox sites within the polymer film, efficient electrocatalysis, and physical and chemical stability of the polymer and redox site ¹⁷

Extensive studies of the redox polymers used here have shown that they fulfil a number of the cited requirements for a successful electrode modifier¹²⁻¹⁵ The redox sites are immobilised in the polyelectrolyte by coordination bonding, consequently the redox sites are not subject to chemically reversible equilibrium processes such as adsorption or ion exchange, and are therefore permanently immobilised in the polymer film¹²⁻¹⁵ The redox centres of the osmium polymer are also chemically unreactive, and substitution of the potentially labile chloride ligand is difficult¹⁴ As a result, these modified electrodes exhibit good chemical stability Another indication of the stability of these materials is the fact that they can be heated in air to temperatures in excess of 300 °C during differential scanning calorimetry without degradation of the polymer The analogous ruthenium redox sites are chemically less stable and undergo photo-substitution of the chloride ligand to produce the *aqua* complex, $[\text{Ru}(\text{bipy})_2(\text{PVP})_{10}\text{H}_2\text{O}]\text{Cl}$ ^{13,15} This, however, can be controlled to a certain extent by the exclusion of light The effect of this change in the coordination sphere of the ruthenium centre on the charge transport properties of the redox polymer is currently under investigation These redox polymers have also been shown to exhibit facile electrocatalytic behaviour towards a number of substrates, *e.g.* Fe(II) oxidation by the ruthenium polymer and Fe(III) reduction by the osmium polymer^{18,19} The second order rate constants for these cross-exchange reactions being large for both substrates, for Fe(II), $k = 2.3 \times 10^5 \text{ mol}^{-1} \text{ dm}^3 \text{ cm s}^{-1}$ and for Fe(III), $k = 2.8 \times 10^3 \text{ mol}^{-1} \text{ dm}^3 \text{ cm s}^{-1}$ In addition, these materials exhibit rapid charge transport properties and favourable permeability to a variety of substrates¹⁸

These desirable properties suggests that these redox polymers may be useful electrode modifiers, however, the long term physical stability of the polymers under operational conditions have been disappointing²¹ A half life of $\approx 8 \text{ h}$ for the redox polymer $[\text{Ru}(\text{bipy})_2(\text{PVP})_5\text{Cl}]\text{Cl}$ in a thin-layer flow-cell has been observed The physical instability appears to be a result of polymer stripping from the electrode surface It was found that overlaying the ruthenium redox polymer with electro-polymerised conducting (poly(3-methylthiophene) and non-conducting (poly(N-ethyltryamine) polymers resulted in improved life times ($t_{1/2} > 48 \text{ h}$) but decreased sensitivities towards substrates was evident²² The origin of the decreased sensitivities was not assessed but it is likely a result of mass

transport restrictions due to the overlaid polymeric coating. Photo-induced cross-linking with UV radiation was also investigated and similar behaviour observed. In a follow up study, Barisci and Wallace²³ studied the use of the analogous material, electro-polymerised $[\text{Ru}(\text{bipy})_2(\text{vpy})_2]^{2+}$ as an electrode modifier. The resulting material was found to have a higher stability in comparison to the preformed redox polymer, but the magnitude of signal enhancement was significantly less. It is possible that this is due to a surface reaction at the electro-polymerised material while at the preformed polymer a through film reaction is known to occur.²⁴

The use of plasticisers to influence the mechanical properties of polymers is well documented. These materials act by separating the polymer chains and therefore increasing bulk polymer segment motion and therefore bulk flexibility.²⁵ The stabilisation of PVP films has been accomplished by the incorporation of the plasticiser dioctyl phthalate to the film upon casting.²⁶ This resulted in increased durability of the polymer films. The films were found to be more flexible and due to the hydrophobicity of the plasticiser, less susceptible to dissolving in aqueous solution. This simple process also resulted in a considerable improvement in the charge transport properties of the polymer.

The chemical cross-linking of polymers to form insoluble materials appears an attractive approach to increasing the stability of polymeric electrode modifiers. The use of chemically cross-linked films on electrodes have therefore been used by several workers to obtain stable polymer coatings. Facci and Murray²⁷ reported a co-polymer comprising of the monomers 4-vinylpyridine and γ -methacryloxypropyltrimethoxysilane (96/4 mol %) The latter monomer forms cross-links on exposure to moisture. An alternative approach was proposed by Shaw *et al* and involved electro-polymerisation of 4-vinylpyridine in the presence of divinylbenzene to produce a cross-linked polymer.²⁸ Lindholm and Sharp used 1,6-dibromohexane, 1,10-dibromodecane and $\alpha\alpha'$ -dibromo-p-xylene to cross-link PVP.²⁹ The films were subsequently loaded with $[\text{IrCl}_6]^{2-/3-}$ to form films where the electrostatically incorporated redox centre was retained sufficiently for the examination of the mediated oxidation of Fe(II).

The polymer backbone of redox polymers is known to exert considerable influence over the charge and mass transport processes.

occurring at the electrode. For this reason, several examples of co-polymers have been used to control the charge transport properties of such films. Often a consequence of changes in polymer backbone composition, is an increase in stability of the modifying layer compared to the homopolymer.⁴ In a recent study³⁰, the stability of a series of ruthenium-containing redox polymers with various polystyrene (PS) and PVP ratios were investigated, $[\text{Ru}(\text{bipy})_2(\text{PS})_x(\text{PVP})_y\text{Cl}]\text{Cl}$ where $x + y = 10$ and compared to the PVP homopolymer. It was found that for the oxidation of nitrite at the PVP homopolymer, the cross-exchange reaction was through film in nature (L_k) up to a surface coverage of $8 \times 10^{-9} \text{ mol cm}^{-2}$. At higher surface coverages, total catalysis was observed with the change over to the corresponding LS_k kinetic regime.²⁴ Incorporation of styrene up to 50 mol % did not affect the kinetics and transport behaviour of the modified electrode processes for nitrite oxidation. It was found that incorporation of the styrene residues greatly enhanced the stability of the films for flow injection analysis of nitrite compared to the homopolymer, but did not affect the sensitivity of the electrode response towards nitrite as expected from the kinetic data.²⁴ A relative standard deviation of less than 1% was observed for responses recorded over 13 days. The homopolymer was found only to be slowly stripped from the electrode surface, this process being accompanied by a corresponding reduction in response. In another study, Anson and Sumi⁴ compared the charge transport properties of random and block co-polymers of PS and p-(diethylaminoethyl)styrene. In this study, the formation of hydrophobic and hydrophilic domains in the polymer on the electrode surface was evident. When the styrene content was > 50 mol %, the block co-polymers were found to exhibit more desirable electrocatalytic properties than the random co-polymer. At low styrene loadings, the difference between random and block co-polymers was insignificant. For both types of polymer, when the styrene content was < 20 - 30 mol %, a marked decrease in stability of the polymer film was observed. The use of composite materials for electrode modification have also been the subject of active investigation recently. Montgomery *et al*⁵ described composite modifiers comprising of a random ternary co-polymer containing two types of hydrophilic cationic groups and hydrophobic styrene groups and conventional polyelectrolytes such as PVP and poly-(vinylimidazole) (PVI). These stability of the composite materials was considerably enhanced compared to that of the polyelectrolyte alone.

For the films studied here, the instability is a result of physical removal of the polymer from the electrode surface under hydrodynamic conditions²² In order to stabilise these films, this stripping process must be prevented The ideal stabilisation procedure should retain or improve the mass / charge transport and electrocatalytic properties of the redox polymer and the resulting films should be chemically and physically stable It is known that the requirements for stability of redox polymers is mutually opposed to the requirements of rapid mass / charge transport³¹ Good stability is obtained with unswollen compact polymer films, while charge transport is optimum in swollen films This is further complicated by the fact that the conditions for fast electron transport and rapid counter ion motion are mutually opposed, so the optimum degree of polymer swelling is a compromise between electron transport and counter ion motion³² In addition, the electrocatalytic properties of the redox polymer are a direct function of the mass and charge transport properties of the film³³ It is obvious that any stabilisation procedure will affect the properties of the redox polymer and therefore has little hope of fulfilling all the requirements of an ideally stabilised film

The stability problem addressed here appears to involve a slow stripping of the polymer from the electrode It is well known that cross-linking of polymer produce insoluble materials, and it was envisaged that *in situ* cross-linking of the polymer chains on electrode surfaces would prevent the polymer from physical removal from the electrode surface In this chapter, the physical stabilisation of $[\text{Os}(\text{bipy})_2(\text{PVP})_{10}\text{Cl}]\text{Cl}$ films by chemical cross-linked with 1,5-dibromopentane, 1,10-dibromodecane and p-dibromobenzene at various mol % is examined The effect of the nature of the cross-linking agent and also of the extent of cross-linking on the surface behaviour, Nernstian behaviour and charge transport properties of the resulting material are described and compared to the behaviour of the homopolymer In addition, the kinetics of the mediated reduction of Fe(III) at the cross-linked films are analysed and compared to the kinetic data for the reduction at the uncross-linked films The advantages of this approach to electrode stabilisation are also considered

4.2. Experimental

4.2.1 Materials and Reagents

4.2.1.1 *In Situ* Cross-linking of $[\text{Os}(\text{bipy})_2(\text{PVP})_{10}\text{Cl}]\text{Cl}$

The synthesis and characterisation of $[\text{Os}(\text{bipy})_2(\text{PVP})_{10}\text{Cl}]\text{Cl}$ was described in chapter 2. This material was cross-linked directly on the electrode surface *via* the solid state reaction with 1,5-dibromopentane, 1,10-dibromodecane and p-dibromobenzene (Aldrich). This was accomplished by the preparation of separate solutions containing known amounts of the redox polymer and the cross-linking reagent. The preparation of redox polymer solutions of exact composition is difficult as the material is known to retain water even after rigorous drying. For this study, a 1.0 % w/v solution of the redox polymer was prepared in methanol, this solution was then accurately diluted serially to obtain 0.1 %w/v and 0.01 % w/v solutions. The original 1.0 % w/v solution was then “calibrated” by coating known volumes of the redox polymer solution onto electrodes and measuring the surface coverage by integration of slow sweep cyclic voltammograms (1 mV s^{-1}) and by coulometry in $0.1 \text{ mol dm}^{-3} \text{ H}_2\text{SO}_4$ electrolyte. The entire film is electro-active in this electrolyte.¹⁸ In this way, the volume of polymer solution required for a particular surface coverage can be evaluated. Stock solutions of 1,5-dibromopentane, 1,10-dibromodecane and p-dibromobenzene were prepared in methanol. Serial dilution was used to produce solutions of the desired concentrations of cross-linking agent. Appropriate volumes of the the polymer solution and cross-linking agent solutions to give the desired surface coverage and level of cross-linking were then placed on the electrode (using typically 10 μL of each solution) dispensed using a Hamilton μL syringe, mixed gently and allowed to dry slowly in air. The electrodes were then cured *in vacuo* for 24 h at room temperature. The levels of cross-linking used were 1, 5, 10 and 20 mol % per monomer unit per chain. As the stoichiometry of the reaction is 2/1 this results in 2, 10, 20, 40 mol % quaternisation of the total quantity of pyridine groups. It is assumed that the reaction results in inter-molecular cross-linking but the possibility of intra-molecular reaction exists. The reproducibility of cross-linking is critical for a systematic study of the properties of the resulting polymer films. The reproducibility of surface coverage was well within the range $\pm 10\%$ of the desired surface coverage, and it is believe that this is a reflection of the precision of the

syringe used to apply the polymer. Assuming the same level of precision is obtained for the application of the cross-linking agent from an identical syringe, then an estimation of the precision of cross-linking can be made. Calculation based on the worst case situation where the maximum surface coverage is in combination with the minimum amount of cross-linking agent (based on precision) and *visa versa*, gives a theoretical estimate of the precision of $\pm 5\%$ of the desired level of cross-linking. This results in cross-linking levels (cross-links / vinyl pyridine residue per chain) in the range $1 / 100 \pm 5$, $1 / 20 \pm 1$, $1 / 10 \pm 0.5$ and $1 / 5 \pm 0.25$. The structure of the resulting polymeric materials can be seen in Fig 4.1.

The procedures reported previously for the solid state cross-linking of PVP involved elevated temperatures, typically 60 °C to 120 °C.^{29,34,35} Such conditions were undesirable in this work for a number of reasons. Firstly, the commercial electrodes used were found to leak on heating above about 50 °C. This results in very high background currents and difficulty in cleaning, and as a result, the electrodes had to be dismantled, cleaned and remounted after each use. In addition, both 1,5-dibromopentane, 1,10-dibromodecane are liquid at room temperature, although their partial pressures are low, it was envisaged that as only small quantities of cross-linking agent were used and distributed across a considerable area compared to volume, loss due to volatilization at elevated temperatures may be problematic. This is undesirable as the level of cross-linking needs to be known. As room temperature conditions were used for the cross-linking reactions in this study, the solid state reaction was studied using infra red spectroscopy.

4.2.1.2 Electrolytes and Solutions

All solutions of electrolyte were prepared from Milli-Q water. As the kinetics of Fe(III) reduction at $[\text{Os}(\text{bipy})_2(\text{PVP})_{10}\text{Cl}]\text{Cl}$ modified electrodes has been studied thoroughly in $0.1 \text{ mol dm}^{-3} \text{ H}_2\text{SO}_4$, this electrolyte was used throughout this study. The low pH ensured solubility of the iron redox species and also prevents interconversion of the redox states. In addition, the redox polymer is soluble in $0.1 \text{ mol dm}^{-3} \text{ H}_2\text{SO}_4$, therefore this electrolyte presents sufficiently arduous conditions to test the

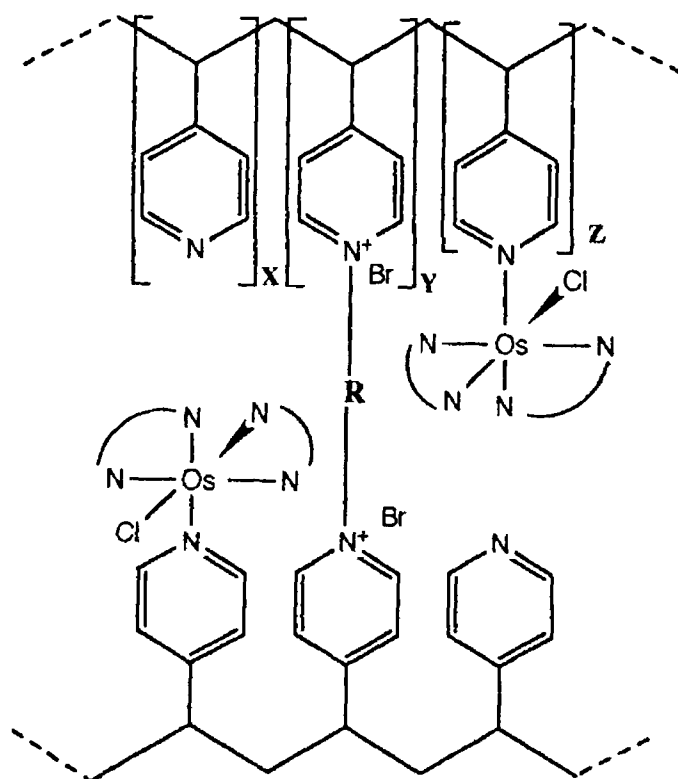


Fig 4 1 Structure of cross-linked redox polymer, where $X = 8$, $Y = 1$ and $Z = 1$ for a 10 mol % cross-linked polymer and $R = 1,5$ -dibromopentane, 1,10-dibromodecane and p -dibromobenzene

stability of cross-linked films The salt $\text{NH}_4[\text{Fe}(\text{SO}_4)_2] \cdot 12\text{H}_2\text{O}$ was used for the preparation of Fe(III) solutions

4.2.1.3 Cyclic Voltammetry and Rotating Disc Electrode Voltammetry

CV and RDE voltammetry were carried out using a conventional three electrode assembly The potentiostat used was the EG&G Princeton Applied Research Model 362 The rotating disc assembly was the Metrohm Model 629-10 Voltammograms were recorded on a Linseis X-Y recorder The working electrodes were 3 mm diameter glassy carbon discs shrouded in Teflon (Metrohm) The counter electrode was 1 cm² platinum gauze placed parallel to the working electrode at distance of ≈ 1 cm The reference electrode was the saturated KCl calomel electrode All potentials are quoted with respect to the SCE without regard to liquid junction potentials Slow sweep rate cyclic voltammetry was also carried out to ascertain the polymer surface coverage with respect to time in the thin-layer flow-cell using the CV option of the EG&G Princeton Applied Research Model 400 electrochemical detector All measurements, unless otherwise stated, were carried out at room temperature

The glassy carbon electrodes were prepared for modification by polishing with 5 μm alumina as an aqueous slurry on a felt cloth The electrodes were rinsed thoroughly with distilled water and methanol The electrodes were then treated with chlorosulphonic acid to promote the formation of surface oxide functional groups The electrodes were again rinsed with distilled water and dried *in vacuo* at room temperature The electrodes were then modified with the redox polymer and the cross-linking agent as described above

4.2.1.4 Flow Injection Apparatus

The flow injection apparatus consisted of a Gilson Miniplus 3 peristaltic pump, a six port Rheodyne injector valve fitted with a 20 μL fixed volume sample loop, an EG&G Princeton Applied Research Model 400 electrochemical detector connected with Teflon HPLC tubing, and a Philips X-t chart recorder In the flow-cell, an Ag/AgCl electrode acted as the reference electrode The stainless steel cell body acted as the counter

electrode. The working electrodes were also 3 mm diameter glassy carbon shrouded in a Teflon block. Modified electrodes were prepared as described above. All potentials are quoted after numerical conversion to the SCE scale. Sample injections were made using a 2 cm³ glass syringe fitted with a Rheodyne injection needle. The carrier electrolyte used was 0.1 mol dm⁻³ H₂SO₄ at a flow rate of 1.0 cm³ min⁻¹.

4.2.1.5 Infra Red Spectroscopy

A solution of poly-(4-vinylpyridine) was prepared in methanol. Similarly, a methanolic solution of p-dibromobenzene was prepared. Appropriate amounts of both solutions to give a 12 mol % quaternisation of the vinyl pyridine residues, were transferred to a Teflon block, mixed thoroughly and allowed to dry slowly in air. When the methanol has dried completely, the polymer films were removed from the Teflon and placed in the sample beam of the Perkin Elmer 599 Infra Red spectrophotometer. A series of IR spectra of the polymer films were recorded over a 21 h period. The cast films were stored in a vacuum desiccator between measurements to prevent the absorption of water. After 21 h the films were heated to 85 °C for a further 24 h and the IR spectra were again recorded.

4.3. Results and Discussion

4.3.1 General Observations and Considerations Concerning Stability

Before embarking on a detailed discussion on the effect of cross-linking on the stability and electrochemical properties of [Os(bipy)₂(PVP)₁₀Cl]Cl, some general observations concerning the stability of the homopolymer must be addressed. From experience, it is clear that the stability of the redox polymer on the electrode surface depends on a number of critical experimental factors. The molecular weight of the polymer is one of these factors. It is generally observed that increased stability is obtained by increasing the molecular weight of the PVP starting material. Increasing molecular weight of the polymer may

have a number of effects which brings about an increase in stability. Firstly, higher molecular weight materials are less soluble than lower molecular weight analogue compounds.³⁶ Secondly, by increasing the molecular weight of the polymer, the likelihood that some part of each polymer chain can come into contact with the electrode surface is increased. The number of vinyl pyridine units per chain for a particular molecular weight which are likely to be adsorbed can be approximated. A monolayer of redox sites is $\approx 1 \times 10^{-10} \text{ mol cm}^{-2}$. As the metal loading is 1/10, then about $1 \times 10^{-9} \text{ mol cm}^{-2}$ vinyl pyridine units are likely to be adsorbed on the surface. For a surface coverage of $1 \times 10^{-7} \text{ mol cm}^{-2}$, (vinyl pyridine groups), the number of polymer chains at the electrode surface is $\approx 1 \times 10^{13}$ for a $600,000 \text{ g mol}^{-1}$ polymer, and $\approx 3 \times 10^{14}$ chains for a $20,000 \text{ g mol}^{-1}$ polymer. As only $\approx 1\%$ of the residues can be involved in the direct adsorption at a surface coverage of $1 \times 10^{-7} \text{ mol cm}^{-2}$ vinyl pyridine residues, and assuming all vinyl pyridine residues have an equal likelihood of adsorption, then ≈ 60 residues per polymer chain are adsorbed for $600,000 \text{ g mol}^{-1}$ polymer and an average of 2 residues per chain for the $20,000 \text{ g mol}^{-1}$ polymer. So, the electrode / polymer chain interaction is, in theory, stronger for higher molecular weight materials. Also, as the adsorption is an equilibrium process, complete desorption of the higher molecular weight polymer is less likely due the large number of "contact points" along the chains. The use of high molecular weight polymers is especially important for high surface coverages, where there is more competition for surface sites and where it is likely that not every chain can come into contact with the adsorptive surface.

Another factor important in ensuring the stability of the modified electrode is the speed of the casting solvent evaporation. The procedure used here involves the slow removal of the solvent to provide stable, well adhered polymer films. Rapid evaporation of solvent results in unstable films which are, frequently, easily stripped from the electrode. The reason for this may be a result of either of two processes. The fast evaporation process may allow residual solvent to be trapped underneath a dry polymer shell at the polymer surface, and the polymer associated with the entrapped solvent is likely to be highly solvated and on immersion into electrolyte is easily dispersed. Secondly, the kinetics of the adsorption of the polymers onto the electrode surface may influence electrode stability. It is characteristic of polymeric materials that adsorption from solution on

to surfaces is typically much slower than that for the monomers and that a true equilibrium layer is not attained^{16,37} Fortunately, desorption rates are even slower¹⁶ A few studies of polyelectrolyte adsorption onto solid electrodes have been reported In these, a rapid initial adsorption process is observed followed by a slow secondary adsorption process^{16,38} The slow nature of the secondary adsorption process has been attributed to the slow conformational changes required in order that the initial adsorbed layer can accommodate further adsorption¹⁶ On carbon, this slow conformational change may involve slow diffusion into voids in the somewhat porous carbon surface¹⁶ It is therefore likely that rapid evaporation of the casting solvent from the electrode surface to leave dry films, may inhibit the adsorption process sufficiently to prevent adequate adhesion of the polymer film to the electrode surface Preparation of the glassy carbon prior to polymer coating is also critical The preparation regime used here produces highly lustrous glassy carbon electrodes The use of chlorosulphonic acid to promote the formation of oxygen-containing surface functionalities allows the preparation of stable, well adhered films This appears to enhance the adsorptive properties of the carbon surface Finally, an observation should be made concerning the adhesive properties of glassy carbon The adhesive properties of the glassy carbon material which have been used here can vary dramatically depending on the supplier and also on the particular batch supplied The reason for this is unclear Poorly adsorptive glassy carbon, however, is visually inhomogeneous

It is possible to prepare stable redox polymer modified electrodes with careful control of the experimental conditions as outlined above for use in quiescent solution However, under the severe hydrodynamic conditions experienced with rotating disc electrode voltammetry and with thin-layer electrochemical flow cells, the physical stripping of the polymer must be addressed It is likely that for thick polymer films of low molecular weight material, that much of the polymer does not contact the underlying glassy carbon, and, as a result is not strongly immobilised at the electrode surface It is conceivable that by cross-linking of the polymer chains, these un-adsorbed or loosely adsorbed polymer molecules can be “anchored” to the surface by stable chemical bonds

4 3 2 Infra Red Analysis of the Solid State Cross-linking Procedure

Infra red spectroscopy is useful for monitoring reactions involving polymeric materials. It is known that the IR stretching frequency for the pyridine moiety in PVP occurs at 1600 cm^{-1} . On quaternisation of the aromatic nitrogen of the pyridine residue, a shift in the stretching frequency to 1640 cm^{-1} occurs.³⁴ The relative intensity of these two frequencies therefore gives a measure of the extent of quaternisation of the pyridine residues. This technique was used to study the cross-linking reaction between PVP and p-dibromobenzene. Pure PVP rather than the redox polymer was used, as this material can be easily cast as thin films from solution which are convenient for IR analysis. Films cast from the redox polymers are extremely brittle.

The procedures reported previously for the solid state cross-linking of PVP with alkyl dihalides involved elevated temperatures, typically 60 to 120°C .^{29,34,35} It has been reported that such high temperatures were required to activate the solid state reaction. Such conditions were undesirable in this work for a number of reasons as outlined earlier. Infra red spectroscopy was used to investigate the possibility that this reaction may proceed at room temperature. The behaviour observed for this material is also assumed to occur in the redox polymer. It is known that the reaction of PVP with dibromoalkanes leads to almost complete cross-linking, *i.e.* no free alkyl bromide.³⁴

After the polymer and the 6 % cross-linking agent had been mixed and the methanol evaporated to produce thin films, IR spectra were recorded at various time intervals. It was assumed that the extinction coefficient for both frequency are the same.³⁴ After a time period of 1 h, the ratio of absorption at the frequencies $1640\text{ cm}^{-1} / 1600\text{ cm}^{-1}$ was 0.11 which indicates $11 \pm 1\text{ mol \%}$ quaternisation. As the target level is 12 mol % quaternisation, it appears that much of the reaction has been completed after 1 h at room temperature. The films were allowed to dry slowly which took, *ca.* 20 min for complete solvent evaporation. It is possible that the cross-linking reaction proceeded quickly while the reactants were in solution at high local concentration on the electrode surface. No further discernible change in the intensity ratio occurred to 3 h. The films were then left for a further 19 h at room temperature and the relative intensities remeasured. These measurements reveal a quaternisation level of 12 ± 1

mol % vinyl pyridine units. At this stage, the reaction appeared to have gone to completion. However, in order to examine the extent of completion of the cross-linking reaction and the need for elevated temperatures, the films were then heated to 85 °C for a further 24 h to complete the cross-linking reaction of any unreacted cross-linking agent. The repeated IR measurements after the elevated temperature conditions indicated that 13 ± 1 mol % of the vinyl pyridine sites were quaternised. The target level was 12 mol % quaternisation. These results suggest complete reaction of the p-dibromobenzene in the polymer film and that this reaction is 90 % complete after 21 h. For this reason, the electrodes used in this study were cross-linked for a 24 h period prior to use. The solubility of the cross-linked films in methanol was examined. The films were observed to swell considerably due to solvation of the polymer chains, as expected, but dispersion of the polymer was not evident. This indicated cross-linking of the polymer.

4.3.3 Stability of Uncross-linked $[\text{Os}(\text{bipy})_2(\text{PVP})_{10}\text{Cl}]\text{Cl}$

In order to ascertain stability improvements of cross-linked polymer films, the stability of the homopolymer must be established and quantified. Using modified electrodes prepared according to the precautions outlined earlier, electrodes were subject to severe hydrodynamic conditions and the surface coverage of the polymer accesses with respect to time using slow sweep rate CV. In Fig. 4.2 a plot of surface coverage, Γ , vs. time can be seen for modified electrodes placed in thin-layer flow cells. The films were allowed to “break-in” by CV cycling for 15 min prior to measurements. The initial surface coverage was 1.0×10^{-8} mol cm⁻², it can be seen that the polymer surface coverage slowly decreases linearly with time. After a period of 24 h, the surface coverage had reduced to 7.4×10^{-9} mol cm⁻² which represents a loss of 26 %. After a period of 46 h, approximately 50 % of the polymer remained on the electrode surface so the half life of the polymer, $t_{1/2}$, is approximately 46 h. This is a considerable improvement compared to the ruthenium analogue compound studied by Wallace *et al*.²² This is likely due to the very high molecular weight material used in this study. As the redox polymer is soluble in the mineral acid used in these experiments, the linear trend seen here probable represents a slow solvation process of the polymer and the resulting physical removal of the

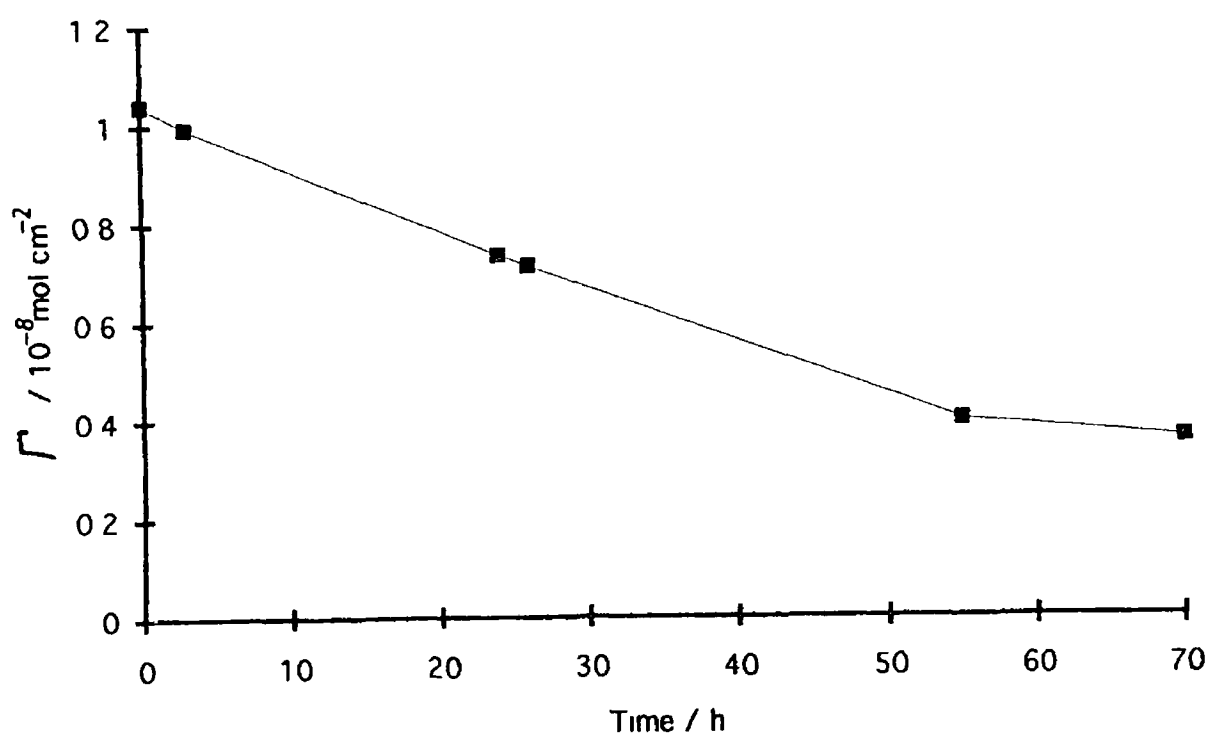


Fig 4 2 Plot of surface coverage of redox polymer with respect to time in the thin-layer flow-cell The electrolyte was $0.1 \text{ mol dm}^{-3} \text{ H}_2\text{SO}_4$ at a flow rate of $1.0 \text{ cm}^3 \text{ min}^{-1}$

dissolved material from the electrode surface. The rate of removal of the polymer is slow, $\approx 1.1 \pm 0.2 \times 10^{-10} \text{ mol cm}^{-2} \text{ h}^{-1}$. At 48 h, the surface coverage is reduced to $4.0 \times 10^{-9} \text{ mol cm}^{-2}$, which is 40 % of the original value. Between 48 h and 70 h the rate of removal drops considerably to $\approx 4.2 \pm 0.2 \times 10^{-11} \text{ mol cm}^{-2} \text{ h}^{-1}$. This appears to suggest that at a surface coverage of about $4 \times 10^{-9} \text{ mol cm}^{-2}$ a change in the stability, and therefore physical nature of the polymer, occurs. It is likely that the polymer chains close to the electrode surface possess more "contact points" of adsorption with the solid electrode surface than chains closer to the electrolyte interface. This would result in less polymer swelling and a more ordered arrangement of chains at the electrode surface. It has been postulated by other workers that the structure of redox polymers close to the electrode/polymer interface is different (more compact) from polymer regions at the polymer/electrolyte interface.²⁰ The results presented here show that there is possibly a difference in the physical properties of these regions and that the material at the polymer/electrode interface appears more strongly adhered to the electrode. At 72 h, the rate of polymer loss levels off. The surface coverage has fallen to $3 \times 10^{-9} \text{ mol cm}^{-2}$ which represents ≈ 30 monolayers of redox sites. From these results, it is evident that the polymer is slowly lost from the electrode surface, by possibly a slow dissolution process to leave a strongly adsorbed layer. The observed instability of the polymer in the thin-layer electrochemical flow-cell has serious consequences for sensor applications in FIA.

We have also studied polymer film stability at rotating disc electrodes at a rotation speed of 1000 rpm. Typically, the $t_{1/2}$ of the redox polymer under continuous rotation conditions is ≈ 24 h. This half-life is therefore approximately only half of that observed in thin-layer flow cells and is a reflection of the more rigorous hydrodynamic conditions encountered with the rotating disc electrode. The rate of polymer stripping was estimated to be $2.1 \pm 0.2 \times 10^{-10} \text{ mol cm}^{-2} \text{ h}^{-1}$ in $0.1 \text{ mol cm}^{-2} \text{ H}_2\text{SO}_4$ at 1000 rpm. After 24 h, the surface coverage was found to remain virtually constant at $\approx 2 \times 10^{-9} \text{ mol cm}^{-2}$. Again, these results suggest that a strongly adsorbed layer of polymer exists at the electrode surface. It seems likely this is due to a large number of adsorption sites per polymer chain close to the electrode surface. This behaviour is consistent with that observed in the thin-layer flow-cell. In light of this, the estimate made earlier concerning the number of monomer residues which may be adsorbed for a particular molecular weight may be considerably

underestimated, as it is likely that the assumption that every pyridine residue has an equal opportunity for adsorption is invalid. Therefore increasing the importance of high molecular weight material for maximum stability of thick polymer films.

The stability of sensor response, for through film reactions, depends on the stability of surface coverage, and stability is therefore of considerable importance for sensor reproducibility. Typically in FIA experiments, sample injections are bracketed by injections of calibration solutions. For a typical 3 injection sequence involving calibration-sample-calibration solutions, with a 12 s peak width, the sequence results in a 36 second time interval. Based on the highest rate of removal in the thin-layer flow-cell detailed above, this corresponds to a loss of $3.2 \times 10^{-14} \text{ mol cm}^{-2}$ over 36 s period. Using the equation for the characteristic kinetic current given by Saveant^{39,40}

$$i_k = n F A k K b_0 L y_\infty \quad (4.1)$$

The characteristic kinetic current for a typical through film reaction can be estimated before and after the 36 s time interval. For a $1.0 \times 10^{-8} \text{ mol cm}^{-2}$ ($b_0 L$) film of $[\text{Os}(\text{bipy})_2(\text{PVP})_{10}\text{Cl}]\text{Cl}$, the reduction of $1.0 \times 10^{-3} \text{ mol dm}^{-3}$ Fe(III) (y_∞) with $kK = 5.6 \times 10^2 \text{ dm}^3 \text{ mol}^{-1} \text{ cm s}^{-1}$ ¹⁸ gives $i_k = 5.4 \times 10^{-4} \text{ A cm}^{-2}$, while after a time period of 36 s, the change in i_k due to polymer stripping is $5.9 \times 10^{-8} \text{ A cm}^{-2}$, which corresponds to a 0.011 % change in i_k . Over this time period, the change in response is therefore negligible. In order to effect an unacceptable 1% change in i_k for a typical measurement sequence, a time interval of 40 min would be required between calibration and sample measurement. Although important, the loss surface coverage is sufficiently slow to ensure no significant difference in the catalytic properties of the modified electrode over typical FIA measurement time scales where calibration is possible. In situations where direct or frequent calibration is impossible, then polymer loss would significantly alter modified electrode sensitivity over protracted time periods.

4.3.4 Stability of Cross-linked $[\text{Os}(\text{bipy})_2(\text{PVP})_{10}\text{Cl}]\text{Cl}$

The osmium redox polymer, $[\text{Os}(\text{bipy})_2(\text{PVP})_{10}\text{Cl}]\text{Cl}$, was cross-linked with 1, 5, 10, 20 mol % of the three cross-linking agents, 1,5-dibromopentane, 1,10-dibromodecane and p-dibromobenzene. In order to assess the stability of these films, the surface coverages with respect to time were recorded for electrodes placed in thin-layer flow-cells and for modified rotating disc electrodes.

It was found that cross-linking with all three cross-linking agents and at all levels resulted in highly stable polymer films. For modified electrodes placed in the thin-layer flow-cell, the surface coverages were found to be maintained within 95 % of their original level over 24 h of continuous flow of $0.1 \text{ mol dm}^{-3} \text{ H}_2\text{SO}_4$. Similar levels of stability were found for the modified rotating disc electrodes. The initial CV (A) and a CV after 24 h (B) for a $1.0 \times 10^{-8} \text{ mol dm}^{-3}$ polymer film cross-linked with 20 mol % p-dibromobenzene can be seen in Fig. 4.3. No significant difference in both CV's is evident. For all cross-linking agents examined, and at all levels, surface coverages for the RDE's were within 10 % of the initial surface coverage after 24 h of continuous electrode rotation.

No apparent difference in the level of stability between cross-linking agents or between different levels of cross-linking was evident. This indicates that the simple anchoring of the outer-layer polymer chains is sufficient to effect stability at cross-linking levels as low as 1 mol %. When it is considered that the polymer at the polymer/glassy carbon interface is strongly adsorbed, it is not surprising that an "all or nothing" result is observed, *i.e.* either cross-linking stabilised the films or it did not.

It is clear from the discussion above, that cross-linking the osmium polymer exerts considerable change in the physical stability of the polymer films. However, as cross-linking levels as low as 1 mol % were effective at completely stabilising the polymer films, no discernible difference between the various cross-linking agents and their respective levels was evident by simple measurements of surface coverage. As already mentioned, the cross-linking reaction has the effect of producing a polymer network structure on the electrode surface where both inter- and intra-molecular

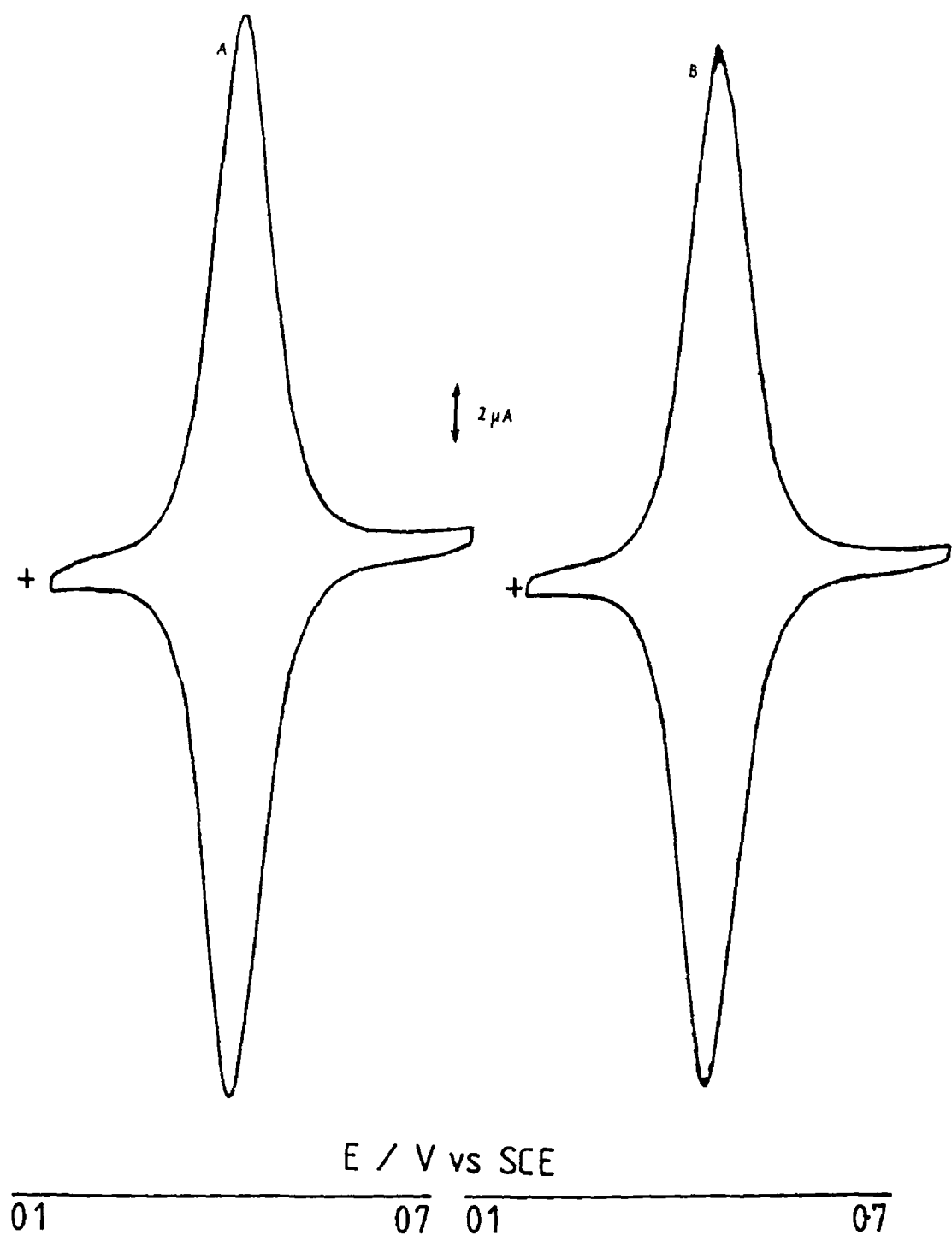


Fig 4.3 Cyclic voltammograms for a $1.0 \times 10^{-8} \text{ mol cm}^{-2}$ polymer film cross-linked with 20 mol % p-dibromobenzene. Curve (A) represents the initial CV while curve (B) shows the CV after 24 h. The electrode was continuously rotated at 1000 rpm over the 24 h period. The electrolyte was $0.1 \text{ mol dm}^{-3} \text{ H}_2\text{SO}_4$ and the potential sweep rate was 50 mV s^{-1} .

bonding is possible. It is well known that cross-linking reduces the possibility of ordered arrangements of polymer molecules in the solid state (polymer crystallinity) ⁴¹. The cross-linking reaction also results in permanent quaternisation of the bridging pyridine residues on the polymer backbone. These effects are likely to lead to gross changes in the bulk structure of the polymer film, altered interactions with electrolyte which ultimately lead to modified electrochemical behaviour. The study of the electrochemical properties of the cross-linked redox polymers may identify subtle differences between the various cross-linking agents and their level of use. For this reason the charge transport, electrocatalytic, Nernstian and surface behaviour of the cross-linked redox polymers were examined. The results will be discussed along these areas.

4.3.5 Charge Transport Characteristics

The rate of charge transport through redox polymer films can be limited by (1) the intrinsic barrier to electron self-exchange (k_{ex}), (2) the transport of charge compensating counter-ions into/out of the polymer film, and (3) polymer segment motion required for redox site juxtapositioning ²⁰. It has recently become clear that the conditions for rapid electron transfer and rapid counter-ion motion are mutually opposed ³². Highly swollen films favour fast ion transport due to the considerable void volume available to accommodate incoming counter ions within the polymer, and the absence of diffusional barriers restricting ion movement. Compact films favour electron transport for two reasons: firstly the redox sites are close together in compact films and secondly, the effective concentration of redox sites within the polymer increases causing a corresponding increase in the rate of self-exchange. The effective rate of electron diffusion, D_e , through redox polymers is given by equation 4.2 ²⁹

$$D_e = \pi k_{ex} \delta^2 c / 4 \quad (4.2)$$

Where, k_{ex} is the rate constant for self-exchange, δ is the contact distance between the reacting species and c is the concentration of electro-active species within the polymer film. Optimisation of D_{ct} is therefore often a

compromise between these opposing requirements. For this reason, any change in polymer structure is likely to result in multiple physical changes of which the net effect is an increase, decrease or negligible effect on charge transport rates. It is therefore difficult to interpret D_{ct} data for the purposes of elucidation of the nature and relative importance of the charge transport controlling processes. The purpose of this work was simply to examine the effect of cross-linking on the overall rate of D_{ct} within the polymer and consider the implications of the results for sensor applications.

The charge transport properties of $[\text{Os}(\text{bipy})_2(\text{PVP})_{10}\text{Cl}]\text{Cl}$ have been extensively studied. From these studies it appears, although not totally conclusively, that the overall rate of charge transport through the osmium polymer is controlled by counter-ion motion.³² In Table 4.1 the charge transport diffusion coefficient, D_{ct} , for the cross-linked redox polymers in the electrolyte used here are shown along with the D_{ct} value for the homopolymer. These values have been estimated by CV using the Randles-Sevcik equation.²⁰ At potential sweep rates $\geq 100 \text{ mV s}^{-1}$ charge transport is diffusionally controlled. This technique yields values more representative of the bulk polymer structure, which is important in the study of the effect of polymer chain cross-linking. These D_{ct} results are also graphed in Fig. 4.4 for clarity. The D_{ct} value for the homopolymer in this electrolyte was estimated to be $1.8 \times 10^{-10} \text{ cm}^2 \text{ s}^{-1}$ which is comparable to that found by Forster *et al.*²⁰ using CV. It can be seen from Table 4.1 and Fig. 4.4 that the D_{ct} values for all mol % for p-dibromobenzene are comparable with that of the homopolymer. Therefore cross-linking with p-dibromobenzene (Fig. 4.4A) does not affect the overall charge transport properties of the redox polymer. Also, no systematic trend appears in the results between different levels of cross-linking. These observations are encouraging as it appears that the D_{ct} properties are maintained and the exact level of cross-linking is not of paramount importance.

It has been observed that cross-linking of redox polymer results in compacting of the polymer film and hindered short range ion motion within redox polymers which yields lowered charge transport rates.⁴² It is therefore expected that increasing the level of cross-linking agent should hinder ion transport and by implication reduce D_{ct} by decreasing the extent of polymer swelling. The polymers studied here are, however, only

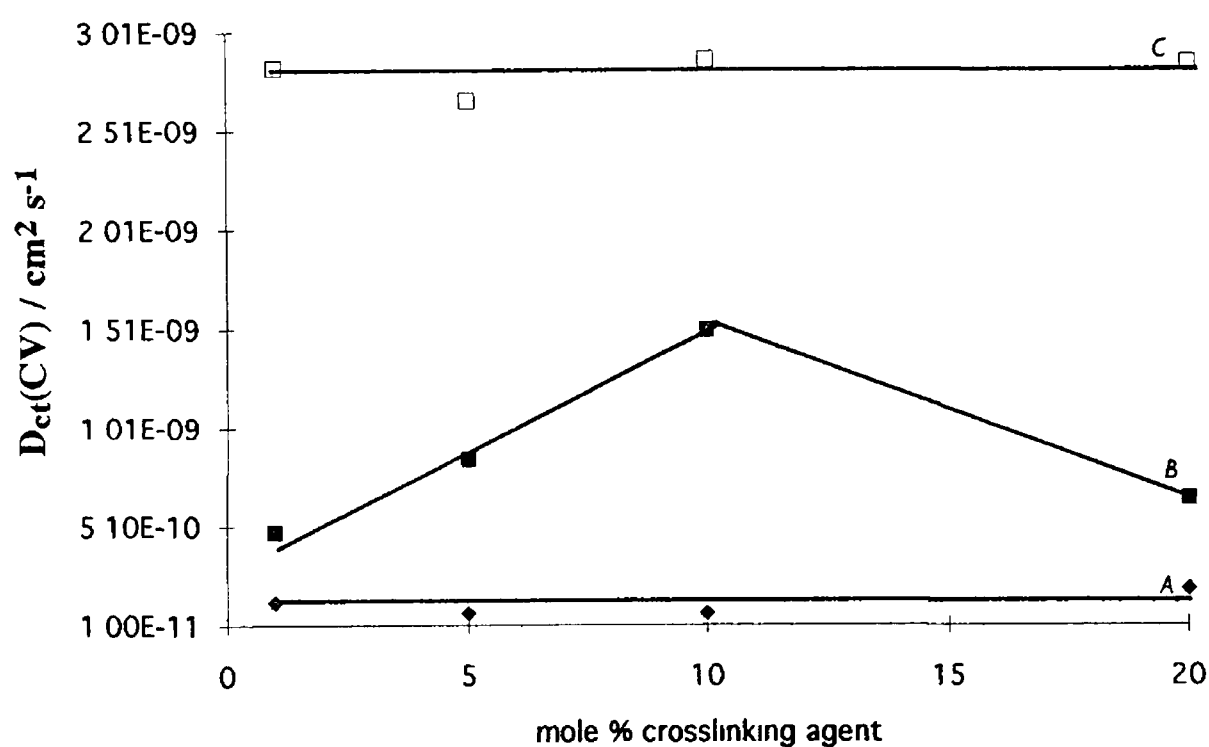


Fig 4.4 Plot of D_{ct} vs mol % cross-linking for (A) p-dibromobenzene, (B) 1,5-dibromopentane and (C) 1,10-dibromodecane D_{ct} values estimated by high sweep rate CV, the electrolyte was $0.1 \text{ mol dm}^{-3} \text{H}_2\text{SO}_4$

mol % crosslinking agent	$D_{ct} / \text{cm}^2 \text{s}^{-1} \text{ §}$		
	1,5-dibromopentane	1,10-dibromodecane	p-dibromobenzene
1	4.8×10^{-10} $\pm 0.3 \times 10^{-10} \ddagger$	2.8×10^{-9} $\pm 0.2 \times 10^{-10}$	1.3×10^{-10} $\pm 0.2 \times 10^{-10}$
5	8.5×10^{-10} $\pm 0.1 \times 10^{-10}$	2.7×10^{-9} $\pm 0.2 \times 10^{-10}$	0.7×10^{-10} $\pm 1.0 \times 10^{-11}$
10	1.5×10^{-9} $\pm 0.3 \times 10^{-10}$	2.9×10^{-9} $\pm 0.2 \times 10^{-10}$	0.7×10^{-10} $\pm 1.0 \times 10^{-11}$
20	6.4×10^{-10} $\pm 0.1 \times 10^{-10}$	2.9×10^{-9} $\pm 0.2 \times 10^{-10}$	2.0×10^{-10} $\pm 2.0 \times 10^{-11}$
homopolymer	$1.8 \times 10^{-10} \pm 0.2 \times 10^{-10}$		

§ Estimated by cyclic voltammetry with $c = 0.7 \times 10^{-3} \text{ mol cm}^{-3}$

‡ Error estimated from measurements for at least two electrodes

Table 4.1 Charge transport diffusion coefficients for various crosslinking agents and various levels of crosslinking. The electrolyte was $0.1 \text{ mol dm}^{-3} \text{ H}_2\text{SO}_4$ and the potential sweep rate was in the region 100 mV s^{-1} to 500 mV s^{-1} .

lightly cross-linked (compared to electro-polymerised and electrostatically cross-linked polymers) (≤ 20 mol %) and are expected to be swollen in the acidic electrolyte due to pyridine protonation and the effect of quaternisation. As a result, mass transport may not be inhibited dramatically by this level of cross-linking. The opposite effect of cross-linking, the reduction in inter-site distances by bringing swollen polymer chains and therefore redox sites into close proximity, should not affect D_{ct} if counter-ion motion is the rate limiting process for the uncross-linked polymer. Assuming counter-ion motion is rate limiting, cross-linking can only decrease or maintain D_{ct} values as the rate of self-exchange appears faster than mass transport.

For the p-dibromobenzene, no significant change in D_{ct} is evident compared to the homopolymer. Nernstian behaviour⁴³ suggests that the p-dibromobenzene cross-linked polymers possess sufficient void volume to accommodate the incoming charge compensating counter-ions (*vide infra*) upon redox. The redox waves are characteristic of an ideal surface species (no diffusional control, *vide infra*) at potential sweep rates < 100 mV s⁻¹, behaviour similar to the homopolymer. Therefore, it appears that the resulting cross-linked structure may not be grossly different from the uncross-linked polymer. It is possible that, as the cross-linking agent is rigid, this may act to keep polymer chains apart to yield an open structure similar to the homopolymer. Through film mediated electrocatalysis of Fe(III) reduction also supports the view of an open structure (*vide infra*) for p-dibromobenzene cross-linked polymer films.

For 1,10-dibromodecane, the rate of charge transport was again found to be constant ($\pm 5\%$) between different levels of cross-linking (Fig 4.4C). No systematic trend was observed. The D_{ct} values are however about one order of magnitude greater than that for the homopolymer, which is again advantageous for sensor applications. This indicates considerable improvement in the charge transport properties of the polymer films upon cross-linking with this compound. The relative importance of mutually opposing effects may be responsible for the magnitude of D_{ct} . As the rate determining process for uncross-linked polymer is suspected to be counter-ion motion, increasing the compaction of the polymer film should decrease or at best maintain D_{ct} values. The cross-linking of the polymer chains is however likely to bring inter-chain redox sites into close proximity compared to the homopolymer (increase

in c), which favours increased electron transport rates. It appears that this may be responsible for the increase in the rate of charge transport. As an increase in D_{ct} is observed, this suggests that counter-ion motion may not in fact be the rate limiting process rather the rate of electron self-exchange. Recent quartz crystal microbalance studies on these materials also indicate that counter-ion transport may not be the charge transport limiting process.⁴⁴ The level of film compaction may not be sufficient to inhibit rapid counter-ion motion and sufficient void volume for charge compensation is available. This view is supported by Nernstian results and surface behaviour (*vide infra*). The n-alkyl chains are long and flexible thus presenting little resistance to ion transport. It is therefore reasonable that D_{ct} should increase under these conditions with respect to the homopolymer.

The D_{ct} results for 1,5-dibromopentane (Fig. 4.4B) are more interesting. At a 1 mol % cross-linking level, the rate of charge transport is slightly faster, by about a factor of two compared to that for the homopolymer. On increasing the level of cross-linking, the rate of D_{ct} increased until about 10 mol % and then decreases again. This clearly shows the gradual improvement and then decline in the charge transport properties of the polymer with cross-linking. This behaviour again may be explained qualitatively on the basis of the interplay between the mutual effects on counter-ion motion and redox site concentration. As the level of cross-linking is increased, the rate of D_{ct} increased due to compaction of the polymer film resulting in a decrease in the inter-site distance (increase in c), the effect of increasing c however, is not as significant as that due to 1,10-dibromodecane as increased ion transport hindrance is likely to occur due to the smaller size of the 1,5-dibromopentane chain. This is reflected in diffusional nature of the CV waves for 1,5-dibromopentane cross-linked films at lower potential sweep rates compared to the 1,10-dibromodecane. At > 10 mol %, the effect of ion transport becomes predominant and limiting and a corresponding decrease in D_{ct} occurs. This is confirmed by the Nernstian behaviour for 20 mol % cross-linked films, where super-Nernstian slopes suggests insufficient free volume for the incoming charge compensating counter-ions (*vide infra*).

The results presented here show that cross-linking of the redox polymer affects the charge transport properties of the redox material significantly. No diminution in D_{ct} is evident for these stabilisation

procedures which was one of the aims of a successful stabilisation scheme. In fact, cross-linking results in an increase in D_{ct} for 1,10-dibromodecane and 1,5-dibromopentane. In addition, D_{ct} values are relatively insensitive to the level of cross-linking (except 1,5-dibromopentane). The increase in D_{ct} appears to be a result of polymer film contraction compared to the uncross-linked state and the corresponding decrease in redox site distance and increase in the rate of self-exchange (as c increases) between the redox sites within the film. Long flexible cross-linking (1,10-dibromodecane) agents appear to present little resistance to counter-ion motion as evident by fast D_{ct} and pure thermodynamic (potential dependent) behaviour at low potential sweep rates. The short flexible cross-linking agent, 1,5-dibromopentane, however, provides more diffusional resistance to ion transport and result in diffusionally controlled behaviour.

4.3.6 Nernstian Behaviour

Recently a model has been developed describing the coupling of mechanical and electrochemical thermodynamics of redox polymer films on electrode surfaces.⁴³ The electrostatically enforced intrusion of compensating counter-ions from the supporting electrolyte is predicted to result in non-Nernstian behaviour because of the inequality of the finite void volume available within the polymer film and the finite molar volume of the compensating ions. The physical consequences of this phenomenon is the forced swelling of the polymer film, a process which in the presence of cross-links, requires energy input in excess of that needed for simple electron transfer to/from the electrode. The electrode potential in this model is given by equation 4.2

$$E = E^{\circ} + (RT/nF) \ln [f / (1-f)] + n v_A^2 c K_m (f - 0.5) / (10^4) Fz^2 \quad (4.3)$$

Where E is the electrode potential, E° is the formal potential, R , T , n and F have their usual meaning, v_A is the molar volume of the anion, c is the concentration of electro-active sites within the film, K_m is the bulk modulus of elasticity of the polymer, f is the fraction of redox sites within the film in the oxidised state and z is the charge on the anion. It is evident

that the mechanical properties of the polymer along with the size of the charge compensating counter-ion can influence the Nernstian behaviour of the redox material. This model has been used to assess the chemical and mechanical properties of plasma-polymerised (highly cross-linked) polyvinylferrocene (PPVF).⁴⁵ The Nernstian behaviour of thin films of PPVF on various electrode materials was examined and the films were found to show super-Nernstian slopes of 120-150 mV decade⁻¹. This was related to the stress induced by the forced inclusion of charge compensating counter-ions. The osmium redox polymer studied here has been observed to exhibit super-Nernstian behaviour in perchlorate electrolyte.¹⁸ This was attributed to the formation of inter-molecular cross-links *via* ion association in the interior of the polymer and the resulting forced inclusion of counter-ions. Similar behaviour has been observed for linear PVF in perchlorate electrolyte.⁴⁶ The model given above was used to distinguish and describe three regions of behaviour in linear PVF, (1) the ion sensitive membrane model (Donnan behaviour), (2) the redox site interaction model (phase separation) and (3) mechanical/electrochemical coupling model.

The Nernstian behaviour of the cross-linked redox polymer at a 20 mol % cross-linking level for each cross-linking agent was examined in order to assess the effect of cross-linking on the electrochemical / mechanical properties of the polymer films.

In Fig. 4.5 the Nernstian plots for the 20 mol % cross-linking of 1,5-dibromopentane, 1,10-dibromodecane, and p-dibromobenzene polymer can be seen. The Nernstian behaviour of the uncross-linked polymer is identical to that for 1,10-dibromodecane and p-dibromobenzene. The plots for 1,10-dibromodecane (A), p-dibromobenzene (B) are linear and have slopes of 58 ± 2 mV decade⁻¹ (at 20 °C) over the region $-2 \leq \log [(\text{Os(II)} / [\text{Os(II)}] \leq +2$. The operational potential, where $[\text{Os(III)}] = [\text{Os(II)}]$ is found at 0.250 ± 0.005 V vs. SCE for both these cross-linking agents. It is evident from these results that the redox polymers exhibit ideal Nernstian behaviour under the conditions examined here. This behaviour suggests that the void volumes of these two cross-linked polymers are sufficient to ensure electro-neutrality without requirement for mechanical Gibbs energy for forced expansion of the polymer for inclusion of the counter-ions.⁴³ It is also possible that the expulsion of solvent can occur to accommodate counter-ion incorporation.

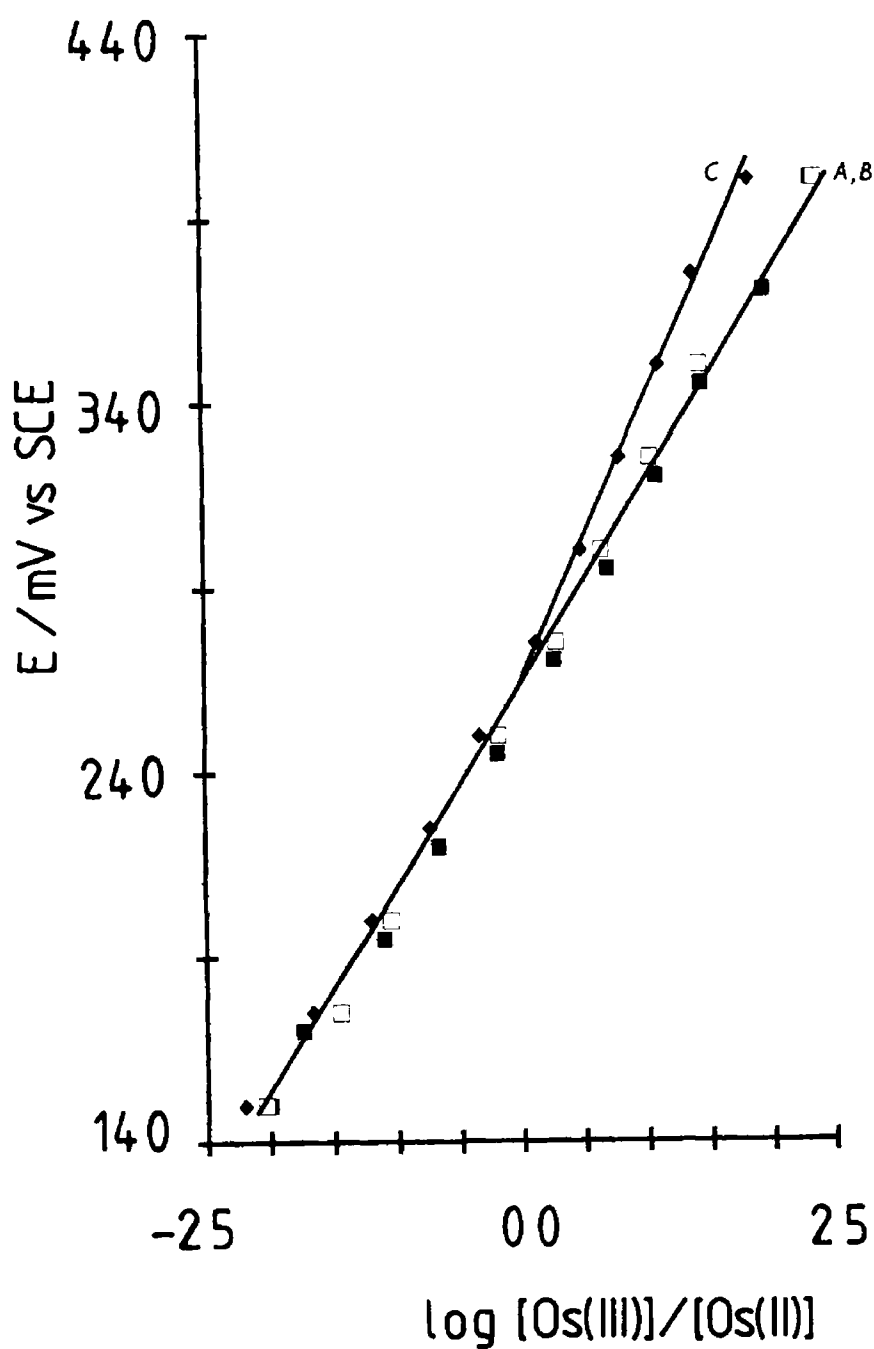


Fig 4.5 Nernstian plot for polymers cross-linked with 20 mol % of (A) \square p-dibromobenzene, (B) \blacksquare 1,10-dibromodecane and (C) \blacklozenge 1,5-dibromopentane. The electrolyte was $0.1 \text{ mol dm}^{-3} \text{ H}_2\text{SO}_4$ and the surface coverages were $1.0 \times 10^{-8} \text{ mol cm}^{-2}$.

again resulting in Nernstian behaviour. These results indicate that these cross-linked redox polymers contain considerable free volume and are therefore possibly gel-like in nature. It will be briefly mentioned in chapter 5 that $[\text{Os}(\text{bipy})_2(\text{PS})_{7.5}(\text{DMAP})_{2.5}\text{Cl}]\text{Cl}$ dissolved in dichloromethane resulted in gel-like suspensions, possible due to inter-molecular cross-linking with the difunctional solvent. It seems likely that similar gel-like structures are possible at the electrode surface. These results are in agreement with the D_{ct} results for 1,10-dibromodecane and *p*-dibromobenzene, where the electrochemistry seems kinetically controlled.

The Nernstian response for 20 mol % of 1,5-dibromopentane cross-linked polymer is found to be linear up to $\log [(\text{Os(III)}) / (\text{Os(II)})] \approx 0.0$ with a slope of $57 \pm 2 \text{ mV decade}^{-1}$. This indicates that the redox polymer possesses sufficient void volume to accommodate the incoming charge compensating counter-ions up to about 50 % oxidation. At $> 50 \%$ oxidation, a super-Nernstian slope of $85 \pm 3 \text{ mV decade}^{-1}$ was observed. The operational potential (where $[\text{Os(III)}] / [\text{Os(II)}] = 1.0$) was found to be $0.265 \pm 0.005 \text{ V vs SCE}$. These results are consistent with and represent forced polymer swelling to incorporate counter-ions to maintain electro-neutrality.⁴³ The increased operational potential is a reflection of the Gibbs mechanical energy for counter-ion incorporation. This observation seems reasonable, as the 1,5-dibromopentane chain is short and normally coiled due to the C—C bond angle. This is likely to result in a more compact film in comparison to the rigid *p*-dibromobenzene (which separates the chains) and the longer flexible alkyl chain of 1,10-dibromodecane. This Nernstian behaviour is in agreement with the charge transport results, i.e. cross-linking with 1,5-dibromopentane causes diffusional restriction on counter-ion movement.

4.3.7 Surface Behaviour of Cross-linked $[\text{Os}(\text{bipy})_2(\text{PVP})_{10}\text{Cl}]\text{Cl}$

Certain criteria for the behaviour of ideal surface immobilised species have been established⁴⁷, these criteria have been discussed in chapter 1. It is useful to examine these parameters as they can be helpful in understanding the redox behaviour of modified electrodes. The parameters, E^0 , ΔE_p , peak width at half maximum height (FWHM), ratio $i_{\text{pa}} / i_{\text{pc}}$ and the sweep rate at which change over from semi-infinite to mixed finite and semi-infinite diffusion behaviour occurs are listed in Table

mol % crosslinking agent	$E_{1/2}^*$ /mV vs SCE	ΔE_p^* /mV	t_{pa}/t_{pc}^*	FWHM* /mV	DC‡ /mV s ⁻¹
<u>p-dibromobenzene</u>					
1	250 ± 5	0.0	1 ± 0.01	90 ± 5	100
5	250 ± 5	0.0	1 ± 0.01	90 ± 5	100
10	250 ± 5	0.0	1 ± 0.01	90 ± 5	100
20	250 ± 5	0.0	1 ± 0.01	90 ± 5	100
<u>1,5-dibromopentane</u>					
1	255 ± 5	20 ± 5	1 ± 0.01	90 ± 5	50
5	255 ± 5	10 ± 5	1 ± 0.01	90 ± 5	50
10	255 ± 5	30 ± 5	1 ± 0.01	90 ± 5	50
20	255 ± 5	10 ± 5	1 ± 0.01	90 ± 5	50
<u>1,10-dibromodecane</u>					
1	250 ± 5	0.0	1 ± 0.01	90 ± 5	100
5	250 ± 5	0.0	1 ± 0.01	90 ± 5	100
10	250 ± 5	0.0	1 ± 0.01	90 ± 5	100
20	250 ± 5	0.0	1 ± 0.01	90 ± 5	100

‡ Potential of change over to semi-infinite diffusional control

* Estimated at 1.0 mV s⁻¹

Table 4.2 Parameters indicative of surface behaviour. The electrolyte was 0.1 mol dm⁻³ H₂SO₄ and the surface coverages were 1.0 × 10⁻⁹ mol cm⁻² for each modified electrode.

4.2 These results are for 1.0×10^{-9} mol cm⁻² surface coverages. It can be seen that the polymers cross-linked with p-dibromobenzene and 1,10-dibromodecane are comparable with the behaviour observed for the homopolymer. The values for ΔE_p , i_{pa} / i_{pc} and FWHM for these cross-linking agents are consistent with rapid reversible surface behaviour of the redox couple. In addition, the plot i_p vs sweep rate is linear up to 100 mV s⁻¹. This indicates the near ideal surface behaviour of the cross-linked films. The $E_{1/2}$ obtained by CV is identical to that obtained from the Nernstian study. Together, these observations indicate the absence of restrictions on ion movement at slow sweep rates and that charge transport is kinetically controlled up to about 100 mV s⁻¹. At higher sweep rates charge transport becomes diffusionally controlled.

Again the results for 1,5-dibromopentane differ slightly from the other cross-linking agents. The $E_{1/2}$ is slightly larger at 255 mV vs SCE, which is consistent with that observed for the Nernstian study. The ΔE_p for all levels of cross-linking with 1,5-dibromopentane was > 0 which is expected for a diffusionally controlled charge transport. In addition, the onset of semi-infinite diffusional behaviour occurs at about 50 mV vs SCE. The i_{pa} / i_{pc} ratio of 1.0 indicates that the kinetics of the forward and reverse reactions are the same. Collectively, these results indicate a mixed finite and semi-infinite diffusional behaviour of the redox polymer under the slow potential sweep rate conditions examined.⁴⁸

It is evident that cross-linking with p-dibromobenzene and 1,10-dibromodecane does not affect the surface behaviour of the osmium redox polymer. This is not surprising since both these cross-linking agents appear not to hinder ion movement or electron transport to any extent (as evident from D_{ct} values). However, cross-linking with 1,5-dibromopentane results in deviation from the ideal behaviour. This is most likely due to the fact that potential increase in the rate of D_{ct} due to a reduction in inter-site distances is not realised as film compaction is sufficient to limit ion availability to a greater extent than that observed for p-dibromobenzene and 1,10-dibromodecane.

4.3.8 Kinetics of Fe(III) Reduction at Cross-linked Redox Polymers

The theory of mediated electrocatalysis have been outlined in detail in chapter 1. According to the theoretical models^{33,39,39,49}, the reaction of substrates at redox polymer modified electrodes can occur at any one of six possible reaction zones. The kinetic situation pertaining for a particular system is controlled by the relative importance of the following parameters, (1) the rate of charge transport through the polymer (D_{ct}) film, (2) the extent of substrate distribution (K), (3) diffusion (D_s) within the film, and (4) the rate of the cross-exchange reaction (k). It is therefore likely that cross-linking of the redox polymer will exert considerable influence over the kinetics and transport processes occurring during mediated electrocatalysis. The mediated reduction of Fe(III) at uncross-linked $[\text{Os}(\text{bipy})_2(\text{PVP})_{10}\text{Cl}]\text{Cl}$ modified electrodes in sulphuric acid electrolyte has been investigated in detail previously¹⁸. Fe(III) was found to partition into the film well ($K \approx 0.2$) and for surface coverages up to $1 \times 10^{-8} \text{ mol cm}^{-2}$, the reaction occurs throughout the polymer film *i.e.* the L_k kinetic regime. At higher surface coverages, total catalysis is obtained and a change over to the LS_k mechanism occurs. The rate of the cross-exchange reaction between the osmium sites and the Fe(III) was found to be rapid with $k = 2.8 \times 10^3 \text{ mol}^{-1} \text{ dm}^3 \text{ cm s}^{-1}$. It was found in perchloric acid electrolyte that the mediated reaction occurred at the polymer/electrolyte interface, S_k'' , with the rate constant for the surface reaction being $3.1 \times 10^{-4} \text{ mol}^{-1} \text{ dm}^3 \text{ cm s}^{-1}$. In this section, the mediated electrocatalytic reduction of Fe(III) at electrodes modified with various surface coverages of redox polymer cross-linked with 1, 5, 10, 20 mol % of p-dibromobenzene, 1,5-dibromopentane and 1,10-dibromodecane is described. The implications for sensor applications are discussed.

4.3.8.1 1,10-Dibromodecane

In Fig. 4.6 Levich plots for the mediated reduction of $1.0 \times 10^{-3} \text{ mol dm}^{-3}$ Fe(III) can be seen for a surface coverage of $1.0 \times 10^{-9} \text{ mol cm}^{-2}$. The polymer was cross-linked at levels of 5, 10 and 20 mol % with 1,10-dibromodecane (A, B and C respectively). The Levich flux (D) is also shown. Similar Levich plots were obtained for surface coverages of 1.0×10^{-9} and $5.0 \times 10^{-10} \text{ mol cm}^{-2}$ at the various levels of cross-linking. It can be seen that the reaction flux from the modified electrode is considerably less than the Levich flux *i.e.* not total catalysis. This indicates that

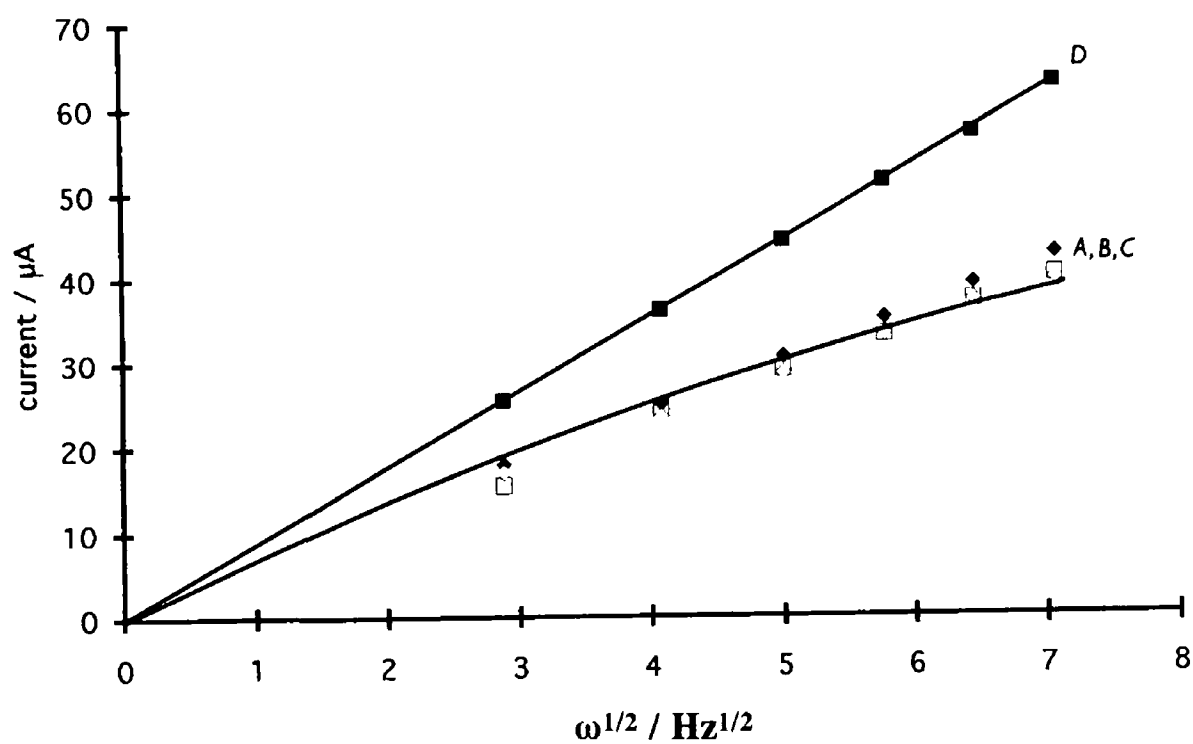


Fig 4.6 Levich plots for the electrocatalytic reduction of Fe(III) at a modified electrode cross-linked with 1,10-dibromodecane where (A) \square 5 mol %, (B) \blacklozenge 10 mol % and (C) \diamond 20 mol % cross-linking and (D) \blacksquare is the Levich flux. The electrolyte was $0.1 \text{ mol dm}^{-3} \text{ H}_2\text{SO}_4$ and the Fe(III) concentration was $1.0 \times 10^{-3} \text{ mol dm}^{-3}$.

transport processes or a chemical limitation control the modified electrode currents rather than simple mass transport from solution. These results suggest that the mediated reaction is controlled by the polymer film. As the rates of the cross-exchange reaction and charge transport are fast, it is likely that substrate partition or diffusion are current limiting. The corresponding Koutecky-Levich plots for 1.0×10^{-8} , 1.0×10^{-9} and 5.0×10^{-10} mol cm⁻² surface coverages cross-linked at a level of 20 mol % are shown in Fig. 4.7. Similar plots were obtained for each level of cross-linking. The diagnostic scheme of Alberly and Hillman^{49,50} can be used to identify the kinetic regime. As the plots are linear and the limiting currents are dependent on the electrode rotation speed, the kinetic regimes S_{te} , LS_{te} and LE_k can be eliminated. This is consistent with rapid D_{ct} within the polymer. The inverse slope of the Koutecky-Levich plots is given by the Levich constant³³, C_{Lev}

$$C_{Lev} = 1.554 D^{2/3} \nu^{-1/6} \quad (4.4)$$

This value has been estimated for clean unmodified electrodes in previous studies to be 1.01×10^{-3} cm s^{-1/2}¹⁸ and 1.04×10^{-3} cm s^{-1/2}⁵⁰. For a poly(hydroxyphenazine) modified electrode, a value of 1.14×10^{-3} cm s^{-1/2} was found for the Levich constant⁵¹. The average Levich slope for all 1,10-dibromodecane cross-linked modified electrodes was found to be $9.1 \pm 0.8 \times 10^{-4}$ cm s^{-1/2}¹⁸ which is close to the reported values above and to the value found for the uncross-linked polymer, $9.4 \pm 0.8 \times 10^{-4}$ cm s^{-1/2}¹⁸. This allows the elimination of the LRZ_{tety} kinetic regime. It can be seen from the Koutecky-Levich plot that modified electrode rate constants, k'_{ME} , are, within experimental error, independent of polymer layer thickness. This allows the elimination of L_k and LE_{ty} kinetic cases. This leaves the regimes S_k'' and LS_k . A plot of $\ln(1-f)$ vs $\ln k'_{ME}$ where f is the fraction of the redox sites in the oxidised state, has a slope of 0.95 ± 0.4 . This indicates that the kinetic regime is S_k'' . In this situation, the electron exchange reaction occurs between redox sites in a region of the redox polymer of molecular dimensions at the polymer/solution interface and the rate constant for the cross-exchange reaction control electrode currents. No partition of the Fe(III) into the film occurs. The S_k'' kinetic case can arise in two situations, a) when charge transport through the

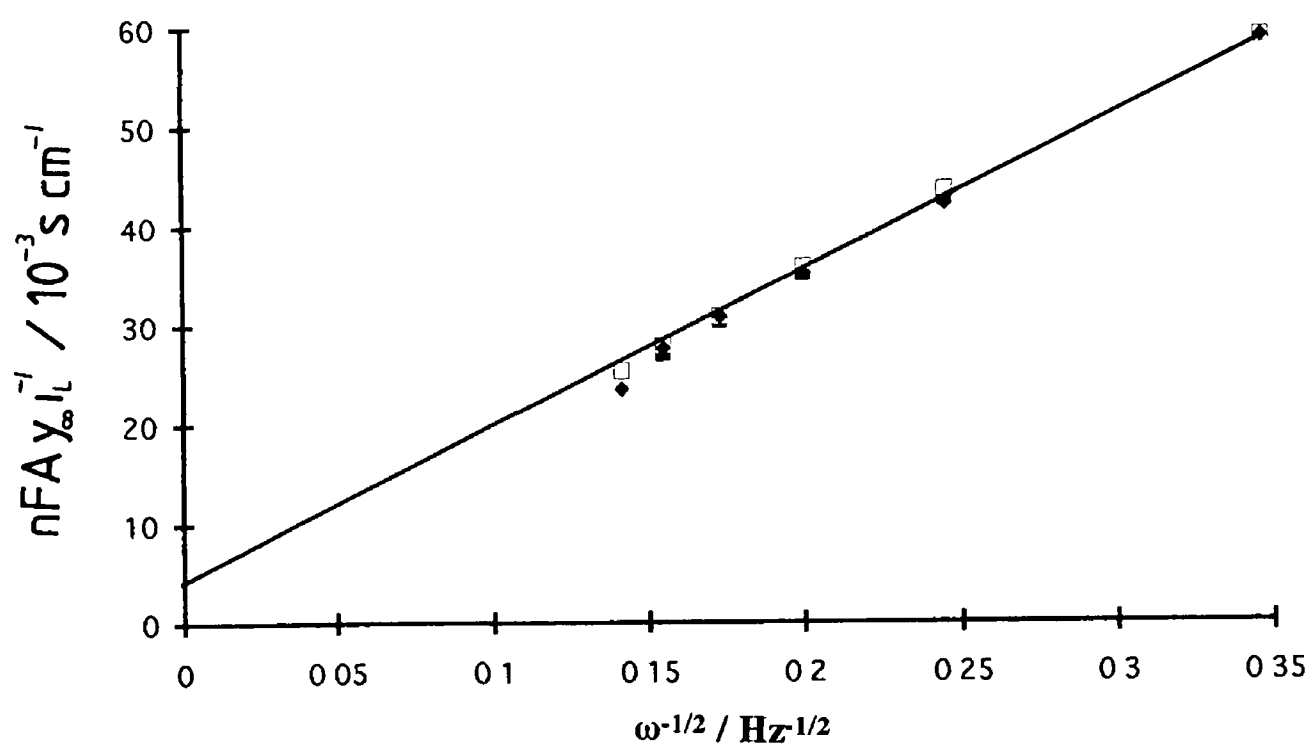


Fig 4.7 Koutecky-Levich plots for the electrocatalytic reduction of $1.0 \times 10^{-3} \text{ mol dm}^{-3} \text{ Fe(III)}$ at a redox polymer modified electrode cross-linked with 20 mol % 1,10-dibromodecane, surface coverages were, $\blacksquare = 1.0 \times 10^{-8}$, $\square = 1.0 \times 10^{-9}$, $\blacklozenge = 5.0 \times 10^{-10} \text{ mol cm}^{-2}$. The electrolyte was $0.1 \text{ mol dm}^{-3} \text{ H}_2\text{SO}_4$.

polymer and the rate of the cross-exchange reaction are so fast that the substrate flux is consumed without penetration of the polymer film, and b) when the substrate is physically unable to penetrate the polymer film. As the observed current flux is considerably less than the predicted Levich flux, it appears that the substrate is unable to penetrate the polymer film. The average value for k'_{ME} is $2.0 \times 10^{-4} \text{ cm s}^{-1}$, and the analytical expression for k'_{ME} under the kinetic regime S_k'' is given by ³³

$$k'_{ME} = k'' b_0 \quad (4.5)$$

As b_0 , the concentration of electro-active centres within the polymer is $0.7 \times 10^{-3} \text{ mol cm}^{-3}$ (neglecting solvent swelling effects), then the second order rate constant for the cross-exchange reaction, k'' , is $2.85 \pm 1.0 \times 10^{-4} \text{ mol}^{-1} \text{ dm}^3 \text{ cm s}^{-1}$. This is equivalent to that found for the reduction of Fe(III) in perchloric acid at the homopolymer which was $3.1 \times 10^{-4} \text{ mol}^{-1} \text{ dm}^3 \text{ cm s}^{-1}$.¹⁸

4.3.8.2 1,5-Dibromopentane

In Fig. 4.8 Levich plots for the mediated reduction of $1.0 \times 10^{-3} \text{ mol dm}^{-3}$ Fe(III) can be seen for a surface coverage of $1.0 \times 10^{-8} \text{ mol cm}^{-2}$. The polymer was cross-linked at levels of 5, 10 and 20 mol % with 1,5-dibromopentane (A, B and C respectively). The Levich flux (D) is also shown. Similar Levich plots were obtained for surface coverages of 1.0×10^{-9} and $5.0 \times 10^{-10} \text{ mol cm}^{-2}$ at the various levels of cross-linking. It can be seen that the reaction flux at the modified electrode is considerably less than the Levich flux indicating that total catalysis is not achieved. This indicates that transport processes or a chemical limitation control the modified electrode currents rather than simple mass transport from solution. These results suggest that the mediated reaction is controlled by the polymer film, probably analyte transport. The current flux at these electrodes is similar to that at 1,10-dibromodecane cross-linked films which suggests a similar kinetic regime. The corresponding Koutecky-Levich plots for 1.0×10^{-8} , 1.0×10^{-9} and $5.0 \times 10^{-10} \text{ mol cm}^{-2}$ films cross-linked with 5 mol % 1,5-dibromopentane are shown in Fig. 4.9. Again, using the

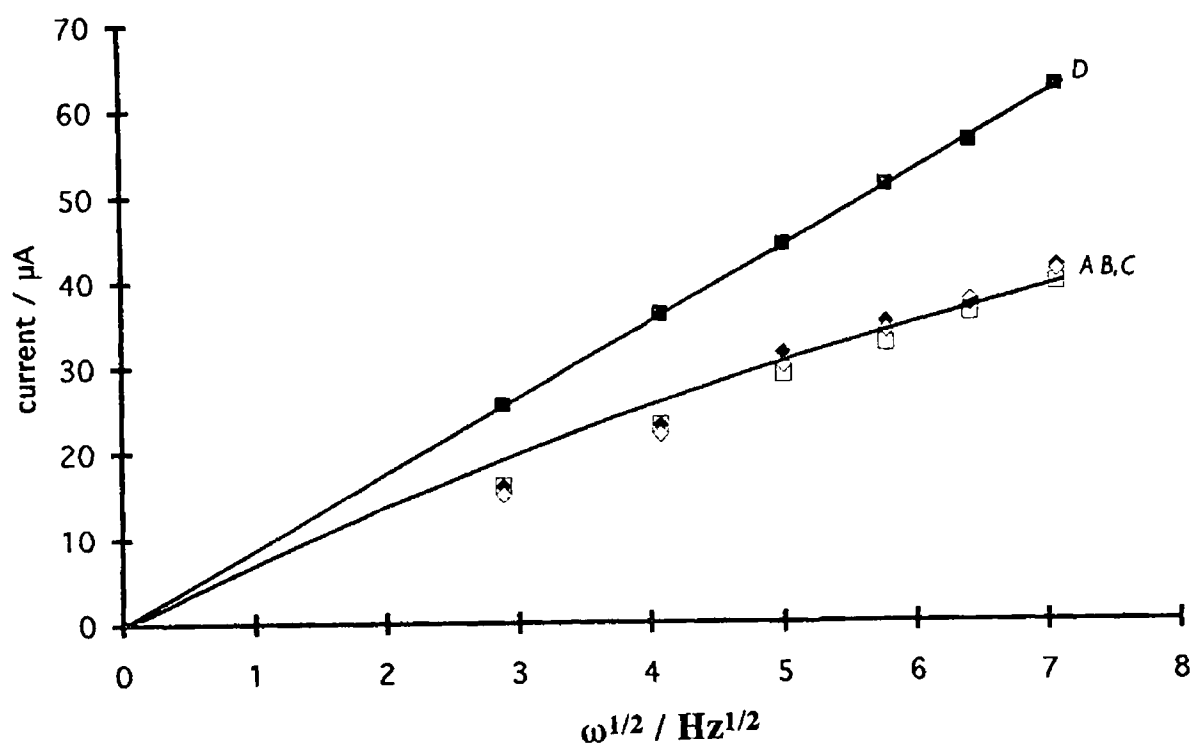


Fig 4.8 Levich plots for the electrocatalytic reduction of Fe(III) at a modified electrode cross-linked with 1,5-dibromopentane where (A) □ 5 mol %, (B) ◆ 10 mol %, (C) ◇ 20 mol % cross-linking and (D) ■ is the Levich flux. The electrolyte was $0.1 \text{ mol dm}^{-3} \text{ H}_2\text{SO}_4$ and the Fe(III) concentration was $1.0 \times 10^{-3} \text{ mol dm}^{-3}$.

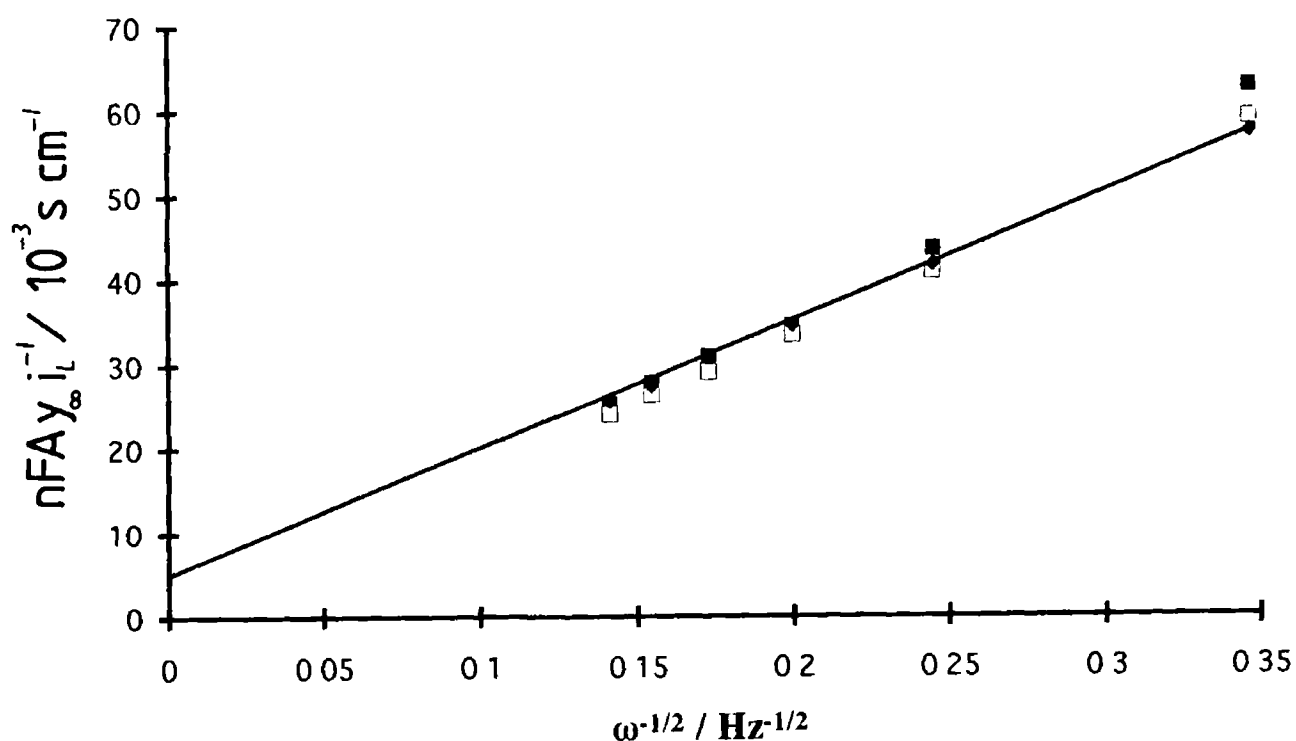


Fig 4.9 Koutecky-Levich plots for the electrocatalytic reduction of $1.0 \times 10^{-3} \text{ mol dm}^{-3} \text{ Fe(III)}$ at a redox polymer modified electrode cross-linked with 20 mol % 1,5-dibromopentane, where □ = 1.0×10^{-8} , ■ = 1.0×10^{-9} , ◆ = $5.0 \times 10^{-10} \text{ mol cm}^{-2}$. The electrolyte was $0.1 \text{ mol dm}^{-3} \text{ H}_2\text{SO}_4$.

Albery and Hillman diagnostic criteria^{49,50}, the exact kinetic regime can be distinguished. The limiting currents are dependent on the electrode rotation speed, and the Koutecky-Levich plots are linear, therefore the S_{te} , LE_k and LS_{te} kinetic cases can be eliminated. The slope of the Koutecky-Levich plots are $9.0 \pm 0.5 \times 10^{-4} \text{ cm s}^{-1/2}$, which is equivalent to that observed previously for the unmodified electrode. This allows the elimination of the LRZ_{tety} kinetic regime. As the modified electrode rate constants, k'_{ME} are independent of layer thickness, this allows the elimination of the L_k and LS_k cases to leave the S_k'' and LS_k regimes. A plot of $\ln(1-f)$ vs $\ln k'_{ME}$ is linear with a slope of 0.95 ± 0.1 which indicates the S_k'' kinetic case. Again, the reaction *locus* is the polymer/electrolyte interface, with the rate constant for the cross-exchange reaction controlling electrode currents. Also, as the Levich flux is greater than the actual measured reaction flux it appears that hindered substrate partition is current limiting. The average modified electrode rate constant was estimated to be $2.1 \times 10^{-4} \text{ cm s}^{-1}$. This yields a value for the second order rate constant, k'' , of $2.95 \pm 1.0 \times 10^{-4} \text{ mol}^{-1} \text{ dm}^3 \text{ cm s}^{-1}$. This is equivalent to that obtained at the same cross reaction for the homopolymer in perchlorate electrolyte.

4.3.8.3 p-Dibromobenzene

Levich plots for the reduction of Fe(III) at electrodes with surface coverages of $1.0 \times 10^{-9} \text{ mol cm}^{-2}$ cross-linked with 1, 5, and 10 mol % p-dibromobenzene (A, B and C respectively) can be seen along with the Levich flux (D) in Fig. 4.10. Again, the modified electrode current flux is less than that for the Levich flux, suggesting film control of the mediated reaction. Koutecky-Levich plot for 1.0×10^{-8} , 1.0×10^{-9} and a $5.0 \times 10^{-10} \text{ mol cm}^{-2}$ surface coverages cross-linked with 1 and 10 mol % p-dibromobenzene can be seen in Fig. 4.11. The behaviour observed is clearly different to that for observed for 1,10-dibromodecane and 1,5-dibromopentane. The Koutecky-Levich plots are linear and the limiting currents are dependent on the rotation speed of the electrode. The average Levich slope for these plots is $1.4 \pm 1.5 \times 10^{-3} \text{ cm s}^{-1/2}$, which is close to those cited earlier. These observations allow the elimination of the kinetic cases, S_{te} , LS_{te} , LE_k and LRZ_{tety} . The intercepts of the Koutecky-Levich plots are inversely related to layer thickness, therefore, the modified

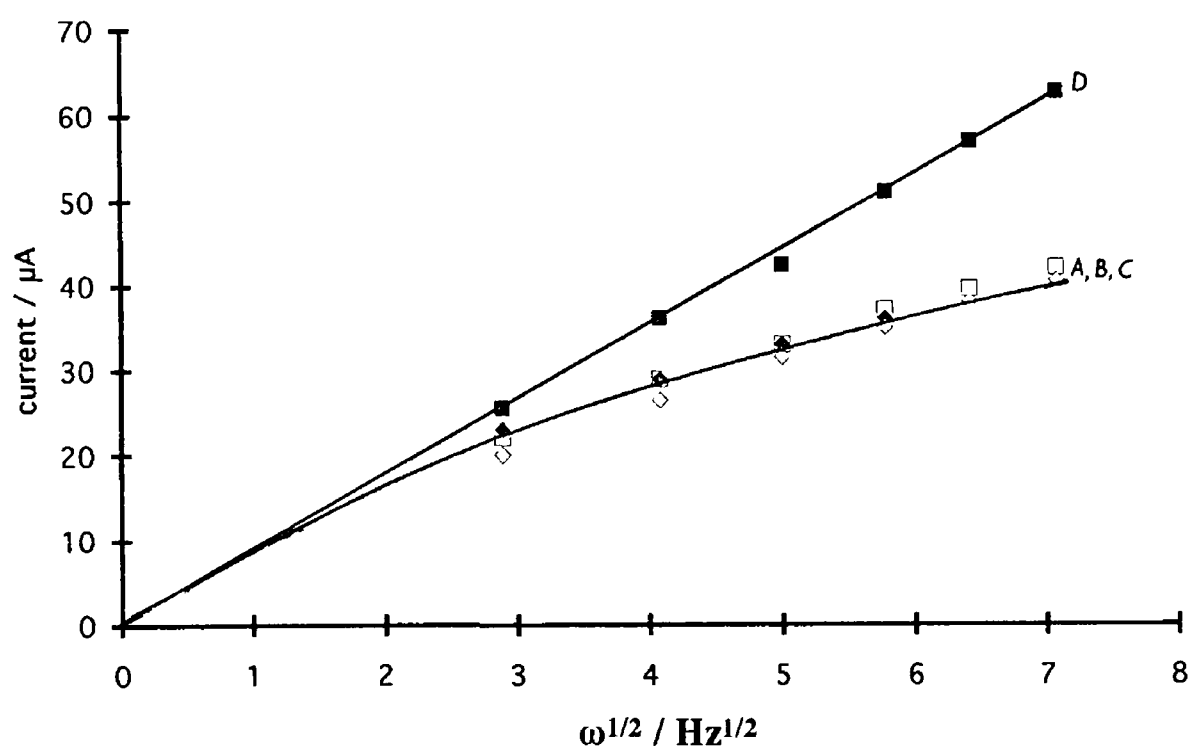


Fig 4 10 Levich plots for the electrocatalytic reduction of Fe(III) at a modified electrode cross-linked with p-dibromobenzene where (A) \square 1 mol %, (B) \blacklozenge 5 mol %, (C) \diamond 10 mol % cross-linking and (D) \blacksquare is the Levich flux. The electrolyte was $0.1 \text{ mol dm}^{-3} \text{ H}_2\text{SO}_4$ and the Fe(III) concentration was $1.0 \times 10^{-3} \text{ mol dm}^{-3}$.

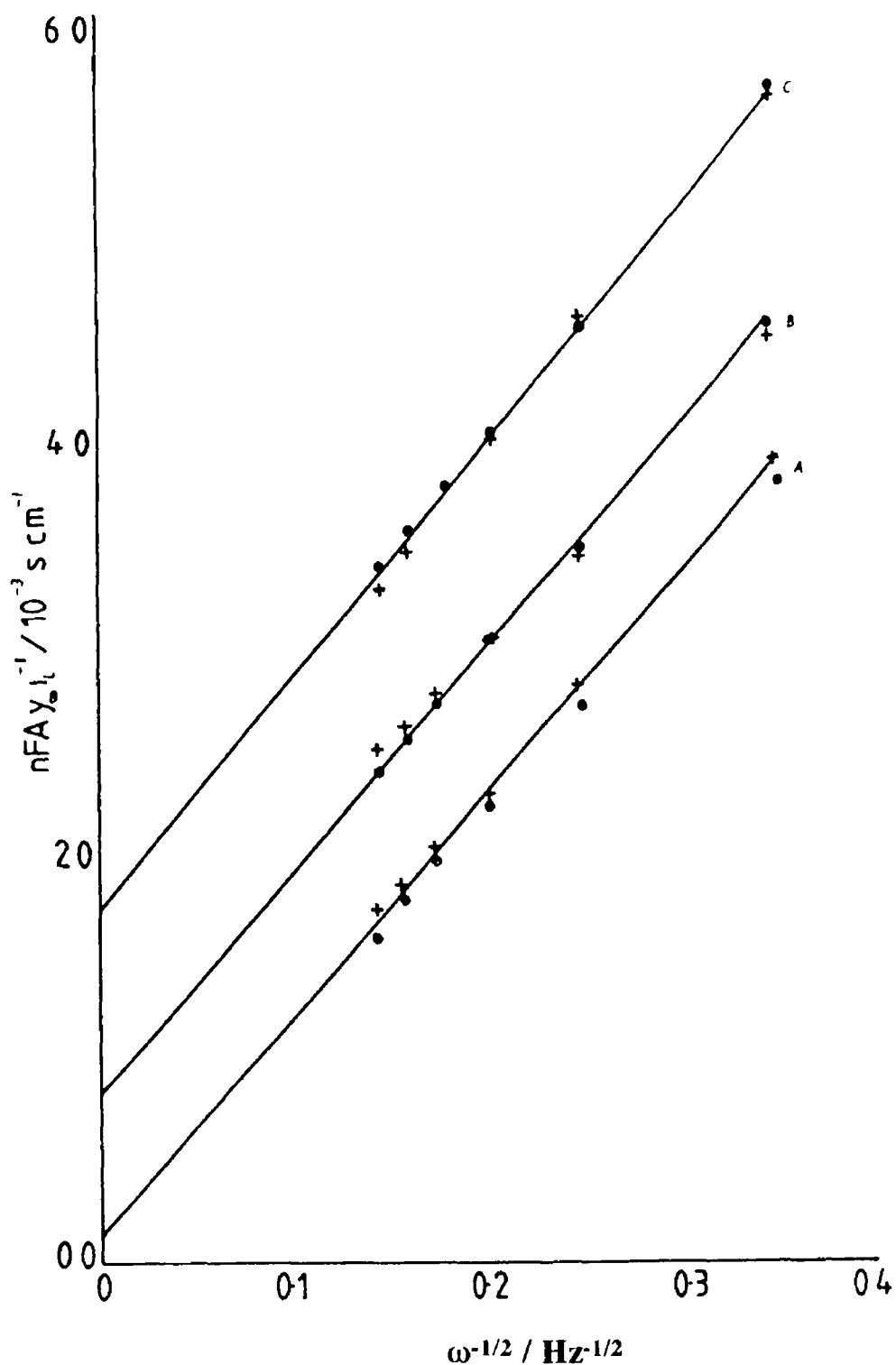


Fig 4 11 Koutecky-Levich plots for the electrocatalytic reduction of $1.0 \times 10^{-3} \text{ mol dm}^{-3} \text{ Fe(III)}$ at redox polymer modified electrodes cross-linked with 1 mol % (●) and 10 mol % (+) p-dibromobenzene. The surface coverages were (A) 1.0×10^{-10} , (B) 1.0×10^{-9} and (C) $5.0 \times 10^{-10} \text{ mol cm}^{-2}$. The electrolyte was $0.1 \text{ mol dm}^{-3} \text{ H}_2\text{SO}_4$.

electrode rate constant, k'_{ME} , is dependent of polymer layer thickness, a plot of $\ln L$ vs $\ln k'_{ME}$ has a slope of 1.1 ± 0.1 indicating a first order relationship. This indicates that the kinetic regime is L_k . This suggests that the Fe(III) penetrates the polymer film and the mediated reaction occurs throughout the film with the rate constant for the cross-exchange reaction controlling electrode currents. The average values for k'_{ME} at the following thickness of film, calculated from the dry density of the polymer are, $L = 3.5 \text{ nm}$, $k'_{ME} = 5.88 \times 10^{-5} \text{ cm s}^{-1}$, $L = 7.5 \text{ nm}$, $k'_{ME} = 1.18 \times 10^{-4} \text{ cm s}^{-1}$, $L = 35 \text{ nm}$, $k'_{ME} = 6.7 \times 10^{-4} \text{ cm s}^{-1}$. The analytical expression relating k'_{ME} to the second order rate constant for the L_k regime is given by³³

$$k'_{ME} = k K b_o L \quad (4.6)$$

This yields a value of $2.5 \pm 0.2 \times 10^2 \text{ dm}^3 \text{ mol}^{-1} \text{ cm s}^{-1}$ for the apparent rate constant, kK . Assuming that the rate constant for the cross-exchange reaction is similar for the cross-linked polymer compared to the homopolymer, $k = 2.8 \times 10^3 \text{ mol}^{-1} \text{ dm}^3 \text{ cm s}^{-1}$, then the partition coefficient, K , can be estimated to be ≈ 0.1 . This value is approximately half of that obtained for the homopolymer. As the Koutecky-Levich lines for each level of cross-linking are co-incident, it appears that K is relatively insensitive to the level cross-linking over the range 1-20 mol %

4.3.8.4 Polymer Cross-linking and Mediated Electrocatalysis

Optimum conditions for mediated electrocatalysis corresponds to the situation where the maximum amount of the redox polymer participates in the reaction. This corresponds to the LS_k and LE_k kinetic regimes. A consequence of the cross-linking the redox polymer is compaction of the films on the electrode surface. The D_{ct} values for the cross-linked films were generally found to increase, in combination with near ideal Nernstian and surface behaviour, it appears, therefore, that the cross-linked polymer films are sufficiently swollen to incorporate charge compensation counter-ions without physical restrictions. From the kinetic results for 1,10-dibromodecane and 1,5-dibromopentane, it is evident that

cross-linking with these agents results in polymer films which are impermeable to Fe(III). Cross-linking at levels as low as 1 mol % was sufficient to prevent penetration of the polymer by the substrate. In fact, the co-incidence of the Koutecky-Levich plots is somewhat surprising. The complete impermeability seems surprising considering the expected open structure of the cross-linked films. The Fe(III) ion, however, is known to be hydrated with six *aqua* species, $[\text{Fe}(\text{H}_2\text{O})_6]^{2+}$, therefore the overall ionic radius of the substrate may be sufficient to physically prevent distribution into the cross-linked polymer film. In addition, the driving forces for the incorporation of counter-ions and substrates are different, the partition of the Fe(III) is concentration driven, while the incorporation of charge compensating counter-ions involves potential driven active transport. A direct comparison of the permeability of counter-ions and substrates is therefore not necessarily appropriate. As the rate constants for the surface reactions are similar to that for the homopolymer, this suggests that the surface redox site micro-environment (and concentration) is preserved upon cross-linking. This indicates structural similarity between cross-linked and uncross-linked polymers.

From the kinetic results for p-dibromobenzene, it is clear that cross-linking with this material results in polymer films which are permeable to Fe(III). This suggests a more open structure in comparison to the other cross-linking agents. This confirms the belief that the rigid cross-links act to separate the polymer chains, however, the reduced rate of substrate permeation ($K \approx 0.1$) is indicative of some film compaction. The ability to “fine tune” film permeability in this fashion may be of considerable advantage.

4.4. Conclusions

The principle objective of this study was the development of a simple *in situ* stabilisation protocol for osmium redox polymer. It is clear that this objective was realised by the cross-linking of the polymer chains with 1,5-dibromopentane, 1,10-dibromodecane and p-dibromobenzene. The levels of stability obtained for all cross-linking agents and at all levels of cross-linking examined are sufficient for long term operation of the

modified electrodes under rigorous hydrodynamic conditions such as those observed in thin-layer flow cells and rotating disc electrodes. The cross-linking approach has a number of advantages compared to other stabilisation techniques, such as, overlaying with polymer and manipulation of the polymer backbone. The rate of charge transport for cross-linked polymers is maintained or enhanced in comparison to the homopolymer. This is advantageous as the responses from sensors constructed from these cross-linked redox polymers are not subject to electron transport limitation at high substrate concentration, such as that observed for the analogue polymer $[\text{Os}(\text{bipy})_2(\text{PS})_{7.5}(\text{DMAP})_{2.5}\text{Cl}]\text{Cl}$ (chapter 5).

The rate of charge transport, D_{ct} , is relatively insensitive to the level of cross-linking used (with the exception of 1,5-dibromopentane). Also the permeation of the electro-active substrate is insensitive to the levels of cross-linking. This is desirable, as providing exact levels cross-linking is not critical, in order to maintain the response characteristics of the modified electrodes. For future commercialisation of operational sensors, this would be of considerable significance.

The mass production of chemical sensors by lithographic technology is crucial for successful commercialisation of the devices. It is obvious that simple construction is of benefit if commercialisation is to be realised. The simple stabilisation procedure adopted here is conducive to mass production technology. The cross-linking agent need only be added to the polymer solution prior to deposition. As the cross-linking reaction proceeds in the solid state, the stabilisation reaction occurs after manufacture. There is no requirement for overlaying of the polymer film or exposure to UV radiation to induce stabilisation. *In situ* cross-linking, by virtue of its simplicity, results in potentially simple manufacturing processes.

It was also evident from this study that the reaction *locus* for the mediated electrocatalytic reaction can be controlled by the choice of cross-linking agent. This can be used to control the magnitude of response from the modified electrode. In situations where a through film reaction is desirable, cross-linking with *p*-dibromobenzene is useful. Surface reactions can be achieved by cross-linking with the *n*-dibromoalkanes. It is possible that careful choice of the nature of the cross-linking agent may control the extent of partition, K , and the reaction *loci* of analytes and

interferences at these electrodes. This may be used to exclude interfering species from permeating the redox polymer film while simultaneously obtaining efficient electrocatalysis of the analyte of interest. In addition, the construction of electrode arrays with deliberately controlled selectivity coefficients based on selective transport (K , D_s) and thermodynamic (ΔG) control of the processes involved in mediated electrocatalysis for the detection of co-existing electro-active species may be possible. Such arrays, in combination with multi-variate calibration protocols may provide powerful, selective multi-species sensors.

A final note concerning the calculation of the second-order rate constant for the cross-exchange reaction at the surface of the polymer.⁵² According to the theory of Alberly and Hillman³³, k'' is calculated from equation 4.5 where b_0 is the concentration of electro-active sites within the polymer film, with units mol dm^{-3} , to give k'' in units of $\text{mol}^{-1} \text{dm}^3 \text{cm s}^{-1}$. As the surface reaction is generally considered a heterogeneous process, then a more appropriate form for the calculation should reflect the surface concentration of electro-active sites in mol cm^{-2} rather than the bulk concentration of redox sites. This should yield $\text{mol}^{-1} \text{cm s}^{-1}$ as the units for k'' . All the literature values for k'' are calculated according to the calculation proposed by Alberly and Hillman, therefore the values quoted here are calculated on the same basis for comparative purposes.

4.5. References

- 1 S Dong, Y Wang, *Electroanalysis*, 1989 1 99
- 2 R W Murray, *Acc Chem Res* , 1980 13 135
- 3 R A Durst, E A Blubaugh, *Fundamentals and Applications of Chemical Sensors*, D Schuetzle, R Hammond, (Eds), ACS Symp Ser , 1984 309 p 245
- 4 K Sumi, F C Anson, *J Phys Chem* , 1986 90 3845
- 5 D M Montgomery, F C Anson, *J Am Chem Soc* , 1985 107 3431
- 6 R F Lane, A T Hubbard, *J Phys Chem* , 1973 77 1401
- 7 R F Lane, A T Hubbard, *J Phys Chem* , 1973 77 1411
- 8 D G Davis, R W Murray, *Anal Chem* , 1977 49 194
- 9 P R Moses, L Weir, R W Murray, *Anal Chem* , 1975 47 1882
- 10 N Oyama, F C Anson, *J Am Chem Soc* , 1979 101 1634
- 11 N Oyama, F C Anson, *Anal Chem* , 1981 53 1192
- 12 J M Clear, J M Kelly, C M O'Connell, J G Vos, *J Chem Res* , (M) 1981 3037
- 13 S M Geraty, J G Vos, *J Chem Soc , Dalton Trans* , 1987 3073
- 14 R J Forster, J G Vos, *Macromolecules*, 1990 23 4372
- 15 O Haas, M Kriens, J G Vos, *J Am Chem Soc* , 1981 103 1318
- 16 S E Creager, M A Fox, *J Electroanal Chem* , 1989 258 431
- 17 R W Murray, A G Ewing, R A Durst, *Anal Chem* , 1987 59 379A
- 18 R J Forster, J G Vos, *J Chem Soc , Faraday Trans* , 1991 87 1863
- 19 C P Andrieux, O Haas, J M Saveant, *J Am Chem Soc* , 1986 108 8175
- 20 R J Forster, A J Kelly, J G Vos, M E G Lyons, *J Electroanal Chem* , 1989 270 365
- 21 N Barisci, E Wilke, G G Wallace, M Meaney, M R Smyth, J G Vos, *Electroanalysis*, 1989 1 245

- 22 G G Wallace, M Meaney, M R Smyth, J G Vos, *Electroanalysis*, 1989 1 357
- 23 J N Barasci, G G Wallace, *Anal Lett* , 1991 24 2059
- 24 D P Leech, Ph D Thesis, Dublin City University, 1991
- 25 *The Technology of Plasticisers*, J K Sears, J R Darby, (Eds), Wiley, NY, 1982, Chp 2
- 26 K K Shiu, R Chemerika, D J Harrison, *Anal Chem* , 1989 61 570
- 27 J Facci, R W Murray, *J Phys Chem* , 1981 85 2870
- 28 B R Shaw, G P Haight, L R Faulkner, *J Electroanal Chem* , 1982 140 147
- 29 B Lindholm, M Sharp, *J Electroanal Chem* , 1986 198 37
- 30 D Leech, R J Forster, M R Smyth, J G Vos, *J Mats Sci* , 1991 1 629
- 31 R J Forster, J G Vos in *Comprehensive Analytical Chemistry*, Vol XXVII, M R Smyth, J G Vos, (Eds), Elsevier, Amsterdam, 1992, Ch 7
- 32 R J Forster, J G Vos, *Electrochimica Acta*, 1992 37 159
- 33 W J Albery, A R Hillman, *Ann Rep Prog Chem* , 1981 (C) 78 377
- 34 H Nishide, J Deguchi, E Tsuchida, *Bull Chem Soc , Jpn* , 1976 49 3498
- 35 J F Cassidy, K Tokuda, *J Electroanal Chem* , 1990 285 287
- 36 F W Billmeyer, *Textbook of Polymer Science*, Wiley Interscience, NY 1984 Chp 7
- 37 A Silberg, *Encyclopedia of Polymer Science and Engineering*, Vol 1, J I Kroschwitz, (Ed), Wiley, NY, 1987 p 557
- 38 A Takahoshi, M K Kawaguchi, *Adv Polym Sci* , 1982 46 1
- 39 C P Andrieux, J M Dumas-Bouchiat, F M'Halla, J M Saveant, *J Electroanal Chem* , 1980 113 19
- 40 C P Andrieux, J M Dumas-Bouchiat, J M Saveant, *J Electroanal Chem* , 1982 131 1
- 41 F W Billmeyer, *Textbook of Polymer Science*, Wiley Interscience, NY, 1984, Ch 12

- 42 S M Oh, L R Faulkner, *J Electroanal Chem* , 1989 269 77
- 43 E F Bowden, M F Dautartas, J F Evans, *J Electroanal Chem* , 1987 219 49
- 44 A P Clarke, Ph D Thesis, Dublin City University, 1992
- 45 M F Dautartas, E F Bowden, J F Evans, *J Electroanal Chem* , 1987 219 71
- 46 E F Bowden, M F Dautartas, J F Evans, *J Electroanal Chem* , 1987 219 91
- 47 A R Hillman, in *Electrochemical Science and Technology of Polymers*, R G Linford, (Ed), Elsevier, Amsterdam, 1987, Ch 5
- 48 P Daum J R Lehnard, D R Rolinson, R W Murray, *J Am Chem Soc* , 1980 102 4649
- 49 W J Albery, A R Hillman, *J Electroanal Chem* , 1984 170 27
- 50 W J Albery, M G Boutelle, A R Hillman, *J Electroanal Chem* , 1985 182 99
- 51 O Haas, H R Zumbrennen, *Helv Chim Acta* , 1981 64 854
- 52 P N Bartlett, private communication, 1992

Chapter 5

Synthesis, Characterisation and Analytical Application of [Os(bipy)₂(PS)_{7.5}(DMAP)_{2.5}Cl]Cl

5.1. Introduction

An important property of modified electrodes is their physical stability. Many modified electrodes possess very useful and interesting properties which may be utilised for analytical purposes. However, their application in typical solutions with extremes of pH and complex matrices remain difficult due to the instability of the modifying layer.¹ It was stated in chapter 1 that many different polymeric materials have been used for electrode modification and that preformed polymers offered the advantages of synthetic variability and control of the physical properties of the electro-active materials. Although these materials tend to be less stable than electro-polymerised materials, manipulation of the chemical structure of the polymer backbone can result in significant enhancement of the physical stability of the polymer film.² It has been demonstrated that the redox polymer, $[\text{Ru}(\text{bipy})_2(\text{PVP})_5\text{Cl}]\text{Cl}$, is unstable under the hydrodynamic conditions of thin-layer electrochemical flow-cells³ and that overlaying the redox polymer with conducting and non-conducting polymers is relatively unsuccessful in stabilising the polymer.⁴ It has, however, been shown that simple incorporation of styrene moieties into the polymer backbone, at various mole ratios, results in a significant stability improvement.² This is thought to be due to the glass-like, hydrophobic nature of the styrene residues in aqueous electrolytes. Such manipulation of the physical properties of the polymer can result in changes in the mass and charge transport properties of the polymer. It is often found that procedures used for the enhancement of modified electrode stability can have a detrimental effect on their catalytic efficiency. As a result, effects caused by electrode stabilisation must be assessed fully in order to understand the charge and mass transport properties of the electrode, and predict the kinetic behaviour and catalytic efficiency of the modifying layer.⁵

The use of polymer-bound catalysts for thermal reactions is well established due to the advantages associated with such systems.⁶ In particular, the use of the polymeric analogue of DMAP (where DMAP = 4-(N,N-dimethylamino) pyridine and the polymer is poly[styrene-co-4-(N-methyl-N-p-vinylbenzylamino) pyridine]) is well documented.⁷ In the late 1960's the catalytic efficiency of DMAP for difficult acylation reactions was reported.^{8,9} Since then, many applications for this pyridine moiety have been developed including the formation of polyurethanes¹⁰,

esterification ¹¹ reactions and the catalysis of the polymerisation of acrylic resin formulations ¹² Verlaan *et al* ¹³ discovered that copper complexes of DMAP are among the most active and specific catalysts for the oxidative polymerisation of 2,6-dimethylphenol to produce the engineering plastic, poly-2,6-dimethyl-1,4-phenyleneoxide. This copper complex of the DMAP residue incorporated into a styrene polymer backbone was found to be very stable under the reaction conditions employed for the oxidative coupling of the phenolic compounds ^{14,15}. Due to the stability of this polymer backbone and the relative instability of PVP-based modifiers used previously ^{3,4}, the analogous electro-active osmium metallo-polymer, $[\text{Os}(\text{bipy})_2(\text{PS})_{7.5}(\text{DMAP})_2\text{Cl}]\text{Cl}$, was prepared in order to investigate the possibility of constructing stable modified electrodes for electroanalysis.

In this chapter, the synthesis of $[\text{Os}(\text{bipy})_2(\text{PS})_{7.5}(\text{DMAP})_2\text{Cl}]\text{Cl}$ is described. The resulting material was characterised using UV/visible and luminescence spectroscopy. The electrochemical and charge transport properties of the polymer were then investigated using cyclic voltammetry. The electrocatalytic and transport properties and analytical application of the material as an electrode modifier are also described. A brief overview of charge transport processes which can occur at redox polymer modified electrodes is also given.

5.1.1 Charge Transport Properties of Redox Polymers

A model for the interior of polyelectrolyte coatings on electrodes has been proposed by Anson *et al* ¹⁶. In this model, it is envisaged that the polymer is swollen with electrolyte and is comprised of two domains. Firstly, a tangled polyelectrolyte chain network with their accompanying counter ions and secondly, “islands” of electrolyte devoid of polymer. It is assumed that Donnan equilibria ¹⁷ prevail within the volume of electrolyte close to the polyelectrolyte chains. The solution that occupies the region outside the Donnan domain has a composition that is determined by the composition of the bulk electrolyte ¹⁶. In the case of highly swollen polymeric coatings, the electrolyte inside and outside the polymer may be essentially identical. However, some partitioning of electrolyte components may be evident ¹⁸. Charge transport through electro-active polymers with fixed redox sites occurs due to any one or combination of the

following processes ¹⁶, self-exchange (“electron hopping”) between fixed redox sites, ion diffusion within the Donnan and electrolyte “islands”, or migration of counter ions due to the influence of applied electric fields. However, it is generally accepted that the predominant process of charge transport through the redox polymers studied here is electron hopping between fixed redox sites ¹⁹. The rate of charge transport is normally controlled by one of three processes which can occur at the modified electrode upon redox reaction ²⁰. These are, a) the intrinsic barrier to self-exchange, b) counter ion movement to maintain electro-neutrality, and c) physical displacement of the polymer chains to allow the mean separation between fixed redox sites to become sufficiently small to allow electron transfer to take place (typically ≈ 1 nm). Factors which affect rates of charge transport include electrolyte type and concentration, pH, redox site loading, polymer backbone and temperature ^{20,21}. A schematic depiction of heterogeneous and homogeneous charge transport processes can be seen in Fig. 5.1. Heterogeneous electron transfer is characterised by a standard rate constant, k^0 , and a symmetry factor, α ²². Normal pulse techniques have been used to determine these parameters for redox polymer modified electrodes ²³. Heterogeneous electron transfer at redox polymers is thought to obey conventional Butler-Volmer kinetics (i e potential controlled), and in situations where no mass transfer effects are encountered, an over-potential associated with any current serves solely as an activation energy ²⁴. It is generally recognised that the rate of heterogeneous electron transfer is significantly faster than homogeneous transfer ²⁵. Homogeneous charge transfer processes appears to be concentration driven and can be characterised by a charge transport diffusion coefficient, D_{ct} ^{26,27}. Methods such as CV, chronoamperometry and chronocoulometry have been used to estimate D_{ct} ²⁸. It has been observed by many authors that D_{ct} values estimated by different techniques can result in different D_{ct} values ^{29,30}. This phenomenon is thought to be due to the differing time scales of measurements ^{29,30}. In addition, CV appears to probe greater portions of the film compared to potential step techniques. For this reason, D_{ct} values have been estimated almost entirely by CV in this study.

The success of any attempt to exploit polymer modified electrodes for the electrocatalytic detection of substrates lies in the detailed understanding of the mechanisms and rates of charge transport. The rate of charge transport must be sufficiently fast so as not to limit the response

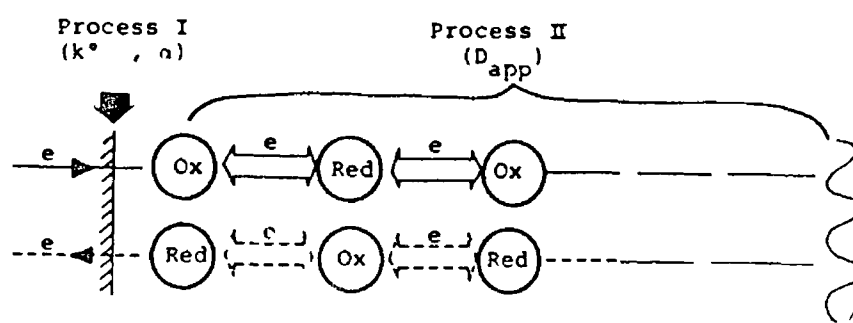


Fig 5 1 Schematic depiction of the charge transport processes at redox polymer modified electrodes. Processes I and II represent the heterogeneous and homogeneous charge transfer respectively (Reproduced from Ohsaka *et al*, *Bull Chem Soc, Jpn*, 1984 57 1844)

of the sensor. In such an event, limited linear ranges would be encountered. The investigation of charge transport rates through polymeric materials has been carried out by many workers.^{20,28-30} The techniques used for the estimation of charge transport rates have been described in chapter 1. A feature of early publications concerning charge transport was the absence of quantitative data regarding ion and electron movement within the films. Parameters such as wave shape and position were used to broadly discuss possible charge transport mechanisms. In an early paper, Kaufmann *et al.*¹⁹ discussed ion and electron transport in tetrathiafulvalene polymer films using a combination of CV and potential step techniques. Khoo *et al.*³¹ have examined the effect of electrolyte type on the charge transport diffusion coefficient in tetracyanoquinodimethane (TCNQ) and tetracyanoethylene (TCNE) modified electrodes using the Randles-Sevcik equation for cyclic voltammetry, and have attributed the changes in D_{ct} to the ion-pairing effect of the perchlorate anion in the polymer film. Inzelt and co-workers^{32,33} have also studied the effect of the nature and concentration of the counter ion on the wave-shape and the CV behaviour of TCNQ polymer films and have concluded that salt or ion pair formation between the reduced forms of the redox films and the counter ions contribute to the variabilities observed with different electrolyte types and concentration. Charge transport rates through radio frequency plasma-polymerised polyvinylferrocene (PVF) have been shown to be controlled by both polymer chain motions and counter ion diffusion.³⁴ Activation energies and entropies of approximately 16 kJmol⁻¹ and -140 Jmol⁻¹K⁻¹, respectively, corresponding to the rate limiting diffusion of counter ions have been determined for these films.³⁴ Bowden *et al.*^{35,37} have considered the thermodynamics of PVF modified electrodes. In this study controlled potential coulometry and CV were used to examine the reversibility of the redox reactions. A model was developed to explain the observed response in terms of forced inclusion of charge compensating counter ions into the film during redox cycling. Other workers have reported the effect of counter ion size on the rates of charge propagation. Albery *et al.*³⁸ have shown that for thionine coated electrodes, the rate of charge transport is a function of counter ion size. Ohsaka and co-workers³⁹ reported that the rate determining process for charge transport through poly(methylviologen) films was not the electron hopping process between adjacent fixed redox sites, but rather the processes of charge compensating

counter ion motion and/or polymer segment motion, based on D_{ct} variations with different electrolyte type and concentration

For most polymer films studied, an increase in redox site loading within films of equal thickness results in an increase in the rate of charge transport through the film. These observations are not surprising as the swollen polymer may act according to Dahms-Ruff behaviour⁴⁰. Using this formulation, the apparent diffusion coefficient is a function of physical diffusion of the electro-active species and self-exchange reaction, and as the inter-site distance decreases (with increased redox site loading) the apparent diffusion coefficient increases. Anson has reported that the concentration dependence of the diffusion coefficients of redox ions that undergo rapid electron exchange in solution according to the Dahms-Ruff equation has been observed for $[\text{Co}(\text{bipy})_3]^{2+}$ incorporated in Nafion⁴⁰. In a similar study, Oyama demonstrated a linear dependence on the apparent diffusion coefficient, D_{app} on the concentration of electro-active sites within redox polymer films, although the exact slope was not that predicted by theory⁴¹. The variation of homogeneous charge diffusion coefficient with fixed redox site loading has been studied for osmium redox centres bound to films prepared from electro-polymerised bis(bipy)bis(N-4-pyridylcinnamamide)osmium(II) hexafluorophosphate^{42,43}. Facci *et al.*⁴³ used ruthenium redox centres to dilute the osmium centres within the film while keeping the redox site loading constant, and observed three regions of behaviour depending on the inter-site distance. In the more popular ion exchange type membranes, several reports concerning the effect of metal site loading have appeared. Oh and Faulkner³⁰ varied the loading of $[\text{Fe}(\text{CN})_6]^{3-/4-}$ within partially quaternised PVP films and have concluded that counter ion motion is not limiting in these polymers because of similarities between D_{ct} measured by transient and steady-state techniques. It was shown that D_{ct} decreased with increasing redox site loading due to cross-linking of the polymer film by the multicharged redox centre. These workers have also investigated the effects of cross-linking on charge transport through the films of PVP bound $[\text{Ru}(\text{bipy})_2\text{Cl}]^+$, and found that activation energies were linearly dependent on the degree of cross-linking. It was also concluded that the anion dependence observed in D_{ct} values for these films was a structural effect and that polymer segment motion controlled the diffusion process.⁴⁴ In a series of contributions by Forster *et al.*⁴⁵⁻⁴⁷, the charge transport characteristics of the osmium-containing polymers, $[\text{Os}(\text{bipy})_2(\text{Pol})_n\text{Cl}]\text{Cl}$

where Pol = PVP or poly-(N-vinylimidazole), (PVI), were investigated as a function of redox site loading, electrolyte type and concentration and temperature. Increases in D_{ct} with increasing electrolyte concentration was observed in all cases except perchlorate electrolytes. The decrease in D_{ct} with increasing perchlorate concentration was attributed to the ion pairing properties of this anion. The rate limiting step for charge transport through these polymers is believed to be counter ion movement for most systems, with all of the polymers showing variation in D_{ct} and activation parameters with electrolyte concentration and type.

It is evident from this discussion that the rate of charge transfer through the polymer film is of paramount importance for optimum efficiencies of the redox polymer modified electrodes. Charge transfer rates are, however, dependent on a wide number of experimental variables, which are often difficult to control under possible operational conditions. As a result a detailed knowledge of the charge transport characteristics of electro-active materials is required prior to the development of electrochemical sensors.

5.1.2 Activation Parameters

The evaluation of activation parameters for the charge transport processes which can occur at polymer modified electrodes can be helpful in order to delineate the rate determining process.⁴⁸ As discussed earlier, the mechanism of charge transfer in the films studied here is believed to be electron hopping between fixed redox sites accompanied by counter ion movement to maintain electro-neutrality.¹⁹ Both processes can be described by Fick's laws of diffusion and can therefore be described by the Arrhenius equation for activation diffusion or chemical reaction⁴⁹,

$$D_{ct} = D_{ct}^0 \exp(-E_a/RT) \quad (5.1)$$

with the Eyring equation being used to calculate activation entropies

$$D_{ct}^0 = e \delta^2 (k_B T / h) \exp(\Delta S^\ddagger / R) \quad (5.2)$$

In these equations E_a refers to the activation energy of the process, δ denotes the mean separation of the fixed redox sites, e is the base of the natural log, and k_B is the Boltzmann constant and h is the Planck constant. The activation enthalpy, (ΔH^\ddagger) , can be calculated directly from the activation energy using the relation

$$\Delta H^\ddagger = E_a - RT \quad (5.3)$$

Low values for E_a (typically $< 10 \text{ kJ mol}^{-1}$) are characteristic of charge transfer being controlled by the intrinsic barrier to electron self-exchange. Higher values ($\approx 40 \text{ kJ mol}^{-1}$) are believed to represent charge transport control by counter ion movement maintaining electro-neutrality, while values $\approx 100 \text{ kJ mol}^{-1}$ are typical of polymer segment motion controlling charge transport. Entropy values can be used to assess ordering/disordering deformations of the polymer structure upon redox and ion transport. Such information is useful in predicting the limiting process for charge transport.⁴⁹

5.2. Experimental

5.2.1 Materials and Reagents

5.2.1.1 Synthesis of $[\text{Os}(\text{bipy})_2(\text{PS})_{7.5}(\text{DMAP})_2.5\text{Cl}]\text{Cl}$

The polymeric material, poly[styrene-co-4-(N-methyl-N-p-vinylbenzylamino) pyridine, $((\text{PS})_{7.5}(\text{DMAP})_{2.5})$), was supplied by the authors of reference 15. The synthesis of $[\text{Os}(\text{bipy})_2\text{Cl}_2]$ was described in chapter 2. A metal loading of 1/10 (metal centre monomer) was chosen for the redox polymer as this loading exhibits optimum charge transport properties for the PVP-based redox polymers.²⁰ This metal loading was

obtained by the reaction of stoichiometric amounts of co-polymer and $[\text{Os}(\text{bipy})_2\text{Cl}_2]$ 100 mg of the co-polymer, poly[styrene-co-4-(N-methyl-N-p-vinylbenzylamino)pyridine] was weighed accurately and dissolved in 40 cm³ of 2-methoxyethanol (BDH) This solution was then transferred to a 150 cm³ round bottomed flask Next 55.1 mg of $[\text{Os}(\text{bipy})_2\text{Cl}_2]$ was dissolved in 40 cm³ of 2-methoxyethanol, this solution was then added and mixed with the co-polymer solution in the round bottomed flask This solvent was used instead of ethanol due to insolubility of the co-polymer in ethanol The resulting mixture was held under reflux at 125 °C for 48 h The reaction was monitored by UV/visible spectroscopy and electrochemically by CV The formation of a product with a redox wave at 0.25 V vs saturated calomel electrode (SCE) and the disappearance of the wave at 0.0 V vs SCE due to $[\text{Os}(\text{bipy})_2\text{Cl}_2]$ indicated the formation of the redox polymer When the starting material redox wave has disappeared completely, the redox polymer was precipitated twice from 2-methoxy ethanol in diethylether The precipitate was dried *in vacuo* at 80 °C for 24 h 136 mg of product was recovered which corresponds to a 88% yield

5.2.2 Procedures

5.2.2.1 UV/Visible Spectroscopy

The redox polymer was found to be insoluble in the solvents usually used for the dissolution of these redox polymers *e.g.* methanol and ethanol.⁵¹ The polymer was, however, found to be soluble in dichloromethane, but gelling of the solution was evident after several days This was suspected to be a result of quaternisation and possibly cross-linking of the polymer *via* the free pyridine moieties by dichloromethane.⁵² The polymer was found to be soluble and stable in a 1:1 mixture of methanol/acetonitrile This mixed solvent system was used throughout for the preparation of polymer solutions

UV/visible spectroscopy was carried out using a Shimadzu UV 240 spectrophotometer 1 cm matched quartz cells were used UV/visible spectra were recorded in the region 900 nm to 190 nm A scan speed of 10 nm s⁻¹ and a slit width of 2 nm was used Spectra were recorded on 4 polymer solutions over the concentration (of redox centres) range 1.48 x

$10^{-5} \text{ mol dm}^{-3}$ to $1.48 \times 10^{-4} \text{ mol dm}^{-3}$ The methanol/acetonitrile solvent was used in the reference beam These solutions were prepared by serial dilution The λ_{max} values were obtained directly from the recorded spectra The molar extinction coefficient, ϵ , was estimated from the slope of the plot of absorbance vs redox polymer concentration

5.2.2.2 Luminescence Spectroscopy

Luminescence spectroscopy was carried out using the Perkin Elmer LS50 luminescence spectrophotometer interfaced to an Epson AX2e PC For the room temperature luminescence measurements a 1 cm fluorescence cell was used, while at -196°C , a quartz tube and holder were employed The excitation and emission slit widths were 10 nm for all experiments No evidence of luminescence was observed for the redox polymer at both room temperature and at -196°C

5.2.2.3 Cyclic Voltammetry and Rotating Disc Electrode Voltammetry

CV and RDE voltammetry were carried out using a conventional three electrode assembly The potentiostat was the EG&G Princeton Applied Research Model 362 The rotating disc assembly was the Metrohm Model 629-10 Voltammograms were recorded on a Linseis X-Y recorder The working electrodes were 3 mm diameter glassy carbon discs shrouded in teflon (Metrohm) The counter electrode was 1 cm^2 platinum gauze placed parallel to the working electrode at distance of $\approx 1 \text{ cm}$ The reference electrode was the saturated KCl calomel electrode All potentials are quoted with respect to the SCE without regard to liquid junction potentials All measurements, unless otherwise stated, were carried out at room temperature In situations where the temperature was varied, this was carried out using a thermostatically controlled waterbath circulating to a jacketed electrochemical cell The electrolyte and modified electrode were allowed to equilibrate at each temperature ($\pm 1^\circ\text{C}$) for 15 minutes

Modified electrodes were prepared by polishing the glassy carbon electrodes with 5 μm alumina as an aqueous slurry on a felt cloth The electrodes were rinsed thoroughly with distilled water and methanol The electrodes were then treated with chlorosulphonic acid to promote the

formation of surface oxide functional groups. The electrodes were again rinsed with distilled water and dried *in vacuo* at room temperature. The electrodes were modified by drop coating using a 1% w/v solution of the polymer. The electrodes were allowed to dry slowly in air and allowed to cure overnight *in vacuo* before use.

In studies where electrolyte type were varied, all experiments were carried out on fresh coatings in order to prevent any problems associated with “memory effects”, where the rate of charge transport through the films would be affected by the electrolyte to which it had previously been in contact.

5.2.2.4 Coulometry

Coulometry was carried out to investigate the extent of electroactivity of the surface immobilised redox sites. The conventional three electrode assembly described above was used in conjunction with the EG&G Princeton Applied Research Model 379 digital coulometer placed in series between the working electrode and the potentiostat return. The coulometer was operated in the anodic mode with a current scale setting of 10 μA . The instrument output was recorded using a Philips X-t recorder. The charge resulting from the oxidation of osmium within the film was recorded during slow potential sweep (1 mV s^{-1}) of the potential from 0.0 V vs. SCE to 0.6 V vs. SCE. Results were corrected for background charging currents.

5.2.3 Flow Injection Analysis

The flow injection apparatus consisted of a Gilson Miniplus 3 peristaltic pump, a six port Rheodyne injector valve fitted with a 20 μL fixed volume sample loop, a Hewlett Packard 1049A electrochemical detector connected with teflon HPLC tubing, and a Philips X-t chart recorder. In the flow-cell, a solid state silver electrode (SSAg) acted as the reference electrode. A stainless steel electrode acted as the counter electrode. Sample injections were made using a 2 cm^3 glass syringe fitted with a Rheodyne injection needle. The carrier electrolyte used was 0.1 mol dm^{-3} H_2SO_4 . The applied potential was -0.05 V vs. SCE (numerical).

conversion from SSAg) and an optimum carrier electrolyte flow rate of $1.0 \text{ cm}^3 \text{ min}^{-1}$ was used. Iron tablet samples were prepared by dissolution in the electrolyte followed by the addition of excess 35% H_2O_2 to oxidise the ferrous salt to the ferric form. The solutions were then made up to the mark with electrolyte. These solutions were used directly. Calibration solutions (and all other iron solutions) were prepared from $[(\text{NH}_4)\text{Fe}(\text{SO}_4)_2] \cdot 12\text{H}_2\text{O}$ in the sulphuric acid electrolyte. Solutions were prepared fresh daily.

5.2.4 Spectrophotometric Determination of Iron in Therapeutic Formulation

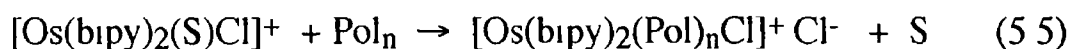
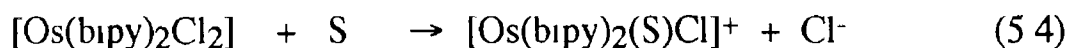
The method used was a standard spectrophotometric technique prescribed by Vogel.⁵³ The tablets were finely ground, weighed and transferred to an evaporating dish. The sample was dissolved with $0.1 \text{ mol dm}^{-3} \text{ H}_2\text{SO}_4$. Dilute KMnO_4 (2 g dm^{-3}) was then added to oxidise Fe(II) to Fe(III). The mixture was then transferred to a volumetric flask and made up to 500 cm^3 . 40 cm^3 of this solution was then transferred to a 50 cm^3 volumetric flask, 3 cm^3 of $4 \text{ mol dm}^{-3} \text{ HNO}_3$ was added along with 5 cm^3 of $2 \text{ mol dm}^{-3} \text{ KSCN}$. The solution was then made up to the mark with deionised water. A blank was prepared in a similar manner. The absorbance was measured at 480 nm using the Shimadzu UV/visible spectrophotometer at fixed wavelength. Standards were prepared in an identical manner from $[(\text{NH}_4)\text{Fe}(\text{SO}_4)_2] \cdot 12\text{H}_2\text{O}$. Solutions were prepared fresh daily.

5.3. Results and Discussion

5.3.1 Characterisation of $[\text{Os}(\text{bipy})_2(\text{PS})_7.5(\text{DMAP})_2.5\text{Cl}]\text{Cl}$

The synthetic strategy used here was that developed previously.^{51,54,55} The polymer backbone was firstly synthesized and then characterised. The organic polymer was subsequently functionalised by coordination with osmium redox centres. This synthetic strategy allows the redox polymer to be isolated and characterised both in solution and as

thin films on electrode surfaces. The formation of the redox polymers is based on the well documented lability of the chloride ligand in the $[\text{Os}(\text{bipy})_2\text{Cl}_2]$ complex according to the following reaction sequence ⁵⁴



where S = solvent (in this case 2-methoxyethanol), Pol is the polymer and n is the number of monomer units/metal centre. Extensive studies have shown that the first chloride ligand is easily removed under reflux in ethanol or methanol (reaction 5.4) leading to the subsequent substitution by the pyridine pendant groups of the polymer ^{51,55,56}. Removal of the second chloride ligand is known to be promoted by the presence of water in the reflux solvent or the use of high boiling point solvents ^{55,56}. Fortunately, the second chloride of $[\text{Os}(\text{bipy})_2\text{Cl}_2]$ is very inert and is not substituted easily. The metal loading of the polymers was based on the quantity of starting material employed during reflux. It was assumed that the reaction goes to completion stoichiometrically. The validity of this assumption is supported by the CV data obtained while monitoring the reaction, which indicates complete consumption of starting redox material and the formation of a single electro-active product. The high product yield (88%) also confirms this. It is also assumed that the co-polymer structural units and the coordinated osmium centres are randomly distributed along the polymer chain. This is an important assumption as the metal-to-metal inter-site distance must be constant and known (or approximated) for the interpretation of the activation parameters ⁴⁹. In the present case, the inter-site distance has been approximated using crystal structure data for the structurally similar polymer, PVP ⁵⁷. This polymer has a mean separation of 0.25 nm between adjacent monomer units and thus, assuming a rigid rod structure in the metallo-polymer studied here, the osmium redox centres are assumed to be separated by 2.5 nm when the metal loading is $n = 1/10$. The structure of the polymer can be seen in Fig. 5.2. It should be noted that the material is the *cis* isomer. The formation of the *trans* isomer is unfavourable due to steric restrictions.

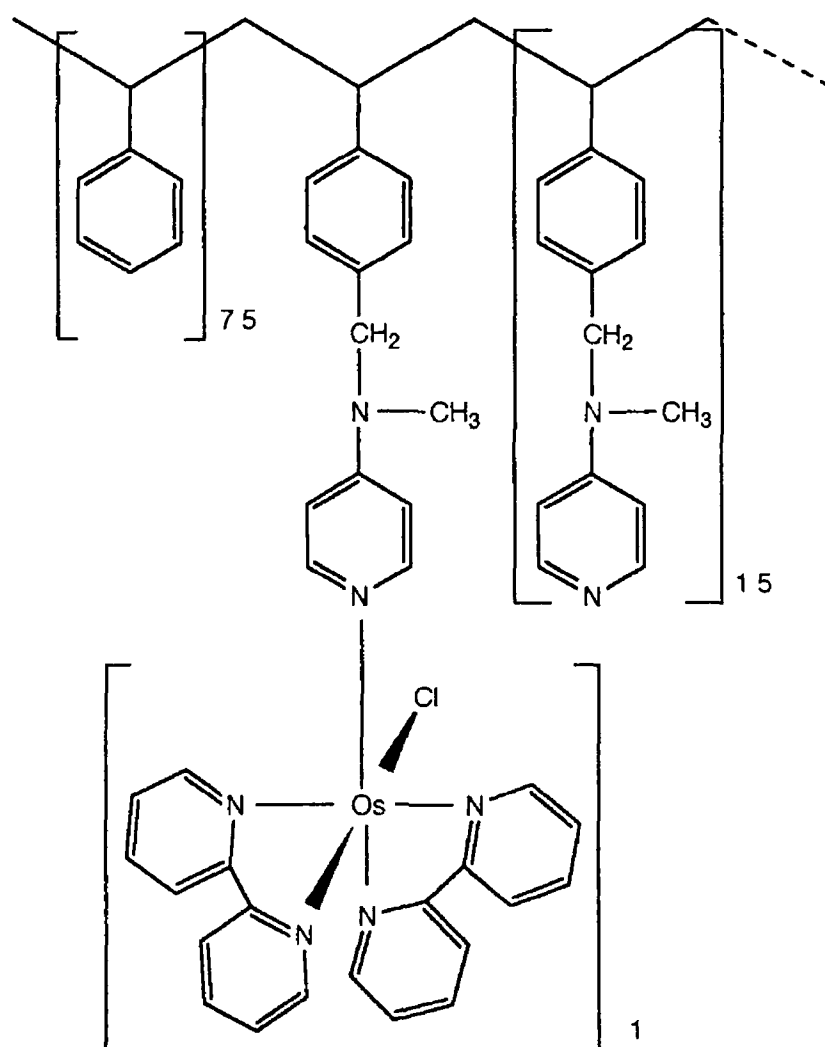


Fig 5 2 Structure of $[\text{Os}(\text{bipy})_2(\text{PS})_{7.5}(\text{DMAP})_{2.5}\text{Cl}]\text{Cl}$

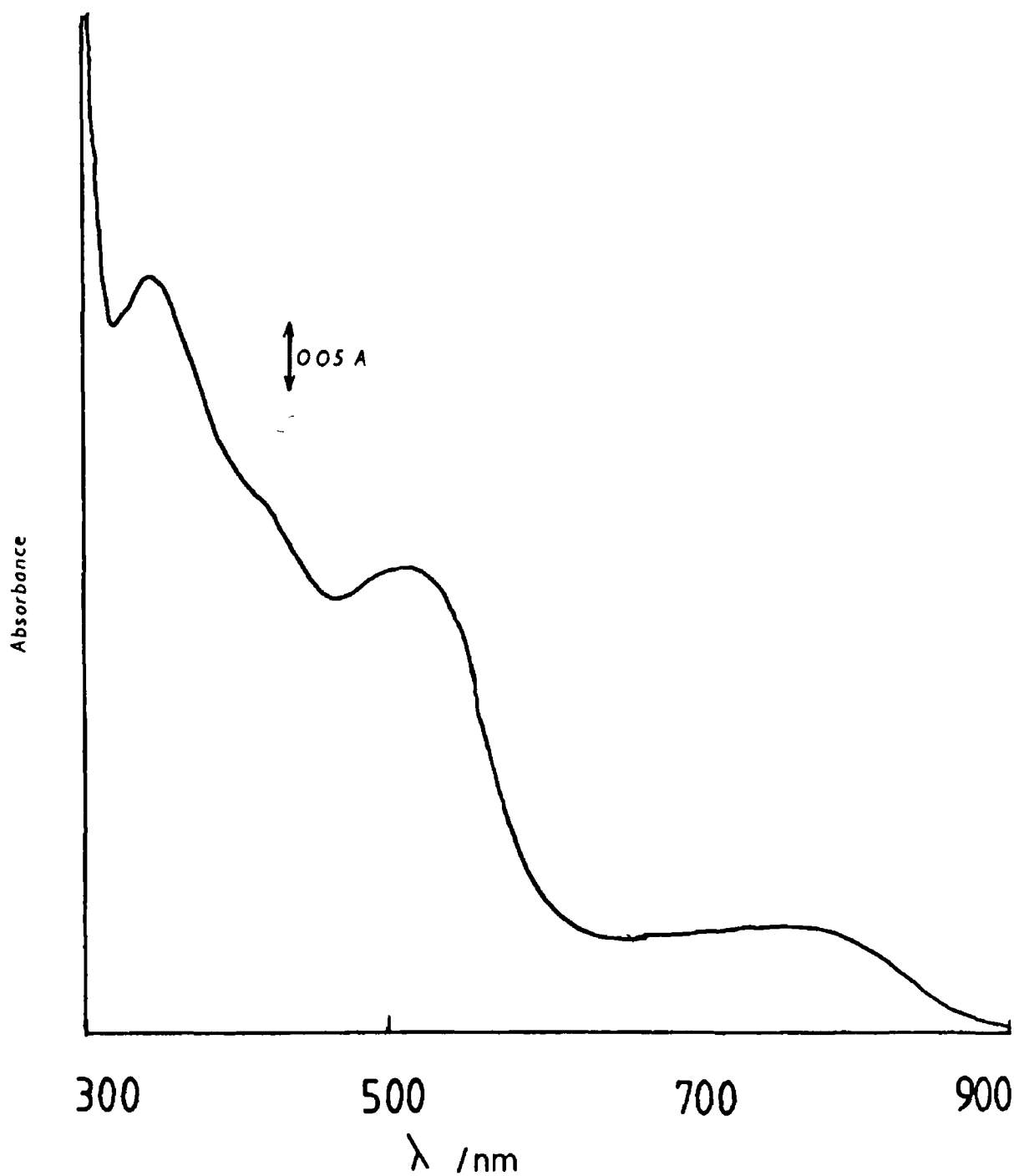


Fig 5 3 The UV/Visible spectrum, recorded in methanol / acetonitrile, of $[\text{Os}(\text{bipy})_2(\text{PS})_{7.5}(\text{DMAP})_{2.5}\text{Cl}]\text{Cl}$

5 3 1 1 Absorption and Emission Spectroscopy

Electronic spectroscopy has proven useful in the characterisation of redox polymers containing coordinated osmium and ruthenium centres^{51,54,55}. In the case of ruthenium^{54,55}, spectroscopic data has been useful in assigning the coordination sphere of the metal centre. Spectroscopic data pertaining to osmium redox polymers have been compared to model compounds and have been used to confirm the structure of the redox polymers.⁵¹ Approximate extinction coefficients were found to be useful in determining the metal loading of the redox polymer.⁵¹ For the redox polymer studied here, the spectroscopic data will be compared to the previously characterised analogous polymer [Os(bipy)₂(PVP)₁₀Cl]Cl. A typical UV/visible spectrum for [Os(bipy)₂(PS)_{7.5}(DMAP)_{2.5}Cl]Cl in methanol/acetonitrile solvent is shown in Fig. 5.3. Two overlapping bands in the UV region occurring at 220 ± 5 nm and 255 ± 5 nm can be identified, and can be attributed to the $\pi \rightarrow \pi^*$ transitions of the aromatic electrons of the styrene and pyridine moieties on the polymer backbone. In the visible region, three electronic transitions are present, occurring at 740 nm ($\log \epsilon = 3.18$), 510 nm ($\log \epsilon = 3.75$) and 358 nm ($\log \epsilon = 3.93$). A shoulder at 430 nm ($\log \epsilon = 3.77$) can also be identified. These transitions are due to metal-to-ligand charge transfer, *i.e.* from the metal d orbital to the π^* orbital of the bipyridyl ligand, (MLCT).⁵⁸ In comparison to the model compound, [Os(bipy)₂(PVP)₁₀Cl]Cl, the wavelengths of transition are in close agreement *i.e.* 358 nm vs 364 nm, 430 nm vs 431 nm, 510 nm vs 486 nm and 740 nm vs 730 nm respectively for the polymer vs the model compound.⁵¹ Molar extinction coefficients are also in good agreement with $\log \epsilon$, 3.93 vs 4.05, 3.77 vs 4.08, 4.05 vs 3.75 and 3.18 vs 3.45 respectively.⁵¹ Slight differences in ϵ and λ may be attributed to factors such as steric and solvent effects and differing degrees of hydration of the polymer chain. Considering that the solvent used in this study and the polymer backbone are entirely different from that of the model compound, these results can be considered to be in good agreement. The results are consistent with the belief that the coordination sphere of the metal centre is [Os(N)₅Cl] and that the metal loading is 1/10 as expected from the synthetic protocol.⁵¹

In luminescence experiments, no evidence of fluorescence was observed at both room temperature and at -196 °C. This indicates that the metal-to-ligand charge transfer occurs from a ground singlet state to an

excited singlet state and that electronic relaxation is radiationless. This observation again confirms the coordination sphere of the metal centre as $[\text{Os}(\text{N})_5\text{Cl}]^{51}$

5.3.1.2 Electrochemistry

The formal potential of a redox couple is a function of the coordination sphere of the metal centre, the supporting electrolyte and electrolyte concentration. For this reason, the use of electrochemistry is valuable in the structural characterisation of redox polymers. A single redox wave was observed in the CV of the redox material. This has been assigned to the Os(II)/Os(III) redox couple.⁵¹ The formal potential of the Os(II)/Os(III) redox couple was determined in several electrolytes using slow sweep rate CV (1 mV s^{-1}). These results can be seen in Table 5.1. In the sulphate electrolytes, the formal potential for the Os(II)/Os(III) couple was found to be $0.245 \pm 0.005 \text{ V vs SCE}$ and $0.250 \pm 0.005 \text{ V vs SCE}$ for Na_2SO_4 and H_2SO_4 respectively. In toluene-p-sulphonic acid, (TpSA), electrolyte the formal potential was $0.200 \pm 0.005 \text{ V vs SCE}$. In perchlorate electrolytes, the formal potentials were determined to be $0.180 \pm 0.005 \text{ V vs SCE}$ and $0.170 \pm 0.005 \text{ V vs SCE}$ for the sodium and acid form respectively. The results are in general agreement with that observed for the model compound and therefore confirm the spectroscopic data concerning the coordination sphere of the metal centre.^{20,51}

It is evident that gross changes in the polymer backbone and consequently the redox centre micro-environment does not exert a significant effect on the spectroscopic properties and electrochemical formal potential of the redox moiety. As a result, the spectroscopic data and electrochemical data presented thus far indicates that the redox polymer has the chemical structure, $[\text{Os}(\text{bipy})_2(\text{PS})_{7.5}(\text{DMAP})_{2.5}\text{Cl}]\text{Cl}$, as expected from the synthetic strategy.

5.3.2 Electrochemistry and Charge Transport Properties of $[\text{Os}(\text{bipy})_2(\text{PS})_{7.5}(\text{DMAP})_{2.5}\text{Cl}]\text{Cl}$

It was stated earlier that it is generally accepted that the mode of charge transport through redox polymer films is by a process of electron self-exchange (“electron hopping”) between fixed redox sites.¹⁹ The rate determining step for charge propagation can be limited by the intrinsic barrier to self-exchange, counter ion movement, or by the rate of polymer segmental motion required for redox site juxtapositioning.²⁰ Traditionally, both qualitative and quantitative descriptions of the charge transport parameters and processes have been presented.²⁹⁻³¹ Here, a qualitative description of the CV behaviour of the electro-active material will be given along with a quantitative investigation of the charge transport properties of the polymer along with possible explanations for the behaviour observed.

A typical CV of $[\text{Os}(\text{bipy})_2(\text{PS})_{7.5}(\text{DMAP})_{2.5}\text{Cl}]\text{Cl}$ in aqueous electrolyte ($0.1 \text{ mol dm}^{-3} \text{ H}_2\text{SO}_4$) can be seen in Fig 5.4 a. The surface coverage (Γ) of the polymer calculated from the amount of material deposited on the electrode was expected to be in the region $2 \times 10^{-8} \text{ mol cm}^{-2}$. Intuitively, from the limited current response, it appears that only a small portion of the immobilised redox centres are electro-active on the CV time scale used. This behaviour was observed in all aqueous electrolytes examined. Using coulometry, it was found that for Γ less than $\approx 5 \times 10^{-9} \text{ mol cm}^{-2}$, the entire film was electro-active at moderate time scales such as at a potential sweep rate (ν) of 1 mV s^{-1} while at higher surface coverages, e.g. $1.2 \times 10^{-8} \text{ mol cm}^{-2}$, the entire film was not electro-active over prolonged time periods. This behaviour is thought to be a result of the high styrene content of the polymer backbone along with the sterically cumbersome pendant coordination group. In Fig 5.4 b, a CV for the same modified electrode in electrolyte comprising 10% ethanol can be seen. It is evident that an increase in the electro-activity of the redox polymer occurs in the presence of ethanol. The organic solvent acts to solvate or plasticise the polymer on the electrode surface and in doing so appears to expose more of the electro-active centres within the polymer film for redox processes. It was found that for thick polymer films, full redox activity can be obtained at *ca.* 25% ethanol, but the films quickly become unstable and are stripped from the electrode surface. The electro-inactivity of large portions of the polymer has serious implications for the charge

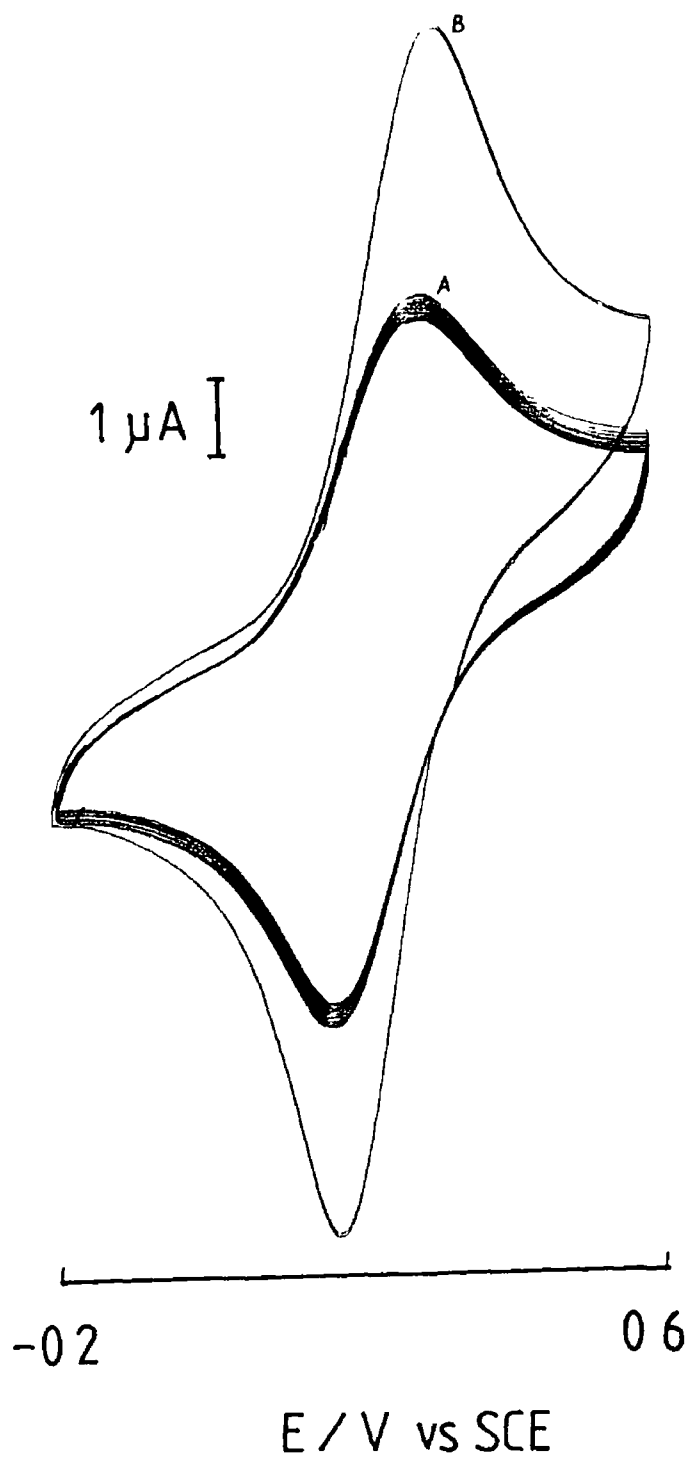


Fig 5.4 CV of $[\text{Os}(\text{bipy})_2(\text{PS})_7.5(\text{DMAP})_2.5\text{Cl}]\text{Cl}$ in (A) $0.1 \text{ mol dm}^{-3} \text{ H}_2\text{SO}_4$ and (B) $0.1 \text{ mol dm}^{-3} \text{ H}_2\text{SO}_4$ containing 10 % ethanol, sweep rate = 100 mV s^{-1}

transport and catalytic properties of the material, which by implication, may affect the performance of sensors constructed from these modified electrodes

Using polymer films with Γ of the order of $\approx 5 \times 10^{-9}$ mol cm $^{-2}$, the CV behaviour of the redox polymer was investigated. Certain criteria for the behaviour of ideal surface immobilised species have been established (*vide supra*)⁵⁹⁻⁶¹. The wave shape illustrated in Fig 5.4 a is characterised by considerable diffusional tailing and considerable peak-to-peak separation, behaviour which is indicative that the charge transport process is diffusionally controlled.⁶² Similar wave shapes have been observed in all electrolytes used. The peak-to-peak separation, (ΔE) , for various electrolytes is presented in Table 5.1. It should also be noted that in the ethanol-containing electrolyte, the general wave shape remains unaltered, although more of the redox centres become electro-active. This indicates that the charge transport limiting process may not change in the presence of the organic component. The ratio of the anodic / cathodic peak currents, i_{pa}/i_{pc} , for various electrolytes are also presented in Table 5.1. These can be seen to deviate from unity (ideal behaviour) therefore indicating non-ideal behaviour. Plots of i_{pa} vs v are useful for the diagnosis of surface behaviour.⁶² For all the electrolytes studied, such plots were found to be non-linear from 1 mV s $^{-1}$ to 500 mV s $^{-1}$. However, plots of i_{pa} vs $v^{1/2}$ were found to be linear. Typical plots can be seen in Fig 5.5 a and b. These results indicate that the polymer does not exhibit any surface behaviour what-so-ever, and the current is limited by semi-infinite diffusional processes and/or by migration effects. As the osmium redox centre is known to exhibit fast self-exchange rates and rapid heterogeneous electron transfer with glassy carbon electrodes, the observations made here indicate that the polymer backbone exerts considerable influence on the charge transport behaviour of this class of material.

The accurate determination of charge transport rates using the models employed in this study requires that the current response be diffusional in character and that migration effects be absent.^{26,30,63} The examination of migration within metallo-polymers of this type have received considerable attention and diagnostic criteria have been established.^{64,65} It appears that migration effects are not observed in the type of polymer used here using potential step techniques such as

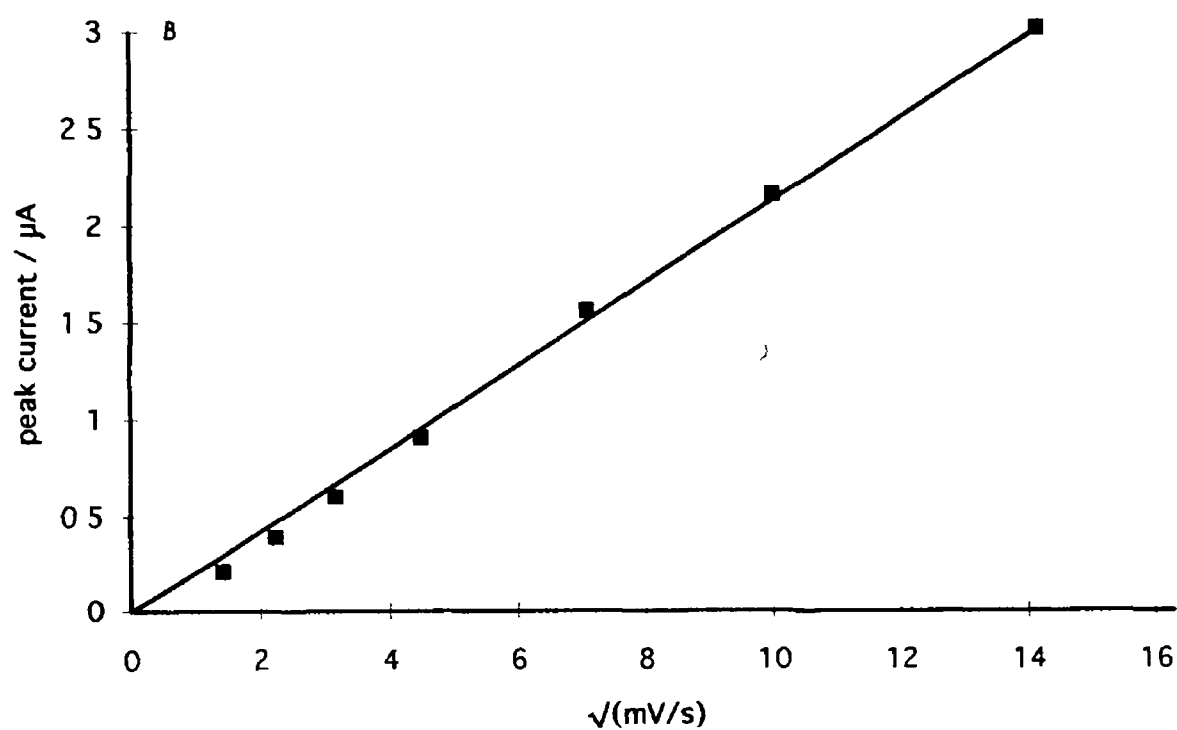
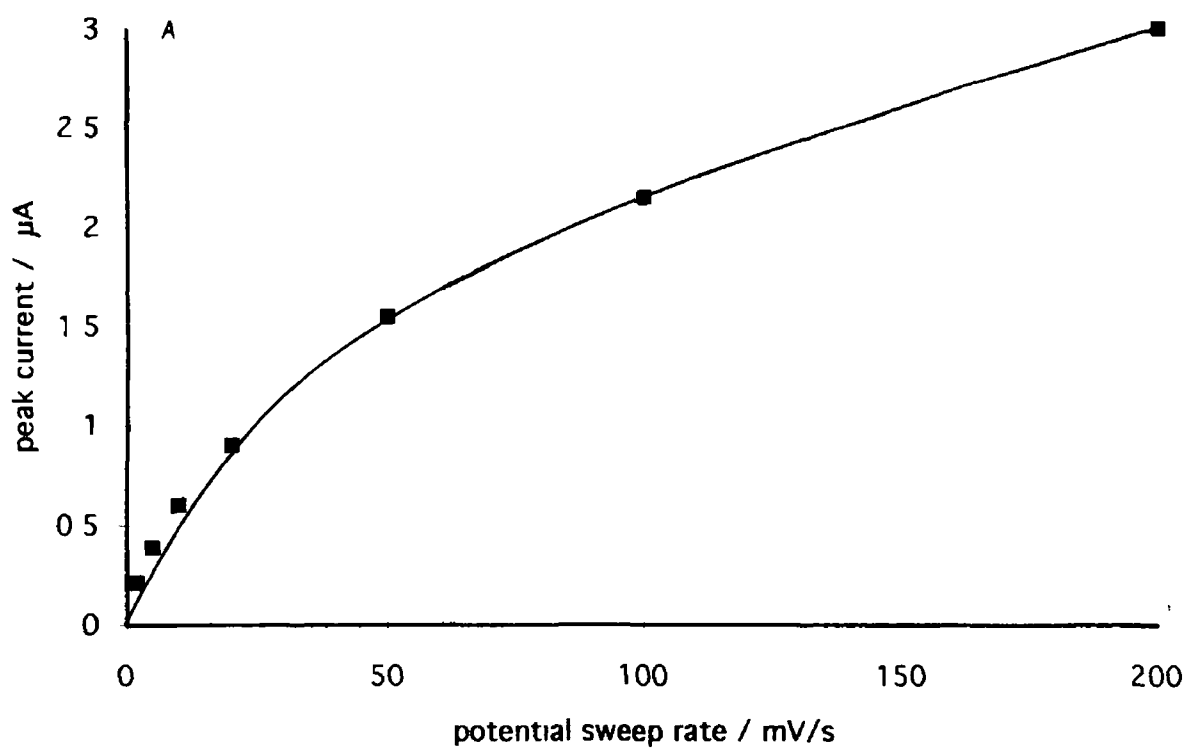


Fig 5.5 The variation of peak current with potential sweep rate for $[\text{Os}(\text{bipy})_2(\text{PS})_{7.5}(\text{DMAP})_2.5\text{Cl}]\text{Cl}$ modified electrodes in $0.1 \text{ mol dm}^{-3} \text{ H}_2\text{SO}_4$

Electrolyte [#]	E _{1/2} / mV*	ΔE _p /mV	t _{pa} /t _{pc}	D _{ct} / 10 ⁻¹² cm ² s ⁻¹
H ₂ SO ₄	250 ± 5	115 ± 5	0.87 ± 0.01	0.45 ± 0.2**
Na ₂ SO ₄	250 ± 5	105 ± 5	0.87 ± 0.01	0.31 ± 0.2
HClO ₄	167 ± 5	115 ± 5	1.03 ± 0.01	1.50 ± 0.3
NaClO ₄	180 ± 5	145 ± 5	0.88 ± 0.01	0.76 ± 0.3
TpSA [§]	200 ± 5	100 ± 5	0.87 ± 0.01	4.4 ± 0.2
H ₂ SO ₄ / 10% Ethanol	250 ± 5	105 ± 5	0.86 ± 0.01	0.63 ± 0.3

All electrolytes are 0.1 mol dm⁻³

* Potentials quoted with respect to SCE

** D_{ct} estimated by CV on at least 3 different films

§ TpSA is toluene-p-sulphonic acid

Table 5.1 The effect of electrolyte on charge transport parameters, surface behaviour and half-wave potential for a [Os(bipy)₂(PS)_{7.5}(DMAP)_{2.5}Cl]Cl modified electrode

chronoamperometry²⁰ Leech *et al*² used co-polymers of vinyl pyridine with high styrene content and also found migration effects to be absent. In the present study, Cottrell plots were found to have a zero current intercept which is indicative of the absence of migration effects. In addition, the diffusional nature of the charge transport process indicates that the charge transport is a result of the Os(II)/Os(III) concentration gradient or hindered counter-ion transport rather than the effect of applied potential. As cyclic voltammetry reveals information representative of the bulk structure of the polymer, and the semi-infinite diffusional behaviour outlined above is ideal for the estimation of D_{ct} by CV, the charge transport diffusion coefficients presented here have been estimated predominantly using this technique.⁶⁶

The rate of charge percolation through the polymer, $[\text{Os}(\text{bipy})_2(\text{PS})_{7.5}(\text{DMAP})_{2.5}\text{Cl}]\text{Cl}$, in various electrolytes are given in Table 5.1. In all cases, the concentration of electro-active species within the redox polymer is assumed to be equal to that of the analogue PVP homopolymer *i.e.* 0.7 mol dm^{-3} .⁵¹ The most striking aspects of these results is the low values for D_{ct} for every electrolyte. The values vary in the range $3.1 \times 10^{-13} \text{ cm}^2 \text{ s}^{-1}$ to $4.4 \times 10^{-12} \text{ cm}^2 \text{ s}^{-1}$. These values are significantly lower, by 1-3 orders of magnitude depending on electrolyte, than those found for $[\text{Os}(\text{bipy})_2(\text{PVP})_{10}\text{Cl}]\text{Cl}$ in the same supporting electrolytes.²⁰ Another significant difference from previously reported D_{ct} studies is that the D_{ct} values obtained for sulphate-based electrolytes in this study, are smaller than those found for perchlorate electrolytes. The reverse situation exists for $[\text{Os}(\text{bipy})_2(\text{PVP})_{10}\text{Cl}]\text{Cl}$.²⁰ The “break in” behaviour of the polymer films also supports this observation, with currents breaking downwards in sulphate electrolyte while breaking upwards in perchlorate. It is noteworthy that the difference in D_{ct} between H_2SO_4 and Na_2SO_4 is small. However, charge transfer appears slightly faster in the acidic electrolyte. As the effect is small, this may be a reflection on the relative insensitivity of the predominantly polystyrene backbone to pH compared to PVP based redox polymers. It can also be seen that the rate of charge transport is increased with the use of electrolyte containing 10% ethanol. The organic electrolyte TpSA exhibits the fastest charge transport characteristics.

It is known that the rate of charge transport through this type of material depends on a large number of factors including temperature, film

thickness, electrolyte type and concentration and polymer morphology^{20,21} It is also becoming clear that the structure of the redox polymer and consequently the redox site micro-environment is important in determining the current carrying capacity of these materials As a result, detailed interpretation of D_{ct} results is difficult In trying to rationalise the D_{ct} values found for this polymer, consideration must be given to the structure of the polymer and the type of electrolyte used As the polymer is predominantly composed of styrene residues, it is envisaged that the model for polyelectrolyte coatings, upon which much of the theory of redox polymers is based¹⁶, may be inappropriate here It is likely that the polymer coated on the electrode surface in aqueous electrolyte is glass-like and unswollen Considering that PVP-based redox polymers in ClO_4^- electrolytes are of similar compact structure but exhibit faster charge transfer, it is likely that an additional physical restriction on charge transfer exists for the polymer studied here The slow rate of charge transport observed for all electrolytes can therefore be attributed, in part, to the intractable nature of $[Os(bipy)_2(PS)_{7.5}(DMAP)_2.5Cl]Cl$ compared to the highly swollen PVP-based systems In addition, considerable portions of the polymer films are electro-inactive, so it is possible that the structure of the polymer on the electrode surface is grossly inhomogeneous with many redox centres being “shielded”, presumably in hydrophobic insulating domains (akin to biological redox centres) from the effect of charge compensating counter-ions or the applied potential Behaviour of this kind was suggested for styrene-containing redox polymers⁶⁷ previously and it is known that the structure of Nafion comprises of hydrophobic and hydrophilic domains⁶⁸ In a series of papers from Anson’s group⁶⁹⁻⁷², the possibility of spontaneous segregation of polymer blends on electrode surfaces into segregated hydrophobic and hydrophilic domains was discussed In a follow up study⁷², the effect of random and block copolymers on the electrochemistry of electrostatically incorporated $Fe(CN)_6^{4-}$ was addressed Again the presence of segregated domains was evident and these were found to affect the electrochemical properties of the redox centre Such a process may also contribute to the severely hindered homogeneous charge transports rates observed This model is supported by the low value obtained for the rate of heterogeneous charge transfer, k^0 , found using sampled current voltammetry in $0.1 \text{ mol dm}^{-3} \text{ H}_2\text{SO}_4$, where $k^0 = 2 \pm 1.5 \times 10^{-6} \text{ cm s}^{-1}$ The value of k^0 found here was *ca* 1-2 orders of magnitude smaller compared to PVP-⁷³ and the

PS/PVP-⁷⁴ based redox polymers. This effect may reflect non-conducting regions of the redox polymer blocking surface sites for heterogeneous electron transfer. Such behaviour has been previously suggested.⁴⁷ It has also been suggested recently that counter-ion movement at short time ranges and redox site juxtapositioning at longer time scales may be responsible for variations in k^0 , however, the orders of magnitude difference suggests that this is unlikely here.⁴⁶ From these observations, the presence of a highly swollen polymer containing Donnan domains¹⁶ and electrolyte “islands” is unlikely. As a result, charge compensating counter-ions must travel from the bulk of solution to the interior of the polymer upon redox and segmental polymer chain motion must occur in a ridged micro-environment.

From the results presented and discussed above, it is clearly evident that D_{ct} values are controlled by a diffusional like process. This process is either polymer chain movement or counter-ion motion. The third possible process, the energy barrier to self-exchange can be discounted due to the large self-exchange rates for the redox sites. In order to delineate the rate limiting process, the activation parameters for charge transport in the more interesting electrolytes, 0.1 mol dm⁻³ HClO₄ and 0.1 mol dm⁻³ TpSA were determined over a temperature range, 16 °C to 50 °C. It should be noted that the assumptions concerning inter-site distances made earlier may not be strictly valid as the redox polymer appears inhomogeneous. However, the activation results may be useful in assigning the rate limiting process for charge transfer. A typical Arrhenius plot obtained with the TpSA electrolyte can be seen in Fig. 5.6. The activation parameters are listed in Table 5.2. In perchloric acid, an intermediate value for the activation energy was obtained. This value (71 kJ mol⁻¹) is indicative of charge transport control by counter-ion motion.⁴⁹ An entropy value close to zero was also obtained which indicates no significant ordering of the polymer chains occurs upon redox. For TpSA, a slightly smaller activation energy was recorded, the magnitude of which, 47 kJ mol⁻¹, suggests that in this electrolyte that counter-ion motion is the charge transport limiting process. A relatively large negative entropy value was obtained in TpSA which suggests considerable ordering of the polymer film upon incorporation of this counter-ion. This is expected as this ion appears to significantly affect the properties of the polymer.

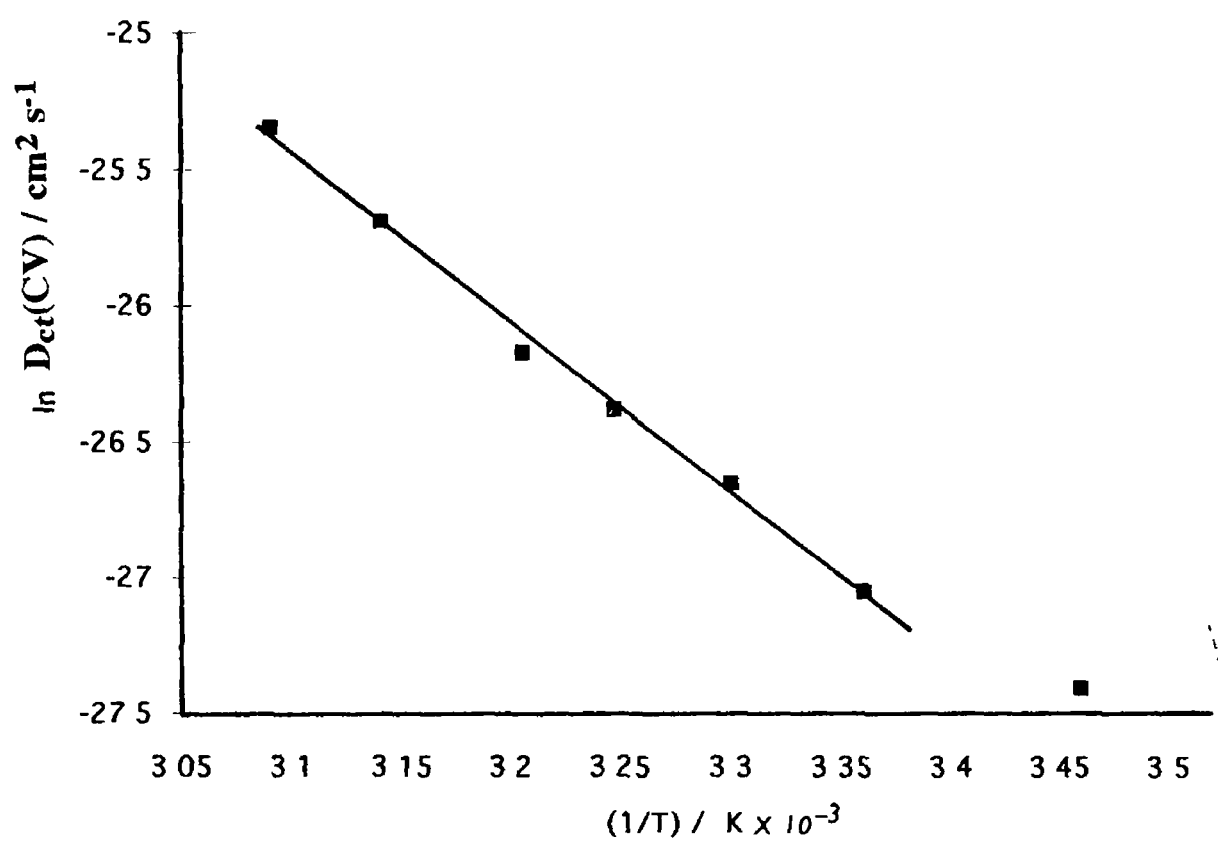


Fig 5.6 Typical Arrhenius plot for 0.1 mol dm^{-3} toluene-p-sulphonic acid electrolyte

Activation Parameter	HClO ₄ 0.1 mol dm ⁻³	TpSA* 0.1 mol dm ⁻³
E _a / kJ mol ⁻¹	71.2 ± 8§	47.4 ± 4§
ΔS [‡] / J mol ⁻¹ K ⁻¹	-5.7 ± 8	-76.6 ± 3
ΔG [‡] / kJ mol ⁻¹	70.4 ± 6	67.8 ± 4
ΔH [‡] / kJ mol ⁻¹	68.7 ± 7	45.0 ± 4

* TpSA is toluene-p-sulphonic acid

§ Errors are calculated from the standard deviation of the slope and intercept of the least squares fit for each line

Table 5.2 Activation parameters for charge transport through [Os(bipy)₂(PS)_{7.5}(DMAP)_{2.5}Cl]Cl in HClO₄ and TpSA

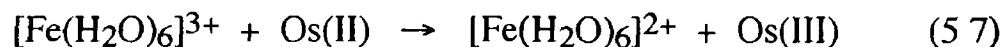
The electrochemical properties and charge transport parameters of $[\text{Os}(\text{bipy})_2(\text{PS})_{7.5}(\text{DMAP})_{2.5}\text{Cl}]\text{Cl}$ suggest that charge transport properties are, at best, poor. This appears to be a result of the intractable and possibly inhomogeneous structure of the redox polymer. Such slow charge transport properties, the compact nature of the polymer and the apparent “shielding” of redox centres will have significant limiting effects on the catalytic efficiency of the redox polymer. In order to study these effects, the mediated electrocatalysis of $[\text{Fe}(\text{H}_2\text{O})_6]^{3+}$ reduction was examined.

5.3.3 Mediated Electrocatalytic Reduction of $[\text{Fe}(\text{H}_2\text{O})_6]^{3+}$ by $[\text{Os}(\text{bipy})_2(\text{PS})_{7.5}(\text{DMAP})_{2.5}\text{Cl}]\text{Cl}$

The electrochemical behaviour of $[\text{Fe}(\text{H}_2\text{O})_6]^{3+}$ at glassy carbon is poor and this substrate does not undergo redox chemistry in the potential region of the electrocatalyst studied here. However, the formal potential for the reduction of $[\text{Fe}(\text{H}_2\text{O})_6]^{3+}$, according to equation 5.6, is 0.46 V vs. SCE⁷⁵, which is positive of the $E_{1/2}$ of the Os(II)/Os(III) redox couple.



On this basis, it is expected that the redox polymer would mediate the reduction of $[\text{Fe}(\text{H}_2\text{O})_6]^{3+}$ with a thermodynamic driving force of 0.21 V according to equation 5.7.



In Fig. 5.7a, a CV for the reduction of $[\text{Fe}(\text{H}_2\text{O})_6]^{3+}$ at a modified electrode can be seen. This CV, when compared to Fig. 5.4a, shows that the redox polymer mediates the reduction of $[\text{Fe}(\text{H}_2\text{O})_6]^{3+}$. It is also evident that a reverse wave is absent, suggesting that the mediated reaction is irreversible. This is expected considering the thermodynamics.

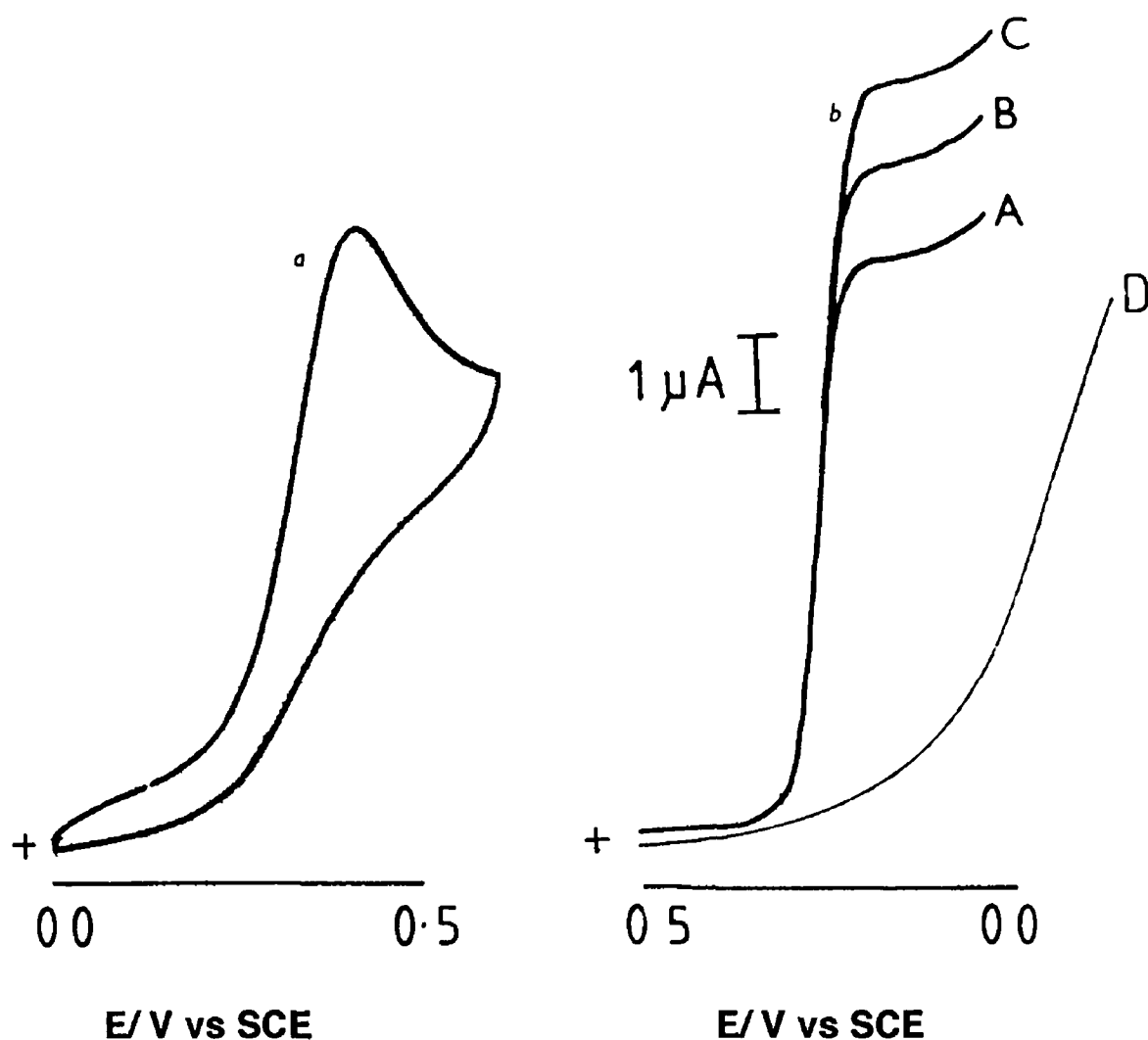


Fig 5.7 CV of (a) $1.0 \times 10^{-3} \text{ mol dm}^{-3} [\text{Fe}(\text{H}_2\text{O})_6]^{3+}$ at an $[\text{Os}(\text{bipy})_2(\text{PS})_{7.5}(\text{DMAP})_{2.5}\text{Cl}]\text{Cl}$ modified electrode and (b) current-potential curves for $[\text{Fe}(\text{H}_2\text{O})_6]^{3+}$ reduction ($1.0 \times 10^{-3} \text{ mol dm}^{-3}$) at (A) 500 rpm, (B) 1000 rpm and (C) 2000 rpm. Curve (D) is the reduction of $[\text{Fe}(\text{H}_2\text{O})_6]^{3+}$ at glassy carbon at 500 rpm.

of the system In Fig 5 7b, current-potential curves for the reduction of $[\text{Fe}(\text{H}_2\text{O})_6]^{3+}$ at a bare glassy carbon electrode and an electrode modified with $[\text{Os}(\text{bipy})_2(\text{PS})_{7.5}(\text{DMAP})_2.5\text{Cl}]\text{Cl}$ are shown These traces again clearly demonstrate that the redox polymer mediates the reduction of $[\text{Fe}(\text{H}_2\text{O})_6]^{3+}$ As the onset of mediation occurs at the onset of Os(II) generation in the film, the electron transfer process occurs *via* redox cycling of the Os(II)/Os(III) sites within the polymer film It is also evident, from the well defined current-potential curves for the mediated reaction, that the electrochemical behaviour of the reduction reaction is significantly improved compared to that at glassy carbon

A number of theoretical models have been described for the analysis of the kinetic and transport properties of mediation at redox polymer modified electrodes ⁷⁶⁻⁸⁴ These models can also be used for the optimisation of modified electrode responses These theories have been discussed in detail in Chapter 1 Rotating disc electrode voltammetry was used to probe the behaviour of the mediated reduction of $[\text{Fe}(\text{H}_2\text{O})_6]^{3+}$ Analysis is carried out by examining the effect of angular velocity of the electrode, ω , the reciprocal slope of the Koutecky-Levich plot, polymer layer thickness, L , and the concentration of electro-active species within the film, b_0 The diagnostic scheme proposed by Alberly, Boutelle and Hillman ⁸⁴ has been used to analyse the transport and kinetic behaviour of $[\text{Fe}(\text{H}_2\text{O})_6]^{3+}$ reduction at the modified electrode

In Fig 5 8, typical Koutecky-Levich plots for the reduction of $[\text{Fe}(\text{H}_2\text{O})_6]^{3+}$ at an $[\text{Os}(\text{bipy})_2(\text{PS})_{7.5}(\text{DMAP})_2.5\text{Cl}]\text{Cl}$ modified electrode are presented At an $[\text{Fe}(\text{H}_2\text{O})_6]^{3+}$ concentration of $8.0 \times 10^{-4} \text{ mol dm}^{-3}$, the plots (Fig 5 8b) are linear and are proportional to the rotation speed of the electrode This information allows the elimination ⁸⁴ of the kinetic situations, S_{te} , LS_{te} and LE_k The inverse slope of the Koutecky-Levich plots are constant for all the surface coverages examined and were found to be $1.0 \pm 0.8 \times 10^{-3} \text{ cm s}^{-1/2}$ This value is equivalent to the Levich constant which is given by,

$$C_{\text{Lev}} = 1.554 D^{2/3} \nu^{-1/6} \quad (5.8)$$

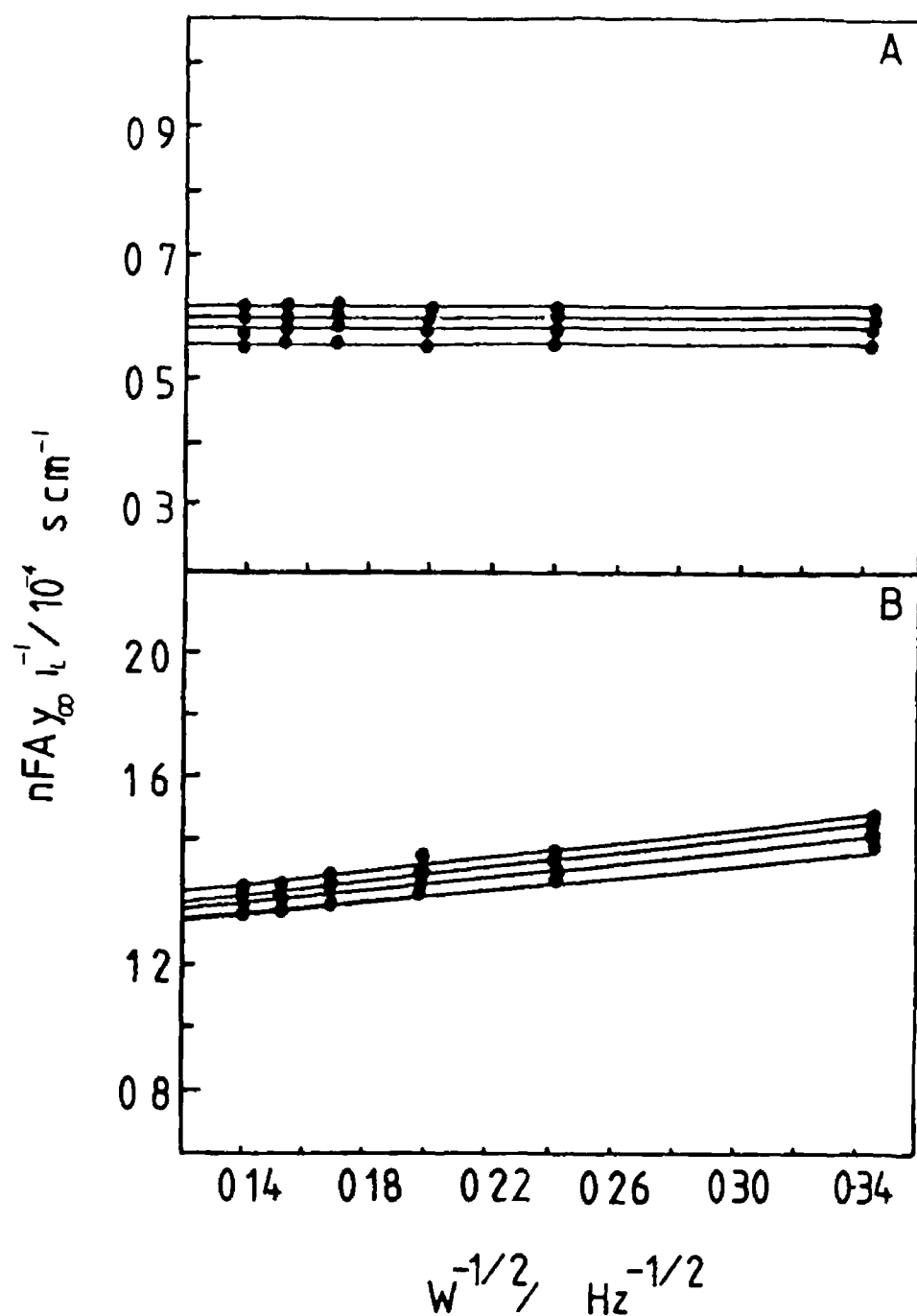


Fig 5.8 Koutecky-Levich plots for the reduction of $[\text{Fe}(\text{H}_2\text{O})_6]^{3+}$ at modified electrodes. A = $1.4 \times 10^{-3} \text{ mol dm}^{-3}$ and B = $8.0 \times 10^{-4} \text{ mol dm}^{-3}$. Surface coverages for both plots are from the top, 3.3×10^{-8} , 4.2×10^{-8} , 1.7×10^{-8} , $4.0 \times 10^{-9} \text{ mol cm}^{-2}$.

where D is the diffusion coefficient of the substrate in the electrolyte and ν is the kinematic viscosity of the electrolyte. This value has been estimated for clean unmodified electrodes in previous studies to be $1.01 \times 10^{-3} \text{ cm s}^{-1/2}$ and $1.04 \times 10^{-3} \text{ cm s}^{-1/2}$.^{84,85} For a poly(hydroxyphenazine) modified electrode, a value of $1.14 \times 10^{-3} \text{ cm s}^{-1/2}$ was found for the Levich constant.⁸⁶ Therefore the Levich slope found for the $[\text{Os}(\text{bipy})_2(\text{PS})_{7.5}(\text{DMAP})_{2.5}\text{Cl}]\text{Cl}$ modified electrode is the same as that obtained at bare electrodes. Armed with this information, the kinetic case, LRZ_{tety} can be eliminated.⁸⁴ With the exclusion of the above cases, the mechanism of the mediated reaction must lie within the S_k'' , LS_k , L_k or LE_{ty} kinetic zones. These cases can be distinguished by the dependence of k'_{ME} (modified electrode rate constant) on L and b_0 . From the Koutecky-Levich plots, it can be seen that k'_{ME} is independent of polymer layer thickness, L , therefore the kinetic cases L_k and LE_{ty} can be eliminated. By examining the dependence of b_0 on k'_{ME} the two cases S_k'' and LS_k can be distinguished. The concentration, b_0 has been estimated at various potentials by step-wise integration of the charge under slow sweep rate CV. In Fig. 5.9, a plot of $\ln(1-f)$ vs $\ln k'_{\text{ME}}$ can be seen (where f = fraction of redox centres in Os(III) oxidation state). The slope of this plot is 1.02 ± 0.11 . This suggests that the kinetic situation is S_k'' . Under this kinetic regime, electron transfer occurs from a region of molecular dimensions at the surface of the polymer to a solution phase $[\text{Fe}(\text{H}_2\text{O})_6]^{3+}$ and the rate constant for the cross-exchange reaction is current limiting. The S_k'' kinetic case can arise in two situations, a) when charge transport through the polymer and the rate of the cross-exchange reaction are so fast that the substrate flux is consumed without penetration of the polymer film, and b) when the substrate is physically unable to penetrate the polymer film. It is evident from the kinetic analysis that $[\text{Fe}(\text{H}_2\text{O})_6]^{3+}$ does not permeate the polymer film. This is a result of the unswollen and intractable nature of the modifying layer. This is not surprising as similar kinetic behaviour has been observed for the reduction of $[\text{Fe}(\text{H}_2\text{O})_6]^{3+}$ at electrodes modified with $[\text{Os}(\text{bipy})_2(\text{PVP})_{10}\text{Cl}]\text{Cl}$ in $1.0 \text{ mol dm}^{-3} \text{ HClO}_4$ electrolyte. In the perchlorate electrolyte, the polymer films are thought to be highly compact and dehydrated, thus preventing partitioning of the substrate.⁸⁵ In both of these cases, it is the physical properties of the polymer which results in the zero permeabilities of the substrate.⁸⁵ It is now evident that the physical properties of the

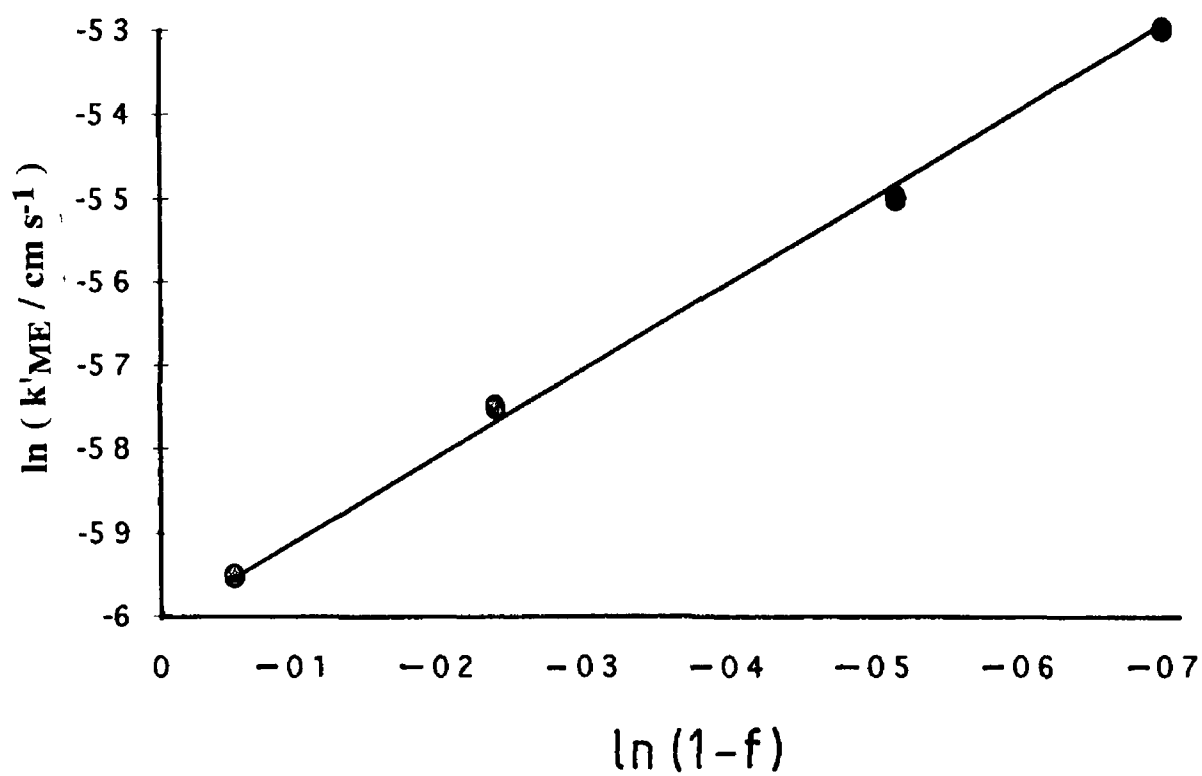


Fig 5 9 Plot of $\ln k'_{ME}$ vs $\ln(1-f)$ for the mediated reduction of $[\text{Fe}(\text{H}_2\text{O})_6]^{3+}$

polymer affect both the charge transport and mass transport behaviour of the polymer film

The analytical expression describing k'_{ME} for the S_k'' kinetic case is of the form ⁷⁶,

$$k'_{ME} = b_0 k'' \quad (5.9)$$

where k'' is the homogeneous second order rate constant for the surface cross-exchange reaction. A value of $1.6 \pm 0.5 \times 10^{-4} \text{ cm s}^{-1}$ has been estimated for k'_{ME} . The relatively large error associated with this value may be a further indication of the apparent inhomogeneity of the polymer films and consequently the variation in available surface redox sites. Using this expression, a value for k'' was estimated to be $2.3 \pm 0.7 \times 10^{-4} \text{ mol}^{-1} \text{ dm}^3 \text{ cm s}^{-1}$. This compares favourably with the value, $3.1 \times 10^{-4} \text{ mol}^{-1} \text{ dm}^3 \text{ cm s}^{-1}$, obtained for the same surface reaction at $[\text{Os}(\text{bipy})_2(\text{PVP})_{10}\text{Cl}]\text{Cl}$ modified electrodes in $1.0 \text{ mol dm}^{-3} \text{ HClO}_4$ electrolyte ⁸⁵. This confirms the surface nature of the mediated reaction and demonstrates that for surface reactions, the rate of the cross-exchange reaction between the mediator and the substrate is independent of the polymer matrix.

At higher $[\text{Fe}(\text{H}_2\text{O})_6]^{3+}$ concentrations, for example $1.4 \times 10^{-3} \text{ mol dm}^{-3}$, the currents generated at the rotating disc electrode become independent of rotation speed (Fig. 5.8a). According to the theory of Alberly and Hillman ⁷⁶, this indicates a change of kinetic case from S_k'' to S_{te} , with the transport of electrons through the polymer film becoming current limiting. This observation is consistent with the slow rates of charge transport observed for the polymer and the zero permeabilities for the iron species.

The use of steady-state techniques for the estimation of charge transport rates through metallo-polymers has received considerable attention recently ^{29,30}. These methods frequently yield charge transport rates significantly faster than the transient techniques such as CV and chronoamperometry. This is believed to be a result of a negligible contribution from counter-ion transport and polymer segment motion in steady-state measurements. At high $[\text{Fe}(\text{H}_2\text{O})_6]^{3+}$ concentrations, with no

substrate permeation of the polymer film and the reduction reaction being controlled by electron transport, (i.e. the S_{te} case), this situation can be considered akin to the sandwich electrode ²⁷ Under these steady-state conditions, according to Saveant, the electron diffusion coefficient, D_e , can be estimated using the equation ¹⁶,

$$i_e = (n F D_e \Gamma) / L^2 \quad (5.10)$$

where i_e is the characteristic electron diffusion current ⁷⁸⁻⁸³ and L is the film thickness. In using this technique, it is assumed that electron transport is slower than both the rate of forced convection of the substrate to the electrode and the rate of the cross-exchange reaction ^{29,30} These assumptions can be shown to be valid by estimation of the substrate mass transport current, i_a , and characteristic kinetic current, i_k , and comparing these to the experimentally estimated electron diffusion current i_e , which is $\approx 2.8 \times 10^{-4} \text{ A cm}^{-2}$. The characteristic solution substrate mass transport current, i_a , given by,

$$i_a = n F D_s Y_\infty / \delta \quad (5.11)$$

i_a has been estimated to be $\approx 3.3 \text{ A cm}^{-2}$, where Y_∞ = the $[\text{Fe}(\text{H}_2\text{O})_6]^{3+}$ concentration at $\approx 1 \times 10^{-1} \text{ mol dm}^{-3}$, D_s , the diffusion coefficient of the substrate in solution is $2 \times 10^{-6} \text{ cm}^2 \text{ s}^{-1}$, and δ is the diffusion layer thickness at $\omega = 8.33 \text{ Hz}$. The characteristic kinetic current, i_k , under these conditions is given by

$$i_k = n F A k'' b_o y_\infty \quad (5.12)$$

For the surface catalytic reaction observed here, this characteristic current has been estimated to be $\approx 2.1 \text{ mA cm}^{-2}$. Therefore $i_a \gg i_e$ and $i_k \gg i_e$,

which is entirely consistent with the charge transport results and kinetic observations as reflected in the zero slopes found for the Koutecky-Levich plots for concentrations of $[\text{Fe}(\text{H}_2\text{O})_6]^{3+}$ greater than $1.0 \times 10^{-3} \text{ mol dm}^{-3}$. Using saturated $[\text{Fe}(\text{H}_2\text{O})_6]^{3+}$ solutions ($\approx 1 \times 10^{-1} \text{ mol dm}^{-3}$ in $0.1 \text{ mol dm}^{-3} \text{ H}_2\text{SO}_4$), the average maximum current flux through the polymer was found to be $2.8 \times 10^{-4} \text{ A cm}^{-2}$. Inserting into equation 5.10, this yields a value for D_e of $6.2 \times 10^{-11} \text{ cm}^2 \text{ s}^{-1}$ with $L = 1.5 \times 10^{-5} \text{ cm}$ and $b_0 = 0.7 \times 10^{-3} \text{ mol cm}^{-3}$. This value is significantly greater than the value for D_{ct} found by CV in the same electrolyte. It is however similar to the value obtained using chronoamperometry in the same electrolyte, which is $1.2 \pm 0.1 \times 10^{-10} \text{ cm}^2 \text{ s}^{-1}$. Many examples of “mis-match” between the current carrying capacity estimated from D_{ct} measurements and those found experimentally have been reported. The reason for this is still unclear. In the present study, it is possible that over the short time-scale measurement using chronoamperometry, where only a small portion of the film is probed, counter-ion availability may not be rate limiting. Therefore the experimentally obtained D_{ct} (PS) value may reflect the true electron diffusion value D_e . The agreement between the chronoamperometry and steady-state results may indicate this. While with the CV measurement, a larger portion of the film is examined and counter-ion availability may then become the rate determining process, as indicated by the thermodynamic parameters discussed earlier, it is also possible that in the compact films of $[\text{Os}(\text{bipy})_2(\text{PS})_{7.5}(\text{DMAP})_2.5\text{Cl}]\text{Cl}$, insufficient void volume exists to accommodate incoming counter-ions for total oxidation of the polymer film during CV. As only a small portion of the film is oxidised with potential step techniques, sufficient void volume within the polymer may exist to ensure rapid electro-neutrality over this time-scale, which may lead to an equivalence in the steady-state measurements and potential step measurements of D_{ct} . These results are a clear demonstration that process controlling charge percolation through metallo-polymers is variable depending on the time-scale of measurement and by implication, the technique used for the estimation.

It was predicted earlier that the slow charge transport properties and the physical properties of the redox polymer may have detrimental effects on the catalytic efficiency of the electro-active material. From the results presented it is clear that modified electrodes constructed from $[\text{Os}(\text{bipy})_2(\text{PS})_{7.5}(\text{DMAP})_2.5\text{Cl}]\text{Cl}$ do not operate in the ideal three dimensional zone. The electrocatalytic material however, significantly

improves the electrochemical behaviour of $[\text{Fe}(\text{H}_2\text{O})_6]^{3+}$ reduction at electrodes, but at high substrate concentration electron transport through the polymer will become current limiting. As the electrode used here is operating under electron transport control at concentrations $> 1 \times 10^{-3} \text{ mol dm}^{-3}$ under steady-state conditions, sensors constructed from these modified electrodes may have limited linear ranges. However, modified electrodes exhibiting similar surface electrocatalytic properties but with rapid electron transport dynamics, currents may be diffusionally controlled (substrate) over considerable concentration ranges. These results demonstrate the need for rapid electron transport through redox polymers. The behaviour of such sensors will be discussed in the next section.

5.3.4 Analytical Application of $[\text{Os}(\text{bipy})_2(\text{PS})_{7.5}(\text{DMAP})_2.5\text{Cl}]\text{Cl}$

The use of redox polymer modified electrodes for electroanalysis is well documented.^{1,3,87-89} The polymer under investigation in this study was applied to the determination of ferrous fumarate in iron supplement tablets. Analysis was carried out using flow injection analysis (FIA) at a constant applied potential. Typical FIA traces can be seen in Fig 5.10. These peaks are well defined and are useful analytically. The sensor was found to have a limit of detection (LOD) of $3 \times 10^{-6} \text{ mol dm}^{-3}$ and to be linear over the concentration range, 1.0×10^{-5} to $1 \times 10^{-3} \text{ mol dm}^{-3}$ of $[\text{Fe}(\text{H}_2\text{O})_6]^{3+}$. This range, although significant, is smaller than that normally found for sensors constructed from redox polymer modified electrodes.⁶⁷ The truncated linear range observed for $[\text{Os}(\text{bipy})_2(\text{PS})_{7.5}(\text{DMAP})_2.5\text{Cl}]\text{Cl}$ is not surprising and can be easily explained from the kinetic/transport data. At low substrate concentrations, the current is controlled by the rate of diffusion of substrate to the electrode surface, consequently, the sensor response obeys a linear relationship with respect to $[\text{Fe}(\text{H}_2\text{O})_6]^{3+}$ concentration. While at higher $[\text{Fe}(\text{H}_2\text{O})_6]^{3+}$ concentrations ($> 1 \times 10^{-3} \text{ mol dm}^{-3}$) the sensor response becomes limited by electron transport dynamics, and because of this the sensor response levels off. This can be seen in Fig 5.11. We have observed that for $[\text{Os}(\text{bipy})_2(\text{PVP})_{10}\text{Cl}]\text{Cl}$ modified electrodes, linear ranges for this substrate extend significantly further, in fact up to $1 \times 10^{-2} \text{ mol dm}^{-3}$, with perchloric acid as the carrier electrolyte. This extended range is a result of

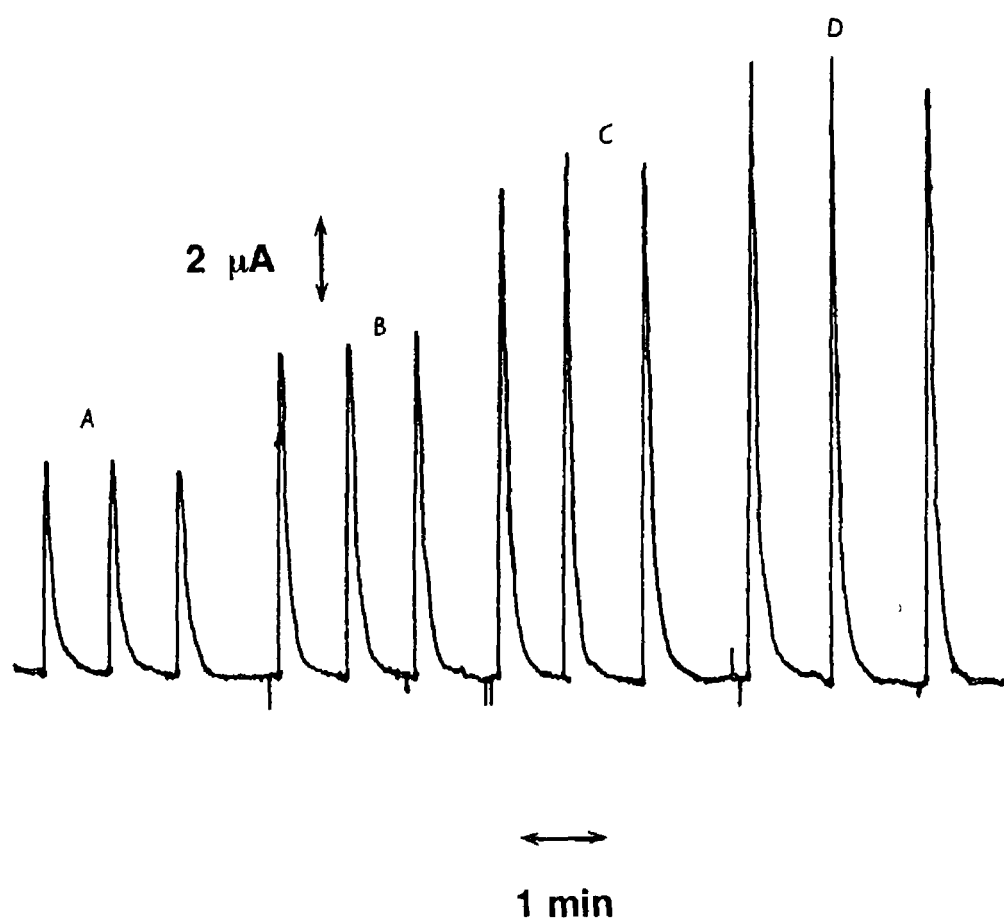


Fig 5 10. Typical FIA peaks for the detection of $[\text{Fe}(\text{H}_2\text{O})_6]^{3+}$ at an $[\text{Os}(\text{bipy})_2(\text{PS})_{7.5}(\text{DMAP})_{2.5}\text{Cl}]\text{Cl}$ modified electrode A, B, C and D are 4.0×10^{-4} , 6.0×10^{-4} , 8.0×10^{-4} and $1.0 \times 10^{-3} \text{ mol dm}^{-3}$ $[\text{Fe}(\text{H}_2\text{O})_6]^{3+}$ respectively. The carrier was 0.1 mol dm^{-3} H_2SO_4 at a flow rate of $1.0 \text{ cm}^3 \text{ min}^{-1}$.

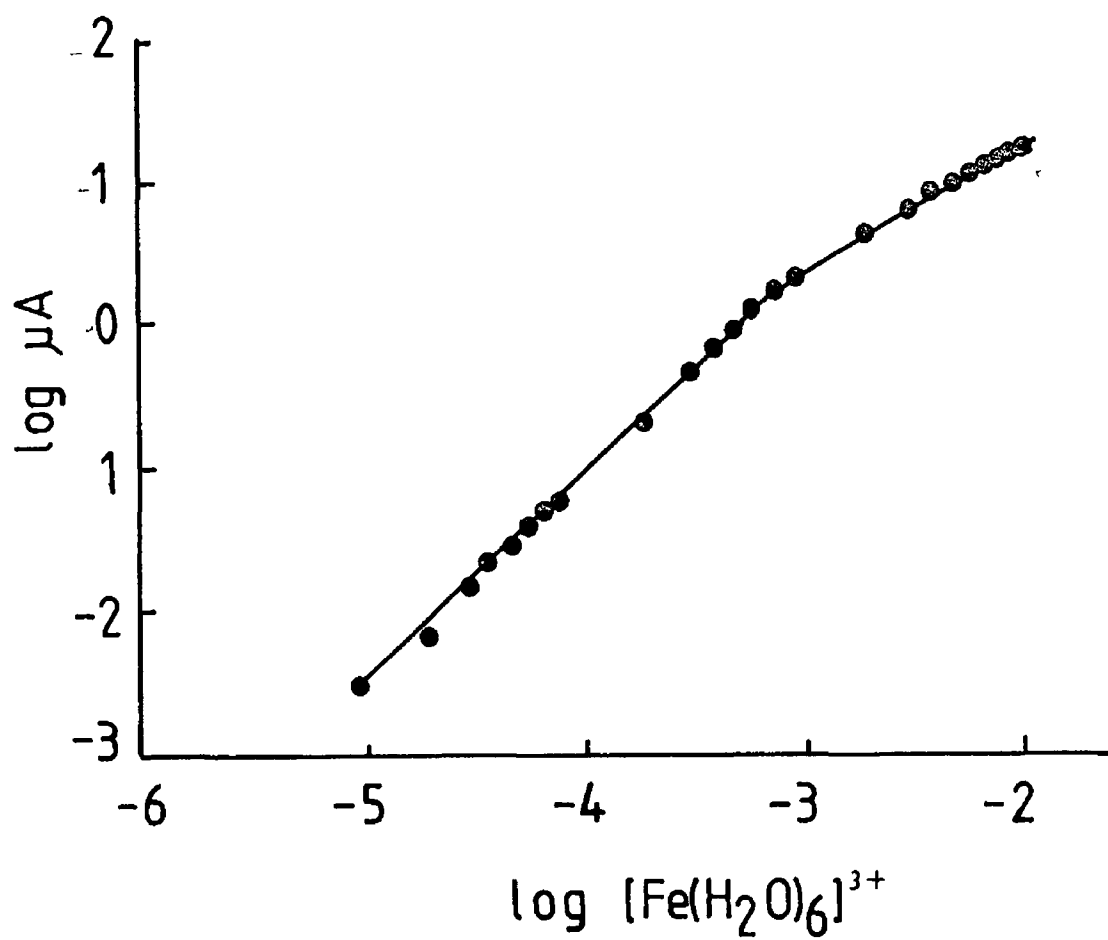


Fig 5 11 Typical calibration plot for the FIA determination of $[\text{Fe}(\text{H}_2\text{O})_6]^{3+}$ Experimental conditions as for Fig 5 10

the significantly more rapid charge transport through the PVP-based polymer although the reaction is also surface in nature. These two examples demonstrate how rapid electron transfer improves the performance of sensors by extending their linear range although the reaction *loci* are identical. The slope (sensitivity) of the sensor over the linear range was $1.8 \pm 0.1 \mu\text{A mmol}^{-1} \text{dm}^3$. Sensor responses were found to be insensitive to changes in polymer layer thickness as expected from a surface reaction under substrate transport control (S_k'').⁸⁴

The primary purpose for the synthesis of $[\text{Os}(\text{bipy})_2(\text{PS})_{7.5}(\text{DMAP})_{2.5}\text{Cl}]\text{Cl}$ was to produce a highly stable redox material. In Fig. 5.12, the response of the sensor in the flow system to various concentrations of $[\text{Fe}(\text{H}_2\text{O})_6]^{3+}$ over several days can be seen. It is evident that the response increased slightly over the first 48 h and then levelled off to a constant value. In this experiment the concentration of the test $[\text{Fe}(\text{H}_2\text{O})_6]^{3+}$ solutions were kept above the linear range to ensure observation of any improvement of the charge transport characteristics of the polymer film. These results demonstrate the excellent long term stability of the modifying layer. Such stability is impressive compared to many modified electrodes proposed previously. The high stability is probably a function of the high styrene content of the polymer which renders the material insoluble in aqueous electrolytes. Some possible explanations for the rise in response over the initial 48 h period include, a) very slow “break-in” effect with release of “shielded” redox centres, or b) mass changes within the polymer. It is becoming evident recently from electrochemical quartz crystal microbalance studies that sudden influxes or egress of mass (solvent and/or electrolyte) can occur to apparently equilibrated, stable polymer films.⁹⁰ The cause and effects of this phenomenon have yet to be established. It can be seen from these results that the stability of the modifying layer is excellent.

For the analysis of iron tablets, a concentration of $105 \pm 3 \text{ mg / tablet}$ of Fe was found using the sensor while $104 \pm 1 \text{ mg / tablet}$ of Fe was found using a standard spectrophotometric assay. The tablet formulation, according to the manufacturers specification, contains 100 mg / tablet Fe. These results clearly demonstrate the utility of redox polymer modified electrodes for electroanalysis. Advantages such as sensitivity, simplicity, stability and ease of automation can be cited for this sensor.

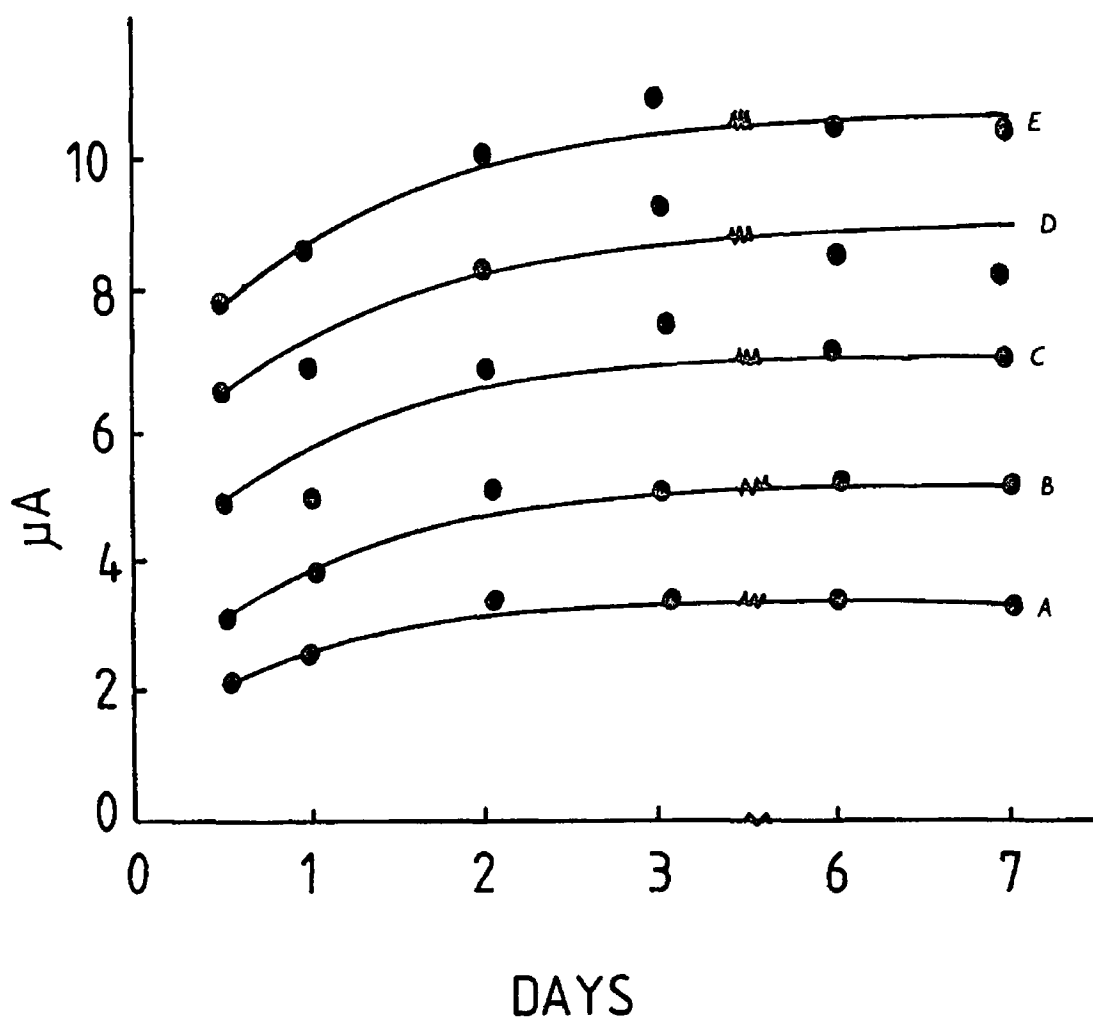


Fig 5.12 Sensor response stability, plot of sensor responses in a thin-layer flow-cell to various concentrations of $[\text{Fe}(\text{H}_2\text{O})_6]^{3+}$ with respect to time. A, B, C, D and E are 2.0 , 3.0 , 4.0 , 5.0 and $6.0 \times 10^{-3} \text{ mol dm}^{-3} [\text{Fe}(\text{H}_2\text{O})_6]^{3+}$ respectively.

5.4. Conclusions

The synthetic strategy developed previously for the preparation of redox polymers from PVP and PVI was successfully applied to the synthesis of the redox polymer used in this study and indicates the general applicability of the synthetic route. The spectroscopic and electrochemical data obtained suggest that the polymer backbone exerts little effect on the spectroscopic properties and electrochemical thermodynamics of the redox centre in solution. These results also indicate that the coordination sphere of the redox centre is that expected *i.e.* $[\text{Os}(\text{N})_5\text{Cl}]$. The ability to characterise the material in this fashion is of particular advantage.

The primary purpose of this study was the preparation of a highly stable redox polymer. This objective was achieved, with the polymer being extremely stable in aqueous electrolyte under the severe hydrodynamic conditions of thin-layer electrochemical flow-cells. From the results presented, it is clear that the conditions required for high stability are mutually opposed to those required for ideal behaviour of the immobilised redox site. In order to ensure rapid homogeneous charge transfer, the redox polymers must have strong interactions with the contacting electrolyte to provide a bulk structure conducive for rapid counter-ion transport and juxtapositioning of the fixed redox sites. For the polymer studied here, these conditions are not satisfied due to the hydrophobic nature of the polymer back-bone. This results in slow charge transport rates and zero permeability of the polymer by the substrate $[\text{Fe}(\text{H}_2\text{O})_6]^{3+}$. As the rate of self-exchange between the osmium redox centres is known to be fast and the rate of cross-exchange reaction with $[\text{Fe}(\text{H}_2\text{O})_6]^{3+}$ is also rapid, then it is obvious that the polymer backbone must be “designed” with physical properties to provide sufficient charge transport rates and analyte permeability to ensure that sensor responses are not limited by the rate of electron transport through the polymer.

Although the sensor described does not operate according to the ideal three dimensional reaction zone, the electrochemical responses to $[\text{Fe}(\text{H}_2\text{O})_6]^{3+}$ are significantly improved compared to the unmodified electrode. According to the theory of Saveant⁹¹, in situations where the direct reaction occurs at rates much less than those predicted by the Marcusian relation, monolayers of redox mediators can be very effective in improving electrode responses. This situation was encountered here and

the improvement in the electrochemical behaviour of $[\text{Fe}(\text{H}_2\text{O})_6]^{3+}$ reduction is clearly evident. The sensor described has the advantages of simplicity, direct detection of the analyte, good sensitivity, moderate linear range, good precision, accuracy and the analysis may be easily automated. Also the analytical protocol is simple compared to the operator intensive spectrophotometric procedure. This shows that in real analytical applications, mediation, even in the non-ideal two dimensional reaction zone, can be very useful for electroanalysis.

5.5. References

- 1 R J Forster, J G Vos in *Comprehensive Analytical Chemistry*, Vol XXVII, M R Smyth, J G Vos,, (Eds), Elsevier, Amsterdam, 1992, Ch 7
- 2 D Leech, R J Forster, M R Smyth, J G Vos, *J Mats Sci* , 1991 1 629
- 3 N Barsci, E Wilke, G G Wallace, M Meaney, M R Smyth, J G Vos, *Electroanalysis*, 1989 1 245
- 4 G G Wallace, M Meaney, M R Smyth, J G Vos, *Electroanalysis*, 1989 1 357
- 5 L L Miller, B Zinger, C Degrand, *J Electroanal Chem* , 1984 178 87
- 6 J Lieto, D Milstein, R L Albright, J V Minkiewitz, B C Gates, *Chem Tech* , 1983 13 46
- 7 G Hofle, W Steglich, H Vorbruggen, *Angew Chem Int Ed Engl* , 1978 17 97
- 8 L M Litvinenko, A I Kirichenko, *Dokl Akad Nauk SSSR, Ser Khim* , 1967 176 97
- 9 W Steglich, G Hofle, *Angew Chem , Int Ed Engl* , 1969 8 981
- 10 H J Twitchett, Brit 990, 633, 1965, *Chem Abstr* , 63 P5861e
- 11 W Steglich, G Hofle, Ger Offen 1, 958, 954 1971, *Chem Abstr* , 75 P34673k
- 12 G M Brauer, D M, Dulik, J M Antonucci, D J Termini, H Argentar, *J Dent Res* , 1979 58 1994
- 13 J P J Verlaan, P J T Alferink, G Challa, *J Mol Catal* , 1984 24 235
- 14 C E Koning, M , G Challa, F B Hulsbergen, J Reedijk, *J Mol Catal* , 1986 34 355
- 15 C E Koning, J J W Eshuis, F J Viersen, G Challa, *Reactive Polym* , 1986 4 293
- 16 F C Anson, J M Saveant, K Shigehara, *J Am Chem Soc* , 1983 105 1096
- 17 A J Bard, L R Faulkner, *Electrochemical Methods*, Wiley, NY, 1980, p 76
- 18 F C Anson, J M Saveant, K Shigehara, *J Phys Chem* , 1983

- 19 F B Kaufman, H Schroeder, E Engler, S R Kramer, J Q Chambers, *J Am Chem Soc* , 1980 102 483
- 20 R J Forster, A J Kelly, J G Vos, M E G Lyons, *J Electroanal Chem* , 1989 270 365
- 21 N Oyama, T Ohsaka, K Chiba, K Takahashi, *Bull Chem Soc Jpn* , 1988 61 1095
- 22 T Ohsaka, H Yamamoto, M Kaneko, A Yamada, M Nakamura, S Nakamura, N Oyama, *Bull Chem Soc Jpn* , 1984 57 1844
- 23 N Oyama, K Sato, S Yamaguchi, H Matsuda, *Denki Kagaku*, 1983 51 91
- 24 A R Hillman, in *Electrochemical Science and Technology of Polymers*, R G Linford, (Ed), Elsevier, Amsterdam, 1987, Ch 5
- 25 F C Anson, *J Phys Chem* , 1980 84 3336
- 26 J C Jernigan, R C Murray, *J Phys Chem* , 1987 91 2030
- 27 C E D Chidsey, R W Murray, *Science*,, 1986 231 25
- 28 N Oyama, T Ohsaka, T Ushirogouchi, S Sanpei, S Nakamura, *Bull Chem Soc Jpn* , 1988 61 3130
- 29 B Lindholm, *J Electroanal Chem* , 1988 250 341
- 30 S M Oh, L R Faulkner, *J Electroanal Chem* , 1989 269 77
- 31 S B Khoo, J K Foley, S Pons, *J Electroanal Chem* , 1980 102 265
- 32 G Inzelt, J Backsai, J Q Chambers, R W Day, *J Electroanal Chem* , 1988 242 265
- 33 G Inzelt, L Szabo, J Q Chambers, R W Day, *J Electroanal Chem* , 1987 219 49
- 34 G Inzelt, L Szabo, *Electrochim Acta*, 1986 31 1382
- 35 E F Bowden, M F Dautartas, J F Evans, *J Electroanal Chem* , 1987 219 49
- 36 M F Dautartas, E F Bowden, J F Evans, *J Electroanal Chem* , 1987 219 71
- 37 E F Bowden, M F Dautartas, J F Evans, *J Electroanal Chem* , 1987 219 91
- 38 W J Albery, M G Boutelle, P J Colby, A R Hillman, *J Electroanal Chem.*, 1982 133 135

- 39 T Ohsaka, N, Oyama, K Sato, H Matsuda, *J Electroanal Chem* , 1985 132 135
- 40 D A Buttry, F C Anson, *J Am Chem Soc* , 1983 105 685
- 41 N Oyama, T Ohsaka, H Yamamoto, M Kaneok, *J Phys Chem* , 1986 90 3850
- 42 H Diafuku, K Aoki, K Tokuda, H Matsuda, *J Electroanal Chem* , 1985 181 1
- 43 J F Facci, R H Schmehl, R W Murray, *J Am Chem Soc* , 1982 104 4959
- 44 S M Oh, L R Faulkner, *J Am Chem Soc* , 1989 111 5613
- 45 R J Forster, M E G Lyons, J G Vos, *J Chem Soc Faraday Trans* , 1991 87 3761
- 46 R J Forster, M E G Lyons, J G Vos, *J Chem Soc Faraday Trans* , 1991 87 3769
- 47 R J Forster, J G Vos, *Electrochimica Acta*, 1992 37 159
- 48 P Daum, J R Lenhard, D Rolinson, R W Murray, *J Am Chem Soc* , 1980 102 4649
- 49 M E G Lyons, H G Fay, J G Vos, A J Kelly, *J Electroanal Chem* , 1988 250 207
- 50 M Tomoi, Y Akada, H Kakiuchi, *Macromol Chem, Rapid Commun* , 1982 3 537
- 51 R J Forster, J G Vos, *Macromolecules*, 1990 23 4372
- 52 H Nishide, J Deguchi, E Tsuchida, *Bull Chem Soc Jpn* , 1976 49 3498
- 53 J Bassett, R C Denny, G H Jeffery, J Mendham, *Vogel's Textbook of Quantitative Inorganic Chemistry*, Edition 6, Longman, 1978, pp 741-742
- 54 J M Clear, J M Kelly, J G Vos, *Makromol Chem* , 1983 184 613
- 55 J M Clear, J M Kelly, C M O'Connell, J G Vos, *J Chem Res* , (M), 1981 3039
- 56 B P Sullivan, P J Salmon, T J Meyer, *Inorg Chem* , 1978 17 3334
- 57 D P Rillema, D S Jones, H A Levy, *J Chem Soc, Chem Commu* , 1979 849
- 58 F E Lytle, D M Hercules, *J Am Chem Soc* , 1969 91 253
- 59 D H Mohilner, *J Electroanal Chem* , 1966 1 241

- 60 K Aoki, K K Tokuda, H Matsuda, *J Electroanal Chem* , 1983 146 417
- 61 K Aoki, K Tokuda, H Matsuda, *J Electroanal Chem* , 1984 160 33
- 62 A R Hillman, in *Electrochemical Science and Technology of Polymers*, R G Linford, (Ed), Elsevier, Amsterdam, 1987 Ch 5
- 63 R Lange, K Dobifhofer, *J Electroanal Chem* , 1987 237 13
- 64 J M Saveant, *J Phys Chem* , 1988 92 4526
- 65 C P Andrieux, J M Saveant, *J Phys Chem* , 1988 92 6761
- 66 P G Pickup, W Kutner, C R Leidner, R W Murray, *J Am Chem Soc* , 1984 106 1991
- 67 D P Leech, Ph D Thesis, Dublin City University, 1991
- 68 M W Espenscheid, A R Ghatak-Roy, R B Moore(III), R M Penner, M N Szturmay, C R Martin, *J Chem Soc Faraday Trans 1*, 1986 82 1051
- 69 D D Montgomery, K Shigehara, E Tsuchida, F C Anson, *J Am Chem Soc* , 1984 106 7991
- 70 D D Montgomery, F C Anson, *J Am Chem Soc* , 1985 107 3431
- 71 M Sharpe, D D Montgomery, F C Anson, *J Electroanal Chem* , 1985 194 247
- 72 K Sumi, F C Anson, *J Phys Chem* , 1986 90 3845
- 73 R J Forster, J G Vos, *J Chem Soc , Faraday Trans* , 1991 87 3769
- 74 T Ohsaka, T Okajima, N Oyama, *J Electroanal Chem* , 1986 215 37
- 75 B G Ateya, L G Austin, *J Electrochem Soc* , 1973 120 1217
- 76 W J Albery, A R Hillman, *Ann Rep Prog Chem* , 1981 C 78 377
- 77 W J Albery, A R Hillman, *J Electroanal Chem* , 1984 170 27
- 78 C P Andrieux, J M Dumas-Bouchiat, F M'Halla, J M Saveant, *J Electroanal Chem* , 1980 113 19
- 79 C P Andrieux, J M Dumas-Bouchiat, J M Saveant, *J Electroanal Chem* , 1982 131 1

- 80 C P Andrieux, J M Dumas-Bouchiat, J M Saveant, *J Electroanal Chem* , 1984 169 9
- 81 C P Andrieux, J M Saveant, *J Electroanal Chem* , 1984 171 65
- 82 C P Andrieux, J M Saveant, *J Electroanal Chem* , 1982 142 1
- 83 C P Andrieux, J M Saveant, *J Electroanal Chem* , 1982 134 163
- 84 W J Albery, M G Boutelle, A R Hillman, *J Electroanal Chem* , 1985 182 99
- 85 R J Forster, J G Vos, *J Chem Soc , Faraday Trans* , 1991 87 1863
- 86 O Haas, H R Zumbrennen, *Helv Chim Acta* , 1981 64 854
- 87 R W Murray, A G Ewing, R A Durst, *Anal Chem* , 1987 59 379A
- 88 A R Guadalupe, H D Abruna, *Anal Chem* , 1985 57 142
- 89 L M Wier, A R Guadalupe, H D Abruna, *Anal Chem* , 1985 57 2011
- 90 A P Clarke, Ph D Thesis, Dublin City University, 1992
- 91 C P, Andrieux, J M Saveant, *J Electroanal Chem* , 1978 93 163

Chapter 6

Sensor Characterisation and Performance

6.1. Introduction

In the preceding chapters, the use of osmium- and ruthenium-containing redox polymers for the preparation of electrocatalytic surfaces for the detection of certain analytes has been described in detail. It was shown that the polymer, $[\text{Os}(\text{bipy})_2(\text{PVP})_{10}\text{Cl}]\text{Cl}$, is a powerful electrocatalyst for the reduction of the nitrosonium ion and that this reaction could be easily harnessed for the development of a novel detection system for nitrite. It was also shown that osmium- and ruthenium-containing redox polymer modified electrodes could, when positioned parallel in thin-layer flow cells, be used for the speciation analysis of the redox pair $\text{Fe}(\text{II})/\text{Fe}(\text{III})$. The potential for the detection of multiple redox pairs using this simple principle is clearly evident. The use of a ruthenium polymer modified electrode as an alternative detection system in the conventional analysis of nitrate was also demonstrated. This approach had a number of advantages such as low limit of detection and large linear range compared to existing spectrophotometric detection systems. These novel examples demonstrate the potential use of these devices for real analytical application. Many other unique and powerful examples of the utility of modified electrodes for sensor development have been described in the literature.¹⁻⁴ Given the unique advantages obtained with the use of these devices and the immense number of potential applications which have been developed, it is disconcerting that to date no chemically modified electrode has been commercialised for analytical purposes. The reason for this is probably a combination of many factors. Some of these factors are however inherent in the problems associated with the application of these devices in real analysis.

The many examples of modified electrodes for electroanalysis which have been described in the literature generally describe the construction of the devices and detection of the analyte of interest in batch type experiments or in flow analysis (HPLC, FIA). Generally, little regard has been given to the detailed performance characteristics of the sensors described.⁴ Parameters such as selectivity, interferences, sensitivity, matrix effects, robustness, reproducibility and response saturation have generally been ignored. It is problems associated with these parameters which, in part, limit the usefulness of modified electrodes for real analysis. In this chapter, the overall performance of the sensors developed in the course of this work from redox polymer modified electrodes will be

discussed. In particular, strategies for the control of sensor sensitivity, selectivity and interference are described. The consequences of possible matrix effects and response saturation will also be addressed. Finally a general discussion concerning the utility of these devices for real analytical application will be given.

6.2. Experimental

6.2.1 Procedures

6.2.1.1 Cyclic Voltammetry and Rotating Disc Electrode Voltammetry

CV and RDE voltammetry were carried out using a conventional three electrode assembly. The potentiostat used was the EG&G Princeton Applied Research Model 362. The rotating disc assembly was the Metrohm Model 629-10. Voltammograms were recorded on a Linseis X-Y recorder. The working electrodes were 3 mm diameter glassy carbon discs shrouded in Teflon (Metrohm). The counter electrode was 1 cm² platinum gauze placed parallel to the working electrode at distance of ≈ 1 cm. The reference electrode was the saturated KCl calomel electrode. All potentials are quoted with respect to the SCE without regard to liquid junction potentials. Slow sweep rate cyclic voltammetry was carried out to ascertain the polymer surface coverage. All measurements, unless otherwise stated, were carried out at room temperature.

The glassy carbon electrodes were prepared for modification by polishing with 5 μm alumina as an aqueous slurry on a felt cloth. The electrodes were rinsed thoroughly with distilled water and methanol. The electrodes were then treated with chlorosulphonic acid to promote the formation of surface oxide functional groups. The electrodes were again rinsed with distilled water and dried *in vacuo* at room temperature.

6 2 1 2 Flow Injection Apparatus

The flow injection apparatus consisted of a Gilson Miniplus 3 peristaltic pump, a six port Rheodyne injector valve fitted with a 20 μL fixed volume sample loop, an EG&G Princeton Applied Research Model 400 electrochemical detector connected with Teflon HPLC tubing, and a Philips X-t chart recorder. In the flow-cell, an Ag/AgCl electrode acted as the reference electrode. The stainless steel cell body acted as the counter electrode. The working electrodes were also 3 mm diameter glassy carbon shrouded in a Teflon block. Modified electrodes were prepared as described above. All potentials are quoted after numerical conversion to the SCE scale. Sample injections were made using a 2 cm^3 glass syringe fitted with a Rheodyne injection needle. The carrier electrolyte used was 0.1 mol dm^{-3} Na_2SO_4 at a flow rate of 1.0 $\text{cm}^3 \text{min}^{-1}$.

6 2 2 Materials and Reagents

The redox polymers $[\text{Os}(\text{bipy})_2(\text{PVP})_{10}\text{Cl}]\text{Cl}$ and $[\text{Ru}(\text{bipy})_2(\text{PVP})_{10}]\text{Cl}$ were synthesised as described in chapters 2 and 3. Ascorbic acid solutions were prepared in 0.1 mol dm^{-3} Na_2SO_4 at pH 4.5. Where the pH was varied, this was achieved by the preparation of a standard 0.05 mol dm^{-3} solution of H_2SO_4 containing and making the appropriate dilutions with distilled water. The Na_2SO_4 concentration was maintained at 0.1 mol dm^{-3} at all pH values. Nitrite, Fe(II) and Fe(III) solutions were prepared as described in chapters 2 and 3.

6.3. Results and Discussion

6 3 1 Sensor Sensitivity Control

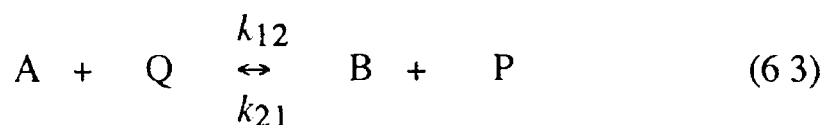
The sensitivity (response per unit concentration) of any sensor is important for a number of reasons. Firstly, high sensitivity results in larger analytical signals and therefore is conducive for lower limits of detection and secondly, highly sensitive detection systems can easily discriminate between samples of similar analyte concentration. There are a number of

approaches which may be utilised in order to increase the sensitivity of redox polymer modified electrodes. The current response from the sensors for a surface reaction (S_k'') is given by the following equation 5-10

$$i = n F A k'' b_o y_{\infty} \quad (6.1)$$

where k'' is the second order rate constant for the cross-exchange reaction, b_o is the concentration of electro-active sites within the polymer film and y_{∞} is the bulk concentration of the substrate. The other symbols have their usual meaning. For a through film reaction (L_k) the additional terms L (polymer film thickness) and K (substrate partition coefficient) are included in this equation (k instead of k''). It is clear from this equation that increasing b_o will increase sensitivity for the S_k'' and L_k mechanisms. This is evident in the dependence of k'_{ME} on b_o for the reactions studied in earlier chapters. Increasing L and K will have a similar effect on sensitivity for through film reactions. However, b_o and L are normally limited by charge and mass transport considerations which are usually a function of the polymer structure and are normally optimised with respect to charge transport (D_{ct}). Ultimately, D_{ct} is the most important parameter to optimise as cathodic or anodic current must be delivered efficiently to ensure that response saturation is not occurring. It was seen that charge transport through the polymer, $[\text{Os}(\text{bipy})_2(\text{PS})_{7.5}(\text{DMAP})_{2.5}\text{Cl}]\text{Cl}$, was sufficiently slow to result in response saturation at $1.0 \times 10^{-3} \text{ mol dm}^{-3}$ Fe(III). A less obvious means of controlling sensor sensitivity is by controlling the rate constant for the cross-exchange reaction, k'' (k) in Alberys notation and k_{12} in Marcusian terms. Any cross-exchange reaction may be considered according to the general reaction scheme 11





Where P/Q is the redox couple of the electrocatalysts and A/B is the substrate redox couple. The equilibrium constant for the cross-exchange reaction is given by

$$K_{12} = k_{12} / k_{21} \quad (6.5)$$

The equilibrium constant is related to standard electrode potentials of the substrate and the mediator catalyst by the relation

$$(RT/F) \ln K_{12} = \pm (E^\circ_{A/B} - E^\circ_{P/Q}) \quad (6.6)$$

Where E° is the formal potentials of the respective redox couples and the + and - sign corresponds to the reduction or oxidation of the substrate respectively. The apparent free energy relationship between the formal potentials of the substrate and electrocatalyst can be examined by the Marcusian relation for outer-sphere electron transfer (neglecting work terms) with the equation ¹²

$$k_{12} = (k_{11} k_{22} K_{12} f)^{1/2} \quad (6.7)$$

Where f is given by,

$$\log f = (\log K_{12})^2 / [4 \log(k_{11} k_{22} / Z^2)] \quad (6.8)$$

Where Z is the bi-molecular collision frequency for two reactants in homogeneous solution. It is obvious from these equations that a logarithmic relationship exists between the rate constant for the cross-exchange reaction and the electrochemical driving force.

In order to investigate the possibility of such a relationship existing for the redox polymer modified electrodes studied here, the rate constants (k'' or k_{12}) for a number of substrates reacting at several polymer modified electrodes were examined. Only surface reactions were considered in order to avoid complications of variations in substrate partition coefficients, K , and diffusion rates within the polymer, D_y . The previously reported reactions which were examined are, the reduction of Fe(III) at a $[\text{Os}(\text{bipy})_2(\text{PVP})_{10}\text{Cl}]\text{Cl}$ modified electrode (k'' taken from Forster *et al.*¹³) and the reduction of Fe(III) at a polythionine modified electrode (k'' taken from Alberly *et al.*¹⁴). The rate constants for the oxidation of Fe(II) at $[\text{Ru}(\text{bipy})_2(\text{PVP})_{10}\text{Cl}]\text{Cl}$ in perchloric acid electrolyte (S_k'') and the oxidation of ascorbic acid (S_k'') at $[\text{Os}(\text{bipy})_2(\text{PVP})_{10}\text{Cl}]\text{Cl}$ were found experimentally (*vide infra*). A plot of $\log k''$ vs ΔE is shown in Fig. 6.1. It can be seen that the rate constants for the cross-exchange reactions increase logarithmically with increasing electrochemical driving force as predicted by the Marcusian relationship above. The general trend is not unexpected, as Leidner and Murray^{15,16} studied the rates of "up hill" electron transfer reaction of a series of metal complexes at an osmium modified electrode with varying formal potentials and found that the rates of the cross-exchange reactions agreed quantitatively with the Marcusian relation. The purpose of modifying electrodes with electrocatalysts is to accelerate electrode reactions, but from these results it can be concluded that the exact level of acceleration can be precisely manipulated by carefully controlling the ΔE between the electrocatalyst and substrate. The $E_{1/2}$ of the electrocatalytic centres used in this study can be easily controlled by manipulation of the coordination sphere of the metal centre. This has previously been demonstrated elegantly by the *in situ* photo-substitution of the labile chloride ligand of ruthenium redox polymers.¹⁷ The manipulation of the $E_{1/2}$ of organic redox polymers is, however, synthetically more difficult and the level of control is

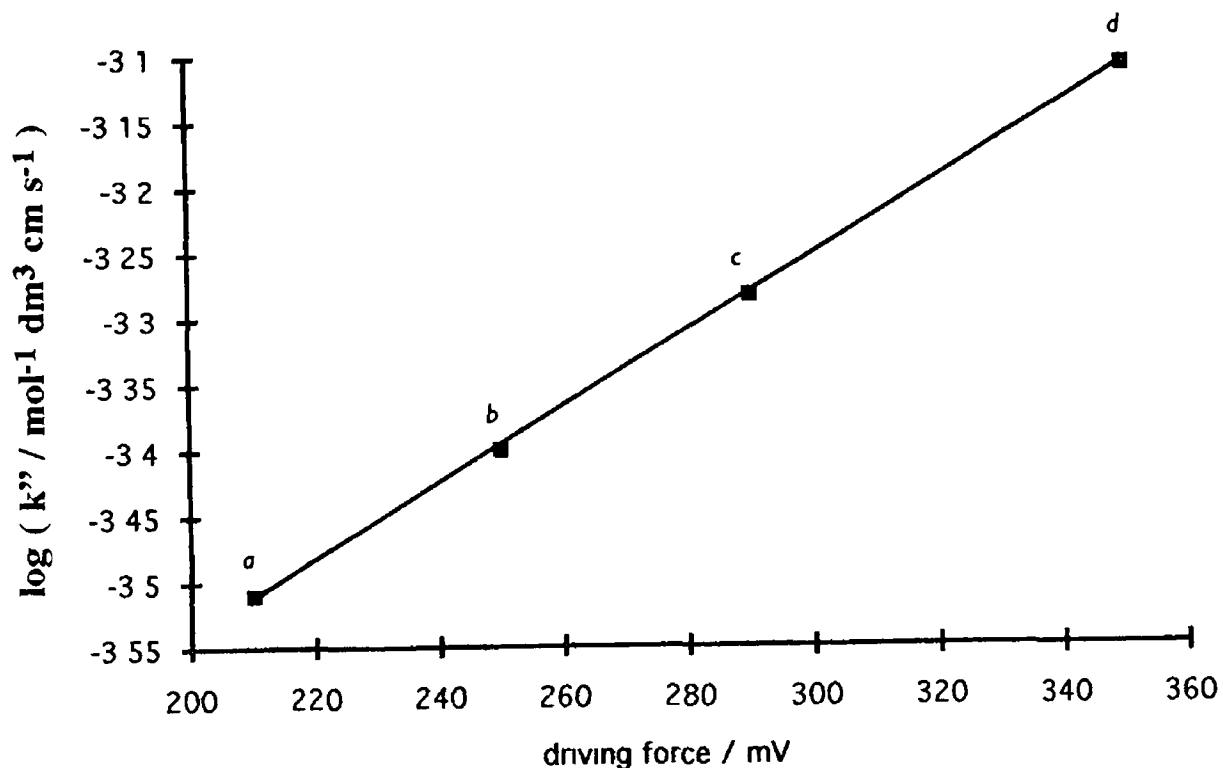


Fig. 6 1 Plot of $\log k''$ vs electrochemical driving force Point a is the reduction of Fe(III) at $[\text{Os}(\text{bipy})_2(\text{PVP})_{10}\text{Cl}]\text{Cl}$, point b is the reduction of the same substrate at thionine modified electrodes, point c is the oxidation of Fe(II) at a $[\text{Ru}(\text{bipy})_2(\text{PVP})_{10}\text{Cl}]\text{Cl}$ modified electrode while point d corresponds to the oxidation of ascorbic acid at the osmium redox polymer All rate constants are for surface reactions

uncertain ¹⁸ The good linearity of the results is surprising and noteworthy for a number of reasons. Firstly, the second point on the graph relates to the reduction of Fe(III) at an organic redox polymer (polythionine ¹⁴) while the rest of the data points correspond to reaction at metallo-polymers. Secondly, the final point on the graph ($\Delta E = 350$ mV) corresponds to the oxidation of the organic substrate, ascorbic acid, which proceeds by an EC mechanism (*vide infra*) ¹⁹ The fact that the experimental data, for the organo-metallic and organic mediators, and metallic and organic substrates fall on a common line is indicative of the general nature of the cross-exchange reactions. That is, the energy barrier for the cross-exchange reaction is a function of ΔE and not on the nature, size or charge on the reactants or any chemical interaction with the electrocatalyst ^{15,16} The results also indicate no difference in the rate of oxidation or reduction with respect to ΔE . This relationship may also be useful in predicting the second order rate constant for reactants with known formal potentials.

In theory, increasing the rate of the cross-exchange reaction should result in a corresponding change in electrode sensitivity. This can be seen in Fig. 6.2 where the log of the theoretical sensitivity (calculated from equation 6.1) vs. ΔE is plotted. The sensitivities are normalised with respect to b_0 and n . It can be seen that increasing ΔE results in the corresponding increase in sensor sensitivity. The ratio of the theoretical sensitivities for Fe(II) oxidation at $[\text{Ru}(\text{bipy})_2(\text{PVP})_{10}\text{Cl}]\text{Cl}$ and Fe(III) reduction at $[\text{Os}(\text{bipy})_2(\text{PVP})_{10}\text{Cl}]\text{Cl}$ is 1.7 while the experimentally (FIA) found ratio is 2.1. Considering that the FIA response is not at steady-state, this close agreement indicates that the values obtained can be used to predict the sensitivity of modified electrodes in thin-layer flow-cells. It should be noted that increasing the free energy difference beyond the point where the currents become diffusionally controlled or fall into the Marcusian “inverted region” is futile from the sensor point of view, as no further increase in electrode current will result and the likelihood of increasing the number of interference is real ^{15,20,21}

In addition to the manipulation of the $E_{1/2}$ of electrocatalyst, formation of complexes which result in an increase in the free energy difference between the redox catalyst and the substrate can increase electrode sensitivity e.g. the 2,2'-bipyridyl complexes of Fe(II) and the thiocyanate complexes of Fe(III). This can be seen in Fig. 6.3. The steady-

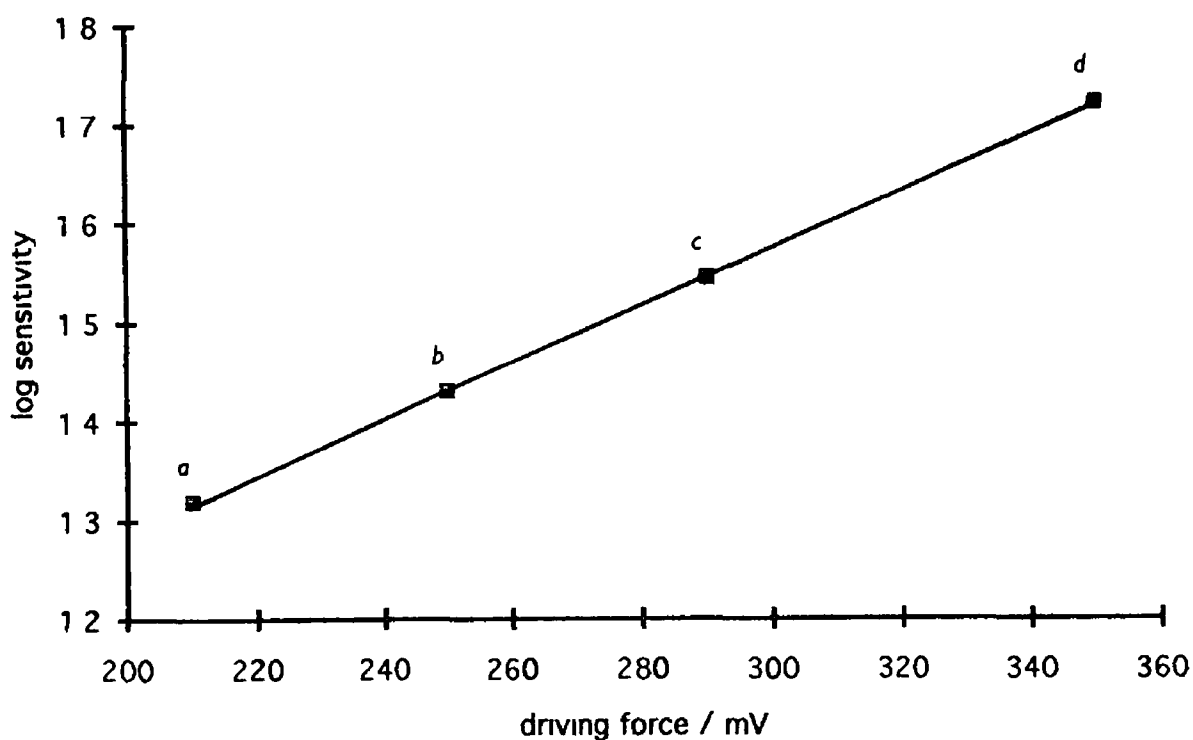


Fig 6 2: Plot of log electrode sensitivity vs electrochemical driving force. Point a is the reduction of Fe(III) at $[\text{Os}(\text{bipy})_2(\text{PVP})_{10}\text{Cl}]\text{Cl}$, point b is the reduction of the same substrate at thionine modified electrodes, point c is the oxidation of Fe(II) at a $[\text{Ru}(\text{bipy})_2(\text{PVP})_{10}\text{Cl}]\text{Cl}$ modified electrode while point d corresponds to the oxidation of ascorbic acid at the osmium redox polymer. All rate constants are for surface reactions.

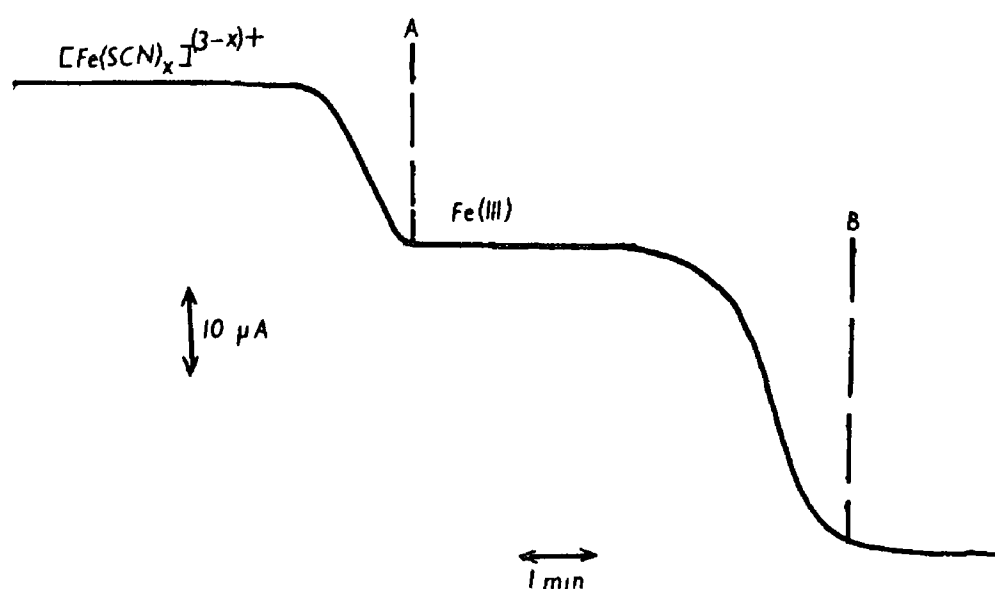


Fig 6.3 The response of an $[Os(bipy)_2(PVP)_{10}Cl]Cl$ modified electrode to $1.0 \times 10^{-3} \text{ mol dm}^{-3} Fe(III)$ and to the same solution following addition of excess SCN^- . Point B represents the addition of the $Fe(III)$ to the electrolyte and point A represents the subsequent addition of SCN^- . The electrode rotation speed was 1000 rpm and the applied potential was 0.120 V vs SCE. The electrolyte was $0.05 \text{ mol dm}^{-3} H_2SO_4$.

state response to $1.0 \times 10^{-3} \text{ mol dm}^{-3}$ Fe(III) reduction at a [Os(bipy)₂(PVP)₁₀Cl]Cl modified electrode is 42.0 μA . Addition of excess SCN⁻ results in the rapid formation of $[\text{Fe}(\text{SCN})_x]^{(3-x)+}$ (where $x = 1, 2$ or 3) and a rapid increase in electrode response to 60.0 μA which corresponds to a 50 % increase in electrode response. A second effect, increase in K due to the reduction in the overall charge of the substrate may also be evident in this example. However, the experiment was carried out with a mono-layer surface coverage ($\approx 1 \times 10^{-10} \text{ mol cm}^{-2}$) to try to eliminate this effect.

6.3.2 Interference / Selectivity Control of Sensors

Traditionally, the greatest limitations of electroanalytical techniques was the lack of selectivity of electrochemical procedures and the severe surface fouling of conventional electrode surfaces.²² Conventional methods of controlling electrode selectivity and prevention of surface fouling have been reviewed recently.²³ These generally are reliant on the masking of interferents, in-line separations, pulsed and sampled current techniques or mathematical deconvolution of mixed signals. These problems have also resulted in the introduction of chemically modified electrode surfaces for selective detection.²² Redox polymer modified electrodes can increase sensor selectivity as acceleration of the electrode reaction of interest allows detection at lower operational potentials resulting in an exponential decrease in potential interference.²⁴ In addition, only simple outer-sphere electron transfer reactions are feasible at the modified electrodes studied in this thesis. This prevents reactions requiring involved inner-sphere electron transfer for reaction. So modification with the redox polymers results in an inherent improvement in selectivity. It is possible, however, that co-existing electro-active species may interfere with the response for the analyte of interest. A typical example of this is the presence of Fe(III) and Cu(II) in samples for the determination of nitrite by electrocatalytic reduction with [Os(bipy)₂(PVP)₁₀Cl]Cl. The formal potential for the Fe(II)/Fe(III) redox couple is 0.46 V vs SCE²⁵, therefore, the reduction of Fe(III) can be mediated by the osmium centres within the polymer film which have an $E_{1/2} = 0.25 \text{ V vs SCE}$. The formal potential of Cu(II)/Cu(I) redox couple is 0.275 V vs SCE²⁶, therefore, the electrocatalytic reduction of Cu(II) is

also possible, although the thermodynamic driving force is small (0.025 V). The effect of these interferents can be easily eliminated by manipulation of the thermodynamics of the system. Formation of the ethylenediamine-tetraacetic acid (EDTA) complexes of these metal ions results in a shift in formal potential to a region negative of the formal potential of the electrocatalyst and therefore are thermodynamically excluded from reaction. The $[\text{Fe}(\text{EDTA})]^+$ formal potential being -0.13 V vs. SCE and for $[\text{Cu}(\text{EDTA})]$ the formal potential is -0.46 V vs. SCE.²⁶ This effect can be seen in Fig. 6.4 for Fe(III). It can be seen from this diagram that simple formation of $[\text{Fe}(\text{EDTA})]^+$ eliminates interference. A large body of information concerning the electrochemical behaviour of metal complexes exists, and this information may be useful in providing simple means of overcoming selectivity problems with co-existing electro-active species.

Another common interferent in the determination of nitrite using the standard spectrophotometric methods is ascorbic acid.²⁷⁻²⁸ Ascorbic acid is known to interfere with the diazotisation step for the colorimetric reaction. This species is ubiquitous in biological samples such as saliva, processed meats and fruit juice and exists at concentrations significantly greater than nitrite, and poses considerable difficulty in determining nitrite in biological matrices. The applied potential for the detection of nitrite by reduction at an $[\text{Os}(\text{bipy})_2(\text{PVP})_{10}\text{Cl}]\text{Cl}$ electrode is 0.120 V vs. SCE. The formal potential of ascorbic acid (at pH 7.0) is -0.190 V vs. SCE,²⁹ therefore the oxidation of this compound is thermodynamically favourable at the osmium polymer modified electrode. Ascorbic acid was however found not to interfere in the detection of nitrite. This is evident from the traces seen in Fig. 6.5. The presence of ascorbic acid in ten fold excess compared to nitrite does not affect the response of the modified electrode in the FIA system to nitrite. The reason for the absence of interference from ascorbic acid oxidation, although thermodynamically favourable can be explained. In order to appreciate this explanation in full, the transport and kinetics of ascorbic acid oxidation at $[\text{Os}(\text{bipy})_2(\text{PVP})_{10}\text{Cl}]\text{Cl}$ will be described.

It has been established that the oxidation of ascorbic acid proceeds *via* two consecutive one-electron processes involving the participation of a radical anion intermediate resulting in the formation of dehydroascorbic acid.³⁰ This species finally undergoes a hydration reaction characteristic of carbonyl groups to form an electro-inactive product. The overall

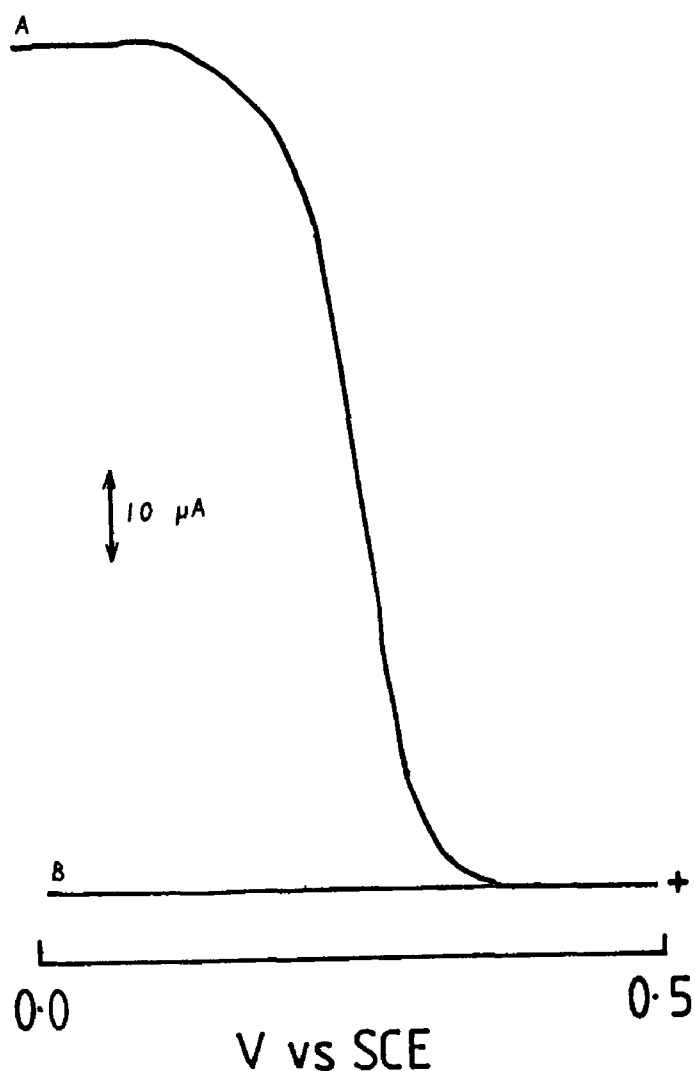


Fig 6 4 Current-potential curves showing the effect of EDTA on the electrocatalytic reduction of Fe(III) at the osmium redox polymer modified electrode. Curve A represents the reduction of free Fe(III) at the redox polymer while curve B shows the current potential curve of the same Fe(III) solution in the presence of excess EDTA. The potential sweep rate was 5.0 mV s^{-1} , the electrode rotation speed was 1000 rpm and the electrolyte was $0.05 \text{ mol dm}^{-3} \text{ H}_2\text{SO}_4$.

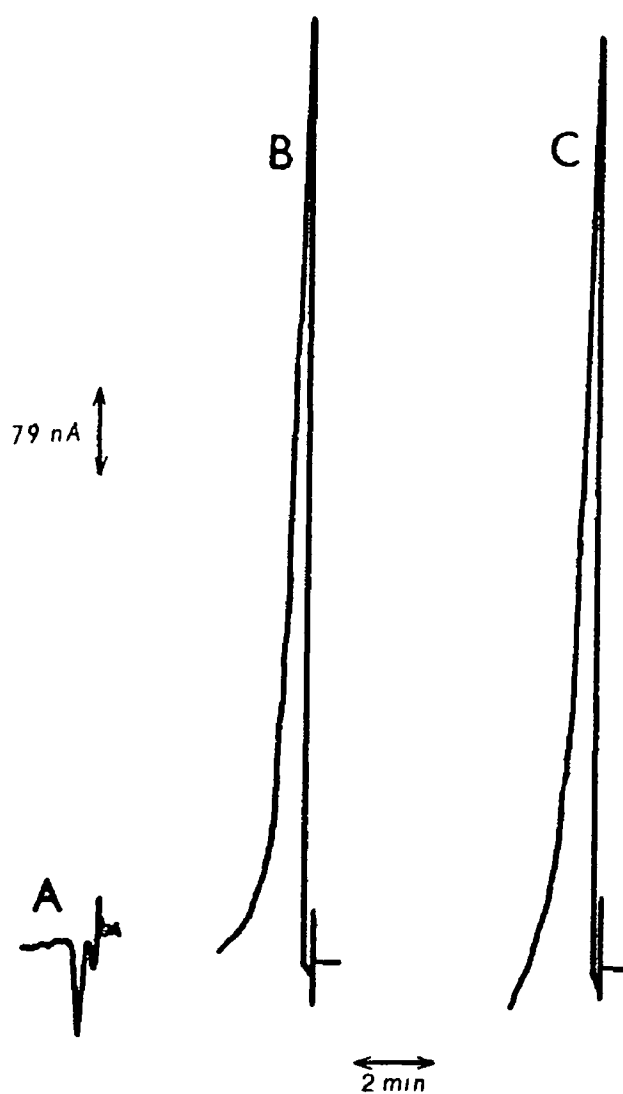


Fig 6 5 The effect of ascorbic acid on the $[\text{Os}(\text{bipy})_2(\text{PVP})_{10}\text{Cl}]\text{Cl}$ modified electrode response to nitrite, (A) $500\ \mu\text{g cm}^{-3}$ ascorbic acid, (B) $50\ \mu\text{g cm}^{-3}\ \text{NO}_2^-$ and (C) $500\ \mu\text{g cm}^{-3}$ ascorbic acid plus $50\ \mu\text{g cm}^{-3}\ \text{NO}_2^-$. The electrolyte was $0.1\ \text{mol dm}^{-3}\ \text{H}_2\text{SO}_4$ at a flow rate of $0.2\ \text{cm}^3\ \text{min}^{-1}$.

reaction process can be classified as an EC process.¹⁹ The fundamental electrode kinetics of this reaction have been studied extensively at conventional electrodes such as Hg³¹, Au³², Pt³⁴ and glassy carbon³⁵. The electrocatalytic oxidation of ascorbic acid at modified electrodes has also been described. The outer-sphere homogeneous oxidation of ascorbic acid by a series of iron(III)-phenanthroline complexes has been studied in detail by Pelizzetti.³⁶ The reaction rate was found to be first order with respect to ascorbic and to the metal complexes. Anson *et al.*³⁷ studied the oxidation at Nafion coated electrodes with [Os(bipy)₃] incorporated electrostatically. Both these studies indicated that the electrocatalytic reaction proceeds *via* the radical anion intermediate and that the rate of the cross-exchange reaction is very facile.

The formal potential (E^0) of the ascorbic acid oxidation is 0.058 V vs SHE at pH 7.0 and 0.140 V vs SHE at pH 5.0.³⁸ As the E^0 for the oxidation reaction is negative of the formal potential of the Os(II)/Os(III) couple, the mediation of the oxidation reaction by the osmium redox polymer is thermodynamically possible. In this study, the reaction order with respect to ascorbic acid and proton concentration was examined in 0.1 mol dm⁻³ Na₂SO₄ at pH = 4.5. The reaction order for ascorbic acid and proton concentration was found to be unity for both reactants (slope = 1.0 ± 0.05 and 0.95 ± 0.05 respectively). These results indicate that the oxidation reaction at [Os(bipy)₂(PVP)₁₀Cl]Cl modified electrode proceeds *via* the two electron process as observed for other modified electrodes.³⁷ In Fig. 6.6 Levich plots for the ascorbic acid oxidation at three modified electrodes with various surface coverages at pH 4.5 can be seen. These plots are linear and all pass through the origin. These observations suggest that the reaction flux is equivalent to the Levich flux, i.e. mass transport controls electrode currents and the reaction occurs at the surface of the polymer. Similar surface behaviour has been observed for ascorbic acid oxidation at Nafion coated electrodes.³⁷ The corresponding Koutecky-Levich plots are shown in Fig. 6.7. Using the diagnostic scheme of Alberly and Hillman, the exact kinetic regime can be elucidated. The Koutecky-Levich plots are linear and the limiting currents are dependent on the rotation speed of the electrode. This allows the elimination of the S_{te} , LS_{te} and LE_k kinetic cases. The Levich slope for the modified electrode was found to be $7.4 \pm 0.2 \times 10^{-4}$ cm s^{-1/2}, while at the bare glassy carbon the slope was $6.2 \pm 0.3 \times 10^{-4}$ cm s^{-1/2}. The slightly smaller slope may be a result of sluggish kinetics at the carbon electrode. These

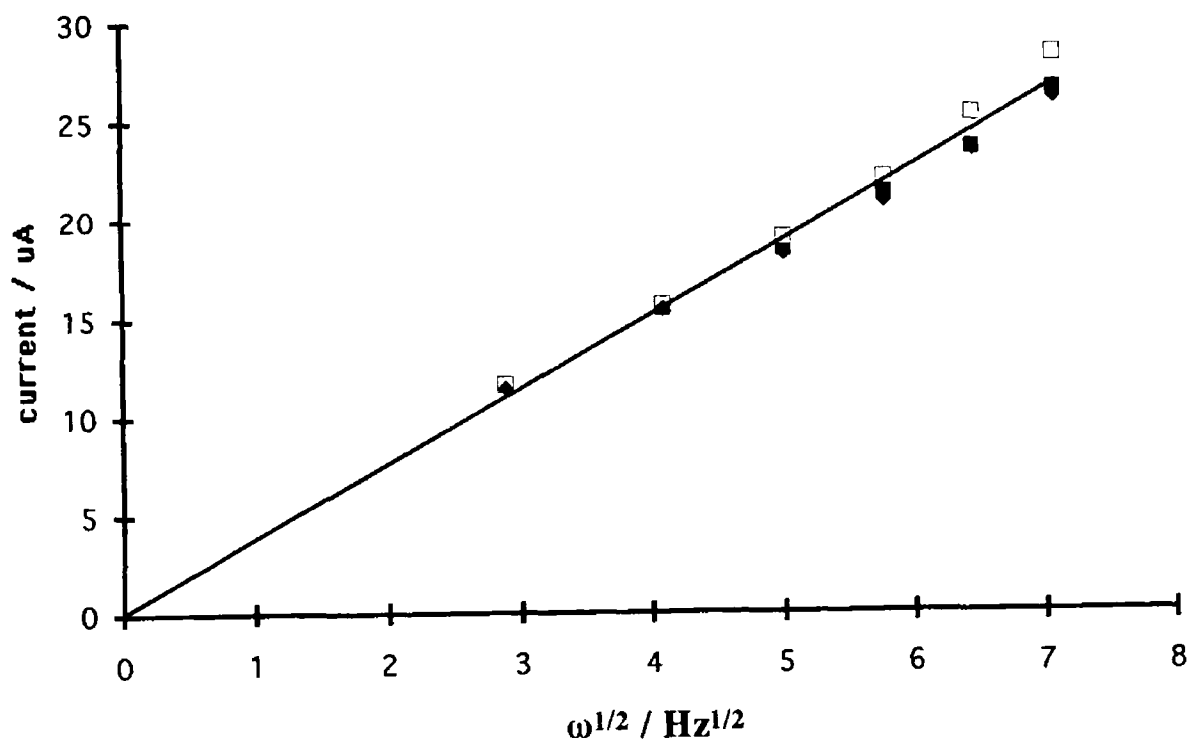


Fig 6 6 Levich plots for the oxidation of $4.0 \times 10^{-4} \text{ mol dm}^{-3}$ ascorbic acid at $[\text{Os}(\text{bipy})_2(\text{PVP})_{10}\text{Cl}]\text{Cl}$ modified electrodes. The points \blacklozenge , \square and \blacksquare represents polymer surface coverages of 3.3×10^{-10} , 5.5×10^{-10} and $2.8 \times 10^{-9} \text{ mol cm}^{-2}$. The electrolyte was $0.1 \text{ mol dm}^{-3} \text{ Na}_2\text{SO}_4$ at pH 4.5. The potential sweep rate was 5 mV s^{-1} .

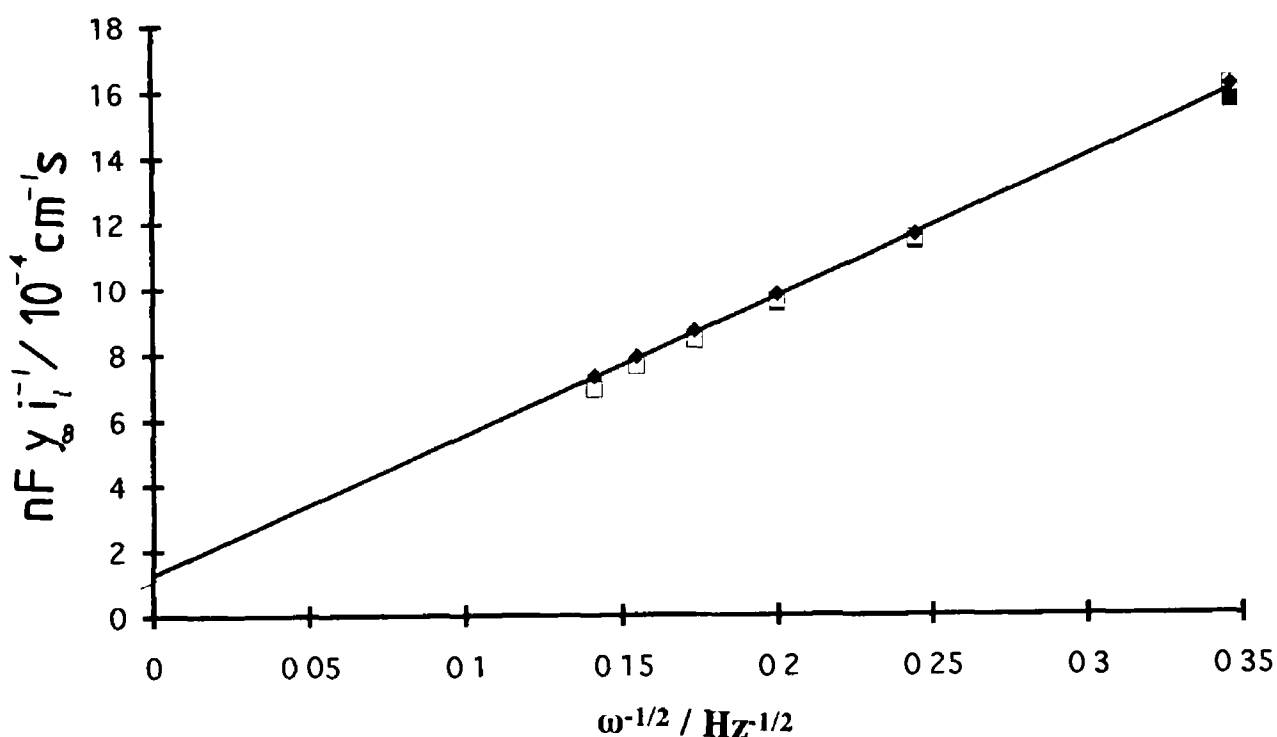


Fig 6 7 Koutecky-Levich plots for the oxidation of $2.0 \times 10^{-4} \text{ mol dm}^{-3}$ ascorbic acid at $[\text{Os}(\text{bipy})_2(\text{PVP})_{10}\text{Cl}]\text{Cl}$ modified electrodes. The points \blacklozenge , \square and \blacksquare represents polymer surface coverages of 3.3×10^{-10} , 5.5×10^{-10} and $2.8 \times 10^{-9} \text{ mol cm}^{-2}$ respectively. The electrolyte was $0.1 \text{ mol dm}^{-3} \text{ Na}_2\text{SO}_4$ at pH 4.5. The potential sweep rate was 5 mV s^{-1} .

values are however, within experimental error the same, therefore the LRZ_{tety} case can be eliminated. The reaction order with respect to L and b_o was found to be zero for L and unity for b_o , slopes of 0.0 ± 0.05 and 0.95 ± 0.05 respectively. This indicates that the kinetic regime is S_k . This is expected from the linearity and zero intercept of the Levich plots. The second order rate constant k'' can now be estimated from the modified electrode rate constant, k'_{ME} by the relation³⁷

$$k'_{ME} = n k'' b_o \quad (6.9)$$

Where $n = 2$. The value of k'_{ME} was found to be $1.10 \pm 0.05 \times 10^{-4} \text{ cm s}^{-1}$. This yields a value for k'' of $7.8 \pm 0.4 \times 10^{-4} \text{ dm}^3 \text{ mol}^{-1} \text{ cm s}^{-1}$. The cross-exchange reaction therefore occurs between solution phase substrate and osmium redox sites at the surface of the polymer. Ascorbic acid does not permeate the polymer film under these conditions.

According to the theory of Saveant³⁹ and Laviron⁴⁰, the rate constant for the self-exchange reaction between the osmium sites within the polymer film can be calculated from the following equation

$$D_e = 1/6 \delta^2 b_o k_{ex} \quad (6.10)$$

Where δ is the inter-site distance, $\approx 0.2 \text{ nm}$, and D_e is the electron diffusion coefficient (assumed equal to $D_{ct}(CV) \approx 1 \times 10^{-10} \text{ cm}^2 \text{ s}^{-1}$). This gives a value of $\approx 4.85 \times 10^4 \text{ dm}^3 \text{ mol}^{-1} \text{ s}^{-1}$ for k_{ex} . As D_{ct} values measured by transient techniques tend to under estimate the true current carrying capacity of redox polymers, this estimate for k_{ex} is likely to be conservative.

The processes which may occur at the $[\text{Os}(\text{bipy})_2(\text{PVP})_{10}\text{Cl}]\text{Cl}$ modified electrode in the presence of nitrite (as NO^+) and ascorbic acid (H_2AA) are schematically represented in Fig. 6.8. NO^+ partitions into the polymer film with $K \approx 1$ where upon the following cross-exchange reaction occurs

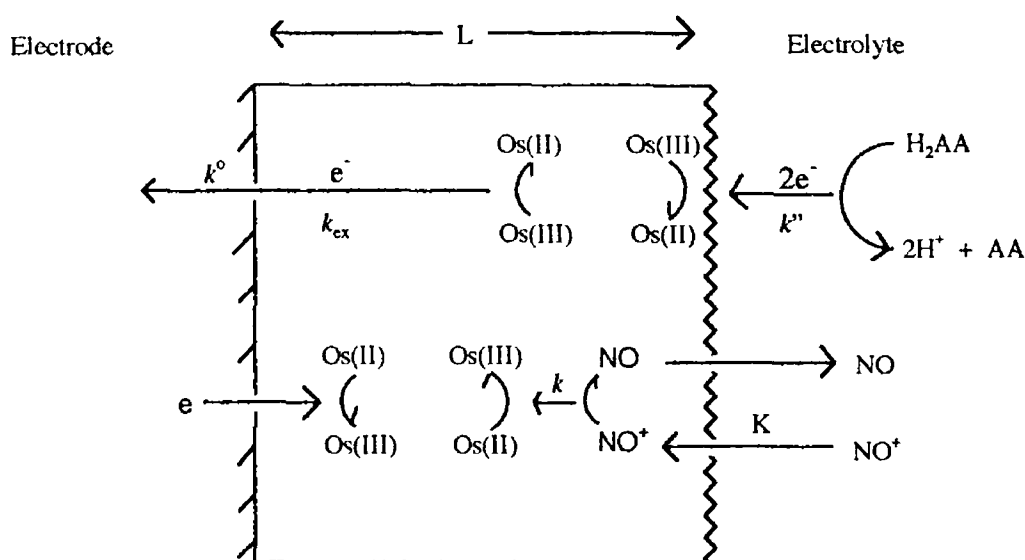
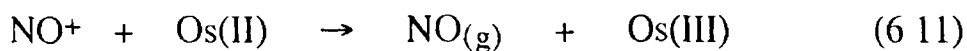
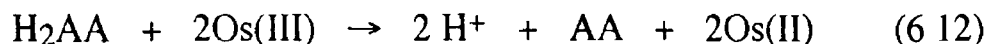


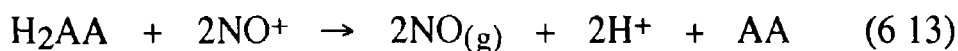
Fig 6 8 Schematic representation of the mediated reactions occurring at the $[\text{Os}(\text{bipy})_2(\text{PVP})_{10}\text{Cl}]\text{Cl}$ modified in the presence of ascorbic acid (H_2AA) and nitrite (as NO^+). The symbols have the following meaning, K = partition coefficient, k , k' are the second order rate constants for the layer reaction and surface reaction respectively, k_{ex} and k^o are the self-exchange and heterogeneous electron transfer rate constants



Thermodynamically, oxidation of Os(II) by H₂AA can not occur. However, the Os(III) sites generated by reaction 6.11 can theoretically participate in following reaction



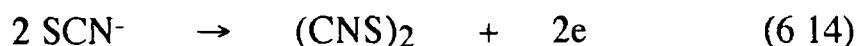
If reaction 6.12 proceeds then the overall reaction can be given by



The net effect of this would be electron flow from the ascorbic acid to the nitrosonium ion and a suppression in the cathodic electrode current. This is not observed for a number of reasons. Firstly, the ascorbic acid does not penetrate the polymer film ($K = 0$) therefore only a mono-layer of osmium sites may come into close enough proximity to participate in reaction 6.12. Secondly, the rate of self-exchange between the Os(II) and Os(III) sites ($\approx 4.85 \times 10^4 \text{ dm}^3 \text{ mol}^{-1} \text{ s}^{-1}$) is significantly faster than the cross-exchange reaction between the Os(III) and ascorbic acid ($7.8 \times 10^{-4} \text{ dm}^3 \text{ mol}^{-1} \text{ cm s}^{-1}$). And finally, since the nitrite reaction is carried out at pH 1.0, as the reaction order for H₂AA oxidation is -1 for [H⁺], and as the reaction is unfavourable under these conditions. The overall effect of the possible mediated electron transfer from H₂AA to NO⁺ would therefore be negligible. Also no direct reduction of NO⁺ by H₂AA is evident over the time-scale of the measurements made. From this, the redox polymer can be seen to act as an “electron valve” at the electrode surface allowing unidirectional current flow.

Another biologically important anion which causes considerable interference in the detection of nitrite by electrochemical methods is

thiocyanate, SCN^- ²⁷ The oxidation of this anion results in the formation of $(\text{CNS})_2$ according to the following reaction ²⁶



The product of the oxidation reaction adsorbs onto the electrode surface and results in rapid electrode passivation. This is evident from the following observations. The alternating injection of $1.0 \times 10^{-3} \text{ mol dm}^{-3}$ NO_2^- and $1.0 \times 10^{-4} \text{ mol dm}^{-3}$ SCN^- solutions results in a 15 % decrease in response to nitrite over a 12 alternating injection sequence at the bare glassy carbon electrode, while no significant change in response to nitrite at the $[\text{Ru}(\text{bipy})_2(\text{PVP})_{10}\text{Cl}]\text{Cl}$ modified electrode (RSD = 0.87 %) was evident. This behaviour may be attributed to the lack of adsorptive properties of the polymer films and also to the catalytic nature of the reaction which ensures that any SCN^- permeating the film to the underlying surface does not react there. It should be noted that the ruthenium polymer mediates the oxidation of thiocyanate, therefore SCN^- interferes electrochemically with the determination of nitrite oxidatively. However, reduction of nitrite at low potentials using the osmium redox polymer eliminates this electrochemical interference in addition to eliminating the passivation effect. The lack of adsorptive properties of the redox polymers is also responsible for the absence of surface fouling found for the direct oxidation and reduction of nitrite at carbon electrodes ⁴¹. This, and the absence of passivation due to protein, have been discussed in chapter 2.

In the speciation analysis of Fe(II) and Fe(III), Cu(II) was found to interfere with the detection of Fe(III). Presumably this is a result of the reduction of Cu(II). The coordination chemistry of Fe(III) and Cu(II) are similar, therefore the use of complexing reagents to discriminate between these complexes is difficult. This is further complicated by the fact that Cu(II) complexes are relatively un-stable at the low pH's required for the speciation analysis. A certain degree of selectivity can however be obtained by increasing the polymer layer thickness. The exact kinetic and transport processes have not been evaluated for Cu(II) reduction at $[\text{Os}(\text{bipy})_2(\text{PVP})_{10}\text{Cl}]\text{Cl}$, however, increasing the surface coverage of the

Surface Coverage/ mol cm ⁻²	Fe(III) <i>i</i> _p / μA	Cu(II) <i>i</i> _p / μA	Ratio of Responses
1.0 × 10 ⁻¹⁰	37.6	10.0	3.9
1.0 × 10 ⁻⁹	43.2	9.2	4.7
1.0 × 10 ⁻⁸	52.3	8.9	5.9

Table 6.1 The effect of surface coverage on Fe(III) sensor response to Fe(III) and Cu(II). The concentrations were 1.0 × 10⁻³ mol dm⁻³ for both species. The electrolyte was 0.1 mol dm⁻³ H₂SO₄ at a flow rate of 1.0 cm³ min⁻¹.

polymer results in a decrease in the response due to Cu(II) and increases the response due to Fe(III). This effect is seen in Table 6.1. From these results it appears that the Cu(II) reduction occurs in a small portion of the polymer film or possibly at the surface of the polymer. Increased selectivity is achieved by increasing the number of catalytic sites available for reaction with the analyte.

6.3.3 Background, LOD and Linear Ranges

The background current (neglecting electronic noise and environment fluctuations) at electrodes can be attributed to a number of sources.⁴² Firstly, non-faradaic charging currents (capacitance) are evident in voltammetric techniques where the electrode potential is changing with respect to time. As the sensors used here operate at constant applied potential, this allows the capacitance current to decay to zero during measurement. Charging currents therefore generally do not present a problem for these sensors. However, injection of samples into the FIA carrier stream with matrix composition grossly different from the composition of the carrier, *i.e.* widely different pH or ionic strength, may present difficulty. The structure of the electrode double layer at the electrode surface at constant potential is a function of the applied potential and the composition of the electrolyte. Sample plugs with differing composition therefore results in a transient response due to the perturbation of the double layer. This process has been detailed recently for glassy carbon electrodes in flow cells.⁴³ We have observed that the transient charging current under the usual experimental conditions is about 2.5 times less than that for the bare glassy carbon electrode under identical conditions. So modification of the electrodes decreases sensitivity to small changes in the double layer structure.

This type behaviour has been observed for the detection of nitrite described in chapter 2 because the sample plug is about pH 7 while the carrier is pH 1.0. This presents difficulties at low nitrite concentration. This can be overcome by using injection volumes sufficiently large such that the resident time of the sample plug in the thin-layer flow-cell is greater than the decay time of the capacitance current.⁴³ Under these conditions pure faradaic current can then be measured. Fortunately, injection of

samples with matrices identical to the carrier results in minimal disturbance of the normal background such as for the detection of Fe(II) and Fe(III)

Another source of background response is faradaic current. This originates from the oxidation or reduction of electro-active impurities in the carrier electrolyte. In order to minimise this source of noise, electrolyte concentrations should be kept as low as possible while sufficient to still maintain efficient charge transport through the redox polymer film. It is expected that the three dimensional arrangement of electro-active sites at the modified electrodes would significantly increase the background faradaic current. This behaviour however is not observed. The background faradaic currents at the modified electrode are typically $\approx 25\%$ of that observed for the bare glassy carbon. The reason for this is not clear. It is however known that the level of porosity of glassy carbon electrodes determines to a large extent the level of background current experienced under operational conditions.⁴⁴ The presence of adsorbed polymer on the surface may decrease the effect of porosity by blocking pores from the contacting electrolyte and thus suppressing this source of background current. The magnitude of background current is of significant importance as this determines the limit of detection ($S/N = 2/1$). Thus, the modified electrodes can lower limit of detection by decreasing background noise (N) as well as increasing the analytical signal (S).

The theoretical limit of detection, *i.e.* the concentration of substrate required to produce a signal twice that of the background current, for the Fe(III), Fe(II) and NO_2^- sensors can be estimated under conditions of infinite mass transport ($\delta \rightarrow 0$) using equation 6.15-10

$$i = n F A k K b_o L y_{\infty} \quad (6.15)$$

Using this equation, assuming a normal background current of $\approx 0.1 \text{ nA}$, 5% conversion efficiencies at the optimum flow rate for each sensor, and surface coverages of about $1 \times 10^{-8} \text{ mol cm}^{-2}$, the following theoretical LODs were found, for Fe(II), $6.5 \times 10^{-11} \text{ mol dm}^{-3}$, Fe(III), $5.2 \times 10^{-9} \text{ mol cm}^{-2}$ and NO_2^- , $3.1 \times 10^{-6} \text{ mol dm}^{-3}$. The experimentally estimated LOD were, Fe(II), $5.0 \times 10^{-8} \text{ mol dm}^{-3}$, Fe(III), $5.0 \times 10^{-8} \text{ mol dm}^{-3}$ and NO_2^- ,

$5.0 \times 10^{-6} \text{ mol dm}^{-3}$ Under these conditions, the electrode responses should be under kinetic control, *i.e.* $L \ll L_k$. It is evident that the experimentally observed LODs for nitrite agrees well with that found using equation 6.15. This is probably due to the rapid permeation of the polymer film by the substrate ($K \approx 1.0$) and the absence of mass transport control on the electrode currents, *i.e.* the catalytic reaction is controlled by k rather than K or D_s (diffusion of substrate in solution). This is confirmed by the strict first order relationship with respect to L in the thin-layer flow-cell (Fig. 2.20). For both Fe(II) and Fe(III) sensors the theoretical LOD's are significantly lower than that obtained experimentally. It is likely that the partitioning of these substrates into the films under flow conditions is far from equilibrium (equilibrium conditions are used to calculate the apparent second order rate constant k/K used above), and as a result the electrode currents are likely to be less than those predicted by equation 6.15. This again is reflected in the effect of surface coverage on electrode response in the flow cells where the slopes of $\ln \Gamma$ vs $\ln i$ are $\ll 1.0$ for both Fe(II) and Fe(III) sensors (Fig. 3.8). It is possible that steady-state conditions may be fulfilled, and therefore results in lowering of the LOD's obtained with the use of larger injection volumes or slower carrier flow rates. However due to the thin-layer nature of the sample plug in the flow-cell, the possibility of complete depletion of the substrate in the interfacial region may limit the usefulness of these measures.

We can also calculate the theoretical sensitivity ($\mu\text{A mmol}^{-1} \text{ dm}^3$) for each sensor at steady-state from equation 6.15 and compare the values to those found experimentally. The theoretical sensitivity of the nitrite sensor calculated (from the experimental conditions) is $\approx 1.3 \mu\text{A mmol}^{-1} \text{ dm}^3$ while the experimentally estimated value is $2.3 \mu\text{A mmol}^{-1} \text{ dm}^3$. These are, within experimental error, identical. This close agreement again appears to be a result of the rapid permeation of the substrate into the film and the kinetic control of the reaction in the thin-layer flow-cell. The calculated sensitivity for the Fe(III) is $\approx 40 \mu\text{A mmol}^{-1} \text{ dm}^3$ while the experimental value is $3.08 \mu\text{A mmol}^{-1} \text{ dm}^3$. The experimental value is considerably less than the predicted value. This may be attributed to the non-steady-state conditions in the thin-layer flow cells. Similar deviant behaviour is observed for the Fe(II) sensor. The estimated sensitivity for the Fe(II) sensor is $\approx 3 \text{ mA mmol}^{-1} \text{ dm}^3$ while the experimental value is $6.4 \mu\text{A mmol}^{-1} \text{ dm}^3$. This may also be attributed to non-steady-state conditions in the flow-cell for this reaction.

The theoretical lower limit of detection has been calculated using equation 6 15 The upper limit of linearity can also be estimated using this equation Direct comparison between the top of the linear range estimated theoretically is not directly comparable to that found experimentally in the thin-layer flow-cell as the hydrodynamic conditions are different for both situations It is however informative to compare these parameters as this gives an estimate of the “saturation concentration” The current response for a particular concentration of substrate at any redox polymer modified electrode is a function of the four characteristic currents defined by Saveant 5-10, these are, the electron transport current, i_e , the Levich current, i_a , the kinetic current, i_k and the substrate diffusion current, i_s For the osmium and ruthenium redox polymers used for the detection of Fe(II), Fe(III) and NO₂⁻, the rate of charge transport measured by chronoamperometry, (D_{ct} (PS)), in sulphuric acid electrolyte is $\approx 1 \times 10^{-9} \text{ cm}^2 \text{ s}^{-1}$ 45 Using this value and equation 6 16 for i_e , the maximum current flux possible at the modified electrodes can be estimated

$$i_e = F D_{ct} \Gamma / L^2 \quad (6 16)$$

This yields a value for the maximum current flux for a $1.0 \times 10^{-8} \text{ mol cm}^{-2}$ surface coverage of 4.3 mA cm^{-2} The characteristic kinetic current, i_k , for the oxidation of $1.0 \times 10^{-3} \text{ mol dm}^{-3}$ Fe(II) at the ruthenium modified electrode is estimated from equation 6 15 to be 43.4 mA cm^{-2} The corresponding Levich current (i_a) estimated from equation 6 17 is 47.1 mA cm^{-2}

$$i_a = F y_{\infty} D_s / \delta \quad (6 17)$$

As the kinetic current is smaller the Levich current at this surface coverage, the electrode responses are kinetically controlled under these conditions As the kinetic current increases with increasing substrate concentration, the sensor response will deviate from linearity when the

magnitude of the kinetic current reaches that of the maximum electron diffusion current. For the Fe(III) sensor, the kinetic current is 0.54 mA cm^{-2} while the Levich current is 47.1 mA cm^{-2} . Again, under these conditions the sensor response will deviate from linearity when the kinetic current approaches the electron diffusion current. Using equation 6.15 this situation arises for the Fe(III) sensor when the substrate concentration reaches $8.3 \times 10^{-3} \text{ mol dm}^{-3}$ for the 0.3 cm diameter electrodes used in the flow-cell. This is slightly less than that found experimentally, i.e. $1.0 \times 10^{-2} \text{ mol dm}^{-3}$. For the Fe(II) sensor, the substrate concentration, where i_k exceeds i_e , is $1.0 \times 10^{-4} \text{ mol dm}^{-3}$. This is considerably less than that found experimentally, i.e. $1.0 \times 10^{-2} \text{ mol dm}^{-3}$. The larger linear range found experimentally may be attributed to the non-steady-state conditions operating in the flow-cell for this reaction.

For the NO_2^- sensor, the slow nature of the cross-exchange reaction ensures that $i_k \ll i_a$ and i_e , so the electrode current is limited by the kinetics of the cross-exchange reaction rather than electron transport (i_e) or by mass transport (i_a) of the substrate to the electrode surface. Using equation 6.15 the concentration of nitrite required for $i_k = i_e$ is 5.2 mol dm^{-3} . The reason for this extended linear range is the slow nature of the electrocatalytic reaction and the absence of mass transport control.

6.3.4 Inter-Electrode Variability

The application of polymer modified electrodes for routine analysis requires reproducibility of inter-electrode responses to be within an acceptable limit. In situations where direct calibration is impossible, such as remote sensors or *in vivo* sensors, then strict reproducibility of the electrodes is essential. The use of automated lithographic technology appears the most fruitful approach to the production of mass produced modified electrodes. Such processes have the advantage of very reproducible production of the electrode surface. The manual method for the modification of electrodes probably represents the least reproducible form of electrode production. It is useful to quantify the exact level of reproducibility attainable by manual methods in order to estimate the worst case. It has already been shown in previous chapters that intra-

electrode reproducibility is excellent at less than 1.5 % RSD for the Fe(II), Fe(III) and NO₂⁻ sensors. This level of reproducibility is probably a reflection on the reproducibility of injection of the sample into the FIA system rather than an inherent feature of the sensors.

The inter-electrode reproducibility was estimated by preparing a series of 8 electrodes from [Os(bipy)₂(PVP)₁₀Cl]Cl and measuring the response for standard solutions of 1.0×10^{-3} mol dm⁻³ Fe(III) and ascorbic acid. These substrates reflect the effect of electrode reproducibility on through film reactions (Fe(III)) and surface reactions (ascorbic acid). It was found that for the detection of ascorbic acid the relative standard deviation over 8 electrodes was of 2.7 %. This level of variation may be considered low taking into account the minute quantities of electrocatalysts deposited on the electrode surfaces. For the through film reaction the RSD over the same number of electrodes was 4.4%. The slightly higher value here represents the greater sensitivity to small changes in polymer layer thickness. This level of reproducibility may also be considered excellent. With the use of automated coating procedures increases in the reproducibility of electrode preparation is inevitable.

6.4. Conclusions

In this chapter it was demonstrated that the polymer bound electrocatalysts behave in a general fashion. These materials can therefore be applied to the analysis of a wide range of potential analytes. The only requirement is that electron transfer is outer-sphere in nature and that the Gibbs free energy of the reaction is negative. This has been demonstrated by the construction of sensors for the analysis of substrates such as Fe(II) and Fe(III). The general nature of the behaviour observed also allows to a certain extent the prediction of the behaviour of potential analytes under operational conditions. It has also been shown that the basic thermodynamic principles can be used to control the sensitivity of the sensors. In addition, greatly enhanced selectivity can also be accomplished by manipulation of the formal potentials of the redox catalysts and that of the analyte and potential interferents. The large body of information available in the literature concerning the electrochemistry of electro-active

species can be applied to control the reactivity of the modified electrode and also the reactivity of the substrates. This results in the elimination of many potential interferences in real analytical systems. It was also shown that thermodynamically favourable electron transfer reactions of interferences such as ascorbic acid were suppressed due to rapid electron self-exchange rates between the catalytic sites within the polymer film. The polymer was seen to act as an “electron valve” by allowing current flow in cathodic direction only. At conventional electrodes the net current is a sum of both anodic and cathodic currents. Obviously, ascorbic acid oxidation proceeds at the operational potentials used in this study using conventional electrode materials.

Modified electrodes also exhibit lower background currents and lower transient capacitance currents than conventional electrode material. This, along with the acceleration of the electrode reaction of interest, results in lower limits of detection. The upper limit of the linear range for the sensors can also be calculated using conventional theory in order to access the “saturation concentration”. For modified electrodes in flow cells extended linear ranges are possible due to the non-steady-state conditions prevailing under these hydrodynamic conditions. In general, the use of the theory of mediated electrocatalysis is very useful in predicting and describing electrode responses in FIA applications.

It was also shown that modified electrodes could be prepared reproducibly ($< 5\%$ RSD) by manual methods. By implication automated procedures for the manufacture of such devices could produce devices with highly controlled electrocatalytic and transport properties. This is of considerable advantage for the commercialising of such devices for routine analytical applications.

6.5. References

- 1 A R Guadalupe, H D Abruna, *Anal Chem* , 1985 57 142
- 2 L M Wier, A R Guadalupe, H D Abruna *Anal Chem* , 1985 57 2011
- 3 S K Cha H D Abruna. *Anal Chem* 1990 62 274
- 4 R J Forster, J G Vos in *Comprehensive Analytical Chemistry* Vol XXVII, M R Smyth, J G Vos, (Eds) Elsevier, Amsterdam, 1992, Ch 7
- 5 C P Andrieux, J M Dumas-Bouchiat, F M'Halla, J M Saveant *J Electroanal Chem* , 1980 113 19
- 6 C P Andrieux, J M Dumas-Bouchiat, J M Saveant, *J Electroanal Chem* , 1982 131 1
- 7 C P Andrieux, J M Dumas-Bouchiat, J M Saveant, *J Electroanal Chem* , 1984 169 9
- 8 C P Andrieux, J M Saveant, *J Electroanal Chem* , 1984 171 65
- 9 C P Andrieux, J M Saveant, *J Electroanal Chem* , 1982 142 1
- 10 C P Andrieux, J M Saveant, *J Electroanal Chem* , 1982 134 163
- 11 F C Anson, T Ohsaka, J M Saveant, *J Am Chem Soc* , 1983 105 4883
- 12 R A Marcus, *Annu Rev Phys Chem* , 1964 15 155
- 13 R J Forster, J G Vos, *J Chem Soc , Faraday Trans* , 1991 87 1863
- 14 W J Albery, M G Boutelle, A R Hillman *J Electroanal Chem* , 1985 182 99
- 15 C R Leidner, R W Murray, *J Am Chem Soc* , 1984 106 1606
- 16 C R Leidner, R W Murray, *J Am Chem Soc* , 1985 107 1606
- 17 O Haas, M Kriens, J G Vos, *J Am Chem Soc* , 1981 103 1318
- 18 A Ivaska, *Electroanalysis*, 1991 3 247
- 19 M E G Lyons, W Breen, F Cassidy, *J Chem Soc , Faraday Trans* , 1991 87 115
- 20 R Engleman, J Jortner *J Mol Phys* , 1970 18 145

- 21 K F Freed, J Jortner, *J Chem Phys* , 1970 52 6272
- 22 R W Murray, A G Ewing, R A Durst, *Anal Chem* , 1987 59 379A
- 23 K Stulik, V Pacakova, *Selective Electrode Rev* , 1992 14 87
- 24 P T Kissinger, *Anal Chem* , 1977 49 445A
- 25 C P Andrieux, O Haas, J M Saveant, *J Am Chem Soc* , 1986 108 8175
- 26 R C Weast, (Ed), *Handbook of Physics and Chemistry* 66th Edition, CRC Press, Florida, 1986, Table D-163
- 27 J E Newbery, M P Lopez de Haddad, *Analyst*, 1985 110 81
- 28 G Norwitz, P Keliher, *Analyst*, 1987 112 903
- 29 R M C Dawson, D C Elliott, W H Elliott, K M Jones, *Data for Biochemical Research*, Edition 3, Claredon Press, Oxford, 1986
- 30 A Aldaz, A M Aquie, *J Electroanal Chem* , 1973 47 532
- 31 J J Ruiz, A Aldaz, M Dominguez, *Can J Chem* , 1978 56 1533
- 32 M Rueda, A Aldaz, F Sanchez-Buggos, *Electrochim Acta* , 1978 23 419
- 33 P Karabinas, D Jannakoudakis, *J Electroanal Chem* , 1984 160 159
- 34 E Pelizzetti, E Mentasti, E Pramauro, *Inorg Chem* , 1976 15 2898
- 35 I Feng Hu, T Kuwana, *Anal Chem* , 1986 58 3235
- 36 E Pelizzetti, E Mentasti, E Pramauro, *Inorg Chem* , 1978 17 1181
- 37 F C Anson, Y-M, Tsou, J M Saveant, *J Electroanal Chem* , 1984 178 113
- 38 N H Williams, J K Yandell, *Aust J Chem* , 1982 35 1133
- 39 W J Albery, A R Hillman, *Ann Rep Prog Chem* , 1981 (C) 78 377
- 38 C P Andrieux, J M Saveant, *J Electroanal Chem* , 1980 111 377
- 40 E Laviron, *J Electroanal Chem* , 1980 112 1
- 41 G Mengoli, M M Musiani, *J Electroanal Chem* , 1989 269 99

- 42 D C Johnson, S G Weber, A M Bond, R M Wrightman,
R E Shoup, I S Krull, *Anal Chim Acta* , 1986 180 187
- 43 Y Xu, H B Halsall, W R Heineman, *Electroanalysis*, 1992
4 33
- 44 J Lankelma, H Poppe, *J Chromatogr* , 1976 125 375
- 45 R J Forster, A J Kelly, J G Vos, M E G Lyons, *J*
Electroanal Chem , 1989 270 365

Chapter 7

8

Concluding Comments

•

Much of the previously published work concerning redox polymer modified electrodes involved the fundamental aspects of these devices. These studies included theoretical models of charge transport processes and mediated electrocatalysis. Generally, studies of electrocatalysis at these electrodes were designed for the testing of proposed theoretical models rather than the development of strategies for electroanalysis, however the potential for sensor development has often been alluded to. As a result relatively little attention has been given to the detailed investigation of the analytical applications of such modified electrodes. The purpose of the work reported in this thesis was to investigate some concepts for the development of redox polymer modified electrodes for electroanalysis and consider general strategies for analytical applications.

Much of current interest in electrocatalysis revolves around the use of under-potential deposition, adatoms and inorganic films at electrode surfaces. Although useful and elegant, such approaches are often severely limited by stability problems and synthetic difficulties. The use of polymeric redox catalysts offer many advantages over other modified electrodes for electroanalysis. These advantages can be attributed to the possibility of three dimensional reaction zones, and more importantly, the level of synthetic variability which can be used in the preparation of organo-metallic polymers. Throughout this thesis, the predominant underlying theme is of, control, by manipulation of the inherent properties of the mediating layer. By controlling the properties of the redox polymer, the reactivity of the electrode can be regulated, and with this the possibility of performing selective detection of target analytes becomes real. With the ability to manipulate the properties of the redox polymer, consideration must be given to what parameters are to be optimised and for what reason. The implications of such manipulations on the various processes occurring at the electrode must also be considered. The parameters which can be manipulated that are useful in designing electrochemical sensors from redox polymer modified electrodes are, polymer layer thickness, L , the concentration of electro-active sites within the film, b_0 , the rate constant for the cross-exchange reaction, k , partition and diffusion of the substrate into the film, K and D_y respectively and the rate of charge transport, D_{ct} . Traditionally, all of these parameters are considered difficult to control with the exception of L . Probably the reason for this view is the predominance of electro-polymerisation of both organic redox polymers.

and organo-metallic materials. Such synthetic approaches offer limited scope for variability.

Probably the most frequently measured parameter in the study of redox polymers is the rate of charge transport, D_{ct} . It has often been stated that the first parameter to be optimised for the development of redox polymer modified electrodes is charge transport. An example of the importance of rapid charge transport was seen in chapter 5, where the response for Fe(III) at an $[\text{Os}(\text{bipy})_2(\text{PS})_{7.5}(\text{DMAP})_{2.5}\text{Cl}]\text{Cl}$ modified electrode was limited by electron transport at substrate concentrations greater than $1.0 \times 10^{-3} \text{ mol dm}^{-3}$. The assumption that charge transport must always be rapid appears to originate in the field of electro-synthesis rather than in the arena of sensor development. Obviously, electro-synthetic procedures require maximum efficiency from the working electrode. However, this assumption begs the question: how fast should D_{ct} be for operational sensors? The answer to this question is simply only as fast as required. The strategy for the development of any sensor must be application specific. For most potential sensor applications, the approximate concentration, and the level of variability of the target analyte concentration is generally known. In addition, environmentally important analytes tend to exist at low concentrations *e.g.* ppb – ppm. As a result, there is little to be gained from the use of modified electrodes where the current carrying capacity of the polymer greatly exceeds the expected reactant flux to the electrode surface. In terms of Saveant's theory, the characteristic electron diffusion current, i_e , need only exceed the expected characteristic mass transport current, i_a . In fact, conditions for rapid charge transport are mutually opposed to those for maximum polymer stability, so, much can be gained by using polymers with application specific charge transport rates. Only in situations where the analyte concentration varies over several orders of magnitude or exists at high concentration are optimum charge transport rates required.

It was demonstrated in chapter 4 that cross-linking $[\text{Os}(\text{bipy})_2(\text{PVP})_{10}\text{Cl}]\text{Cl}$ with various levels of 1,5-dibromopentane resulted in polymer films with varying charge transport properties. In addition, previous studies on these materials demonstrate that the structure of the polymer backbone and the composition of the contacting electrolyte can influence the charge transport properties of these materials remarkably. Also, manipulation of b_0 has a marked influence on the

charge transport rates. The results suggest that D_{ct} is more controllable than originally believed. With the synthetic strategy used for the preparation of these materials, the polymer backbone, concentration of electro-active sites, the type and level of cross-linking can be controlled at will.

With the prospect of modified electrodes with controlled charge transport rates, certain applications become apparent. Controlled charge transport allows the possibility of defined maximum current fluxes through the polymer. For example, many analytical procedures for environmental monitoring are designed to indicate when the analyte concentration exceeds the maximum permitted level for that species. It is possible that devices constructed from redox polymer modified electrodes may be used to indicate a specified upper limit for the concentration of the target analyte. In designing such a system, the maximum electron flux through the redox polymer under operational conditions would correspond to the analyte mass transport flux at the maximum permitted concentration. Simple measurement of the electrode current would indicate when the maximum current flux has been attained and consequently the upper concentration limit. Such "on/off" devices would however require precise control of hydrodynamic conditions and potential interferences.

It was seen in chapter 6 that the sensitivity and selectivity of sensors for electro-active substrates depended on the free energy difference between the substrate and the electrocatalyst. The free energy difference can be controlled by either manipulation of the $E_{1/2}$ of the electrocatalyst or of the interfering species. A very clear example of this was the simultaneous detection of Fe(II) and Fe(III) in a single sample aliquot by enveloping the formal potential of the Fe(II)/Fe(III) redox couple by the half-wave potentials of the osmium and ruthenium electrocatalysts. This allows speciation analysis of the free metal species without manipulation of the oxidation states of the analyte redox pair. This approach has considerable advantages compared to existing techniques and the potential for application to other redox couples and multiple redox states is clearly evident. The same principles were applied to enhance the sensitivity of [Os(bipy)₂(PVP)₁₀Cl]Cl modified electrodes for the detection of Fe(III) by the formation of iron-thiocyanate complex, $[\text{Fe}(\text{SCN})_x]^{(3-x)+}$. Removal of Fe(III) and Cu(II) interference was also accomplished in this manner. The use of the slow cross-exchange reaction for the nitrite sensor was also

shown to be advantageous. The independence of mass transport controlled allowed the electrode response to be directly related to known and easily measurable parameters. The equation describing the sensor response may be used for the internal calibration of the sensor. Due to the well established coordination chemistry of osmium and ruthenium, control of the free energy difference between the analyte and the redox catalysts is relatively straight forward in comparison to organic redox polymers or electro-polymerised organo-metallic materials.

In the case of the nitrite sensor, ascorbic acid interference was prevented by inhibiting the oxidation reaction although the applied potential was favourable. Oxidation of ascorbic acid was prevented as the redox polymer acted as an "electron valve" and allowed uni-directional (cathodic) current flow. Essentially, a co-existing electro-active species was prevented from interfering by manipulation of the thermodynamic of the system. At conventional electrodes, this analysis would be impossible. It is conceivable that the other simple concepts may be exploited to carry out unique electroanalytical measurements. A possible example of this is the determination of co-existing electro-active substrates by control of the reaction zones. If we consider a system where species A can permeate the polymer film and react in a three dimensional reaction zone, L_k , (e.g. Fe(II) in $[\text{Ru}(\text{bipy})_2(\text{PVP})_{10}\text{Cl}]\text{Cl}$) and species B which can not permeate the polymer film and reacts at the polymer/electrolyte interface, S_k , (e.g. ascorbic acid at $[\text{Ru}(\text{bipy})_2(\text{PVP})_{10}\text{Cl}]\text{Cl}$). Assuming sufficient charge transport to accommodate both reactions simultaneously at a polymer film of thickness, L_1 , then the current flux is the sum of the fluxes for both reactions. At another modified electrode with a thicker polymer film, L_2 , the current flux again is the sum of the surface and film reactions, however, the difference in current response is due to the differences in layer thickness, ΔL , and consequently the oxidation of A. Under identical hydrodynamic conditions, the current for the oxidation of A at L_1 can be isolated and consequently the current response for B. Again, this concept would be impossible to implement at conventional electrodes or monolayer devices. These novel approaches are a direct consequence of the unique, controllable behaviour of the redox polymers.

Currently, much attention is being directed towards the development of electrode arrays, for example, potentiometric arrays for the determination of a range of ions in blood. These approaches stemmed

from the success of multi-linear regression techniques applied to near IR spectroscopy in the 1970's. In these applications, the absolute specificity of each sensory element is not critical, the calibration procedure models the sensory elements response to various substrates in a series of calibration solutions ("learning sets"). Due to the general nature of the mediated electrocatalysis studied here, it is likely that absolute specificity in complex samples for these electrodes is unattainable unless under very defined conditions. In the above discussion, numerous approaches are available to impart certain levels of selectivity and sensitivity to individual sensors. It is likely that arrays of modified electrodes may be constructed with synthetically controlled selectivity and sensitivity for a range of analytes. The use of the well developed calibration procedures using multi-linear regression may prove successful in establishing modified electrodes as real analytical devices.

In summary, the use of redox polymer modified electrodes for electroanalysis is in an early stage of development. It is quite clear that the metallo-polymers used for sensor development offer a range of advantages over the more commonly used electrocatalytic surfaces. The use of simple synthetic strategies to control selectivity on the basis of partition (K), free energy (k) and reaction *loci* is of particular advantage. Many simple concepts which can be implemented for the isolation of information for analytical purposes are available and it is certain that many more will be proposed and developed. The future prospect for these devices lies in the "fine tuning" of the properties of the polymer layers, truly engineering on the molecular scale.